

JAERI-Research

95-018



**BULK SHIELDING EXPERIMENT ON A LARGE SS316/WATER
ASSEMBLY BOMBARDED BY D-T NEUTRONS
VOLUME II : ANALYSIS**

March 1995

Fujio MAEKAWA, Chikara KONNO, Masayuki WADA, Yukio OYAMA
Yujiro IKEDA, Yoshitomo UNO, Yuriy VERZILOV* and Hiroshi MAEKAWA

**日本原子力研究所
Japan Atomic Energy Research Institute**

本レポートは、日本原子力研究所が不定期に公刊している研究報告書です。

入手の問合せは、日本原子力研究所技術情報部情報資料課（〒319-11 茨城県那珂郡東海村）あて、お申し越しください。なお、このほかに財団法人原子力弘済会資料センター（〒319-11 茨城県那珂郡東海村日本原子力研究所内）で複写による実費頒布をおこなっております。

This report is issued irregularly.

Inquiries about availability of the reports should be addressed to Information Division, Department of Technical Information, Japan Atomic Energy Research Institute, Tokaimura, Naka-gun, Ibaraki-ken 319-11, Japan.

© Japan Atomic Energy Research Institute, 1995

編集兼発行 日本原子力研究所
印 刷 いばらき印刷株

Bulk Shielding Experiment on a Large SS316/Water Assembly
Bombarded by D-T Neutrons
Volume II : Analysis

Fujio MAEKAWA, Chikara KONNO, Masayuki WADA, Yukio OYAMA
Yujiro IKEDA, Yoshitomo UNO, Yuriy VERZILOV* and Hiroshi MAEKAWA

Department of Reactor Engineering
Tokai Research Establishment
Japan Atomic Energy Research Institute
Tokai-mura, Naka-gun, Ibaraki-ken

(Received February 8, 1995)

As a part of the Engineering Design Activities (EDA) of the International Thermonuclear Experimental Reactor (ITER), the bulk shielding experiment on a large SS316/water assembly bombarded by D-T neutrons were carried out at the FNS facility in JAERI. The experimental details are described in the separate issue, Volume I. In this report, Volume II, methods and results of the experimental analysis, and comparisons of the calculated results with the experiments are compiled. Two transport calculation codes, MCNP-4 and DOT-3.5, and cross section libraries based on JENDL-3.1 and JENDL-3.2 were used in the analysis. As a result, the following facts were found for shielding properties of the SS316/water shield to both neutrons and gamma-rays; (i) Neutron fluxes from 14 MeV down to thermal energy and gamma-ray heating rates can be predicted with high accuracy within 20% by the MCNP calculation with JENDL-3.2 and the DOT calculation with consideration of the self-shielding correction and 125-neutron and 40-gamma-ray energy groups. (ii) Although influences of the self-shielding correction and the number of energy groups are not so large as in the case of SS316 assemblies, further uncertainty of about 20% should be taken into the calculated results when the

This report was submitted to the Joint Central Team (JCT) of ITER.

* Research Fellow

correction is omitted or 42-neutron and 21-gamma-ray energy groups are used. (iii) If thermal neutron fluxes are expressed in one energy group in multi-group calculations, a large error may be involved in the calculated results of thermal neutron flux in some cases.

Keywords: ITER/EDA, FNS, Shielding Experiment, SS316, Water, MCNP, DOT, JENDL-3.1, JENDL-3.2, Self-shielding, Energy Group Number

D-T中性子による大型SS316／水体系におけるバルク遮蔽実験
第2部：解析

日本原子力研究所東海研究所原子炉工学部
前川 藤夫・今野 力・和田 政行・大山 幸夫
池田裕二郎・宇野 喜智・Yuriy VERZILOV*・前川 洋

(1995年2月8日受理)

国際熱核融合実験炉（ITER）の工学設計活動（EDA）の一環として、D-T中性子により照射された大型SS316／水体系におけるバルク遮蔽実験が原研FNS施設で行われ、実験の詳細が本レポートの別刷である第1部に述べられている。本レポート、第2部は、この実験解析の方法とその結果、および計算結果と実験値との比較をまとめたものである。解析には2つの輸送計算コードMCNP-4とDOT-3.5、およびJENDL-3.1とJENDL-3.2に基づく断面積ライブラリを用いた。その結果、SS316／水遮蔽体の中性子、2次 γ 線の双方に対する遮蔽性能について、次のことが分った。（i）JENDL-3.2を使用したMCNP計算、自己遮蔽を考慮したDOT計算（中性子125群+ γ 線40群）により、14MeV～熱エネルギーまでの中性子束及び γ 線核発熱を20%以内で精度良く予測することができる。（ii）自己遮蔽補正及びエネルギー群数の影響はSS316体系の時ほど大きくないが、自己遮蔽補正を考慮しない時、あるいは中性子42群 γ 線21群で計算を行う時には、それぞれさらに20%程度の不確定性を計算結果に見込む必要がある。（iii）多群計算で熱中性子を1つの群で表現すると、場合によっては熱群の中性子束の計算結果に大きな誤差を生じることがある。

このレポートはITER/JCTに提出したものである。
東海研究所：〒319-11 茨城県那珂郡東海村白方字白根2-4
*リサーチフェロー

Contents

1. Introduction	1
2. Analysis	3
2. 1 Calculation Conditions	3
2. 2 MCNP Calculation	3
2. 3 DOT Calculation	4
2. 4 Post Processing	6
3. Comparison of the Calculation with the Experiment	7
3. 1 Reaction Rate	7
3. 2 Neutron Spectrum	7
3. 3 Gamma-ray Heating Rate	8
3. 4 Gamma-ray Spectrum	8
3. 5 Room Returned Background	9
4. Discussions	10
4. 1 Energy Profile of the Dosimetry Reaction Rate	10
4. 2 Comparison among DOT Calculations	11
4. 3 Comparison between DOT and MCNP Calculation	11
4. 4 Comparison of JENDL-3.1 and JENDL-3.2	12
4. 5 Comparison of the MCNP Calculation with the Experiment	12
4. 6 Treatment of Thermal Neutron	13
5. Concluding Remarks	15
Acknowledgment	16
References	17

目 次

1. はじめに	1
2. 解析	3
2.1 計算条件	3
2.2 MCNP計算	3
2.3 DOT計算	4
2.4 後処理	6
3. 計算と実験との比較	7
3.1 反応率	7
3.2 中性子スペクトル	7
3.3 γ 線発熱率	8
3.4 γ 線スペクトル	8
3.5 壁反射バックグラウンド	9
4. 検討	10
4.1 ドジメトリー反応のエネルギープロファイル	10
4.2 DOT計算同士の比較	11
4.3 DOTとMCNP計算の比較	11
4.4 JENDL-3.1とJENDL-3.2の比較	12
4.5 MCNPによる計算値と実験値の比較	12
4.6 热中性子の取り扱い	13
5. 結論	15
謝辞	16
参考文献	17

List of Tables

- Table 2.1 Atomic densities adopted to the analysis.
- Table 2.2 Cross section libraries used in the analysis. Libraries outside the parentheses are used for the transport calculations, and those inside the parentheses are the original cross section data bases.
- Table 2.3 Energy group structure of neutron 125-group, gamma-ray 40-group, neutron 42-group and gamma-ray 21-group used in the DOT analysis. The unit of energy is eV.
- Table 3.1 Measured and calculated reaction rates and their C/E ratios.
- Table 3.2 Neutron spectra at the eight positions in the assembly calculated by MCNP with the FSXLIB-J3 library.
- Table 3.3 Neutron spectra at the eight positions in the assembly calculated by MCNP with the FSXLIB-J3R2 library.
- Table 3.4 Neutron spectra at the eight positions in the assembly calculated by DOT with the JSSTDL library of 125 neutron groups.
- Table 3.5 Neutron spectra at the eight positions in the assembly calculated by DOT with the FUSION-J3 library of 125 neutron groups.
- Table 3.6 Neutron spectra at the eight positions in the assembly calculated by DOT with the JSSTDL library of 42 neutron groups.
- Table 3.7 Neutron spectra at the eight positions in the assembly calculated by DOT with the FUSION-40 library of 42 neutron groups.
- Table 3.8 Measured and calculated integral neutron fluxes and their C/E ratios.
- Table 3.9 Measured and calculated gamma-ray heating rates in [Gy/Source Neutron] and their C/E ratios.
- Table 3.10 Gamma-ray spectra at the four positions in the assembly calculated by MCNP with the FSXLIB-J3 library.
- Table 3.11 Gamma-ray spectra at the four positions in the assembly calculated by MCNP with the FSXLIB-J3R2 library.
- Table 3.12 Gamma-ray spectra at the four positions in the assembly calculated by DOT with the JSSTDL library of 125 neutron and 40 gamma-ray groups.
- Table 3.13 Gamma-ray spectra at the four positions in the assembly calculated by DOT with the FUSION-J3 library of 125 neutron and 40 gamma-ray groups.
- Table 3.14 Gamma-ray spectra at the four positions in the assembly calculated by DOT with the JSSTDL library of 42 neutron and 21 gamma-ray groups.
- Table 3.15 Gamma-ray spectra at the four positions in the assembly calculated by DOT with the FUSION-40 library of 42 neutron and 21 gamma-ray groups

List of Figures

- Fig. 2.1 Calculation model for the SS316/water assembly.
- Fig. 2.2 Input data of MCNP for the analysis of the SS316/water assembly with the FSXLIB-J3R2 library.
- Fig. 2.3 Input data of FNSUNCL for the DOT analysis of the SS316/water assembly with the FUSION-J3 library (125-n + 40- γ).
- Fig. 2.4 Input data of the DOT analysis for the SS316/water assembly with the FUSION-J3 library (125-n + 40- γ).
- Fig. 2.5 Input data of FNSUNCL for the DOT analysis of the SS316/water assembly with the FUSION-40 library (42-n + 21- γ).
- Fig. 2.6 Input data of the DOT analysis for the SS316/water assembly with the FUSION-40 library (42-n + 21- γ).
- Fig. 2.7 Input data of FNSUNCL for the DOT analysis of the SS316/water assembly with the JSSTDL library (125-n + 40- γ).
- Fig. 2.8 Input data of the DOT analysis for the SS316/water assembly with the JSSTDL library (125-n + 40- γ).
- Fig. 2.9 Input data of FNSUNCL for the DOT analysis of the SS316/water assembly with the JSSTDL library (42-n + 21- γ).
- Fig. 2.10 Input data of the DOT analysis for the SS316/water assembly with the JSSTDL library (42-n + 21- γ).
- Fig. 3.1 Dosimetry reaction cross sections of the $^{27}\text{Al}(\text{n},\alpha)^{24}\text{Na}$ and $^{32}\text{S}(\text{n},\text{p})^{32}\text{P}$ reactions taken from JENDL Dosimetry File.
- Fig. 3.2 Dosimetry reaction cross sections of the $^{93}\text{Nb}(\text{n},2\text{n})^{92m}\text{Nb}$ and $^{115}\text{In}(\text{n},\text{n}')^{115m}\text{In}$ reactions taken from JENDL Dosimetry File.
- Fig. 3.3 Dosimetry reaction cross sections of the $^{10}\text{B}(\text{n},\alpha)^7\text{Li}$ and $^{197}\text{Au}(\text{n},\gamma)^{198}\text{Au}$ reactions taken from JENDL Dosimetry File.
- Fig. 3.4 Dosimetry reaction cross sections of the $^{235}\text{U}(\text{n,fission})$ and $^{238}\text{U}(\text{n,fission})$ reactions taken from JENDL Dosimetry File.
- Fig. 3.5 The C/E ratios of the $^{10}\text{B}(\text{n},\alpha)^7\text{Li}$ reaction rate for four different DOT calculations.
- Fig. 3.6 The C/E ratios of the $^{10}\text{B}(\text{n},\alpha)^7\text{Li}$ reaction rate for MCNP and DOT calculations.
- Fig. 3.7 The C/E ratios of the $^{27}\text{Al}(\text{n},\alpha)^{24}\text{Na}$ reaction rate for four different DOT calculations.
- Fig. 3.8 The C/E ratios of the $^{27}\text{Al}(\text{n},\alpha)^{24}\text{Na}$ reaction rate for MCNP and DOT calculations.
- Fig. 3.9 The C/E ratios of the $^{32}\text{S}(\text{n},\text{p})^{32}\text{P}$ reaction rate for four different DOT calculations.
- Fig. 3.10 The C/E ratios of the $^{32}\text{S}(\text{n},\text{p})^{32}\text{P}$ reaction rate for MCNP and DOT calculations.
- Fig. 3.11 The C/E ratios of the $^{93}\text{Nb}(\text{n},2\text{n})^{92m}\text{Nb}$ reaction rate for four different DOT calculations.

- Fig. 3.12 The C/E ratios of the $^{93}\text{Nb}(\text{n},2\text{n})^{92\text{m}}\text{Nb}$ reaction rate for MCNP and DOT calculations.
- Fig. 3.13 The C/E ratios of the $^{115}\text{In}(\text{n},\text{n}')^{115\text{m}}\text{In}$ reaction rate for four different DOT calculations.
- Fig. 3.14 The C/E ratios of the $^{115}\text{In}(\text{n},\text{n}')^{115\text{m}}\text{In}$ reaction rate for MCNP and DOT calculations.
- Fig. 3.15 The C/E ratios of the $^{197}\text{Au}(\text{n},\gamma)^{198}\text{Au}$ reaction rate for four different DOT calculations.
- Fig. 3.16 The C/E ratios of the $^{197}\text{Au}(\text{n},\gamma)^{198}\text{Au}$ reaction rate for MCNP and DOT calculations.
- Fig. 3.17 The C/E ratios of the $^{235}\text{U}(\text{n,fission})$ reaction rate for four different DOT calculations.
- Fig. 3.18 The C/E ratios of the $^{235}\text{U}(\text{n,fission})$ reaction rate for MCNP and DOT calculations.
- Fig. 3.19 The C/E ratios of the $^{238}\text{U}(\text{n,fission})$ reaction rate for four different DOT calculations.
- Fig. 3.20 The C/E ratios of the $^{238}\text{U}(\text{n,fission})$ reaction rate for MCNP and DOT calculations.
- Fig. 3.21 The measured neutron spectra in MeV energy region at the front surface of the assembly in comparisons with four different DOT calculations.
- Fig. 3.22 The measured neutron spectra in MeV energy region at the front surface of the assembly in comparisons with MCNP and DOT calculations.
- Fig. 3.23 The measured neutron spectra in MeV energy region at 127 mm depth in comparisons with four different DOT calculations.
- Fig. 3.24 The measured neutron spectra in MeV energy region at 127 mm depth in comparisons with MCNP and DOT calculations.
- Fig. 3.25 The measured neutron spectra in MeV energy region at 229 mm depth in comparisons with four different DOT calculations.
- Fig. 3.26 The measured neutron spectra in MeV energy region at 229 mm depth in comparisons with MCNP and DOT calculations.
- Fig. 3.27 The measured neutron spectra in MeV energy region at 330 mm depth in comparisons with four different DOT calculations.
- Fig. 3.28 The measured neutron spectra in MeV energy region at 330 mm depth in comparisons with MCNP and DOT calculations.
- Fig. 3.29 The measured neutron spectra in MeV energy region at 457 mm depth in comparisons with four different DOT calculations.
- Fig. 3.30 The measured neutron spectra in MeV energy region at 457 mm depth in comparisons with MCNP and DOT calculations.
- Fig. 3.31 The measured neutron spectra in MeV energy region at 610 mm depth in comparisons with four different DOT calculations.
- Fig. 3.32 The measured neutron spectra in MeV energy region at 610 mm depth in comparisons with MCNP and DOT calculations.
- Fig. 3.33 The measured neutron spectra in MeV energy region at 762 mm depth in comparisons with four different DOT calculations.
- Fig. 3.34 The measured neutron spectra in MeV energy region at 762 mm depth in comparisons with MCNP and DOT calculations.

- Fig. 3.35 The measured neutron spectra in MeV energy region at 914 mm depth in comparisons with four different DOT calculations.
- Fig. 3.36 The measured neutron spectra in MeV energy region at 914 mm depth in comparisons with MCNP and DOT calculations.
- Fig. 3.37 The measured neutron spectra in keV energy region at the front surface of the assembly in comparisons with four different DOT calculations.
- Fig. 3.38 The measured neutron spectra in keV energy region at the front surface of the assembly in comparisons with MCNP and DOT calculations.
- Fig. 3.39 The measured neutron spectra in keV energy region at 127 mm depth in comparisons with four different DOT calculations.
- Fig. 3.40 The measured neutron spectra in keV energy region at 127 mm depth in comparisons with MCNP and DOT calculations.
- Fig. 3.41 The measured neutron spectra in keV energy region at 229 mm depth in comparisons with four different DOT calculations.
- Fig. 3.42 The measured neutron spectra in keV energy region at 229 mm depth in comparisons with MCNP and DOT calculations.
- Fig. 3.43 The measured neutron spectra in keV energy region at 330 mm depth in comparisons with four different DOT calculations.
- Fig. 3.44 The measured neutron spectra in keV energy region at 330 mm depth in comparisons with MCNP and DOT calculations.
- Fig. 3.45 The measured neutron spectra in keV energy region at 457 mm depth in comparisons with four different DOT calculations.
- Fig. 3.46 The measured neutron spectra in keV energy region at 457 mm depth in comparisons with MCNP and DOT calculations.
- Fig. 3.47 The measured neutron spectra in keV energy region at 610 mm depth in comparisons with four different DOT calculations.
- Fig. 3.48 The measured neutron spectra in keV energy region at 610 mm depth in comparisons with MCNP and DOT calculations.
- Fig. 3.49 The measured neutron spectra in keV energy region at 762 mm depth in comparisons with four different DOT calculations.
- Fig. 3.50 The measured neutron spectra in keV energy region at 762 mm depth in comparisons with MCNP and DOT calculations.
- Fig. 3.51 The measured neutron spectra in keV energy region at 914 mm depth in comparisons with four different DOT calculations.
- Fig. 3.52 The measured neutron spectra in keV energy region at 914 mm depth in comparisons with MCNP and DOT calculations.
- Fig. 3.53 The measured neutron spectra in eV energy region at 127 mm depth in comparisons with four different DOT calculations.

- Fig. 3.54 The measured neutron spectra in eV energy region at 127 mm depth in comparisons with MCNP and DOT calculations.
- Fig. 3.55 The measured neutron spectra in eV energy region at 229 mm depth in comparisons with four different DOT calculations.
- Fig. 3.56 The measured neutron spectra in eV energy region at 229 mm depth in comparisons with MCNP and DOT calculations.
- Fig. 3.57 The measured neutron spectra in eV energy region at 330 mm depth in comparisons with four different DOT calculations.
- Fig. 3.58 The measured neutron spectra in eV energy region at 330 mm depth in comparisons with MCNP and DOT calculations.
- Fig. 3.59 The measured neutron spectra in eV energy region at 457 mm depth in comparisons with four different DOT calculations.
- Fig. 3.60 The measured neutron spectra in eV energy region at 457 mm depth in comparisons with MCNP and DOT calculations.
- Fig. 3.61 The measured neutron spectra in eV energy region at 610 mm depth in comparisons with four different DOT calculations.
- Fig. 3.62 The measured neutron spectra in eV energy region at 610 mm depth in comparisons with MCNP and DOT calculations.
- Fig. 3.63 The measured neutron spectra in eV energy region at 762 mm depth in comparisons with four different DOT calculations.
- Fig. 3.64 The measured neutron spectra in eV energy region at 762 mm depth in comparisons with MCNP and DOT calculations.
- Fig. 3.65 The C/E ratios of the integrated neutron flux above 10 MeV for four different DOT calculations.
- Fig. 3.66 The C/E ratios of the integrated neutron flux above 10 MeV for MCNP and DOT calculations.
- Fig. 3.67 The C/E ratios of the integrated neutron flux between 0.1 and 1 MeV for four different DOT calculations.
- Fig. 3.68 The C/E ratios of the integrated neutron flux between 0.1 and 1 MeV for MCNP and DOT calculations.
- Fig. 3.69 The C/E ratios of the integrated neutron flux between 10 and 100 keV for four different DOT calculations.
- Fig. 3.70 The C/E ratios of the integrated neutron flux between 10 and 100 keV for MCNP and DOT calculations.
- Fig. 3.71 The C/E ratios of the integrated neutron flux between 10 and 100 eV for four different DOT calculations.
- Fig. 3.72 The C/E ratios of the integrated neutron flux between 10 and 100 eV for MCNP and DOT calculations.

- Fig. 3.73 The C/E ratios of the integrated neutron flux between 1 and 10 eV for four different DOT calculations.
- Fig. 3.74 The C/E ratios of the integrated neutron flux between 1 and 10 eV for MCNP and DOT calculations.
- Fig. 3.75 The C/E ratios of the integrated neutron flux below 1 eV for four different DOT calculations.
- Fig. 3.76 The C/E ratios of the integrated neutron flux below 1 eV for MCNP and DOT calculations.
- Fig. 3.77 The C/E ratios of the gamma-ray heating rate of SS316 for four different DOT calculations.
- Fig. 3.78 The C/E ratios of the gamma-ray heating rate of SS316 for MCNP and DOT calculations.
- Fig. 3.79 The measured gamma-ray spectra at 457 mm depth in comparisons with four different DOT calculations.
- Fig. 3.80 The measured gamma-ray spectra at 457 mm depth in comparisons with MCNP and DOT calculations.
- Fig. 3.81 The measured gamma-ray spectra at 610 mm depth in comparisons with four different DOT calculations.
- Fig. 3.82 The measured gamma-ray spectra at 610 mm depth in comparisons with MCNP and DOT calculations.
- Fig. 3.83 The measured gamma-ray spectra at 762 mm depth in comparisons with four different DOT calculations.
- Fig. 3.84 The measured gamma-ray spectra at 762 mm depth in comparisons with MCNP and DOT calculations.
- Fig. 3.85 The measured gamma-ray spectra at 914 mm depth in comparisons with four different DOT calculations.
- Fig. 3.86 The measured gamma-ray spectra at 914 mm depth in comparisons with MCNP and DOT calculations.
- Fig. 4.1 Energy profile of $^{10}\text{B}(\text{n},\alpha)^7\text{Li}$ reaction at each measuring positions.
- Fig. 4.2 Energy profile of $^{27}\text{Al}(\text{n},\alpha)^{24}\text{Na}$ reaction at each measuring positions.
- Fig. 4.3 Energy profile of $^{32}\text{S}(\text{n},\text{p})^{32}\text{P}$ reaction at each measuring positions.
- Fig. 4.4 Energy profile of $^{93}\text{Nb}(\text{n},2\text{n})^{92m}\text{Nb}$ reaction at each measuring positions.
- Fig. 4.5 Energy profile of $^{115}\text{In}(\text{n},\text{n}')^{115m}\text{In}$ reaction at each measuring positions.
- Fig. 4.6 Energy profile of $^{197}\text{Au}(\text{n},\gamma)^{198}\text{Au}$ reaction at each measuring positions.
- Fig. 4.7 Energy profile of $^{235}\text{U}(\text{n,fission})$ reaction at each measuring positions.
- Fig. 4.8 Energy profile of $^{238}\text{U}(\text{n,fission})$ reaction at each measuring positions.

1. Introduction

Shielding designs¹⁻⁶⁾ of the inboard blanket/shield of the International Thermonuclear Experimental Reactor, ITER, is one of the crucial issues for the optimization of the reactor. In the latest design^{2, 3, 6)} of ITER, a combination of type 316 stainless steel (SS316) with coolant water is chosen as the shield material for the reference design of the non-breeding shielding blanket option. The combination of SS316 and water is also the second candidate¹⁾ for the vacuum vessel of ITER for both the shielding blanket option and the breeding blanket option. The reasons why SS316 is frequently used in the designs are as follows; i) superior shielding performance in conjunction with water, ii) a large number of databases, iii) supported by the conventional fabrication technology, iv) relatively low helium production rate by neutron irradiation, and so on.

In order to experimentally investigate shielding properties of the SS316 shields without coolant water, the bulk shielding experiments on large SS316 assemblies^{7, 8)} have been already carried out at the intense D-T neutron source facility, Fusion Neutronics Source⁹⁾ (FNS), in the Japan Atomic Energy Research Institute (JAERI). The experiments were a part of the '94 Task of ITER/EDA, T-16, "Preparation of Neutronic Experiments and Measuring Technique." The experimental analyses¹⁰⁻¹²⁾ have also been performed as a part of the '93 Task of ITER/EDA, Shield/Blanket JA-3, "Bulk Shielding Experiments: Phase IA Pre- & Post-Analyses and Preparation of SS316 and SS316/Water Experiments."

The bulk shielding experiment on a large SS316/water assembly, which is also a part of '94 Task of ITER/EDA, T-16, is planned along with the SS316 experiments. The experimental assembly for the SS316/water shield has been determined by the pre-analyses¹³⁾ of the experiments as a part of '93 Task of ITER/EDA, Blanket/Shield JA-3. Since the SS316/water experimental assembly is designed taking full advantage of the previous SS316 assemblies, the SS316/water assembly has the similar appearance as the SS316 assemblies just replacing the shielding materials. It is intended to obtain the experimental data for both SS316 and SS316/water assemblies up to 914 mm in thickness of the shield, which almost corresponds to or a little thicker than the sum of thicknesses of inboard blanket/shield and vacuum vessel of ITER on the mid-plane. The SS316/water shield has a superior shielding property to the SS316 shield, that is, gamma-rays heating rate of SS316 attenuates by about 4.5 and 2.5 orders of magnitude for SS316/water and SS316 shields of 914 mm in thickness, respectively. Since penetrated neutrons and gamma-rays through the SS316/water shield are much fewer than those through the SS316 shield, it is required from a view point of experiment that room returned neutron and gamma-ray background should be negligibly low even at the deepest measuring position of 914 mm in the SS316/water assembly. Influence and reduction of the

room returned background have been intensively investigated in the pre-analyses¹³⁾. It is found according to the pre-analyses that the low background level of less than one tenth to the foreground at the 914 mm position can be attained when an additional shield made of polyethylene of 100 mm thickness is placed around a rear part of the SS316/water assembly.

The bulk shielding experiment on a large SS316/water assembly have been conducted as it is described in detail in the Volume I¹⁴⁾. Various quantities were measured with high accuracy up to 914 mm in depth in the experiments; (i) neutron spectrum in almost whole energy range from 14 MeV down to thermal energy, (ii) many dosimetry reaction rates, (iii) gamma-ray spectrum and (iv) gamma-ray heating rate. The room returned background was experimentally confirmed to be small enough to the foreground events. Since not only the energy-integrated quantities but also neutron and gamma-ray spectra are measured in wide energy ranges, these experimental data supply very useful informations to the shielding designs of ITER.

In order to provide databases for estimation of safety factors to the shielding design of ITER, the bulk shielding experiments on SS316/water assembly were analyzed as a part of the '93 Task of ITER/EDA, Shield/Blanket JA-3. Two transport calculation codes, the continuous energy Monte Carlo code MCNP-4¹⁵⁾ and the two dimensional discrete ordinates code DOT-3.5¹⁶⁾, and the Japanese Evaluated Nuclear Data Library, JENDL-3.1¹⁷⁾ were used for the present analysis as similar to the previous one¹⁴⁾. Besides the latest version of JENDL-3, JENDL-3.2^{18, 19)}, which has been released since the end of June, 1994, was used for the MCNP calculation.

This report describes the calculation methods, calculated results and comparison of the calculations with the measured results for the SS316/water experiments. Since most of methods of the present analyses for the SS316/water experiments are the same as those of the previous analyses for the SS316 experiments, explanations of the calculation methods are briefly given in Chapter 2. Detailed descriptions can be found in the previous report¹⁰⁾. The calculated results are presented and compared with the experiment in Chapter 3. The results are discussed in Chapter 4 including comparisons with the SS316 experiments. Chapter 5 summarizes this report.

2. Analysis

2.1 Calculation Conditions

Two transport codes were used for the experimental analyses. One is the three-dimensional Monte Carlo transport code MCNP-4¹⁵⁾ and the other is the two-dimensional discrete ordinates transport code DOT-3.5¹⁶⁾. Cross sections are treated in the continuous energy form in the MCNP-4 code while group-wise cross sections are used in the DOT-3.5 code. In order to calculate the first collision sources for DOT, the modified version of the GRTUNCL code¹⁶⁾, namely, FNSUNCL³²⁾, was used.

The calculation model is illustrated in Fig. 2.1. The appearance of the model is almost the same as that of the assembly #2 of the previous experiments¹⁰⁾. It consists of the test region simulating the SS316/water shield and the source reflector. The test region has a simple cylindrical shape, 1200 mm in diameter and 1372 mm in thickness, and seven water layers of 26.8 mm thickness. The volume ratio of the water layers to the SS316/water shield up to 914 mm is 20.5 %, which is nearly the optimum value^{2, 6)} for the shields of fusion devices. There are eight measuring positions; the front surface of the test region, and 127, 229, 330, 457, 610, 762 and 914 mm from the front surface of the test region. Atomic densities adopted to the analysis are listed in Table 2.1. An additional shield made of water and polyethylene was attached around the rear part of the real experimental assembly in order to reduce the room returned background. The additional shield was omitted in the present calculations since it was found that influences of the additional shield to all the measured parameters were negligibly small as described in the Volume I of this report.

The angle-dependent spectra of D-T source neutrons were precisely simulated in both DOT and MCNP calculations as described in the previous report¹⁰⁾. The measured quantities were normalized by the number of source neutrons. In the experiment, the number of source neutrons means the number of generated neutrons by the D-T reaction, not the number of emitted neutrons from the target. The number of emitted neutrons from the target is 1.03 times as many as the number of D-T reactions because of (n,2n) reactions with the structural materials of the target. All the calculated values are exactly normalized by the number of D-T reactions as it is done in the experiment.

2.2 MCNP Calculation

Two nuclear data files, JENDL-3.1¹⁷⁾ and JENDL-3.2^{18, 19)}, were adopted to the MCNP analyses. The processed cross section libraries for MCNP derived from the two files

were FSXLIB-J3^{20), 21)} and FSXLIB-J3R2²²⁾ for JENDL-3.1 and JENDL-3.2, respectively. The FSXDOSJ3²³⁾ library in continuous energy form based on JENDL Dosimetry File²⁴⁾ was used as a dosimetry reaction cross section library. As for a photon transport cross section library, the MCPLIB1¹⁵⁾ library was used. Cross section data used in the analyses are summarized in Table 2.2.

Figure 2.2 is the input data of MCNP used in the analysis. The methods and techniques adopted to the present analysis, such as the source subroutine, variance reduction techniques, tallies, and so on were almost the same as the previous ones¹⁰⁾. An engineering work station, HP9000/730 (Hewlett-Packard Co.), was used for the analysis. Number of histories and computation time were 3.0 millions and 106 hours for the calculation with JENDL-3.1, and 4.0 millions and 142 hours for the calculation with JENDL-3.2, respectively.

Owing to the appropriate variance reduction techniques and the enough computation time, good statistical accuracies were achieved for all the calculated results. Statistical errors of the calculated results with JENDL-3.2 were a little better than those with JENDL-3.1 because of the larger number of histories, but they did not differ so much. Statistical errors of the typical threshold reactions of $^{27}\text{Al}(\text{n},\alpha)^{24}\text{Na}$ and $^{115}\text{In}(\text{n},\text{n}')^{115\text{m}}\text{In}$ were less than 5.0 % and 1.8 % at all the measurement points, respectively. As for non-threshold reactions, statistical errors for both $^{10}\text{B}(\text{n},\alpha)^7\text{Li}$ and $^{235}\text{U}(\text{n},\text{fission})$ reactions ranged between 2 and 9 %.

Statistical errors of $^{197}\text{Au}(\text{n},\gamma)^{198}\text{Au}$ reaction rates were a little larger than the other reaction rates as they ranged between 5 and 17 % because of the existence of the giant resonance peak at 4.9 eV. If a neutron of 4.9 eV crossed one of the detector surfaces during the Monte Carlo calculation, considerably larger contribution, i.e., particle weight multiplied by the cross section at 4.9 eV, was scored comparing with the case of neutrons with any other energies. Thus the reaction rate was dominated by few numbers of neutrons which energies were close to 4.9 eV. Hence in order to minimize the statistical errors, the reaction rates were calculated by summing products of the neutron spectra and the group-wise reaction cross section in 125 energy groups. The statistical errors were reduced down to 4 - 11 %.

Statistical errors of the neutron spectra in most of the energy bins except those around 10 MeV were between 4 and 10 %. The errors larger than 10 % were occasionally seen in the energy bins around 10 MeV, but those larger than 20 % appeared in few cases. As for gamma-ray heating rates, the statistic error was small as they ranged between 2 and 5 %. The errors for gamma-ray spectra ranged around 10 - 15 % in each energy bin.

2.3 DOT Calculation

Calculation methods and databases for the DOT analysis were almost the same as

those for the previous analyses for SS316 experiments. Cross section data used in the DOT analysis are listed in Table 2.2. Two different energy group structures, 125-neutron + 40-gamma-ray groups and 42-neutron + 21-gamma-ray groups, were adopted to the calculations. The energy group structures are summarized in Table 2.3. In order to investigate the effect of self-shielding correction in group constants, two series of DOT calculations were done with and without considering the self-shielding correction. The FUSION-J3²⁵⁾ (125-n + 40- γ) and FUSION-40²⁵⁾ (42-n + 21- γ) libraries were used for calculations without the correction while the JSSTDL library^{26, 27)} was used for calculations with the correction. The original JSSTDL library in 295-neutron and 104-gamma-ray groups was collapsed to the smaller energy group number for the analyses. All the libraries for DOT were based on JENDL-3.1. Photon transport cross sections contained in the FUSION-J3 and FUSION-40 libraries were based on DLC-99²⁸⁾, and those in the JSSTDL library were on the DLC-137²⁹⁾ (PHOTX).

Input data of FNSUNCL and DOT calculations are shown in Figs. 2.3 - 2.10. The P5-S16 approximation was adopted through all the calculations. Mesh intervals toward the Z-direction in the water layers were 6.7 mm, and those in the SS316 regions were 6 - 20 mm. The mesh intervals used were fixed through all the calculations to keep the calculation condition constant. In the input data of FNSUNCL, normalization factor of 1.0 was assigned on the first 2** card. But the real normalization was made taking account of the angular dependent source intensity table given on the 14** card. All the calculations were normalized to one D-T reaction.

The vectorized super computer of the JAERI Computing and Information System Center, FACOM VP-2600, was used for all the FNSUNCL and DOT calculations. Since the DOT code used had been vectorized, the calculations were speeded up. Consumed computation time for calculations with 125-neutron and 40-gamma-ray groups was about 16 and 23 minutes for FNSUNCL and DOT, respectively. That for calculations with 42-neutron and 21-gamma-ray groups was about 2 and 9 minutes for FNSUNCL and DOT, respectively.

There are four different DOT calculations. In order to easily identify the four calculations from each other, they are abbreviated as follows through this report;

- DOT with FUSION-J3 (125-n + 40- γ) without self-shielding correction: DOT-F-125,
- DOT with FUSION-40 (42-n + 21- γ) without self-shielding correction: DOT-F-42,
- DOT with JSSTDL (125-n + 40- γ) with self-shielding correction: DOT-J-125,
- DOT with JSSTDL (42-n + 21- γ) with self-shielding correction: DOT-J-42.

2.4 Post Processing

In order to extract neutron and gamma-ray spectra, and to calculate reaction rates at the measurement positions with flux files by DOT, the reaction rate and spectrum editing code INTERF²⁷⁾ was used. The group-wise dosimetry reaction cross section libraries in 125 and 42 neutron groups, JDOS125²³⁾ and JDOS42²³⁾, respectively, were used to calculate the reaction rates for the DOT calculations. The JDOS125 and JDOS42 libraries were also derived from the JENDL Dosimetry File.

The photon interaction cross section library, DLC-99²⁸⁾, was converted to group-wise photon KERMA factor library³¹⁾ in 40 and 21 energy groups. The calculated gamma-ray spectra by DOT and MCNP were multiplied by the KERMA factors of SS316, and summed up over all the groups to yield gamma-ray heating rates of SS316.

The measured gamma-ray spectra were given with their energy resolution. In order to compare the measured and calculated spectra appropriately, the calculated gamma-ray spectra by both DOT and MCNP were broadened by the energy resolution of the experiments.

3. Comparison of the Calculation with the Experiment

3.1 Reaction Rate

Eight kinds of dosimetry reaction rates were measured. Cross sections of the reactions taken from the JENDL Dosimetry File are shown in Figs. 3.1 - 3.4. Calculated to experimental ratios (C/E ratios) of the reaction rates are obtained for all the calculations. Numerical values of the measured and calculated reaction rates and their C/E ratios are presented in Table 3.1. Figures 3.5 - 3.20 show all the C/E ratios. Curves of the experimental errors are indicated in the figures with the C/E values. Statistical errors of the MCNP calculation are attached to each symbol of the C/E ratio. The C/Es for four different DOT calculations are plotted in the figures indicated by odd figure number such as Figs. 3.5, 3.7, 3.9 and so on. In order to compare the DOT calculation with MCNP and to investigate differences of the two nuclear data files, JENDL-3.1 and JENDL-3.2, the MCNP calculations with both files and the DOT-J-125 calculations are plotted in the figures indicated by even figure number. This rule of the odd and even figure number is adopted to all the following figures.

3.2 Neutron Spectrum

Numerical data of the calculated neutron spectra are presented in Tables 3.2 - 3.7. The measured and calculated neutron spectra in energy regions of MeV, keV and eV are shown in Figs. 3.21 - 3.36, 3.37 - 3.52 and 3.53 - 3.64, respectively.

It should be noticed that assigned errors to the measured neutron spectra in the energy region of MeV in the tables and figures do not include all the errors. The additional errors are described in detail in the Ref. 14. At the front surface of the assemblies where 14 MeV neutron peak is prominent, measured spectra between 5 and 10 MeV might be assessed to be smaller as seen in Figs. 3.21 and 3.22 because of the difficulties in the experiment. In the positions deeper than 457 mm, larger spectra are given below 10 MeV as seen in Figs. 3.29 - 3.36 because of difficulty in the measurements.

Because the calculated spectra are not broadened with energy resolution of the measured spectra, 14 MeV peaks by the calculations are sharper than the measured ones. In the energy region of keV, energy bin widths of the calculated spectra in 125 energy groups seem to nearly correspond to the energy resolution of the measured one. But those in 40 energy groups are much broader than the measured spectra, and fine structures of the spectra are not expressed appropriately.

Fluxes of thermal energy are measured and calculated in one energy group. Energy

ranges of the thermal fluxes for the experiments, MCNP and DOT calculations with 125 energy groups are from 1.001×10^{-5} eV to 0.32241 eV, while those for DOT calculations with 42 energy groups are from 1.0×10^{-3} eV to 0.215 eV. The lethargy width of the two energy bins are different as they are 10.38 and 5.371, respectively. Quantitative comparisons are not valid when the spectra are represented in the unit of flux / lethargy. Hence the thermal fluxes for all the experiments and calculations are multiplied by the following factors. The factor for the experiments, MCNP and DOT calculations with 125 energy groups is

$$\frac{\ln(3.2241 \times 10^{-1}) - \ln(1.001 \times 10^{-5})}{\ln(3.2241 \times 10^{-1}) - \ln(1.0 \times 10^{-1})} = 8.867,$$

and that for DOT calculations with 42 energy groups is

$$\frac{\ln(2.15 \times 10^{-1}) - \ln(1.0 \times 10^{-3})}{\ln(3.2241 \times 10^{-1}) - \ln(1.0 \times 10^{-1})} = 4.588.$$

Now all the thermal fluxes are expressed in the same energy range between 0.1 and 0.32241 eV, and direct comparisons of the fluxes on the figure are possible.

Both measured and calculated neutron spectra are integrated within six energy ranges; above 10 MeV, 0.1 - 1 MeV, 10 - 100 keV, 10 - 100 eV, 1 - 10 eV and below 1 eV. The obtained integral fluxes by experiments and calculations are summarized in Table 3.8. The C/E ratios of the integral fluxes are presented in the table and Figs. 3.65 - 3.76. The mismatches of energy resolution between the experiments and the calculations can be avoided by the integration procedures. This procedure of integration makes it possible to compare the calculated spectra with the measured ones quantitatively.

3.3 Gamma-Ray Heating Rate

Numerical values of the measured and calculated gamma-ray heating rates of SS316 and their C/E ratios are summarized in Table 3.9. The C/E ratios are also shown in Figs. 3.77 and 3.78.

3.4 Gamma-Ray Spectrum

Numerical values of the calculated gamma-ray spectra broadened by the energy resolution of the measured spectra are tabulated in Tables 3.10 - 3.15. The measured and calculated spectra are presented in Figs. 3.79 - 3.86. It should be remarked that errors of the measured spectra include statistical ones only. There are additional errors of about 10 % in

the spectra.

3.5 Room Returned Background

As it is described in the experimental part of this report, Volume I¹⁴⁾, the room returned background might be superposed on the measured data at 914 mm position because the excellent shielding property of the SS316/water shield results in a low signal to noise ratio. The background is experimentally determined by the U-235 fission chamber. It is estimated that the background to the foreground for $^{235}\text{U}(\text{n},\text{fission})$ reaction is negligibly small and about 8 % at the 764 mm and the 914 mm position, respectively. The ratio of the background is as almost the same value as in the pre-analyses¹³⁾ for this experiment. Although the background is negligible for energy region higher than 10 MeV according to the pre-analyses, the room returned background less than 10 % might be included in the measured quantities related to low energy neutrons and gamma-rays at the 914 mm position. The experimental data are not corrected for the background.

4. Discussions

4.1 Energy Profile of the Dosimetry Reaction Rate

Eight dosimetry reaction rates are measured in the experiment. Cross sections of the reactions have been already presented in Figs. 3.1 - 3.4. Though these cross sections have their own shapes, the reaction rates are governed by not only the cross section but also the neutron spectrum at each measuring positions. Figures 4.1 - 4.8 illustrate energy profiles of the reaction rates to recognize in which neutron energy ranges the reactions dominantly occur. These figures are based on the MCNP calculation with JENDL-3.2 and JENDL Dosimetry File.

Since more than 99 % and 90 % of reactions for $^{93}\text{Nb}(\text{n},2\text{n})^{92m}\text{Nb}$ and $^{27}\text{Al}(\text{n},\alpha)^{24}\text{Na}$, respectively, are induced by neutrons above 10 MeV at any measuring positions as seen in Figs. 4.2 and 4.4, these reactions are excellent indices to examine transmission of 14 MeV neutrons.

As for $^{32}\text{S}(\text{n},\text{p})^{32}\text{P}$ and $^{238}\text{U}(\text{n,fission})$ reactions shown in Figs. 4.3 and 4.8, contribution of neutrons above 10 MeV is about a half while the reactions are also sensitive to energy ranges of 2 - 10 MeV and 1 - 10 MeV, respectively. Whereas the cross section of $^{238}\text{U}(\text{n,fission})$ is sensitive to neutrons below 1 MeV and has large resonance peaks around 1 keV as shown in Fig. 3.4, contribution of neutrons below 1 MeV is negligibly small.

As presented in Fig. 3.2, since $^{115}\text{In}(\text{n},\text{n}')^{115m}\text{In}$ reaction has large cross section for the energy range between 1 and 12 MeV, it is not so sensitive to 14 MeV neutrons. Hence the reaction provides precious information for neutron fluxes in the MeV energy range excluding contributions from prominent 14 MeV neutrons. It is seen from Fig. 4.5 that contributions of the energy range between 1 and 5 MeV are dominant.

Cross section of $^{197}\text{Au}(\text{n},\gamma)^{198}\text{Au}$ reaction has the giant resonance peak at 4.9 eV as well known. It is found in Fig. 4.6 that about 80 - 90 % of the reaction rates is caused by neutrons in the energy range between 1 and 10 eV in which the resonance peak presents.

Energy profiles of $^{10}\text{B}(\text{n},\alpha)^7\text{Li}$ and $^{235}\text{U}(\text{n,fission})$ reactions have a similar trend as seen in Figs. 4.1 and 4.7. Both reactions are mainly caused by neutrons below 1 keV. At all the measuring positions except 914 mm, contributions of thermal neutrons are large especially at the measuring positions near the front surface of the experimental assembly where the water layers and measuring positions are the closest. Since the position at 914 mm is far from the water layers, thermal neutrons hardly contribute to the reactions. The $^{235}\text{U}(\text{n,fission})$ reaction rates are measured in both the previous experiment for SS316 assemblies and the present experiment for SS316/Water assembly. It should be noted that sensitive energy

regions of the $^{235}\text{U}(\text{n},\text{fission})$ reaction for the SS316 and SS316/Water assemblies are much different each other.

4.2 Comparison among DOT Calculations

Influence of energy group number, that is, 125-n + 40- γ or 42-n + 21- γ , and that of the self-shielding correction are discussed in this section by comparing four different DOT calculations; DOT-J-125, DOT-F-125, DOT-J-42 and DOT-F-42.

Influence of energy group number is similar to that observed in the previous experiment for the SS316 assemblies. Most of discrepancies for the reaction rates and integral fluxes at all the measuring positions are less than 20 % between 42 and 125 group calculations. Differences of gamma-ray heating rates between the two energy group structures are less than 7 % at all the measuring positions.

Influence of the self-shielding correction is observed in the reaction rates having sensitivity to low energy neutrons, integral fluxes below 1 MeV and gamma-ray heating rates. In most cases, these quantities calculated with and without the correction are nearly the same at the front surface of assembly. Calculated neutron and gamma-ray fluxes without the correction become smaller than those with the correction when the penetration thickness increases. Because in the case that the self-shielding correction is neglected, absorption cross section used in the transport calculations is larger than the effective one and absorption of neutrons is enhanced. At the deepest position of 914 mm, most of the quantities related to neutrons below 1 MeV calculated without the correction are smaller by about 20 % than those with the correction.

In the previous experimental analysis¹⁰⁾ for the SS316 assemblies, the self-shielding correction strongly affect the calculated neutron fluxes, reaction rates and gamma-rays induced by neutrons. For example, fission rates of U-235 and gamma-ray heating rates at 914 mm position calculated without the correction are about 3 times smaller than those with the correction. In the present analysis, however, the correction is less effective comparing with the previous experiment on the SS316 shields. The reason is that deep valleys of a neutron spectrum made by resonance peaks were flattened due to hydrogen atoms and as a result the influence of the self-shielding became less effective.

4.3 Comparison between DOT and MCNP Calculation

The MCNP calculation with JENDL-3.1 and DOT-J-125 calculation are compared in this section. The DOT-J-125 calculation is selected for the comparisons because it is the

most precise among the four DOT calculations and based on JENDL-3.1 as same as the MCNP calculation.

Energy-integrated quantities, such as reaction rates, integral fluxes and gamma-ray heating rates, by both calculations are in good agreement within 10 % except for two specific cases. This fact suggests that transport calculations with the SN approximation and multi-group constants to this kind of bulk shields have adequate accuracies comparable to continuous energy Monte Carlo calculation if calculation conditions are carefully selected.

One of the two specific cases is that reaction rates of $^{10}\text{B}(\text{n},\alpha)^7\text{Li}$, $^{197}\text{Au}(\text{n},\gamma)^{198}\text{Au}$ and $^{235}\text{U}(\text{n,fission})$ at the front surface by DOT-J-125 are larger by 50 %, 20 % and 50 %, respectively, than those by MCNP. Another case is that integral fluxes below 1 eV by DOT-J-125 are about 20 % smaller than those by MCNP as seen in Fig. 3.76. These two cases can be attributed to inadequate treatment of neutrons in thermal energy. This matter of concern will be discussed in detail in the section 4.6.

4.4 Comparison of JENDL-3.1 and JENDL-3.2

Two nuclear data libraries can be compared in the two MCNP calculations. It is seen from the figures concerning with neutrons that calculated results with both libraries are nearly identical as they agree within 10 %. Gamma-ray heating rates with JENDL-3.1 are larger by about 20 % than those with JENDL-3.2 at most of measuring positions. This fact can be attributed to the modification¹⁸⁾ of energy balance of secondary gamma-ray data for neutron capture reaction for many nuclides. The energy balance in JENDL-3.1 does not always satisfy the law of conservation of energy. The balance in JENDL-3.2 is modified so as to meet the law.

4.5 Comparison of the MCNP Calculation with the Experiment

The calculated results are compared with the experiments in this section. Because comparisons among the calculations have been discussed and differences of them have been clarified in the former sections, discussions in this section are focused on comparisons between the MCNP calculation with JENDL-3.2 and the experiment. Validity of JENDL-3.2 for shielding calculations will be assessed through the comparisons.

As seen in C/E ratios of $^{93}\text{Nb}(\text{n},2\text{n})^{92m}\text{Nb}$ reaction in Fig. 3.12, those of $^{115}\text{In}(\text{n},\text{n}')^{115m}\text{In}$ reaction in Fig. 3.14 and those of integral flux above 10 MeV in Fig. 3.66, the calculations are in good agreement with the experiment within 10 %. Both transmission of 14 MeV neutrons and scattered neutrons in MeV energy region are predicted with high accuracy up to

914 mm position.

The calculated integral fluxes agree well within 5 % with the experiment in the energy range of 0.1 - 1 MeV at positions up to 610 mm, while those at 762 and 914 mm positions are smaller by 20 % than the experiment as seen in Fig. 3.68. As for the energy range of 10 - 100 keV, the calculations are about 15 % smaller than the experiment at all the positions as seen in Fig. 3.70. The calculated neutron spectra in the keV energy region shown in Figs. 3.38 - 3.52 appropriately reproduce the experiment.

In the energy region of eV, agreement between the calculated spectra and the measured ones is good as seen in Figs. 3.54 - 3.64. For the C/E ratios of the integral fluxes in energy regions of 10 - 100 eV and 1 - 10 eV as presented in Figs. 3.72 and 3.74, calculations agree with the experiment within the experimental error ranges of about 20 and 10 %, respectively. As for integral fluxes below 1 eV which represent thermal fluxes, calculated fluxes are slightly larger than the measured ones although statistical errors of MCNP calculation are somewhat large. Three dosimetry reactions of $^{10}\text{B}(\text{n},\alpha)^7\text{Li}$, $^{197}\text{Au}(\text{n},\gamma)^{198}\text{Au}$ and $^{235}\text{U}(\text{n,fission})$ have also large sensitivity to the eV energy region. The C/E values for both $^{10}\text{B}(\text{n},\alpha)^7\text{Li}$ and $^{235}\text{U}(\text{n,fission})$ reactions are about 0.9 at all the positions except the front surface where C/E's are 1.2. The C/E's for $^{197}\text{Au}(\text{n},\gamma)^{198}\text{Au}$ reaction range between 0.95 and 1.15. Thus the agreement of these three reactions between the calculations and the experiments is fairly good.

As for the gamma-ray heating rates shown in Fig. 3.78, although the C/E values are slightly larger than unity up to 457 mm depth, the calculation agrees with the experiment within 30 %. The shapes of calculated gamma-ray spectra presented in Figs. 3.80, 3.82, 3.84 and 3.86 are in good agreement with the measured ones.

Although discrepancies of about 20 - 30 % are found between the calculation and the experiment, it can be concluded as a whole that the MCNP calculation with JENDL-3.2 can predict the neutron fluxes in the energy range from 14 MeV to thermal energy as well as gamma-ray fluxes with high accuracy, typically within 20 %.

4.6 Treatment of Thermal Neutron

As pointed out in the section 4.3, there are two large discrepancies between the DOT-J-125 and the MCNP calculations; (i) reaction rates of $^{10}\text{B}(\text{n},\alpha)^7\text{Li}$, $^{197}\text{Au}(\text{n},\gamma)^{198}\text{Au}$ and $^{235}\text{U}(\text{n,fission})$ by DOT-J-125 are considerably larger than those by MCNP at the front surface and (ii) integral fluxes below 1 eV by DOT-J-125 are smaller than those by MCNP. The reason can be explained as follows.

In the present DOT calculations, and probably in most of all transport calculations for

nuclear designs of fusion reactor with multi-group cross section constants, thermal neutrons are represented in one energy group. The Maxwell distribution at the room temperature is usually assumed as a weighting function to derive group cross sections of thermal energy. This weighting function is valid when a medium is a low absorbing material and neutrons are well thermalized. In the present experiment, however, the water layer of 26.8 mm is not so thick and the measuring positions are not in the water layers but in the SS316 layers. Since nuclides contained in the SS316 such as Cr, Fe, Ni and Mo have larger neutron capture cross sections of the $1/v$ shape around the thermal energy, the SS316 layer is more liable to absorb thermal neutrons of lower energy comparing with higher energy. The spectrum of thermal neutrons at the measuring positions in the SS316 layers are harder than that of the Maxwell distribution at the room temperature. If a cross section has the $1/v$ shape around the thermal energy, such as cross sections of $^{10}\text{B}(\text{n},\alpha)^7\text{Li}$, $^{197}\text{Au}(\text{n},\gamma)^{198}\text{Au}$, $^{235}\text{U}(\text{n,fission})$ or usual (n,γ) reactions, their effective cross sections for thermal neutrons weighted by the harder spectrum are smaller than those calculated with assumption of the usual Maxwell distribution at the room temperature. In fact, the cross section of $^{10}\text{B}(\text{n},\alpha)^7\text{Li}$ for usual thermal neutrons is 3837 b while the effective cross section at the measuring positions is much smaller, i.e., about 2300 b, according to the MCNP calculation. This discrepancy between the effective cross sections and the weighted ones by the Maxwell distribution for thermal neutrons is the reason of the former discrepancy indicated at the beginning of this section. Since the (n,γ) cross sections for thermal neutrons adopted in the DOT calculations are larger than the effective ones, the calculated thermal flux becomes smaller. This is the reason of the latter discrepancy mentioned earlier.

Thus it should be noted that when one treats thermal neutrons in one energy group, the calculated fluxes, reaction rates and so on involve large ambiguity. This effect appears when two materials of high and low absorption cross sections are close by each other.

5. Concluding Remarks

The bulk shielding experiment for the SS316/water assembly was analyzed with the MCNP and DOT codes, and the calculated results were compared with the experiment. The following facts were found through the comparisons.

- (i) Most of experimental results were predicted within 20 % accuracy by the MCNP calculation with JENDL-3.2.
- (ii) The JENDL-3.1 and JENDL-3.2 libraries give almost identical results for neutron, but JENDL-3.2 is superior for calculation of gamma-ray heating rates.
- (iii) The DOT calculation with 125-neutron and 40-gamma-ray energy groups and the self-shielding correction has almost the same accuracy as MCNP.
- (iv) Effects of energy group number and the self-shielding correction on multi-group calculations are not so large, though the self-shielding correction are highly important in the previous analysis for the SS316 experiments.
- (v) Treatment of thermal neutrons in one energy group may cause large ambiguity for multi-group calculations.

The MCNP calculation with JENDL-3.2, which is regarded as the most precise calculation in the present analysis, agreed with the most of experimental results. The DOT-J-125 calculation has comparable accuracy as the MCNP calculation. These fact implies that if the geometry is precisely modeled and calculation parameters such as energy group number, consideration of the self-shielding correction, spacial mesh intervals, source conditions, and so on, are carefully examined and selected, experimental results can be predicted by both MCNP and DOT with a high accuracy of about 20 %.

Variety of quantities for both neutrons and gamma-rays, not only energy-integrated values but also energy spectra, are measured. The measured neutron spectra cover nearly whole energy ranges from 14 MeV down to thermal energy. Hence it should be emphasized that validity of prediction accuracy of any design parameters has been demonstrated through the present experimental and analytical studies. In other words, there are several shielding design parameters for ITER; gamma-ray heating rate, insulator dose of super-conducting magnet (SCM), displacement damage of copper in SCM, fast neutron flux and helium production rate. Only the gamma-ray heating rate among the five design parameters mentioned is actually measured and it is compared with the calculations. The rest of four design parameters, however, can be indirectly examined through the present study. Any design parameters can be calculated by integrating products of the neutron or gamma-ray fluxes and the energy-dependent response functions of each parameter. According to the present studies, prediction

accuracy for both neutron and gamma-ray fluxes in nearly all the energy ranges has been proved to be considerably high. Hence if the response functions are given appropriately, it can be concluded that prediction accuracies of any design parameters by the transport calculation are high as they are better than about 20 %.

Acknowledgment

The authors are grateful to Drs. S. Matsuda, Y. Seki, H. Takatsu and S. Sato of Naka Fusion Research Establishment of JAERI, and Dr. T. Mori of Department of Reactor Engineering for their useful suggestions and discussions to the present work. They wish to express their thanks to Drs. K. Maki of Hitachi, Ltd. and K. Hayashi of Hitachi Engineering Co., Ltd. for their valuable collaboration to this work. They also thank Mr. A. Iwai for his assistance with many calculations.

accuracy for both neutron and gamma-ray fluxes in nearly all the energy ranges has been proved to be considerably high. Hence if the response functions are given appropriately, it can be concluded that prediction accuracies of any design parameters by the transport calculation are high as they are better than about 20 %.

Acknowledgment

The authors are grateful to Drs. S. Matsuda, Y. Seki, H. Takatsu and S. Sato of Naka Fusion Research Establishment of JAERI, and Dr. T. Mori of Department of Reactor Engineering for their useful suggestions and discussions to the present work. They wish to express their thanks to Drs. K. Maki of Hitachi, Ltd. and K. Hayashi of Hitachi Engineering Co., Ltd. for their valuable collaboration to this work. They also thank Mr. A. Iwai for his assistance with many calculations.

References

- 1) Ioki K., Johnson G., Shimizu K. and Williamson D.: "Design of ITER Vacuum Vessel," Proc. 3rd Symposium on Fusion Nuclear Technology, Los Angeles, California, USA, June 27 - July 1, 1994, to be published in Fusion Eng. Des.
- 2) Gohar Y., Parker R. and Rebut P. -H.: "ITER Blanket Designs," ibid.
- 3) Santoro R. T., et al.: "ITER Shielding Analysis," ibid.
- 4) Green L., et al.: Proc. 11th Topical Meeting on Technology of Fusion Energy, New Orleans, Louisiana, USA, June 19 - 23, 1994; Fusion Technol., 26 pp. 300 - 315 (1994).
- 5) Maki K., et al.: "Japanese Contributions to ITER Shielding Neutronics Design," JAERI-M 91-46 (1991).
- 6) Maki K., et al.: "Shielding Design of Reactor Core Region in Fusion experimental Reactor," JAERI-M 91-17 (1991, in Japanese).
- 7) Konno C., et al.,: "Bulk Shielding Experiments on Large SS316 Assemblies Bombarded by D-T Neutrons, Volume I: Experiment." JAERI-Research 94-43 (1994).
- 8) Konno C., et al.: Fusion Technol., 21 pp. 2169 - 2173 (1992).
- 9) Nakamura T., Maekawa H., Ikeda Y. and Oyama Y., "A D-T Neutron Source for Fusion Neutronics Experiments at JAERI," Proc. Int'l Ion Engineering Congress-ISIAT '83 & IPAT '83, 567, Kyoto (1983).
- 10) Maekawa F., et al.,: "Bulk Shielding Experiments on Large SS316 Assemblies Bombarded by D-T Neutrons, Volume II: Analysis." JAERI-Research 94-44 (1994).
- 11) Maekawa F., et al.: Fusion Technol., 21 pp. 2107 - 2111 (1992).
- 12) Maekawa F., et al.: "Importance of Self-Shielding Effect on Shielding Design of Fusion Devices," Proc. 17th Symposium on Fusion Technology, Rome, Italy, pp. 1419 - 1423 (1992).
- 13) Konno C., et al.: "Pre-Analyses of SS316 and SS316/Water Bulk Shielding Experiments," JAERI-Tech 94-19 (1994).
- 14) Konno C., et al.,: "Bulk Shielding Experiment on a Large SS316/Water Assembly Bombarded by D-T Neutrons, Volume I: Experiment," JAERI-Research 95-17 (1995).
- 15) Briesmeister J. F. (Ed.): "MCNP - A General Monte Carlo Code for Neutron and Photon Transport, Version 4," RSIC/CCC-200, Radiation Shielding Information Center (1991).
- 16) Rhoades W. A. and Mynatt F. R.: "The DOT III Two-Dimensional Discrete Ordinates Transport Code," ORNL/TM-4280 (1973).
- 17) Shibata K., et al.: "Japanese Evaluated Nuclear Data Library, Version-3 -- JENDL-3 --," JAERI 1319 (1990).

- 18) Nakagawa T.: "JENDL-3 Revision 2," Proc. of the 1993 Symposium on Nucl. Data, JAERI-M 94-19, pp. 68 - 78 (1994).
- 19) Kikuchi Y.: "JENDL-3 Revision-2 - JENDL-3.2 -," Proc. International Conference on Nuclear Data for Science and Technology, Gatlinburg, Tennessee, May 9 - 13, pp. 685-691 (1994).
- 20) Kosako K., et al.: "FSXLIB-J3: MCNP Continuous Energy Cross Section Library Based on JENDL-3," JAERI-M 91-187 (1991, in Japanese).
- 21) Kosako K., Oyama Y. and Maekawa H.: "FSXLIB-J3 MCNP Continuous Cross Section Library Based on JENDL-3." Proc. New Horizons in Radiation Protection and Shielding, Pasco, Washington, April 26 - May 1, 1992, pp. 357 - 363, (1992).
- 22) Kosako K., et al.: "FSXLIB-J3R2: A Continuous Energy Cross Section Library for MCNP Based on JENDL-3.2," JAERI-Data/Code 94-20 (1994).
- 23) Kosako K., et al.: To be published.
- 24) Nakazawa M., et al.: "JENDL Dosimetry File," JAERI 1325 (1992).
- 25) Maki K., et al.: "Nuclear Group Constant Set FUSION-J3 for Fusion Reactor Nuclear Calculations based on JENDL-3," JAERI-M 91-72 (1991, in Japanese).
- 26) Hasegawa A.: "Development of a Common Nuclear Group Constants Library System: JSSTDL-295n-104γ Based on JENDL-3 Nuclear Data Library," Proc. Int'l Conf. on Nuclear Data, Jülich, Germany, pp. 232 - 234 (1991).
- 27) Hasegawa A.: "JSSTDL-295n-104γ; a Common Nuclear Group Cross-Section Library Based on JENDL-3 Nuclear Data File," Proc. 2nd Specialists' Meeting on Nuclear Data for Fusion Reactor, JAERI-M 91-62 pp. 15 - 25 (1991).
- 28) Roussin, et al.: "Description of the DLC-99/HUGO Package of Photon Interaction Data in ENDF/B-V Format," ORNL/RSIC-46, ENDF-335 (1986).
- 29) Turbey D. K., Berger M. J. and Hubbell J. H.: "DLC-136/PHOTX: Photon Interaction Cross Section Library," RSIC/DLC-136, Radiation Shielding Information Center (1989).
- 30) Kosako K.: "INTERF: The Reaction rates and Spectra Editing Code for Analysis of Fusion Neutronics Experiments," JAERI-M 90-199 (1990, in Japanese).
- 31) Maki. K., et al.: "Nuclear Heating Constant KERMA Library - Nuclear Heating Library for Fusion Nuclear Group Constant Set FUSION-J3 -", JAERI-M 91-73 (1991, in Japanese).
- 32) Oyama Y., et al.: "Phase III Experiments of the JAERI/USDOE Collaborative Program on Fusion Blanket Neutronics - Line Source and Annular Blanket Experiments - Volume I: Experiment," JAERI-M 94-15 (1994).

Table 2.1 Atomic densities adopted to the analysis.

Nuclide	SS316 in the test region	SS316 in the source reflector	Air	Water
H-1	-	-	-	6.6659×10^{22}
N-14	-	-	3.8810×10^{19}	-
O-16	-	-	1.0400×10^{19}	3.3329×10^{22}
Si	1.0341×10^{21}	8.1608×10^{20}	-	-
Cr	1.5482×10^{22}	1.5025×10^{22}	-	-
Mn-55	1.0355×10^{21}	1.3561×10^{21}	-	-
Fe	5.7904×10^{22}	5.8331×10^{22}	-	-
Ni	9.3405×10^{21}	9.1456×10^{21}	-	-
Mo	1.0585×10^{21}	1.0254×10^{21}	-	-

unit: [atoms / cm³]

Table 2.2 Cross section libraries used in the analysis. Libraries outside the parentheses are used for the transport calculations, and those inside the parentheses are the original cross section data bases.

	MCNP	DOT without self-shielding correction	DOT with self-shielding correction
Neutron transport	FSXLIB-J3 & FSXLIB-J3R2 (JENDL-3.1, -3.2)	FUSION-J3 FUSION-40 (JENDL-3.1)	JSSTDL (JENDL-3.1)
Photon transport	MCPLIB1 (DLC-7E & STORM-ISRAEL)	FUSION-J3 FUSION-40 (DLC-99)	JSSTDL (DLC-137, PHOTX)
Dosimetry reaction	FSXDOSJ3 (JENDL Dosimetry File)	JDOS125 (JENDL Dosimetry File)	JDOS42 (JENDL Dosimetry File)
Photon kerma factor	FUSION-J3 (DLC-99)	FUSION-J3 FUSION-40 (DLC-99)	FUSION-J3 FUSION-40 (DLC-99)

Table 2.3 Energy group structures of neutron 125-groups, gamma-ray 40-groups, neutron 42-groups and gamma-ray 21 groups used in the DOT analyses. The unit of energy is eV.

Neutron 125G					Gamma-Ray 40G					Neutron 42G					Gamma-Ray 21G				
Group	Upper-Energy	Group	Upper-Energy	Group	Upper-Energy	Group	Upper-Energy	Group	Upper-Energy	Group	Upper-Energy	Group	Upper-Energy	Group	Upper-Energy	Group	Upper-Energy	Group	Upper-Energy
1	1.6487e+07	43	5.3525e+06	85	8.6515e+04	1	1.4000e+07	1	1.5000e+07	1	1.40e+07	1	1.20e+07	2	1.3720e+07	2	1.20e+07	2	
2	1.6231e+07	44	5.3525e+06	86	7.6349e+04	2	1.2000e+07	2	1.2540e+07	3	1.00e+07	3	1.00e+07	3	1.2540e+07	3	1.00e+07	3	
3	1.5980e+07	45	4.7236e+06	87	6.7378e+04	3	1.0000e+07	4	1.1478e+07	4	8.00e+06	4	8.00e+06	4	1.1478e+07	4	8.00e+06	4	
4	1.5732e+07	46	4.4374e+06	88	5.9461e+04	4	9.0000e+06	5	1.0500e+07	5	7.50e+06	5	7.50e+06	5	1.0500e+07	5	7.50e+06	5	
5	1.5488e+07	47	4.1686e+06	89	5.2474e+04	5	8.0000e+06	6	9.3104e+06	6	7.00e+06	6	7.00e+06	6	9.3104e+06	6	7.00e+06	6	
6	1.5248e+07	48	3.9160e+06	90	4.6304e+04	6	7.0000e+06	7	8.2610e+06	7	6.50e+06	7	6.50e+06	7	8.2610e+06	7	6.50e+06	7	
7	1.5012e+07	49	3.6787e+06	91	4.0857e+04	7	7.0000e+06	7	7.3280e+06	8	6.00e+06	8	6.00e+06	8	7.3280e+06	8	6.00e+06	8	
8	1.4779e+07	50	3.4559e+06	92	3.6067e+04	8	6.5000e+06	9	6.5000e+06	9	5.50e+06	9	5.50e+06	9	6.5000e+06	9	5.50e+06	9	
9	1.4550e+07	51	3.2465e+06	93	3.1827e+04	9	10	5.5000e+06	10	5.7570e+06	10	5.00e+06	10	5.00e+06	10	5.7570e+06	10	5.00e+06	10
10	1.4324e+07	52	3.0488e+06	94	2.8087e+04	11	5.0000e+06	11	5.0990e+06	11	4.50e+06	11	4.50e+06	11	5.0990e+06	11	4.50e+06	11	
11	1.4102e+07	53	2.8650e+06	95	2.4787e+04	12	4.5000e+06	12	4.5160e+06	12	4.00e+06	12	4.00e+06	12	4.5160e+06	12	4.00e+06	12	
12	1.3883e+07	54	2.6914e+06	96	2.1874e+04	13	4.0000e+06	13	4.0000e+06	13	3.50e+06	13	3.50e+06	13	4.0000e+06	13	3.50e+06	13	
13	1.3668e+07	55	2.5284e+06	97	1.9304e+04	14	3.5000e+06	14	3.1620e+06	14	3.00e+06	14	3.00e+06	14	3.1620e+06	14	3.00e+06	14	
14	1.3456e+07	56	2.3752e+06	98	1.5034e+04	15	3.0000e+06	15	2.5000e+06	15	2.50e+06	15	2.50e+06	15	2.5000e+06	15	2.50e+06	15	
15	1.3248e+07	57	2.2313e+06	99	1.1709e+04	16	2.5000e+06	16	1.8710e+06	16	2.00e+06	16	2.00e+06	16	1.8710e+06	16	2.00e+06	16	
16	1.3042e+07	58	2.0961e+06	100	9.1118e+03	17	2.2500e+06	17	1.4000e+06	17	1.50e+06	17	1.50e+06	17	1.4000e+06	17	1.50e+06	17	
17	1.2840e+07	59	1.9691e+06	101	7.1016e+03	18	2.0000e+06	18	1.0000e+06	18	1.00e+06	18	1.00e+06	18	1.0000e+06	18	1.00e+06	18	
18	1.2641e+07	60	1.8498e+06	102	5.5307e+03	19	1.7500e+06	19	8.0000e+05	19	8.00e+05	19	8.00e+05	19	8.0000e+05	19	8.00e+05	19	
19	1.2445e+07	61	1.7377e+06	103	4.3073e+03	19	1.5000e+06	20	1.5000e+06	20	5.6600e+05	20	2.00e+05	20	5.6600e+05	20	2.00e+05	20	
20	1.2252e+07	62	1.5335e+06	104	3.3546e+03	21	1.375e+06	21	1.375e+06	21	4.0000e+05	21	1.00e+05	21	4.0000e+05	21	1.00e+05	21	
21	1.2062e+07	63	1.3533e+06	105	2.6125e+03	22	2.1250e+06	22	2.1250e+06	22	2.8300e+05	22	2.00e+05	22	2.8300e+05	22	2.00e+05	22	
22	1.1873e+07	64	1.1943e+06	106	2.0346e+03	23	1.1250e+06	23	1.1250e+06	23	2.00e+05	23	2.00e+05	23	2.00e+05	23	2.00e+05	23	
23	1.1691e+07	65	1.0546e+06	107	1.5846e+03	24	1.0000e+06	24	1.0000e+06	24	1.4100e+05	24	1.4100e+05	24	1.4100e+05	24	1.4100e+05	24	
24	1.1510e+07	66	9.3013e+05	108	1.2341e+03	25	9.0000e+05	25	9.0000e+05	25	1.0000e+05	25	1.0000e+05	25	1.0000e+05	25	1.0000e+05	25	
25	1.1331e+07	67	8.2084e+05	109	9.6110e+02	25	26	8.0000e+05	26	8.0000e+05	26	4.6500e+04	26	4.6500e+04	26	4.6500e+04	26	4.6500e+04	26
26	1.1156e+07	68	7.2438e+05	110	5.8293e+02	27	7.0000e+05	27	7.0000e+05	27	2.1500e+04	27	2.1500e+04	27	2.1500e+04	27	2.1500e+04	27	
27	1.0983e+07	69	6.3927e+05	111	3.5927e+02	28	6.0000e+05	28	6.0000e+05	28	1.0000e+04	28	1.0000e+04	28	1.0000e+04	28	1.0000e+04	28	
28	1.0812e+07	70	5.6415e+05	112	2.1445e+02	29	5.2000e+05	29	5.2000e+05	29	4.6500e+03	29	4.6500e+03	29	4.6500e+03	29	4.6500e+03	29	
29	1.0645e+07	71	4.9786e+05	113	1.3007e+02	29	4.0000e+05	30	5.0000e+05	30	2.1500e+03	30	2.1500e+03	30	2.1500e+03	30	2.1500e+03	30	
30	1.0480e+07	72	4.3936e+05	114	7.8891e+01	30	3.5000e+05	31	4.0000e+05	31	3.0000e+03	31	3.0000e+03	31	3.0000e+03	31	3.0000e+03	31	
31	1.0317e+07	73	3.8774e+05	115	4.7850e+01	31	3.0000e+05	32	3.0000e+05	32	4.6500e+02	32	4.6500e+02	32	4.6500e+02	32	4.6500e+02	32	
32	1.0157e+07	74	3.4217e+05	116	3.9023e+01	32	2.5000e+05	33	2.5000e+05	33	2.1500e+02	33	2.1500e+02	33	2.1500e+02	33	2.1500e+02	33	
33	9.9999e-06	75	3.0197e+05	117	1.7603e+01	33	2.0000e+05	34	1.5000e+05	34	1.0000e+02	34	1.0000e+02	34	1.0000e+02	34	1.0000e+02	34	
34	9.3940e-06	76	2.6849e+05	118	1.0677e+01	34	1.5000e+05	35	1.0000e+05	35	4.6500e+01	35	4.6500e+01	35	4.6500e+01	35	4.6500e+01	35	
35	8.8249e-06	77	2.3517e+05	119	6.4758e+00	35	3.0000e+04	36	8.0000e+04	36	2.1500e+01	36	2.1500e+01	36	2.1500e+01	36	2.1500e+01	36	
36	8.2902e-06	78	2.0554e+05	120	3.9278e+00	36	3.0000e+04	37	6.0000e+04	37	1.0000e+01	37	1.0000e+01	37	1.0000e+01	37	1.0000e+01	37	
37	7.7879e-06	79	1.8315e+05	121	2.3823e+00	37	3.0000e+04	38	4.5000e+04	38	4.6500e+00	38	4.6500e+00	38	4.6500e+00	38	4.6500e+00	38	
38	7.3161e-06	80	1.6163e+05	122	1.4449e+00	38	3.0000e+04	39	3.0000e+04	39	2.1500e+00	39	2.1500e+00	39	2.1500e+00	39	2.1500e+00	39	
39	6.8728e-06	81	1.4266e+05	123	8.7640e-01	39	3.0000e+04	40	2.0000e+04	40	1.0000e+00	40	1.0000e+00	40	1.0000e+00	40	1.0000e+00	40	
40	6.4564e-06	82	1.2588e+05	124	5.3156e-01	40	2.0000e+04	41	1.0000e+04	41	4.6500e-01	41	4.6500e-01	41	4.6500e-01	41	4.6500e-01	41	
41	6.0652e-06	83	1.1109e+05	125	3.2241e-01	41	1.0000e+04	42	1.0000e-01	42	2.1500e-01	42	2.1500e-01	42	2.1500e-01	42	2.1500e-01	42	
42	5.6978e-06	84	9.8035e+04	125	1.0010e-05	42	1.0000e-03	43	1.0000e-03	43	1.0000e-03	43	1.0000e-03	43	1.0000e-03	43	1.0000e-03	43	

Table 3.1 Measured and calculated reaction rates and their C/E ratios.

Position [mm]	Expt. Error [s]	Calculated Reaction Rate						Calculated Reaction Rate						Calculated Reaction Rate					
		MCNP-J31	Error	MCNP-J32	Error	MCNP-J125	Error	DOT-F-42	DOT-F-42	MCNP-J31	Error	MCNP-J32	Error	MCNP-J125	Error	DOT-F-125	DOT-F-125	DOT-F-42	DOT-F-42
$^{10}_B(n,\alpha)^{7}_Li$	4.35	3.528e-26	7.37	3.5639e-26	6.77	5.050e-26	4.987e-26	4.947e-26	4.960e-26	1.179	8.69	1.191	8.06	1.688	1.667	1.653	1.658		
-7.0	2.992e-26	4.35	1.308e-26	7.21	1.4866e-26	9.57	1.466e-26	1.370e-26	1.434e-26	1.342e-26	0.815	5.88	0.927	8.87	0.914	0.854	0.894	0.836	
127.0	1.604e-26	4.28	5.966e-27	6.67	5.6943e-27	4.95	5.225e-27	5.4225e-27	5.754e-27	5.238e-27	0.905	6.03	0.863	4.27	0.898	0.822	0.872	0.794	
228.6	6.596e-27	4.08	2.290e-27	6.96	2.0734e-27	4.92	2.084e-27	1.870e-27	2.009e-27	1.779e-27	0.949	6.60	0.859	4.23	0.863	0.775	0.832	0.737	
330.2	2.414e-27	3.98	1.887e-28	5.64	2.1768e-28	5.74	2.303e-28	1.998e-28	2.181e-28	1.851e-28	0.759	4.28	0.876	5.03	0.927	0.804	0.878	0.745	
457.2	2.485e-28	3.86	4.373e-29	4.28	4.2403e-29	4.34	4.529e-29	3.811e-29	4.265e-29	3.484e-29	0.913	3.91	0.885	3.84	0.945	0.795	0.890	0.727	
609.6	4.791e-29	3.76	6.713e-30	3.91	7.1486e-30	3.28	7.691e-30	6.148e-30	7.118e-30	5.481e-30	0.805	3.15	0.857	2.81	0.942	0.737	0.853	0.657	
762.0	8.342e-30	3.69	7.567e-31	4.03	8.3722e-31	3.15	8.793e-31	5.884e-31	8.312e-31	5.509e-31	0.813	3.28	0.854	2.69	0.897	0.600	0.848	0.562	
$^{27}Al(n,\alpha)^{24}Na$	3.02	1.077e-29	0.92	1.0884e-29	0.81	1.087e-29	1.087e-29	1.150e-29	1.150e-29	1.150e-29	0.981	0.90	0.991	0.80	0.990	0.990	1.048	1.047	
-1.0	1.098e-29	3.02	1.794e-30	1.41	1.7857e-30	1.19	1.829e-30	1.828e-30	1.868e-30	1.866e-30	0.952	1.34	0.947	1.13	0.970	0.970	0.991	0.990	
127.0	1.885e-30	3.21	3.728e-31	1.85	3.9988e-31	1.55	3.954e-31	3.950e-31	3.964e-31	3.964e-31	0.890	1.65	0.955	1.48	0.944	0.943	0.948	0.946	
228.6	4.189e-31	3.54	8.559e-32	2.56	8.7799e-32	2.15	8.905e-32	8.891e-32	8.860e-32	8.786e-32	0.877	2.25	0.921	1.98	0.934	0.933	0.924	0.922	
330.2	9.532e-32	3.59	1.253e-32	3.38	1.2967e-32	2.80	1.356e-32	1.353e-32	1.319e-32	1.315e-32	0.965	3.94	0.974	3.40	1.024	1.020	0.978	0.974	
457.2	1.355e-33	3.25	1.308e-33	4.08	1.3194e-33	3.49	1.387e-33	1.383e-33	1.325e-33	1.319e-33	0.977	4.36	1.056	3.81	1.059	1.055	0.945	0.990	
609.6	1.363e-34	4.20	1.333e-34	4.46	1.4404e-34	3.61	1.444e-34	1.438e-34	1.3549e-34	1.349e-34	0.977	5.24	1.152	4.86	1.173	1.167	1.094	1.087	
762.0	1.062e-35	8.02	1.111e-35	5.01	1.2231e-35	4.22	1.246e-35	1.239e-35	1.162e-35	1.154e-35	1.047	5.24	1.152	4.86	1.173	1.167	1.094	1.087	
$^{32}S(n,p)^{32}P$	2.458e-29	0.47	2.4910e-29	0.83	2.545e-29	2.543e-29	2.667e-29	2.6663e-29	2.6663e-29	2.6663e-29	0.914	0.43	0.926	0.77	0.946	0.945	0.991	0.990	
-1.0	2.690e-29	3.80	5.884e-30	0.50	5.9022e-30	0.82	6.059e-30	6.055e-30	6.349e-30	6.341e-30	0.940	0.47	0.943	0.77	0.968	0.967	1.014	1.013	
127.0	6.260e-30	3.80	1.406e-30	0.59	1.4681e-30	0.98	1.447e-30	1.4644e-30	1.512e-30	1.508e-30	0.919	0.55	0.960	0.94	0.959	0.957	0.988	0.986	
228.6	1.530e-30	3.80	3.379e-31	0.77	3.4575e-31	1.25	3.534e-31	3.526e-31	3.598e-31	3.585e-31	0.923	0.71	0.945	1.18	0.965	0.963	0.983	0.980	
330.2	3.660e-31	3.80	5.319e-32	0.93	5.4989e-32	1.50	5.727e-32	5.708e-32	5.7568e-32	5.730e-32	0.927	0.87	0.958	1.44	0.998	0.994	1.003	0.998	
457.2	5.740e-32	3.80	5.772e-33	1.05	5.7572e-33	1.66	6.101e-33	6.072e-33	6.050e-33	6.010e-33	0.953	1.00	0.950	1.57	1.007	1.002	0.998	0.992	
609.6	6.060e-33	4.20	6.110e-34	1.05	6.5136e-34	1.59	6.514e-34	6.475e-34	6.377e-34	6.319e-34	0.874	0.92	0.932	1.48	0.932	0.926	0.911	0.904	
762.0	6.990e-34	5.90	5.567e-35	1.33	5.5734e-35	2.07	5.895e-35	5.848e-35	5.752e-35	5.691e-35	0.389	0.52	0.390	0.81	0.412	0.409	0.402	0.398	
$^{93}Nb(n,2n)^{92m}Nb$	4.499e-29	0.92	4.5411e-29	0.80	4.531e-29	4.531e-29	4.525e-29	4.525e-29	4.525e-29	4.525e-29	1.011	0.93	1.021	0.82	1.018	1.018	1.017	1.017	
-1.0	4.450e-29	3.00	6.971e-30	1.46	6.9276e-30	1.23	7.119e-30	7.116e-30	6.916e-30	6.912e-30	1.000	1.46	0.993	1.22	1.021	1.021	0.992	0.991	
127.0	6.973e-30	3.12	1.411e-30	1.94	1.5040e-30	1.64	1.499e-30	1.497e-30	1.433e-30	1.433e-30	0.929	1.80	0.990	1.62	0.987	0.986	0.945	0.944	
228.6	1.519e-30	3.36	3.094e-31	2.72	3.2238e-31	2.31	3.309e-31	3.301e-31	3.123e-31	3.117e-31	0.913	2.48	0.950	2.20	0.975	0.974	0.921	0.919	
330.2	3.390e-31	3.15	4.564e-32	3.71	4.6733e-32	3.05	4.953e-32	4.941e-32	4.612e-32	4.600e-32	0.906	3.36	0.927	2.83	0.983	0.981	0.915	0.913	
457.2	5.039e-32	5.05	4.679e-33	4.47	4.6552e-33	3.86	4.990e-33	4.973e-33	4.570e-33	4.553e-33	0.988	4.42	0.983	3.79	1.054	1.050	0.965	0.961	
609.6	4.7356e-33	3.07	4.722e-34	4.99	5.0201e-34	4.02	5.1309e-34	5.107e-34	4.628e-34	4.606e-34	0.994	4.96	1.057	4.25	1.079	1.075	0.974	0.969	
762.0	4.753e-34	3.35	3.934e-35	5.56	4.3305e-35	4.67	4.428e-35	4.403e-35	3.978e-35	3.953e-35	0.956	5.32	1.052	4.91	1.076	1.070	0.967	0.961	
914.4	4.115e-35	7.09																	

Table 3.1 Continued.

Position [nm]	Expt. Error [%]	MCNP- J31 [%)	MCNP- J32 [%)	Calculated Reaction Rate			DOT- F-125	DOT- J-42	DOT- F-42	MCNP- J31 [%)	MCNP- J32 [%)	Calc. / Expt.		
				Error	MCNP- Error [%]	DOT- J-125 [%)						MCNP- Error [%]	DOT- J-125 [%)	
115In(n,n')115mIn														
-1.0	1.878e-29	2.90	1.835e-29	1.43	1.7838e-29	1.24	1.865e-29	1.865e-29	1.879e-29	1.876e-29	0.977	1.40	0.950	1.18
127.0	8.076e-30	2.93	7.919e-30	1.08	7.7035e-30	0.93	7.887e-30	7.874e-30	7.782e-30	7.757e-30	0.981	1.06	0.954	0.89
228.6	2.411e-30	3.00	2.229e-30	1.18	2.2465e-30	0.99	2.250e-30	2.240e-30	2.213e-30	2.197e-30	0.924	1.09	0.932	0.929
330.2	6.270e-31	3.35	5.785e-31	1.29	5.7118e-31	1.05	5.891e-31	5.846e-31	5.786e-31	5.733e-31	0.923	1.19	0.911	0.918
457.2	1.165e-31	4.09	1.109e-31	1.42	1.0869e-31	1.18	1.122e-31	1.108e-31	1.098e-31	1.080e-31	0.933	1.35	0.951	0.943
609.6	1.270e-32	3.25	1.335e-32	1.56	1.2946e-32	1.31	1.335e-32	1.308e-32	1.309e-32	1.275e-32	1.051	1.64	1.019	1.34
762.0	1.402e-33	3.71	1.530e-33	1.53	1.5407e-33	1.32	1.549e-33	1.505e-33	1.523e-33	1.468e-33	1.092	1.67	1.099	1.45
914.4	2.187e-34	4.90	2.085e-34	1.78	2.1227e-34	1.57	2.140e-34	2.020e-34	2.188e-34	2.030e-34	0.953	1.70	0.970	1.52
197Au(n, γ)198Au														
-1.0	5.323e-27	3.03	5.854e-27	8.40	5.93e-27	5.56	6.806e-27	6.799e-27	6.865e-27	6.954e-27	1.100	9.24	1.115	6.20
127.0	4.545e-27	3.06	4.941e-27	5.14	5.15e-27	4.00	5.009e-27	4.798e-27	4.943e-27	4.688e-27	1.086	5.59	1.135	4.54
228.6	2.177e-27	3.14	2.065e-27	5.32	2.13e-27	4.43	2.110e-27	1.985e-27	2.073e-27	1.921e-27	0.949	5.05	0.977	4.33
330.2	7.760e-28	3.25	7.319e-28	5.71	7.336e-28	4.66	7.354e-28	6.781e-28	6.464e-28	6.464e-28	0.943	5.39	0.949	4.42
457.2	1.410e-28	3.25	1.338e-28	5.87	1.35e-28	4.49	1.470e-28	1.279e-28	1.416e-28	1.187e-28	0.949	5.57	0.958	4.30
609.6	2.828e-29	4.22	2.719e-29	6.15	2.79e-29	5.61	2.927e-29	2.472e-29	2.805e-29	2.266e-29	0.951	5.91	0.988	5.55
762.0	4.680e-30	5.11	4.670e-30	7.34	5.15e-30	7.38	4.893e-30	3.868e-30	4.583e-30	3.446e-30	0.998	7.33	1.099	8.12
914.4	7.800e-31	5.30	8.087e-31	9.60	8.86e-31	10.79	8.608e-31	5.382e-31	8.553e-31	5.298e-31	1.037	9.95	1.136	12.25
235U(n,fission)														
-4.0	4.766e-27	3.65	5.662e-27	6.85	5.6960e-27	6.12	8.115e-27	8.030e-27	7.966e-27	8.009e-27	1.188	8.14	1.195	7.31
127.0	2.405e-27	3.65	2.123e-27	6.43	2.395e-27	8.94	2.435e-27	2.275e-27	2.385e-27	2.232e-27	0.883	5.68	0.996	8.91
228.6	9.922e-28	3.65	9.408e-28	6.01	9.1704e-28	4.45	9.771e-28	8.953e-28	9.511e-28	8.669e-28	0.948	5.70	0.924	4.11
330.2	3.634e-28	3.65	3.674e-28	6.28	3.2495e-28	4.47	3.400e-28	3.054e-28	3.286e-28	2.913e-28	1.011	6.35	0.894	4.00
457.2	4.395e-29	3.67	3.551e-29	4.42	3.9811e-29	4.53	4.289e-29	3.713e-29	4.080e-29	3.472e-29	0.808	3.57	0.906	4.10
609.6	8.837e-30	3.68	7.815e-30	3.55	7.8603e-30	3.49	8.366e-30	7.016e-30	6.468e-30	6.468e-30	0.884	3.14	0.889	3.10
762.0	1.550e-30	3.86	1.306e-30	3.24	1.3294e-30	2.91	1.450e-30	1.156e-30	1.345e-30	1.039e-30	0.843	2.73	0.858	2.50
914.4	3.214e-31	4.28	2.406e-31	3.75	2.4150e-31	2.46	2.555e-31	1.8335e-31	2.431e-31	1.729e-31	0.748	2.81	0.751	1.85
238U(n,fission)														
-4.0	1.3778e-28	3.72	1.334e-28	0.88	1.3355e-28	0.77	1.347e-28	1.306e-28	1.306e-28	1.306e-28	0.969	0.85	0.969	0.75
127.0	2.924e-29	3.85	2.889e-29	1.10	2.8462e-29	0.94	2.191e-29	2.911e-29	2.801e-29	2.795e-29	0.988	1.09	0.973	0.928
228.6	6.971e-30	4.16	6.807e-30	1.29	7.0422e-30	1.11	7.032e-30	7.015e-30	6.721e-30	6.695e-30	0.976	1.26	1.010	1.12
330.2	1.672e-30	4.71	1.615e-30	1.62	1.6396e-30	1.39	1.688e-30	1.681e-30	1.609e-30	1.599e-30	0.966	1.56	0.981	1.36
457.2	2.835e-31	6.16	2.716e-31	1.97	2.6996e-31	1.66	2.8333e-31	2.814e-31	2.665e-31	2.665e-31	0.958	1.89	0.952	1.58
609.6	3.317e-32	8.92	3.620e-32	2.28	2.9269e-32	1.99	3.095e-32	3.063e-32	2.959e-32	2.890e-32	0.911	2.08	0.882	1.76
762.0	3.863e-33	26.12	3.251e-33	2.42	3.3119e-33	2.04	3.368e-33	3.320e-33	3.173e-33	3.116e-33	0.842	2.04	0.857	1.75
914.4	1.380e-33	33.55	3.407e-34	2.44	3.4441e-34	2.19	3.575e-34	3.483e-34	3.423e-34	3.314e-34	0.247	0.60	0.250	0.55

Table 3.2 Neutron spectra at the eight positions in the assembly calculated by MCNP with the FSXLIB-J3 library.

Energy [MeV] Upper Lower		Flux / Lethargy / Source Neutron							
		-10 mm	127 mm	229 mm	330 mm	457 mm	610 mm	762 mm	914 mm
1.5488e+01	1.5248e+01	8.196e-04	8.343e-05	1.505e-05	2.483e-06	2.556e-07	1.888e-08	2.402e-09	1.654e-10
1.5248e+01	1.5012e+01	1.302e-03	1.364e-04	2.395e-05	4.956e-06	6.901e-07	4.957e-08	4.726e-09	3.261e-10
1.5012e+01	1.4779e+01	2.323e-03	2.739e-04	4.671e-05	8.263e-06	1.078e-06	1.116e-07	9.097e-09	4.727e-10
1.4779e+01	1.4550e+01	1.387e-03	2.026e-04	4.069e-05	8.934e-06	1.142e-06	1.070e-07	1.018e-08	9.174e-10
1.4550e+01	1.4324e+01	1.913e-04	6.995e-05	1.807e-05	3.931e-06	7.214e-07	6.866e-08	9.004e-09	7.447e-10
1.4324e+01	1.4102e+01	6.111e-05	3.194e-05	8.084e-06	2.527e-06	4.134e-07	5.082e-08	5.307e-09	3.878e-10
1.4102e+01	1.3883e+01	2.825e-05	2.722e-05	6.214e-06	1.513e-06	2.798e-07	3.077e-08	2.978e-09	3.613e-10
1.3883e+01	1.3668e+01	3.489e-05	1.837e-05	4.243e-06	1.133e-06	2.739e-07	3.347e-08	2.732e-09	4.082e-10
1.3668e+01	1.3456e+01	2.927e-05	1.249e-05	4.516e-06	1.085e-06	1.708e-07	3.246e-08	2.123e-09	2.448e-10
1.3456e+01	1.3248e+01	2.576e-05	1.284e-05	3.783e-06	9.624e-07	1.502e-07	1.832e-08	1.543e-09	1.465e-10
1.3248e+01	1.3042e+01	1.938e-05	8.503e-06	2.306e-06	1.203e-06	1.278e-07	1.258e-08	2.212e-09	1.788e-10
1.3042e+01	1.2840e+01	1.899e-05	9.143e-06	2.110e-06	7.395e-07	1.484e-07	1.150e-08	1.515e-09	1.661e-10
1.2840e+01	1.2641e+01	1.619e-05	8.074e-06	2.370e-06	4.819e-07	8.742e-08	1.098e-08	1.411e-09	1.065e-10
1.2641e+01	1.2445e+01	2.206e-05	5.488e-06	1.707e-06	4.840e-07	7.926e-08	9.760e-09	1.319e-09	1.323e-10
1.2445e+01	1.2252e+01	1.476e-05	5.616e-06	1.304e-06	3.395e-07	5.813e-08	8.289e-09	1.010e-09	7.912e-11
1.2252e+01	1.2062e+01	1.510e-05	5.949e-06	1.706e-06	4.755e-07	9.278e-08	7.629e-09	1.185e-09	9.422e-11
1.2062e+01	1.1875e+01	1.128e-05	5.620e-06	1.331e-06	5.069e-07	7.518e-08	8.832e-09	9.253e-10	7.376e-11
1.1875e+01	1.1691e+01	1.271e-05	4.440e-06	1.120e-06	3.799e-07	8.872e-08	7.596e-09	1.024e-09	6.399e-11
1.1691e+01	1.1510e+01	6.740e-06	4.335e-06	1.258e-06	3.429e-07	5.487e-08	7.406e-09	9.303e-10	7.122e-11
1.1510e+01	1.1331e+01	6.449e-06	3.451e-06	1.058e-06	3.068e-07	5.361e-08	1.211e-08	7.300e-10	6.575e-11
1.1331e+01	1.1156e+01	1.845e-06	4.341e-06	1.084e-06	2.402e-07	4.987e-08	6.300e-09	7.455e-10	5.557e-11
1.1156e+01	1.0983e+01	4.024e-06	4.468e-06	1.177e-06	2.739e-07	4.642e-08	5.894e-09	7.098e-10	4.534e-11
1.0983e+01	1.0812e+01	6.177e-06	4.224e-06	1.031e-06	2.775e-07	4.026e-08	4.126e-09	5.424e-10	4.684e-11
1.0812e+01	1.0645e+01	3.557e-06	3.649e-06	1.144e-06	3.031e-07	5.050e-08	7.084e-09	7.839e-10	5.101e-11
1.0645e+01	1.0480e+01	1.712e-06	4.400e-06	1.238e-06	3.238e-07	5.780e-08	5.893e-09	6.024e-10	4.740e-11
1.0480e+01	1.0317e+01	5.312e-06	4.975e-06	1.309e-06	2.890e-07	5.856e-08	6.854e-09	6.462e-10	5.582e-11
1.0317e+01	1.0157e+01	4.986e-06	4.913e-06	1.356e-06	5.836e-07	6.093e-08	7.829e-09	5.674e-10	5.498e-11
1.0157e+01	9.9999e+00	4.125e-06	5.575e-06	1.086e-06	2.780e-07	7.380e-08	8.144e-09	5.995e-10	5.205e-11
9.9999e+00	9.3940e+00	5.483e-06	4.616e-06	1.152e-06	3.309e-07	4.907e-08	5.461e-09	6.143e-10	5.619e-11
9.3940e+00	8.8249e+00	6.009e-06	4.482e-06	1.089e-06	2.507e-07	4.172e-08	5.032e-09	5.823e-10	4.269e-11
8.8249e+00	8.2902e+00	5.716e-06	4.203e-06	1.296e-06	2.946e-07	4.801e-08	5.018e-09	5.342e-10	4.304e-11
8.2902e+00	7.7879e+00	5.681e-06	5.214e-06	1.236e-06	3.219e-07	4.986e-08	5.338e-09	5.756e-10	3.286e-11
7.7879e+00	7.3161e+00	6.427e-06	5.018e-06	1.430e-06	3.081e-07	4.950e-08	5.453e-09	5.616e-10	4.192e-11
7.3161e+00	6.8728e+00	7.426e-06	5.122e-06	1.233e-06	2.788e-07	4.678e-08	5.634e-09	6.131e-10	5.402e-11
6.8728e+00	6.4564e+00	1.003e-05	4.987e-06	1.416e-06	3.110e-07	6.018e-08	4.972e-09	5.990e-10	4.078e-11
6.4564e+00	6.0652e+00	8.430e-06	4.594e-06	1.452e-06	3.504e-07	5.626e-08	6.143e-09	5.514e-10	5.135e-11
6.0652e+00	5.6978e+00	1.051e-05	5.174e-06	1.381e-06	3.645e-07	5.712e-08	6.346e-09	6.175e-10	4.755e-11
5.6978e+00	5.3525e+00	1.211e-05	5.620e-06	1.546e-06	3.552e-07	6.280e-08	6.620e-09	6.756e-10	5.748e-11
5.3525e+00	5.0282e+00	1.270e-05	6.110e-06	1.629e-06	3.835e-07	7.263e-08	7.525e-09	6.961e-10	5.803e-11
5.0282e+00	4.7236e+00	1.276e-05	5.828e-06	1.722e-06	4.286e-07	6.821e-08	6.231e-09	8.946e-10	7.130e-11
4.7236e+00	4.4374e+00	1.263e-05	6.010e-06	1.626e-06	3.690e-06	7.246e-08	8.157e-09	8.499e-10	6.636e-11
4.4374e+00	4.1686e+00	1.263e-05	8.188e-06	1.575e-06	4.541e-07	8.170e-08	8.812e-09	9.348e-10	7.322e-11
4.1686e+00	3.9160e+00	1.526e-05	8.928e-06	1.927e-06	4.930e-07	8.061e-08	1.161e-08	9.601e-10	7.470e-11
3.9160e+00	3.6787e+00	1.463e-05	8.039e-06	2.414e-06	4.900e-07	7.486e-08	7.452e-09	9.779e-10	1.292e-10
3.6787e+00	3.4595e+00	1.629e-05	8.728e-06	1.996e-06	5.599e-07	8.869e-08	1.028e-08	1.240e-09	8.271e-11
3.4595e+00	3.2465e+00	1.707e-05	8.114e-06	2.615e-06	6.827e-07	1.131e-07	1.219e-08	1.250e-09	1.192e-10
3.2465e+00	3.0498e+00	1.570e-05	1.118e-05	2.674e-06	7.915e-07	1.217e-07	1.524e-08	1.304e-09	2.001e-10
3.0498e+00	2.8650e+00	2.207e-05	1.157e-05	3.385e-06	7.193e-07	1.516e-07	1.601e-08	1.735e-09	1.699e-10
2.8650e+00	2.6914e+00	2.075e-05	1.170e-05	3.672e-06	8.423e-07	1.651e-07	1.810e-08	2.150e-09	2.138e-10
2.6914e+00	2.5284e+00	2.189e-05	1.246e-05	3.922e-06	9.325e-07	1.700e-07	2.157e-08	2.241e-09	2.446e-10
2.5284e+00	2.3752e+00	2.794e-05	1.445e-05	4.324e-06	1.158e-06	2.103e-07	2.259e-08	2.648e-09	3.285e-10
2.3752e+00	2.2313e+00	3.033e-05	1.611e-05	4.624e-06	1.368e-06	2.629e-07	3.207e-08	3.779e-09	3.779e-10
2.2313e+00	2.0961e+00	2.627e-05	1.497e-05	4.595e-06	1.316e-06	2.612e-07	3.061e-08	3.501e-09	4.034e-10
2.0961e+00	1.9691e+00	3.116e-05	1.494e-05	4.553e-06	1.254e-06	2.643e-07	2.940e-08	3.281e-09	3.873e-10
1.9691e+00	1.8498e+00	2.811e-05	1.583e-05	4.665e-06	1.324e-06	2.503e-07	3.388e-08	3.665e-09	4.261e-10
1.8498e+00	1.7377e+00	3.379e-05	1.898e-05	6.045e-06	1.499e-06	3.068e-07	3.953e-08	4.134e-09	5.924e-10
1.7377e+00	1.5335e+00	3.339e-05	1.832e-05	5.622e-06	1.501e-06	3.088e-07	3.964e-08	4.730e-09	5.857e-10
1.5335e+00	1.3533e+00	3.469e-05	2.033e-05	6.770e-06	1.709e-06	3.569e-07	4.846e-08	5.392e-09	7.763e-10
1.3533e+00	1.1943e+00	4.219e-05	2.187e-05	6.658e-06	1.948e-06	4.036e-07	5.315e-08	6.320e-09	1.061e-09
1.1943e+00	1.0540e+00	3.974e-05	2.495e-05	7.144e-06	2.157e-06	4.888e-07	6.597e-08	8.875e-09	1.579e-09
1.0540e+00	9.3013e-01	3.830e-05	2.329e-05	7.367e-06	1.932e-06	4.849e-07	6.853e-08	8.040e-09	1.890e-09
9.3013e-01	8.2084e-01	4.434e-05	2.339e-05	7.688e-06	2.143e-06	5.642e-07	7.574e-08	1.091e-08	1.777e-09
8.2084e-01	7.2438e-01	4.611e-05	2.515e-05	8.144e-06	2.692e-06	5.924e-07	7.873e-08	1.003e-08	2.447e-09
7.2438e-01	6.3927e-01	6.099e-05	3.040e-05	1.121e-05	3.436e-06	8.755e-07	1.395e-07	1.744e-08	4.343e-09
6.3927e-01	5.6415e-01	6.408e-05	2.655e-05	1.142e-05	2.852e-06	9.184e-07	1.400e-07	2.331e-08	6.723e-09
5.6415e-01	4.9786e-01	4.980e-05	2.209e-05	8.694e-06	2.369e-06	7.197e-07	1.231e-07	1.847e-08	5.978e-09
4.9786e-01	4.3936e-01	4.901e-05	2.110e-05	7.134e-06	2.146e-06	6.844e-07	1.515e-07	1.848e-08	5.260e-09
4.3936e-01	3.8774e-01	4.060e-05	1.632e-05	5.429e-06	1.729e-06	4.579e-07	8.309e-08	1.295e-08	5.430e-09
3.8774e-01	3.4217e-01	6.274e-05	2.286e-05	8.544e-06	2.447e-06	7.639e-07	1.212e-07	2.246e-08	8.934e-09
3.4217e-01	3.0197e-01	5.761e-05	2.208e-05	7.539e-06	2.137e-06	6.410e-07	1.311e-07	2.330e-08	9.616e-09
3.0197e-01	2.6649e-01	4.980e-05	1.857e-05	6.261e-06	2.094e-06	6.782e-07	1.183e-07	1.794e-08	9.891e-09
2.6649e-01	2.3517e-01	4.275e-05	1.434e-05	6.096e-06	1.685e-06	5.			

Table 3.2 Continued.

Energy [MeV] Upper	Lower	Flux / Lethargy / Source Neutron							
		-10 mm	127 mm	229 mm	330 mm	457 mm	610 mm	762 mm	914 mm
5.2474e-02	4.6308e-02	1.530e-05	4.397e-06	2.008e-06	8.495e-07	1.854e-07	3.055e-08	7.873e-09	4.691e-09
4.6308e-02	4.0867e-02	1.658e-05	5.600e-06	2.439e-06	9.848e-07	2.249e-07	5.340e-08	8.573e-09	6.186e-09
4.0867e-02	3.6065e-02	1.487e-05	5.262e-06	2.266e-06	7.445e-07	1.644e-07	4.154e-08	7.333e-09	4.755e-09
3.6065e-02	3.1827e-02	1.202e-05	3.941e-06	1.599e-06	5.736e-07	1.174e-07	2.402e-08	6.292e-09	3.016e-09
3.1827e-02	2.8087e-02	4.230e-06	2.367e-06	9.300e-07	1.684e-07	6.412e-08	1.048e-08	2.989e-09	1.685e-09
2.8087e-02	2.4787e-02	1.202e-05	5.961e-06	2.519e-06	7.633e-07	1.804e-07	3.930e-08	1.125e-08	5.278e-09
2.4787e-02	2.1874e-02	2.016e-05	7.678e-06	3.496e-06	1.248e-06	3.677e-07	6.443e-08	1.533e-08	8.790e-09
2.1874e-02	1.9304e-02	1.242e-05	4.810e-06	1.675e-06	5.798e-07	1.811e-07	4.481e-08	1.056e-08	5.732e-09
1.9304e-02	1.5034e-02	7.024e-06	2.646e-06	1.233e-06	3.409e-07	1.075e-07	2.080e-08	4.902e-09	2.820e-09
1.5034e-02	1.1709e-02	6.567e-06	2.874e-06	1.160e-06	3.538e-07	8.553e-08	1.760e-08	4.904e-09	2.663e-09
1.1709e-02	9.1186e-03	7.609e-06	4.248e-06	1.801e-06	6.027e-07	1.355e-07	1.910e-08	6.433e-09	2.947e-09
9.1186e-03	7.1016e-03	4.042e-06	2.091e-06	9.289e-07	2.530e-07	4.655e-08	1.673e-08	3.126e-09	1.212e-09
7.1016e-03	5.5307e-03	4.731e-06	2.629e-06	1.380e-06	4.139e-07	7.214e-08	1.771e-08	4.132e-09	1.821e-09
5.5307e-03	4.3073e-03	5.892e-06	3.802e-06	1.932e-06	4.966e-07	1.275e-07	1.989e-08	4.756e-09	2.256e-09
4.3073e-03	3.3545e-03	5.638e-06	3.881e-06	1.881e-06	4.702e-07	2.129e-07	2.259e-08	4.754e-09	1.856e-09
3.3545e-03	2.6125e-03	7.224e-06	5.635e-06	2.158e-06	7.033e-07	1.795e-07	3.229e-08	6.335e-09	2.364e-09
2.6125e-03	2.0346e-03	4.346e-06	3.309e-06	1.321e-06	4.834e-07	1.288e-07	2.920e-08	4.660e-09	1.507e-09
2.0346e-03	1.5846e-03	7.837e-06	5.511e-06	1.964e-06	6.618e-07	1.918e-07	3.626e-08	7.033e-09	2.840e-09
1.5846e-03	1.2341e-03	7.186e-06	4.651e-06	1.728e-06	7.474e-07	1.786e-07	3.386e-08	7.025e-09	2.430e-09
1.2341e-03	9.6110e-04	5.083e-06	3.510e-06	1.551e-06	4.599e-07	1.421e-07	2.937e-08	4.946e-09	1.904e-09
9.6110e-04	5.8293e-04	5.9237e-06	3.649e-06	1.627e-06	5.220e-07	1.565e-07	2.966e-08	5.516e-09	1.996e-09
5.8293e-04	3.5357e-04	5.0012e-06	3.224e-06	1.495e-06	4.125e-07	1.220e-07	2.529e-08	4.424e-09	1.528e-09
3.5357e-04	2.1445e-04	4.4387e-06	2.957e-06	1.175e-06	4.736e-07	9.425e-08	1.749e-08	3.495e-09	9.187e-10
2.1445e-04	1.3007e-04	4.8246e-06	3.983e-06	1.748e-06	5.913e-07	1.142e-07	2.332e-08	5.056e-09	1.149e-09
1.3007e-04	7.8891e-05	4.8474e-06	3.478e-06	1.553e-06	5.322e-07	1.448e-07	2.597e-08	4.683e-09	1.209e-09
7.8891e-05	4.7850e-05	4.4824e-06	3.622e-06	1.462e-06	5.638e-07	1.253e-07	2.501e-08	4.187e-09	1.290e-09
4.7850e-05	2.9023e-05	3.9131e-06	2.867e-06	1.175e-06	4.240e-07	9.408e-08	1.913e-08	3.315e-09	7.978e-10
2.9023e-05	1.7603e-05	3.7951e-06	3.258e-06	1.175e-06	4.676e-07	8.228e-08	1.846e-08	3.446e-09	7.246e-10
1.7603e-05	1.0677e-05	3.4271e-06	3.196e-06	1.528e-06	5.170e-07	8.388e-08	2.209e-08	4.018e-09	6.327e-10
1.0677e-05	6.4758e-06	3.3355e-06	2.875e-06	1.438e-06	4.941e-07	8.901e-08	1.885e-08	3.097e-09	5.335e-10
6.4758e-06	3.9278e-06	3.0067e-06	2.951e-06	1.222e-06	4.286e-07	8.280e-08	1.670e-08	2.893e-09	4.811e-10
3.9278e-06	2.3823e-06	3.6667e-06	2.995e-06	1.118e-06	3.642e-07	7.091e-08	1.542e-08	2.378e-09	3.374e-10
2.3823e-06	1.4449e-06	2.6269e-06	2.653e-06	1.033e-06	3.636e-07	6.691e-08	1.429e-08	1.876e-09	3.416e-10
1.4449e-06	8.7640e-07	2.7428e-06	2.275e-06	9.187e-07	3.283e-07	5.870e-08	1.048e-08	1.445e-09	1.667e-10
8.7640e-07	5.3156e-07	1.7902e-06	1.864e-06	7.650e-07	2.445e-07	3.941e-08	9.361e-09	1.341e-09	1.023e-10
5.3156e-07	3.2241e-07	1.9411e-06	1.218e-06	6.030e-07	1.843e-07	3.085e-08	5.212e-09	9.207e-10	5.052e-11
3.2241e-07	1.0010e-11	1.0724e-06	3.294e-07	1.601e-07	6.531e-08	2.797e-09	7.846e-10	1.058e-10	6.270e-13

Table 3.3 Neutron spectra at the eight positions in the assembly calculated by MCNP with the FSXLIB-J3R2 library.

Energy [MeV] Upper	Lower	Flux / Lethargy / Source Neutron							
		-10 mm	127 mm	229 mm	330 mm	457 mm	610 mm	762 mm	914 mm
1.5488e+01	1.5248e+01	8.344e-04	8.385e-05	1.472e-05	2.654e-06	2.476e-07	2.565e-08	2.325e-09	1.252e-10
1.5248e+01	1.5012e+01	1.338e-03	1.426e-04	2.566e-05	4.987e-06	5.503e-07	4.472e-08	3.933e-09	4.141e-10
1.5012e+01	1.4779e+01	2.418e-03	2.677e-04	5.004e-05	9.272e-06	1.096e-06	8.932e-08	8.872e-09	7.586e-10
1.4779e+01	1.4550e+01	1.432e-03	1.977e-04	4.248e-05	8.538e-06	1.371e-06	1.207e-07	1.238e-08	1.066e-09
1.4550e+01	1.4324e+01	1.922e-04	6.603e-05	1.993e-05	4.506e-06	8.225e-07	8.121e-08	1.044e-08	7.861e-10
1.4324e+01	1.4102e+01	5.855e-05	3.200e-05	9.465e-06	2.477e-06	4.659e-07	3.995e-08	5.200e-09	6.099e-10
1.4102e+01	1.3883e+01	3.216e-05	2.320e-05	7.107e-06	1.495e-06	2.593e-07	3.640e-08	2.612e-09	2.501e-10
1.3883e+01	1.3668e+01	3.726e-05	2.217e-05	5.234e-06	1.454e-06	2.275e-07	2.759e-08	2.737e-09	2.078e-10
1.3668e+01	1.3456e+01	2.931e-05	1.484e-05	3.699e-06	1.243e-06	1.223e-07	2.512e-08	2.391e-09	1.369e-10
1.3456e+01	1.3248e+01	2.130e-05	1.049e-05	3.196e-06	1.021e-06	1.924e-07	2.103e-08	2.362e-09	1.742e-10
1.3248e+01	1.3042e+01	1.918e-05	1.191e-05	2.636e-06	8.204e-07	1.268e-07	2.028e-08	2.665e-09	2.216e-10
1.3042e+01	1.2840e+01	1.777e-05	8.815e-06	2.502e-06	7.446e-07	8.243e-08	1.174e-08	1.711e-09	1.412e-10
1.2840e+01	1.2641e+01	1.735e-05	6.938e-06	1.945e-06	5.524e-07	8.725e-08	1.121e-08	1.692e-09	1.446e-10
1.2641e+01	1.2445e+01	1.315e-05	6.793e-06	2.011e-06	4.379e-07	1.163e-07	9.624e-09	1.228e-09	1.122e-10
1.2445e+01	1.2252e+01	1.195e-05	5.075e-06	1.925e-06	4.895e-07	7.185e-09	8.161e-09	1.050e-09	9.638e-11
1.2252e+01	1.2062e+01	9.461e-06	4.524e-06	1.631e-06	3.663e-07	5.755e-08	6.890e-09	1.070e-09	9.582e-11
1.2062e+01	1.1875e+01	8.594e-06	5.092e-06	1.430e-06	3.498e-07	6.844e-08	7.978e-09	8.051e-10	1.031e-10
1.1875e+01	1.1691e+01	1.185e-05	4.714e-06	1.195e-06	4.117e-07	6.695e-08	7.135e-09	7.887e-10	6.955e-11
1.1691e+01	1.1510e+01	3.989e-06	4.689e-06	1.388e-06	3.024e-07	5.152e-08	7.261e-09	7.772e-10	6.886e-11
1.1510e+01	1.1331e+01	6.889e-06	4.417e-06	1.306e-06	3.351e-07	8.030e-08	8.001e-09	9.890e-10	6.053e-11
1.1331e+01	1.1156e+01	6.155e-06	4.087e-06	1.429e-06	4.047e-07	4.839e-08	7.143e-09	7.629e-10	6.452e-11
1.1156e+01	1.0983e+01	6.062e-06	4.130e-06	1.419e-06	3.331e-07	6.531e-08	6.856e-09	7.748e-10	5.292e-11
1.0983e+01	1.0812e+01	5.112e-06	4.546e-06	1.135e-06	3.803e-07	4.481e-08	6.480e-09	7.536e-10	6.192e-11
1.0812e+01	1.0645e+01	2.907e-06	4.863e-06	1.253e-06	3.206e-07	5.189e-08	6.838e-09	7.465e-10	6.084e-11
1.0645e+01	1.0480e+01	5.303e-06	5.383e-06	1.362e-06	3.248e-07	6.390e-08	7.910e-09	8.062e-10	7.002e-11
1.0480e+01	1.0317e+01	4.661e-06	4.660e-06	1.482e-06	3.165e-07	7.105e-08	6.773e-09	5.827e-10	5.917e-11
1.0317e+01	1.0157e+01	3.026e-06	4.735e-06	1.435e-06	3.850e-07	5.878e-08	7.169e-09	7.196e-10	5.496e-11
1.0157e+01	9.9999e+00	5.211e-06	5.424e-06	1.418e-06	3.811e-07	6.190e-08	7.781e-09	8.454e-10	5.391e-11
9.9999e+00	9.3940e+00	7.348e-06	4.625e-06	1.507e-06	3.635e-07	5.642e-08	5.804e-09	7.400e-10	6.545e-11
9.3940e+00	8.8249e+00	8.251e-06	4.454e-06	1.370e-06	3.702e-07	5.746e-08	6.724e-09	8.047e-10	5.199e-11
8.8249e+00	8.2902e+00	5.668e-06							

Table 3.3 Continued.

Energy [MeV] Upper Lower	-10 mm	127 mm	Flux / Lethargy / Source Neutron						914 mm
			229 mm	330 mm	457 mm	610 mm	762 mm	914 mm	
6.4564e+00	6.0652e+00	1.113e-05	4.809e-06	1.352e-06	3.744e-07	5.746e-08	6.074e-09	6.933e-10	5.379e-11
6.0652e+00	5.6978e+00	9.528e-06	4.894e-06	1.572e-06	3.685e-07	6.156e-08	6.352e-09	6.569e-10	5.536e-11
5.6978e+00	5.3525e+00	9.340e-06	6.562e-06	1.500e-06	3.831e-07	7.662e-08	7.164e-09	6.947e-10	6.607e-11
5.3525e+00	5.0282e+00	1.065e-05	5.691e-06	1.657e-06	4.036e-07	7.353e-08	7.083e-09	7.460e-10	6.077e-11
5.0282e+00	4.7236e+00	8.119e-06	5.867e-06	1.450e-06	3.648e-07	7.054e-08	8.404e-09	8.641e-10	7.446e-11
4.7236e+00	4.4374e+00	1.137e-05	6.062e-06	1.822e-06	4.805e-07	8.340e-08	8.996e-09	8.678e-10	8.513e-11
4.4374e+00	4.1686e+00	1.144e-05	6.711e-06	1.974e-06	4.851e-07	8.440e-08	7.442e-09	1.108e-09	7.538e-11
4.1686e+00	3.9160e+00	1.361e-05	6.839e-06	1.838e-06	4.063e-07	6.631e-08	7.315e-09	1.010e-09	7.117e-11
3.9160e+00	3.6787e+00	1.157e-05	6.595e-06	1.785e-06	4.993e-07	7.583e-08	7.964e-09	9.816e-10	8.616e-11
3.6787e+00	3.4559e+00	1.415e-05	7.823e-06	2.097e-06	5.267e-07	7.885e-08	7.889e-09	1.072e-09	1.284e-10
3.4559e+00	3.2465e+00	1.539e-05	8.630e-06	2.091e-06	5.555e-07	8.836e-08	8.745e-09	1.074e-09	1.156e-10
3.2465e+00	3.0498e+00	1.621e-05	9.476e-06	2.600e-06	5.977e-07	1.087e-07	9.997e-09	1.252e-09	9.478e-11
3.0498e+00	2.8650e+00	1.935e-05	9.682e-06	3.140e-06	7.183e-07	1.274e-07	1.268e-08	1.621e-09	1.465e-10
2.8650e+00	2.6914e+00	2.142e-05	1.256e-05	3.097e-06	8.191e-07	1.421e-07	1.415e-08	1.886e-09	1.473e-10
2.6914e+00	2.5284e+00	2.315e-05	1.254e-05	3.300e-06	8.947e-07	1.405e-07	1.864e-08	2.079e-09	1.919e-10
2.5284e+00	2.3752e+00	2.380e-05	1.253e-05	3.945e-06	9.731e-07	1.848e-07	1.874e-08	2.189e-09	2.213e-10
2.3752e+00	2.2313e+00	2.697e-05	1.514e-05	4.809e-06	1.158e-06	2.144e-07	2.609e-08	2.685e-09	3.045e-10
2.2313e+00	2.0961e+00	2.567e-05	1.474e-05	4.567e-06	1.123e-06	2.133e-07	2.450e-08	2.597e-09	3.179e-10
2.0961e+00	1.9691e+00	2.651e-05	1.597e-05	4.674e-06	1.183e-06	2.148e-07	2.372e-08	3.036e-09	3.446e-10
1.9691e+00	1.8498e+00	2.767e-05	1.615e-05	4.687e-06	1.342e-06	2.453e-07	3.237e-08	3.601e-09	4.852e-10
1.8498e+00	1.7377e+00	3.163e-05	1.865e-05	5.190e-06	1.478e-06	3.026e-07	3.536e-08	4.454e-09	5.737e-10
1.7377e+00	1.5335e+00	3.324e-05	1.786e-05	6.296e-06	1.486e-06	3.197e-07	3.989e-08	4.544e-09	6.284e-10
1.5335e+00	1.3533e+00	3.519e-05	2.102e-05	6.738e-06	1.804e-06	3.924e-07	5.169e-08	5.663e-09	8.300e-10
1.3533e+00	1.1943e+00	3.973e-05	2.255e-05	7.454e-06	1.954e-06	4.457e-07	5.724e-08	7.326e-09	1.151e-09
1.1943e+00	1.0540e+00	4.084e-05	2.270e-05	8.504e-06	2.289e-06	5.559e-07	7.293e-08	8.920e-09	1.738e-09
1.0540e+00	9.3013e-01	4.085e-05	2.324e-05	7.876e-06	2.106e-06	5.284e-07	7.458e-08	9.306e-09	2.227e-09
9.3013e-01	8.2084e-01	4.519e-05	2.209e-05	7.747e-06	2.202e-06	5.361e-07	7.951e-08	1.096e-08	2.149e-09
8.2084e-01	7.2438e-01	4.814e-05	2.396e-05	8.225e-06	2.576e-06	5.986e-07	8.811e-08	1.115e-08	2.569e-09
7.2438e-01	6.3927e-01	6.275e-05	3.234e-05	1.084e-05	3.306e-06	8.524e-07	1.418e-07	1.871e-08	5.352e-09
6.3927e-01	5.6415e-01	5.998e-05	2.877e-05	1.030e-05	3.067e-06	8.840e-07	1.560e-07	2.137e-08	6.758e-09
5.6415e-01	4.9786e-01	5.164e-05	2.014e-05	8.539e-06	2.620e-06	7.126e-07	1.276e-07	2.007e-08	6.203e-09
4.9786e-01	4.3936e-01	4.537e-05	1.907e-05	7.212e-06	2.359e-06	6.773e-07	1.038e-07	2.034e-08	6.074e-09
4.3936e-01	3.8774e-01	4.495e-05	1.668e-05	6.084e-06	1.918e-06	5.145e-07	9.041e-08	1.517e-08	4.806e-09
3.8774e-01	3.4217e-01	5.826e-05	2.262e-05	8.987e-06	2.628e-06	7.738e-07	1.287e-07	2.362e-08	9.169e-09
3.4217e-01	3.0197e-01	5.204e-05	1.974e-05	8.363e-06	2.225e-06	6.673e-07	1.061e-07	2.419e-08	9.781e-09
3.0197e-01	2.6649e-01	4.745e-05	1.626e-05	6.897e-06	2.047e-06	6.391e-07	1.061e-07	2.057e-08	9.861e-09
2.6649e-01	2.3517e-01	4.238e-05	1.410e-05	5.622e-06	1.696e-06	5.022e-07	8.548e-08	1.671e-08	8.207e-09
2.3517e-01	2.0754e-01	3.377e-05	1.216e-05	4.691e-06	1.446e-06	3.909e-07	8.591e-08	1.450e-08	6.639e-09
2.0754e-01	1.8315e-01	3.055e-05	1.064e-05	3.936e-06	1.366e-06	3.575e-07	6.397e-08	1.215e-08	5.252e-09
1.8315e-01	1.6163e-01	3.419e-05	1.385e-05	5.175e-06	1.580e-06	4.811e-07	8.679e-08	1.471e-08	8.097e-09
1.6163e-01	1.4264e-01	2.610e-05	9.425e-06	3.131e-06	1.136e-06	3.316e-07	5.537e-08	1.074e-08	4.947e-09
1.4264e-01	1.2588e-01	4.096e-05	1.343e-05	6.301e-06	1.816e-06	5.096e-07	1.009e-07	2.153e-08	1.0028e-08
1.2588e-01	1.1109e-01	3.109e-05	9.717e-06	4.081e-06	1.307e-06	4.148e-07	7.555e-08	1.824e-08	8.583e-09
1.1109e-01	9.8035e-02	2.121e-05	6.295e-06	2.257e-06	8.444e-07	2.718e-07	5.136e-08	1.042e-08	5.230e-09
9.8035e-02	8.6515e-02	2.039e-05	6.974e-06	2.755e-06	7.681e-07	2.321e-07	4.653e-08	1.039e-08	5.597e-09
8.6515e-02	7.6349e-02	2.901e-05	9.057e-06	4.066e-06	1.337e-06	3.487e-07	8.562e-08	1.598e-08	9.553e-09
7.6349e-02	6.7378e-02	2.153e-05	6.922e-06	2.946e-06	9.909e-07	3.111e-07	5.163e-08	1.197e-08	7.282e-09
6.7378e-02	5.9461e-02	5.627e-05	2.527e-06	5.257e-06	7.955e-07	2.674e-07	3.873e-08	1.063e-08	5.389e-09
5.9461e-02	5.2474e-02	1.679e-05	5.328e-06	2.578e-06	7.631e-07	2.513e-07	5.568e-08	1.067e-08	6.260e-09
5.2474e-02	4.6308e-02	1.459e-05	4.954e-06	1.913e-06	7.369e-07	2.140e-07	3.866e-08	8.665e-09	4.845e-09
4.6308e-02	4.0867e-02	1.510e-05	4.850e-06	2.531e-06	9.214e-07	2.218e-07	4.251e-08	1.194e-08	6.246e-09
4.0867e-02	3.6065e-02	1.261e-05	4.580e-06	1.842e-06	7.788e-07	2.134e-07	3.468e-08	8.080e-09	4.307e-09
3.6065e-02	3.1827e-02	8.669e-06	3.600e-06	1.399e-06	4.374e-07	1.368e-07	2.792e-08	6.375e-09	2.884e-09
3.1827e-02	2.8087e-02	4.078e-06	1.416e-06	6.411e-06	1.705e-07	6.787e-08	1.271e-08	2.489e-09	1.306e-09
2.8087e-02	2.4787e-02	1.205e-05	5.620e-06	2.166e-06	7.606e-07	1.949e-07	4.075e-08	7.730e-09	4.357e-09
2.4787e-02	2.1874e-02	1.790e-05	8.084e-06	3.282e-06	1.113e-06	3.424e-07	7.215e-08	1.482e-08	8.005e-09
2.1874e-02	1.9304e-02	1.150e-05	4.593e-06	1.718e-06	6.523e-07	1.638e-07	3.884e-08	9.120e-09	4.690e-09
1.9304e-02	1.5034e-02	6.912e-06	2.718e-06	9.890e-07	4.151e-07	1.034e-07	2.072e-08	4.753e-09	2.501e-09
1.5034e-02	1.1709e-02	6.923e-06	2.824e-06	1.328e-06	4.465e-07	1.060e-07	2.171e-08	4.289e-09	2.257e-09
1.1709e-02	9.1186e-03	7.742e-06	4.022e-06	1.944e-06	6.404e-07	1.492e-07	2.963e-08	6.159e-09	2.917e-09
9.1186e-03	7.1016e-03	4.946e-06	1.945e-06	8.231e-07	3.171e-07	6.164e-08	1.489e-08	2.830e-09	1.151e-09
7.1016e-03	5.5307e-03	6.310e-06	3.160e-06	1.200e-06	4.013e-07	9.591e-08	2.145e-08	3.851e-09	1.462e-09
5.5307e-03	4.3073e-03	6.368e-06	3.645e-06	1.640e-06	6.604e-07	1.177e-07	2.507e-08	5.210e-09	1.662e-09
4.3073e-03	3.3546e-03	6.382e-06	4.055e-06	1.610e-06	6.140e-07	1.181e-07	2.599e-08	5.040e-09	1.824e-09
3.3546e-03	2.6125e-03	6.565e-06	4.987e-06	2.139e-06	7.400e-07	1.681e-07	3.630e-08	6.509e-09	2.447e-09
2.6125e-03	2.0346e-03	5.362e-06	3.368e-06	1.297e-06	5.644e-07	1.244e-07	2.504e-08	4.779e-09	1.939e-09
2.0346e-03	1.5846e-03	8.457e-06	4.564e-06	1.981e-06	7.625e-07	1.865e-07	3.578e-08	6.507e-09	2.569e-09
1.5846e-03	1.2341e-03	6.969e-06	4.108e-06	1.938e-06	7.494e-07	1.830e-07	3.696e-08	8.070e-09	2.941e-09
1.2341e-03	9.6110e-04	5.778e-06	3.806e-06	1.449e-06	5.522e-07	1.327e-07	2.606e-08	5.497e-09	2.099e-09
9.6110e-04	5.8293e-04	6.128e-06	3.962e-06	1.635e-06	5.935e-07	1.516e-07	2.811e-08	5.136e-09	2.005e-09
5.8293e-04	3.5357e-04	4.929e-06	3.212e-06	1.286e-06	4.902e-07	1.291e-07	2.504e-08	4.744e-09	1.687e-09
3.5357e-04	2.11445e-04	4.396e-06	2.943e-06	1.210e-06	4.406e				

Table 3.4 Neutron spectra at the eight positions in the assembly calculated by DOT with the JSSTD library of 125 neutron groups.

Energy [MeV] Upper Lower	-10 mm	127 mm	Flux / Lethargy / Source Neutron						762 mm	914 mm
			229 mm	330 mm	457 mm	610 mm	762 mm	914 mm		
1.5488e+01	1.5248e+01	8.547e-04	8.716e-05	1.504e-05	2.755e-06	3.339e-07	2.627e-08	2.130e-09	1.491e-10	
1.5248e+01	1.5012e+01	1.332e-03	1.496e-04	2.771e-05	5.445e-06	7.219e-07	6.254e-08	5.533e-09	4.212e-10	
1.5012e+01	1.4779e+01	2.420e-03	2.745e-04	5.074e-05	9.920e-06	1.307e-06	1.138e-07	1.022e-08	7.915e-10	
1.4779e+01	1.4550e+01	1.402e-03	1.968e-04	4.068e-05	8.729e-06	1.264e-06	1.208e-07	1.167e-08	9.575e-10	
1.4550e+01	1.4324e+01	2.464e-04	6.996e-05	1.801e-05	4.481e-06	7.417e-07	8.043e-08	8.595e-09	7.657e-10	
1.4324e+01	1.4102e+01	9.915e-05	3.459e-05	9.147e-06	2.394e-06	4.210e-07	4.900e-08	5.595e-09	5.298e-10	
1.4102e+01	1.3883e+01	6.457e-05	2.600e-05	6.589e-06	1.685e-06	2.924e-07	3.416e-08	3.959e-09	3.805e-10	
1.3883e+01	1.3668e+01	4.741e-05	2.213e-05	5.712e-06	1.449e-06	2.453e-07	2.805e-08	3.205e-09	3.040e-10	
1.3668e+01	1.3456e+01	1.277e-05	1.575e-05	4.446e-06	1.177e-06	2.030e-07	2.354e-08	2.711e-09	2.552e-10	
1.3456e+01	1.3248e+01	6.944e-06	1.145e-05	3.371e-06	9.243e-07	1.636e-07	1.936e-08	2.261e-09	2.134e-10	
1.3248e+01	1.3042e+01	1.266e-05	9.633e-06	2.763e-06	7.575e-07	1.348e-07	1.608e-08	1.894e-09	1.790e-10	
1.3042e+01	1.2840e+01	1.728e-05	8.503e-06	2.374e-06	6.429e-07	1.138e-07	1.353e-08	1.596e-09	1.506e-10	
1.2840e+01	1.2641e+01	1.745e-05	7.617e-06	2.120e-06	5.711e-07	1.004e-07	1.187e-08	1.393e-09	1.300e-10	
1.2641e+01	1.2445e+01	1.608e-05	6.873e-06	1.918e-06	5.160e-07	9.043e-08	1.062e-08	1.240e-09	1.147e-10	
1.2445e+01	1.2252e+01	1.309e-05	6.094e-06	1.728e-06	4.676e-07	8.194e-08	9.608e-09	1.118e-09	1.026e-10	
1.2252e+01	1.2062e+01	1.085e-05	5.447e-06	1.573e-06	4.292e-07	7.529e-08	8.824e-09	1.024e-09	9.316e-11	
1.2062e+01	1.1875e+01	9.957e-06	5.067e-06	1.466e-06	3.995e-07	6.991e-08	8.161e-09	9.425e-10	8.543e-11	
1.1875e+01	1.1691e+01	9.483e-06	4.818e-06	1.383e-06	3.755e-07	6.539e-08	7.599e-09	8.738e-10	7.856e-11	
1.1691e+01	1.1510e+01	9.361e-06	4.638e-06	1.321e-06	3.575e-07	6.190e-08	7.167e-09	8.208e-10	7.322e-11	
1.1510e+01	1.1331e+01	6.675e-06	4.344e-06	1.244e-06	3.382e-07	5.869e-08	6.791e-09	7.777e-10	6.862e-11	
1.1331e+01	1.1156e+01	4.936e-06	4.125e-06	1.183e-06	3.216e-07	5.585e-08	6.447e-09	7.381e-10	6.466e-11	
1.1156e+01	1.0983e+01	4.489e-06	4.075e-06	1.162e-06	3.146e-07	5.428e-08	6.216e-09	7.081e-10	6.112e-11	
1.0983e+01	1.0812e+01	4.195e-06	4.139e-06	1.183e-06	3.193e-07	5.476e-08	6.219e-09	7.037e-10	5.951e-11	
1.0812e+01	1.0645e+01	4.137e-06	4.319e-06	1.229e-06	3.296e-07	5.628e-08	6.342e-09	7.122e-10	5.988e-11	
1.0645e+01	1.0480e+01	4.189e-06	4.496e-06	1.271e-06	3.374e-07	5.726e-08	6.400e-09	7.124e-10	6.004e-11	
1.0480e+01	1.0317e+01	4.178e-06	4.702e-06	1.320e-06	3.471e-07	5.859e-08	6.498e-09	7.177e-10	6.075e-11	
1.0317e+01	1.0157e+01	4.477e-06	4.848e-06	1.351e-06	3.535e-07	5.950e-08	6.547e-09	7.166e-10	6.067e-11	
1.0157e+01	9.9999e+00	5.621e-06	5.090e-06	1.407e-06	3.666e-07	6.162e-08	6.758e-09	7.366e-10	6.242e-11	
9.9999e+00	9.3940e+00	6.097e-06	4.508e-06	1.247e-06	3.279e-07	5.553e-08	6.155e-09	6.767e-10	5.671e-11	
9.3940e+00	8.8249e+00	5.757e-06	4.189e-06	1.156e-06	3.035e-07	5.081e-08	5.586e-09	6.113e-10	5.001e-11	
8.8249e+00	8.2902e+00	5.901e-06	4.731e-06	1.269e-06	3.258e-07	5.289e-08	5.648e-09	6.047e-10	4.791e-11	
8.2902e+00	7.7879e+00	6.114e-06	4.919e-06	1.314e-06	3.357e-07	5.404e-08	5.725e-09	6.093e-10	4.749e-11	
7.7879e+00	7.3161e+00	6.552e-06	4.908e-06	1.306e-06	3.319e-07	5.331e-08	5.623e-09	5.967e-10	4.682e-11	
7.3161e+00	6.8728e+00	7.669e-06	4.861e-06	1.299e-06	3.307e-07	5.330e-08	5.636e-09	5.988e-10	4.747e-11	
6.8728e+00	6.4564e+00	9.354e-06	4.946e-06	1.325e-06	3.372e-07	5.458e-08	5.788e-09	6.153e-10	4.968e-11	
6.4564e+00	6.0652e+00	9.997e-06	5.086e-06	1.364e-06	3.464e-07	5.620e-08	5.964e-09	6.337e-10	5.194e-11	
6.0652e+00	5.6978e+00	1.037e-05	5.340e-06	1.430e-06	3.620e-07	5.892e-08	6.256e-09	6.648e-10	5.543e-11	
5.6978e+00	5.3525e+00	1.080e-05	5.674e-06	1.525e-06	3.854e-07	6.268e-08	6.623e-09	7.020e-10	5.887e-11	
5.3525e+00	5.0282e+00	1.108e-05	5.895e-06	1.581e-06	3.979e-07	6.519e-08	6.907e-09	7.328e-10	6.287e-11	
5.0282e+00	4.7236e+00	1.188e-05	6.272e-06	1.689e-06	4.258e-07	7.023e-08	7.467e-09	7.937e-10	6.915e-11	
4.7236e+00	4.4374e+00	1.300e-05	6.638e-06	1.793e-06	4.517e-07	7.509e-08	8.018e-09	8.536e-10	7.597e-11	
4.4374e+00	4.1686e+00	1.421e-05	6.975e-06	1.892e-06	4.771e-07	7.988e-08	8.582e-09	9.159e-10	8.334e-11	
4.1686e+00	3.9160e+00	1.515e-05	7.395e-06	2.015e-06	5.089e-07	8.602e-08	9.286e-09	9.941e-10	9.224e-11	
3.9160e+00	3.6787e+00	1.567e-05	7.731e-06	2.109e-06	5.319e-07	9.153e-08	9.964e-09	1.071e-09	1.038e-10	
3.6787e+00	3.4559e+00	1.657e-05	8.215e-06	2.248e-06	5.678e-07	9.853e-08	1.079e-08	1.164e-09	1.155e-10	
3.4559e+00	3.2465e+00	1.798e-05	8.987e-06	2.481e-06	6.293e-07	1.104e-07	1.219e-08	1.320e-09	1.346e-10	
3.2465e+00	3.0498e+00	1.959e-05	1.009e-05	2.833e-06	7.264e-07	1.277e-07	1.419e-08	1.542e-09	1.563e-10	
3.0498e+00	2.8650e+00	2.100e-05	1.111e-05	3.175e-06	8.233e-07	1.473e-07	1.656e-08	1.813e-09	1.876e-10	
2.8650e+00	2.6914e+00	2.261e-05	1.203e-05	3.466e-06	9.031e-07	1.635e-07	1.852e-08	2.038e-09	2.152e-10	
2.6914e+00	2.5284e+00	2.394e-05	1.276e-05	3.690e-06	9.616e-07	1.751e-07	1.988e-08	2.193e-09	2.337e-10	
2.5284e+00	2.3752e+00	2.572e-05	1.409e-05	4.162e-06	1.098e-06	2.037e-07	2.341e-08	2.604e-09	2.846e-10	
2.3752e+00	2.2313e+00	2.871e-05	1.613e-05	4.882e-06	1.311e-06	2.503e-07	2.947e-08	3.311e-09	3.819e-10	
2.2313e+00	2.0961e+00	2.825e-05	1.570e-05	4.736e-06	1.268e-06	2.458e-07	2.911e-08	3.307e-09	3.927e-10	
2.0961e+00	1.9691e+00	2.872e-05	1.588e-05	4.762e-06	1.269e-06	2.475e-07	2.931e-08	3.335e-09	4.029e-10	
1.9691e+00	1.8498e+00	2.925e-05	1.628e-05	4.903e-06	1.308e-06	2.590e-07	3.091e-08	3.536e-09	4.441e-10	
1.8498e+00	1.7377e+00	3.178e-05	1.807e-05	5.541e-06	1.496e-06	3.012e-07	3.664e-08	4.245e-09	5.588e-10	
1.7377e+00	1.5335e+00	3.164e-05	1.799e-05	5.531e-06	1.494e-06	3.033e-07	3.711e-08	4.323e-09	5.809e-10	
1.5335e+00	1.3533e+00	3.535e-05	2.039e-05	6.438e-06	1.767e-06	3.725e-07	4.687e-08	5.578e-09	8.119e-10	
1.3533e+00	1.1943e+00	3.918e-05	2.231e-05	7.139e-06	1.974e-06	4.339e-07	5.599e-08	6.818e-09	1.104e-09	
1.1943e+00	1.0540e+00	4.008e-05	2.268e-05	7.336e-06	2.044e-06	4.641e-07	6.139e-08	7.660e-09	1.360e-09	
1.0540e+00	9.3013e-01	4.258e-05	2.318e-05	7.540e-06	2.106e-06	5.066e-07	6.889e-08	8.865e-09	1.868e-09	
9.3013e-01	8.2084e-01	4.360e-05	2.309e-05	7.718e-06	2.195e-06	5.266e-07	7.378e-08	9.749e-09	2.105e-09	
8.2084e-01	7.2438e-01	4.981e-05	2.558e-05	8.702e-06	2.495e-06	6.080e-07	8.633e-08	1.159e-08	2.553e-09	
7.2438e-01	6.3927e-01	6.327e-05	3.1545e-05	1.129e-05	3.348e-06	9.110e-07	1.391e-07	2.020e-08	5.637e-09	
6.3927e-01	5.6415e-01	5.684e-05	2.646e-05	6.685e-06	2.932e-06	8.300e-07	1.327e-07	2.046e-08	6.406e-09	
5.6415e-01	4.9786e-01	5.048e-05	2.224e-05	8.148e-06	2.473e-06	6.979e-07	1.127e-07	1.781e-08	5.692e-09	
4.9786e-01	4.3936e-01	4.791e-05	1.990e-05	7.195e-06	2.168e-06	6.341e-07	1.024e-07	1.658e-08	5.659e-09	
4.3936e-01	3.8774e-01	4.405e-05	1.756e-05	6.308e-06	1.891e-06	5.500e-07	8.850e-08	1.449e-08	5.005e-09	
3.8774e-01	3.4217e-01	6.913e-05	2.520e-05	9.323e-06	2.840e-06	9.023e-07	1.510e-07	2.658e-08	1.109e-08	
3.4217e-01	3.0197e-01	6.								

Table 3.4 Continued.

Energy [MeV]		Flux / Lethargy / Source Neutron								
Upper	Lower	-10 mm	127 mm	229 mm	330 mm	457 mm	610 mm	762 mm	914 mm	
5.2474e-02	4.6308e-02	1.869e-05	6.336e-06	2.685e-06	8.850e-07	2.510e-07	4.870e-08	1.090e-08	6.214e-09	
4.6308e-02	4.0867e-02	1.548e-05	5.533e-06	2.350e-06	7.760e-07	2.168e-07	4.218e-08	9.347e-09	5.219e-09	
4.0867e-02	3.6065e-02	1.222e-05	4.489e-06	1.911e-06	6.323e-07	1.684e-07	3.286e-08	7.179e-09	3.889e-09	
3.6065e-02	3.1827e-02	9.538e-06	3.538e-06	1.511e-06	5.007e-07	1.259e-07	2.461e-08	5.299e-09	2.794e-09	
3.1827e-02	2.8087e-02	3.371e-06	1.078e-06	4.587e-07	1.519e-07	3.763e-08	7.355e-09	1.580e-09	8.306e-10	
2.8087e-02	2.4787e-02	2.833e-05	1.123e-05	4.829e-06	1.607e-06	4.675e-07	9.222e-08	2.042e-08	1.129e-08	
2.4787e-02	2.1874e-02	1.627e-05	6.207e-06	2.685e-06	8.977e-07	2.750e-07	5.468e-08	1.252e-08	7.434e-09	
2.1874e-02	1.9304e-02	1.096e-05	4.129e-06	1.792e-06	6.005e-07	1.719e-07	3.432e-08	7.810e-09	4.565e-09	
1.9304e-02	1.5034e-02	5.223e-06	1.858e-06	8.066e-07	2.707e-07	6.252e-08	1.250e-08	2.750e-09	1.498e-09	
1.5034e-02	1.1709e-02	7.739e-06	3.607e-06	1.566e-06	5.263e-07	1.153e-07	2.312e-08	4.877e-09	2.434e-09	
1.1709e-02	9.1186e-03	7.452e-06	3.893e-06	1.687e-06	5.675e-07	1.262e-07	2.535e-08	5.183e-09	2.385e-09	
9.1186e-03	7.1016e-03	4.833e-06	2.386e-06	1.036e-06	3.486e-07	7.525e-08	1.512e-08	3.051e-09	1.372e-09	
7.1016e-03	5.5307e-03	5.656e-06	2.900e-06	1.258e-06	4.238e-07	8.774e-08	1.764e-08	3.501e-09	1.500e-09	
5.5307e-03	4.3073e-03	6.546e-06	3.771e-06	1.635e-06	5.513e-07	1.144e-07	2.302e-08	4.481e-09	1.802e-09	
4.3073e-03	3.3546e-03	7.609e-06	4.916e-06	2.128e-06	7.185e-07	1.576e-07	3.177e-08	6.088e-09	2.336e-09	
3.3546e-03	2.6125e-03	7.020e-06	4.688e-06	2.028e-06	6.854e-07	1.601e-07	3.225e-08	6.124e-09	2.281e-09	
2.6125e-03	2.0346e-03	6.316e-06	4.226e-06	1.826e-06	6.178e-07	1.469e-07	2.960e-08	5.588e-09	2.051e-09	
2.0346e-03	1.5846e-03	5.717e-06	4.972e-06	2.146e-06	7.272e-07	1.829e-07	3.686e-08	6.959e-09	2.541e-09	
1.5846e-03	1.2341e-03	7.262e-06	4.728e-06	2.038e-06	6.920e-07	1.812e-07	3.652e-08	6.927e-09	2.545e-09	
1.2341e-03	9.6110e-04	6.216e-06	3.951e-06	1.702e-06	5.787e-07	1.502e-07	3.027e-08	5.752e-09	2.101e-09	
9.6110e-04	5.8293e-04	5.848e-06	3.901e-06	1.677e-06	5.721e-07	1.445e-07	2.909e-08	5.476e-09	1.935e-09	
5.8293e-04	3.5357e-04	3.999e-06	2.580e-06	1.108e-06	3.787e-07	8.485e-08	1.709e-08	3.158e-09	1.031e-09	
3.5357e-04	2.1445e-04	5.366e-06	4.145e-06	1.777e-06	6.085e-07	1.382e-07	2.784e-08	5.034e-09	1.558e-09	
2.1445e-04	1.3007e-04	4.692e-06	3.556e-06	1.521e-06	5.222e-07	1.180e-07	2.374e-08	4.245e-09	1.221e-09	
1.3007e-04	7.8891e-05	4.931e-06	4.025e-06	1.718e-06	5.912e-07	1.370e-07	2.756e-08	4.881e-09	1.335e-09	
7.8891e-05	4.7850e-05	4.625e-06	3.847e-06	1.639e-06	5.654e-07	1.322e-07	2.655e-08	4.668e-09	1.223e-09	
4.7850e-05	2.9023e-05	3.965e-06	3.203e-06	1.362e-06	4.710e-07	1.058e-07	2.121e-08	3.699e-09	9.110e-10	
2.9023e-05	1.7603e-05	3.925e-06	3.341e-06	1.419e-06	4.916e-07	1.073e-07	2.147e-08	3.693e-09	8.327e-10	
1.7603e-05	1.0677e-05	3.752e-06	3.313e-06	1.404e-06	4.876e-07	1.046e-07	2.091e-08	3.554e-09	7.331e-10	
1.0677e-05	6.4758e-06	3.553e-06	3.213e-06	1.359e-06	4.730e-07	9.978e-08	1.990e-08	3.344e-09	6.288e-10	
6.4758e-06	3.9227e-06	3.325e-06	3.033e-06	1.281e-06	4.467e-07	9.189e-08	1.829e-08	3.041e-09	5.160e-10	
3.9227e-06	2.3823e-06	3.073e-06	2.795e-06	1.178e-06	4.116e-07	8.155e-08	1.620e-08	2.663e-09	4.007e-10	
2.3823e-06	1.4449e-06	2.795e-06	2.497e-06	1.051e-06	3.677e-07	6.910e-08	1.370e-08	2.224e-09	2.889e-10	
1.4449e-06	8.7640e-07	2.511e-06	2.160e-06	9.069e-07	3.178e-07	5.569e-08	1.101e-08	1.767e-09	1.906e-10	
8.7640e-07	5.3156e-07	2.238e-06	1.819e-06	7.618e-07	2.674e-07	4.299e-08	8.480e-09	1.346e-09	1.146e-10	
5.3156e-07	3.2241e-07	1.971e-06	1.476e-06	6.164e-07	2.166e-07	3.145e-08	6.188e-09	9.741e-10	6.156e-11	
3.2241e-07	1.0010e-11	1.060e-06	2.695e-07	1.064e-07	3.763e-08	2.426e-09	4.697e-10	8.197e-11	8.753e-13	

Table 3.5 Neutron spectra at the eight positions in the assembly calculated by DOT with the FUSION-J3 library of 125 neutron groups.

Energy [MeV]		Flux / Lethargy / Source Neutron								
Upper	Lower	-10 mm	127 mm	229 mm	330 mm	457 mm	610 mm	762 mm	914 mm	
1.5488e+01	1.5248e+01	8.547e-04	8.708e-05	1.502e-05	2.749e-06	3.329e-07	2.615e-08	2.118e-09	1.480e-10	
1.5248e+01	1.5012e+01	1.332e-03	1.495e-04	2.769e-05	5.438e-06	7.205e-07	6.235e-08	5.511e-09	4.190e-10	
1.5012e+01	1.4779e+01	2.420e-03	2.744e-04	5.096e-05	9.906e-05	1.304e-06	1.135e-07	1.018e-08	7.874e-10	
1.4779e+01	1.4550e+01	1.401e-03	1.967e-04	4.061e-05	8.709e-06	1.260e-06	1.203e-07	1.161e-08	9.506e-10	
1.4550e+01	1.4324e+01	2.463e-04	6.994e-05	1.799e-05	4.473e-06	7.396e-07	8.010e-08	8.549e-09	7.603e-10	
1.4324e+01	1.4102e+01	9.914e-05	3.460e-05	9.142e-06	2.390e-06	4.200e-07	4.882e-08	5.568e-09	5.264e-10	
1.4102e+01	1.3883e+01	6.443e-05	2.601e-05	5.587e-06	1.684e-06	2.919e-07	3.406e-08	3.942e-09	3.783e-10	
1.3883e+01	1.3668e+01	4.738e-05	2.216e-05	5.719e-06	1.450e-06	2.453e-07	2.802e-08	3.199e-09	3.030e-10	
1.3668e+01	1.3456e+01	1.2545e-05	1.571e-05	4.435e-06	1.173e-06	2.023e-07	2.345e-08	2.699e-09	2.538e-10	
1.3456e+01	1.3248e+01	6.837e-06	1.144e-05	3.369e-06	9.235e-07	1.634e-07	1.932e-08	2.255e-09	2.127e-10	
1.3248e+01	1.3042e+01	1.260e-05	9.629e-06	2.761e-06	7.568e-07	1.347e-07	1.604e-08	1.889e-09	1.783e-10	
1.3042e+01	1.2840e+01	1.727e-05	8.499e-06	2.372e-06	6.423e-07	1.136e-07	1.350e-08	1.591e-09	1.500e-10	
1.2840e+01	1.2641e+01	1.746e-05	7.614e-06	2.118e-06	5.704e-07	1.003e-07	1.184e-08	1.388e-09	1.294e-10	
1.2641e+01	1.2445e+01	1.611e-05	6.872e-06	1.917e-06	5.154e-07	9.026e-08	1.059e-08	1.236e-09	1.142e-10	
1.2445e+01	1.2252e+01	1.312e-05	6.091e-06	1.726e-06	4.668e-07	8.173e-08	9.575e-09	1.113e-09	1.020e-10	
1.2252e+01	1.2062e+01	1.089e-05	5.455e-06	1.575e-06	4.293e-07	7.525e-08	8.811e-09	1.021e-09	9.282e-11	
1.2062e+01	1.1875e+01	9.978e-06	5.061e-06	1.463e-06	3.985e-07	6.969e-08	8.129e-09	9.380e-10	8.493e-11	
1.1875e+01	1.1691e+01	9.514e-06	4.820e-06	1.383e-06	3.753e-07	6.531e-08	7.583e-09	8.712e-10	7.825e-11	
1.1691e+01	1.1510e+01	9.386e-06	4.640e-06	1.321e-06	3.572e-07	6.182e-08	7.152e-09	8.184e-10	7.293e-11	
1.1510e+01	1.1331e+01	6.712e-06	4.356e-06	1.247e-06	3.388e-07	5.874e-08	6.791e-09	7.770e-10	6.849e-11	
1.1331e+01	1.1156e+01	4.950e-06	4.114e-06	1.179e-06	3.204e-07	5.559e-08	6.411e-09	7.333e-10	6.418e-11	
1.1156e+01	1.0983e+01	4.508e-06	4.076e-06	1.162e-06	3.144e-07	5.422e-08	6.203e-09	7.060e-10	6.090e-11	
1.0983e+01	1.0812e+01	4.206e-06	4.138e-06	1.182e-06	3.189e-07	5.466e-08	6.202e-09	7.012e-10	5.926e-11	
1.0812e+01	1.0645e+01	4.139e-06	4.315e-06	1.228e-06	3.289e-07	5.611e-08	6.318e-09	7.089e-10	5.954e-11	
1.0645e+01	1.0480e+01	4.183e-06	4.496e-06	1.270e-06	3.371e-07	5.718e-08	6.384e-09	7.099e-10	5.977e-11	
1.0480e+01	1.0317e+01	4.189e-06	4.699e-06	1.318e-06	3.465e-07	5.845e-08	6.476e-09	7.147e-10	6.042e-11	
1.0317e+01	1.0157e+01	4.524e-06	4.849e-06	1.350e-06	3.530e-07	5.936e-08	6.525e-09	7.135e-10	6.033e-11	
1.0157e+01	9.9999e+00	5.682e-06	5.096e-06	1.407e-06	3.663e-07	6.153e-08	6.741e-09	7.339e-10	6.212e-11	
9.9999e+00	9.3940e+00	6.129e-06	4.511e-06	1.247e-06	3.278e-07	5.548e-08	6.144e-09	6.749e-10	5.651e-11	
9.3940e+00	8.8249e+00	5.784e-06	4.189e-06	1.155e-06	3.031e-07	5.071e-08	5.570e-09	6.088e-10	4.975e-11	
8.8249e+00	8.2902e+00	5.913e-06	4.730e-06	1.268e-06						

Table 3.5 Continued.

Energy [MeV] Upper	Energy [MeV] Lower	-10 mm	127 mm	Flux / Lethargy / Source Neutron 229 mm 330 mm 457 mm 610 mm 762 mm 914 mm
6.4564e+00	6.0652e+00	1.000e-05	5.081e-06	1.361e-06 3.454e-07 5.598e-08 5.934e-09 6.297e-10 5.155e-11
6.0652e+00	5.6978e+00	1.037e-05	5.335e-06	1.427e-06 3.611e-07 5.872e-08 6.228e-09 6.611e-10 5.506e-11
5.6978e+00	5.3525e+00	1.079e-05	5.670e-06	1.523e-06 3.846e-07 6.248e-08 6.596e-09 6.983e-10 5.851e-11
5.3525e+00	5.0282e+00	1.106e-05	5.885e-06	1.577e-06 3.965e-07 6.490e-08 6.869e-09 7.281e-10 6.247e-11
5.0282e+00	4.7236e+00	1.186e-05	6.267e-06	1.687e-06 4.248e-07 6.999e-08 7.433e-09 7.893e-10 6.870e-11
4.7236e+00	4.4374e+00	1.296e-05	6.633e-06	1.790e-06 4.507e-07 7.484e-08 7.983e-09 8.489e-10 7.547e-11
4.4374e+00	4.1686e+00	1.416e-05	6.964e-06	1.887e-06 4.754e-07 7.950e-08 8.529e-09 9.022e-10 8.263e-11
4.1686e+00	3.9160e+00	1.512e-05	7.390e-06	2.012e-06 5.077e-07 8.573e-08 9.243e-09 9.883e-10 9.162e-11
3.9160e+00	3.6787e+00	1.564e-05	7.715e-06	2.102e-06 5.295e-07 9.104e-08 9.899e-09 1.062e-09 1.029e-10
3.6787e+00	3.4559e+00	1.654e-05	8.207e-06	2.244e-06 5.663e-07 9.813e-08 1.073e-08 1.156e-09 1.145e-10
3.4559e+00	3.2465e+00	1.795e-05	8.984e-06	2.478e-06 6.280e-07 1.100e-07 1.213e-08 1.311e-09 1.335e-10
3.2465e+00	3.0498e+00	1.953e-05	1.007e-05	2.826e-06 7.235e-07 1.270e-07 1.409e-08 1.529e-09 1.548e-10
3.0498e+00	2.8650e+00	2.095e-05	1.110e-05	3.168e-06 8.204e-07 1.466e-07 1.644e-08 1.797e-09 1.855e-10
2.8650e+00	2.6914e+00	2.256e-05	1.202e-05	3.462e-06 9.009e-07 1.629e-07 1.841e-08 2.023e-09 2.130e-10
2.6914e+00	2.5284e+00	2.385e-05	1.272e-05	3.673e-06 9.556e-07 1.736e-07 1.966e-08 2.165e-09 2.299e-10
2.5284e+00	2.3752e+00	2.564e-05	1.405e-05	4.142e-06 1.090e-06 2.017e-07 2.312e-08 2.556e-09 2.791e-10
2.3752e+00	2.2313e+00	2.863e-05	1.608e-05	4.855e-06 1.300e-06 2.475e-07 2.902e-08 3.269e-09 3.727e-10
2.2313e+00	2.0961e+00	2.829e-05	1.572e-05	4.735e-06 1.265e-06 2.447e-07 2.887e-08 3.270e-09 3.864e-10
2.0961e+00	1.9691e+00	2.871e-05	1.585e-05	4.744e-06 1.261e-06 2.453e-07 2.895e-08 3.284e-09 3.945e-10
1.9691e+00	1.8498e+00	2.910e-05	1.611e-05	4.832e-06 1.284e-06 2.530e-07 3.001e-08 3.417e-09 4.241e-10
1.8498e+00	1.7377e+00	3.187e-05	1.808e-05	5.524e-06 1.485e-06 2.978e-07 3.598e-08 4.146e-09 5.401e-10
1.7377e+00	1.5335e+00	3.162e-05	1.791e-05	5.485e-06 1.475e-06 2.980e-07 3.620e-08 4.192e-09 5.569e-10
1.5335e+00	1.3533e+00	3.541e-05	2.033e-05	6.388e-06 1.744e-06 3.651e-07 4.551e-08 5.372e-09 7.683e-10
1.3533e+00	1.1943e+00	3.924e-05	2.219e-05	7.054e-06 1.937e-06 4.225e-07 5.384e-08 6.484e-09 1.026e-09
1.1943e+00	1.0540e+00	4.031e-05	2.265e-05	7.284e-06 2.016e-06 4.539e-07 5.925e-08 7.300e-09 1.262e-09
1.0540e+00	9.3013e-01	4.303e-05	2.318e-05	7.489e-06 2.076e-06 4.949e-07 6.624e-08 8.394e-09 1.709e-09
9.3013e-01	8.2084e-01	4.405e-05	2.316e-05	7.692e-06 2.171e-06 5.165e-07 7.122e-08 9.256e-09 1.938e-09
8.2084e-01	7.2438e-01	4.967e-05	2.538e-05	8.556e-06 2.430e-06 5.852e-07 8.158e-08 1.075e-08 2.280e-09
7.2438e-01	6.3927e-01	6.320e-05	3.127e-05	1.106e-05 3.237e-06 8.634e-07 1.279e-07 1.796e-08 4.664e-09
6.3927e-01	5.6415e-01	5.764e-05	2.672e-05	9.685e-06 2.891e-06 8.053e-07 1.247e-07 1.850e-08 5.402e-09
5.6415e-01	4.9786e-01	5.174e-05	2.265e-05	8.229e-06 2.466e-06 8.894e-07 1.081e-07 1.646e-08 4.960e-09
4.9786e-01	4.3936e-01	4.931e-05	2.023e-05	7.254e-06 2.159e-06 6.294e-07 9.887e-08 1.545e-08 5.021e-09
4.3936e-01	3.8774e-01	4.498e-05	1.766e-05	6.288e-06 1.863e-06 5.402e-07 8.470e-08 1.339e-08 4.426e-09
3.8774e-01	3.4217e-01	6.941e-05	2.502e-05	9.144e-06 2.745e-06 8.585e-07 1.389e-07 2.328e-08 8.958e-09
3.4217e-01	3.0197e-01	7.127e-05	2.308e-05	8.561e-06 2.597e-06 8.427e-07 1.406e-07 2.514e-08 1.101e-08
3.0197e-01	2.6649e-01	5.129e-05	1.677e-05	6.222e-06 1.896e-06 5.845e-07 9.877e-08 1.793e-08 7.968e-09
2.6649e-01	2.3517e-01	4.079e-05	1.384e-05	5.124e-06 1.561e-06 4.553e-07 7.717e-08 1.390e-08 5.977e-09
2.3517e-01	2.0754e-01	4.134e-05	1.419e-05	5.267e-06 1.607e-06 4.672e-07 7.923e-08 1.428e-08 6.064e-09
2.0754e-01	1.8315e-01	3.126e-05	1.079e-05	4.015e-06 1.226e-06 3.426e-07 5.805e-08 1.037e-08 4.269e-09
1.8315e-01	1.6163e-01	4.035e-05	1.416e-05	5.348e-06 1.644e-06 4.810e-07 8.218e-08 1.486e-08 6.236e-09
1.6163e-01	1.4264e-01	2.359e-05	8.140e-06	3.060e-06 9.390e-07 2.605e-07 4.432e-08 7.930e-09 3.227e-09
1.4264e-01	1.2588e-01	4.811e-05	1.623e-05	6.217e-06 1.924e-06 5.914e-07 1.020e-07 1.887e-08 8.179e-09
1.2588e-01	1.1109e-01	3.803e-05	1.193e-05	4.676e-06 1.463e-06 4.720e-07 8.292e-08 1.597e-08 7.516e-09
1.1109e-01	9.8035e-02	2.319e-05	6.988e-06	2.757e-06 8.655e-07 2.621e-07 4.622e-08 8.896e-09 4.141e-09
9.8035e-02	8.6515e-02	2.701e-05	8.462e-06	3.373e-06 1.064e-06 3.197e-07 5.684e-08 1.103e-08 5.160e-09
8.6515e-02	7.6349e-02	3.994e-05	1.160e-05	4.692e-06 1.486e-06 4.863e-07 8.746e-08 1.764e-08 8.837e-09
7.6349e-02	6.7378e-02	3.085e-05	8.469e-06	3.460e-06 1.105e-06 3.671e-07 6.676e-08 1.392e-08 7.336e-09
6.7378e-02	5.9461e-02	2.698e-05	7.296e-06	3.018e-06 9.699e-07 3.173e-07 5.829e-08 1.243e-08 6.771e-09
5.9461e-02	5.2474e-02	1.909e-05	5.358e-06	2.235e-06 7.213e-07 2.202e-07 4.078e-08 8.702e-09 4.712e-09
5.2474e-02	4.6308e-02	2.272e-05	6.623e-06	2.768e-06 8.946e-07 2.698e-07 5.015e-08 1.073e-08 5.840e-09
4.6308e-02	4.0867e-02	1.913e-05	5.887e-06	2.471e-06 8.010e-07 2.374e-07 4.440e-08 9.516e-09 5.181e-09
4.0867e-02	3.6065e-02	1.496e-05	4.700e-06	1.980e-06 6.434e-07 1.817e-07 3.412e-08 7.265e-09 3.894e-09
3.6065e-02	3.1827e-02	1.138e-05	3.595e-06	1.520e-06 4.948e-07 1.313e-07 2.473e-08 5.220e-09 2.749e-09
3.1827e-02	2.8087e-02	3.223e-06	8.825e-07	3.716e-07 1.208e-07 3.190e-08 6.003e-09 1.266e-09 6.651e-10
2.8087e-02	2.4787e-02	2.934e-05	1.036e-05	4.381e-06 1.427e-06 3.815e-07 7.207e-08 1.501e-08 7.824e-09
2.4787e-02	2.1874e-02	2.141e-05	7.443e-06	3.176e-06 1.041e-06 3.123e-07 5.972e-08 1.297e-08 7.326e-09
2.1874e-02	1.9304e-02	1.420e-05	4.681e-06	2.007e-06 6.596e-07 1.923e-07 3.699e-08 8.061e-09 4.548e-09
1.9304e-02	1.5034e-02	5.554e-06	1.633e-06	7.007e-07 2.306e-07 5.597e-08 1.079e-08 2.306e-09 1.255e-09
1.5034e-02	1.1709e-02	9.408e-06	3.696e-06	1.588e-06 5.236e-07 1.180e-07 2.285e-08 4.716e-09 2.382e-09
1.1709e-02	9.1186e-03	3.956e-06	1.701e-06	5.618e-07 1.271e-07 2.470e-08 4.953e-09 2.330e-09 1.991e-09
9.1186e-03	7.1016e-03	5.589e-06	2.357e-06	1.013e-06 3.437e-07 7.360e-08 1.431e-08 2.838e-09 1.309e-09
7.1016e-03	5.5307e-03	6.503e-06	2.863e-06	1.231e-06 4.069e-07 8.548e-08 1.664e-08 3.249e-09 1.439e-09
5.5307e-03	4.3073e-03	7.682e-06	3.821e-06	1.641e-06 5.432e-07 1.138e-07 2.219e-08 4.250e-09 1.777e-09
4.3073e-03	3.3546e-03	8.921e-06	4.943e-06	2.121e-06 7.028e-07 1.548e-07 3.029e-08 5.709e-09 2.288e-09
3.3546e-03	2.6125e-03	8.153e-06	4.705e-06	2.016e-06 6.691e-07 1.562e-07 3.054e-08 5.710e-09 2.227e-09
2.6125e-03	2.0346e-03	7.269e-06	4.218e-06	1.806e-06 5.999e-07 1.422e-07 2.783e-08 4.953e-09 2.330e-09
2.0346e-03	1.5846e-03	8.6474e-06	4.944e-06	2.114e-06 7.034e-07 1.756e-07 3.438e-08 6.386e-09 2.445e-09
1.5846e-03	1.2341e-03	8.391e-06	4.729e-06	2.020e-06 6.734e-07 1.747e-07 3.424e-08 6.384e-09 2.456e-09
1.2341e-03	9.6110e-04	6.100e-06	3.266e-06	1.394e-06 4.653e-07 1.164e-07 2.280e-08 4.244e-09 1.612e-09
9.6110e-04	5.8293e-04	6.028e-06	3.591e-06	1.529e-06 5.121e-07 1.209e-07 2.373e-08 4.301e-09 1.508e-09
5.8293e-04	3.5357e-04	3.858e-06	2.231e-06	9.481e-07 3.183e-07 6.545e-08 1.283e-08 2.272e-09 7.198e-10
3.5357e-04	2.1445e-04	5.249e-06	3.802e-06	1.613e-06 5.422e-07 1.128e-07 2.212e-08 3.785e-09 1.117e-09
2.1445e-04	1.3007e-04	4.538e-06	3.164e-06	1.338e-06 4.509e-07 9.234e-08 1.808e-08 3.048e-09 7.998e-10
1.3007e-04	7.8891e-05	5.036e-06	3.958e-06	1.668e-06 5.636e-07 1.209e-07 2.365e-08 3.934e-09 9.509e-10
7.8891e-05	4.7850e-05	4.732e-06	3.811e-06	1.602e-06 5.424e-07 1.194e-07 2.334e-08 3.847e-09 8.789e-10
4.7850e-05	2.9023e-05	3.694e-06	2.726e-06	1.143e-06 3.879e-07 8.058e-08 1.573e-08 2.570e-09 5.443e-10
2.9023e-05	1.7603e-05	3.804e-06	3.039e-06	1.271e-06 4.322e-07 8.626e-08 1.680e-08 2.696e-09 4.990e-10
1.7603e-05	1.0677e-05	3.686e-06	3.110e-06	1.297e-06 4.420e-07 8.735e-08 1.698e-08 2.688e-09 4.403e-10
1.0677e-				

Table 3.6 Neutron spectra at the eight positions in the assembly calculated by DOT with the JSSTD library of 42 neutron groups.

Energy [MeV] Upper	Energy [MeV] Lower	Flux / Lethargy / Source Neutron							
		-10 mm	127 mm	229 mm	330 mm	457 mm	610 mm	762 mm	914 mm
1.5000e+01	1.3720e+01	1.125e-03	1.360e-04	2.624e-05	5.375e-06	7.487e-07	6.960e-08	6.660e-09	5.541e-10
1.3720e+01	1.2549e+01	1.961e-05	1.923e-06	5.257e-06	1.347e-06	2.261e-07	2.509e-08	2.764e-09	2.520e-10
1.2549e+01	1.1478e+01	1.060e-05	6.392e-06	1.835e-06	4.964e-07	8.697e-08	1.010e-08	1.154e-09	1.053e-10
1.1478e+01	1.0500e+01	6.868e-06	4.650e-06	1.339e-06	3.629e-07	6.257e-08	7.156e-09	8.081e-10	6.945e-11
1.0500e+01	9.3140e+00	5.120e-06	4.641e-06	1.291e-06	3.387e-07	5.686e-08	6.265e-09	6.844e-10	5.689e-11
9.3140e+00	8.2610e+00	6.009e-06	4.400e-06	1.194e-06	3.087e-07	5.072e-08	5.458e-09	5.851e-10	4.674e-11
8.2610e+00	7.3280e+00	6.213e-06	4.922e-06	1.304e-06	3.303e-07	5.272e-08	5.511e-09	5.785e-10	4.480e-11
7.3280e+00	6.5000e+00	7.609e-06	5.013e-06	1.320e-06	3.318e-07	5.269e-08	5.478e-09	5.726e-10	4.480e-11
6.5000e+00	5.7570e+00	9.778e-06	5.150e-06	1.368e-06	3.449e-07	5.529e-08	5.786e-09	6.064e-10	4.892e-11
5.7570e+00	5.0990e+00	1.124e-05	5.792e-06	1.548e-06	3.883e-07	6.262e-08	6.534e-09	6.829e-10	5.687e-11
5.0990e+00	4.5160e+00	1.239e-05	6.432e-06	1.719e-06	4.299e-07	7.019e-08	7.371e-09	7.723e-10	6.681e-11
4.5160e+00	4.0000e+00	1.411e-05	7.183e-06	1.933e-06	4.837e-07	8.006e-08	8.481e-09	8.919e-10	8.013e-11
4.0000e+00	3.1620e+00	1.687e-05	8.388e-06	2.301e-06	5.809e-07	1.001e-07	1.089e-08	1.161e-09	1.148e-10
3.1620e+00	2.5000e+00	2.213e-05	1.169e-05	3.374e-06	8.794e-07	1.536e-07	1.789e-08	1.951e-09	2.058e-10
2.5000e+00	1.8710e+00	2.726e-05	1.496e-05	4.501e-06	1.204e-06	2.325e-07	2.751e-08	3.114e-09	3.727e-10
1.8710e+00	1.4000e+00	3.193e-05	1.762e-05	5.475e-06	1.492e-06	3.058e-07	3.785e-08	4.440e-09	6.136e-10
1.4000e+00	1.0580e+00	3.914e-05	2.132e-05	6.870e-06	1.910e-06	4.255e-07	5.579e-08	6.872e-09	1.191e-09
1.0580e+00	8.0000e-01	4.279e-05	2.231e-05	7.389e-06	2.094e-06	4.997e-07	6.948e-08	9.100e-09	1.938e-09
8.0000e-01	5.6600e-01	5.790e-05	2.686e-05	9.549e-06	2.847e-06	7.803e-07	1.228e-07	1.900e-08	5.979e-09
5.6600e-01	4.0000e-01	4.325e-05	1.810e-05	6.415e-06	1.906e-06	5.286e-07	8.363e-08	1.331e-08	4.365e-09
4.0000e-01	2.8300e-01	5.496e-05	2.022e-05	7.406e-06	2.247e-06	6.780e-07	1.133e-07	1.988e-08	8.265e-09
2.8300e-01	2.0000e-01	3.992e-05	1.416e-05	5.250e-06	1.608e-06	4.723e-07	8.046e-08	1.450e-08	6.089e-09
2.0000e-01	1.4100e-01	2.380e-05	8.851e-06	3.307e-06	1.017e-06	2.727e-07	4.650e-08	8.184e-09	3.104e-09
1.4100e-01	1.0000e-01	3.325e-05	1.163e-05	4.512e-06	1.415e-06	4.297e-07	7.574e-08	1.425e-08	6.255e-09
1.0000e-01	4.6500e-02	2.581e-05	7.813e-06	3.189e-06	1.026e-06	3.323e-07	6.122e-08	1.326e-08	7.345e-09
4.6500e-02	2.1500e-02	2.017e-05	5.761e-06	2.450e-06	8.057e-07	2.572e-07	4.938e-08	1.196e-08	7.776e-09
2.1500e-02	1.0000e-02	8.796e-06	3.633e-06	1.571e-06	5.233e-07	1.295e-07	2.551e-08	5.466e-09	2.954e-09
1.0000e-02	4.6500e-03	6.729e-06	3.307e-06	1.431e-06	4.785e-07	1.061e-07	2.104e-08	4.173e-09	2.038e-09
4.6500e-03	2.1500e-03	6.086e-06	3.517e-06	1.518e-06	5.095e-07	1.108e-07	2.209e-08	4.149e-09	1.739e-09
2.1500e-03	1.0000e-03	6.658e-06	4.154e-06	1.787e-06	6.020e-07	1.419e-07	2.839e-08	5.217e-09	1.979e-09
1.0000e-03	4.6500e-04	5.727e-06	3.761e-06	1.611e-06	5.453e-07	1.288e-07	2.580e-08	4.644e-09	1.607e-09
4.6500e-04	2.1500e-04	5.232e-06	3.753e-06	1.603e-06	5.445e-07	1.271e-07	2.545e-08	4.473e-09	1.473e-09
2.1500e-04	1.0000e-04	4.900e-06	3.643e-06	1.551e-06	5.289e-07	1.221e-07	2.444e-08	4.246e-09	1.278e-09
1.0000e-04	4.6500e-05	4.559e-06	3.586e-06	1.522e-06	5.211e-07	1.188e-07	2.372e-08	4.070e-09	1.121e-09
4.6500e-05	2.1500e-05	3.935e-06	3.139e-06	1.329e-06	4.565e-07	9.887e-08	1.970e-08	3.327e-09	8.160e-10
2.1500e-05	1.0000e-05	3.725e-06	3.184e-06	1.344e-06	4.633e-07	9.728e-08	1.934e-08	3.199e-09	6.804e-10
1.0000e-05	4.6500e-06	3.417e-06	3.026e-06	1.274e-06	4.404e-07	8.981e-08	1.780e-08	2.896e-09	5.294e-10
4.6500e-06	2.1500e-06	3.034e-06	2.703e-06	1.134e-06	3.932e-07	7.618e-08	1.506e-08	2.409e-09	3.674e-10
2.1500e-06	1.0000e-06	2.615e-06	2.252e-06	9.417e-07	3.274e-07	5.837e-08	1.149e-08	1.811e-09	2.183e-10
1.0000e-06	4.6500e-07	2.198e-06	1.751e-06	7.293e-07	2.541e-07	4.023e-08	7.892e-09	1.226e-09	1.076e-10
4.6500e-07	2.1500e-07	9.667e-07	4.289e-07	1.783e-07	6.222e-08	7.781e-09	1.524e-09	2.412e-10	1.656e-11
2.1500e-07	1.0000e-09	2.000e-06	5.197e-07	2.037e-07	7.154e-08	4.693e-09	9.044e-10	1.559e-10	2.140e-12

Table 3.7 Neutron spectra at the eight positions in the assembly calculated by DOT with the FUSION-40 library of 42 neutron groups.

Energy [MeV]		Flux / Lethargy / Source Neutron							
Upper	Lower	-10 mm	127 mm	229 mm	330 mm	457 mm	610 mm	762 mm	914 mm
1.5000e+01	1.3720e+01	1.125e-03	1.358e-04	2.619e-05	5.375e-06	7.461e-07	6.928e-08	6.623e-09	5.504e-10
1.3720e+01	1.2549e+01	1.942e-05	1.908e-05	5.208e-06	1.347e-06	2.234e-07	2.475e-08	2.723e-09	2.478e-10
1.2549e+01	1.1478e+01	1.108e-05	6.740e-06	1.931e-06	4.964e-07	9.116e-08	1.056e-08	1.205e-09	1.095e-10
1.1478e+01	1.0500e+01	6.712e-06	4.551e-06	1.308e-06	3.629e-07	6.100e-08	6.964e-09	7.851e-10	6.730e-11
1.0500e+01	9.3140e+00	5.083e-06	4.593e-06	1.277e-06	3.387e-07	5.611e-08	6.172e-09	6.733e-10	5.586e-11
9.3140e+00	8.2610e+00	6.027e-06	4.393e-06	1.191e-06	3.087e-07	5.051e-08	5.429e-09	5.812e-10	4.636e-11
8.2610e+00	7.3280e+00	6.121e-06	4.844e-06	1.282e-06	3.303e-07	5.174e-08	5.402e-09	5.664e-10	4.376e-11
7.3280e+00	6.5000e+00	7.651e-06	5.070e-06	1.334e-06	3.318e-07	5.316e-08	5.520e-09	5.763e-10	4.502e-11
6.5000e+00	5.7570e+00	9.919e-06	5.230e-06	1.389e-06	3.449e-07	5.601e-08	5.854e-09	6.127e-10	4.939e-11
5.7570e+00	5.0990e+00	1.105e-05	5.679e-06	1.515e-06	3.883e-07	6.116e-08	6.374e-09	6.654e-10	5.539e-11
5.0990e+00	4.5160e+00	1.234e-05	6.418e-06	1.713e-06	4.299e-07	6.982e-08	7.321e-09	7.662e-10	6.619e-11
4.5160e+00	4.0000e+00	1.404e-05	7.163e-06	1.925e-06	4.837e-07	7.954e-08	8.413e-09	8.836e-10	7.928e-11
4.0000e+00	3.1620e+00	1.692e-05	8.426e-06	2.310e-06	5.809e-07	1.003e-07	1.089e-08	1.159e-09	1.145e-10
3.1620e+00	2.5000e+00	2.195e-05	1.160e-05	3.342e-06	8.794e-07	1.565e-07	1.761e-08	1.917e-09	2.016e-10
2.5000e+00	1.8710e+00	2.717e-05	1.488e-05	4.461e-06	1.204e-06	2.287e-07	2.692e-08	3.032e-09	3.610e-10
1.8710e+00	1.4000e+00	3.195e-05	1.756e-05	5.430e-06	1.492e-06	3.000e-07	3.684e-08	4.289e-09	5.851e-10
1.4000e+00	1.0580e+00	3.895e-05	2.122e-05	6.766e-06	9.101e-06	4.119e-07	5.327e-08	6.501e-09	1.090e-09
1.0580e+00	8.0000e-01	4.296e-05	2.219e-05	7.274e-06	2.094e-06	4.817e-07	6.572e-08	8.451e-09	1.741e-09
8.0000e-01	5.6600e-01	5.818e-05	2.677e-05	9.392e-06	2.847e-06	7.402e-07	1.125e-07	1.667e-08	4.855e-09
5.6600e-01	4.0000e-01	4.423e-05	1.822e-05	6.366e-06	1.906e-06	5.128e-07	7.856e-08	1.202e-08	3.754e-09
4.0000e-01	2.8300e-01	5.629e-05	2.039e-05	7.353e-06	2.247e-06	6.509e-07	1.047e-07	1.742e-08	6.679e-09
2.8300e-01	2.0000e-01	4.121e-05	1.435e-05	5.241e-06	1.608e-06	4.589e-07	7.525e-08	1.287e-08	5.036e-09
2.0000e-01	1.4100e-01	2.381e-05	8.491e-06	3.109e-06	1.017e-06	2.454e-07	4.023e-08	6.707e-09	2.380e-09
1.4100e-01	1.0000e-01	3.449e-05	1.197e-05	4.546e-06	1.415e-06	4.130e-07	6.978e-08	1.229e-08	4.902e-09
1.0000e-01	4.6500e-02	2.732e-05	8.142e-06	3.244e-06	1.026e-06	3.283e-07	5.768e-08	1.141e-08	5.604e-09
4.6500e-02	2.1500e-02	2.633e-05	6.485e-06	2.673e-06	8.057e-07	2.845e-07	5.143e-08	1.109e-08	6.596e-09
2.1500e-02	1.0000e-02	1.515e-05	3.706e-06	1.571e-06	5.233e-07	1.336e-07	2.494e-08	5.160e-09	2.786e-09
1.0000e-02	4.6500e-03	8.595e-06	3.223e-06	1.373e-06	4.785e-07	1.038e-07	1.963e-08	3.835e-09	1.902e-09
4.6500e-03	2.1500e-03	6.824e-06	3.285e-06	1.398e-06	5.095e-07	9.850e-08	1.881e-08	3.480e-09	1.516e-09
2.1500e-03	1.0000e-03	7.275e-06	3.776e-06	1.602e-06	6.020e-07	1.167e-07	2.243e-08	4.009e-09	1.546e-09
1.0000e-03	4.6500e-04	6.293e-06	3.608e-06	1.523e-06	5.453e-07	1.117e-07	2.156e-08	3.714e-09	1.258e-09
4.6500e-04	2.1500e-04	5.357e-06	3.424e-06	1.441e-06	5.445e-07	1.047e-07	2.022e-08	3.353e-09	1.075e-09
2.1500e-04	1.0000e-04	5.132e-06	3.449e-06	1.444e-06	5.289e-07	1.034e-07	1.995e-08	3.254e-09	9.175e-10
1.0000e-04	4.6500e-05	4.796e-06	3.490e-06	1.454e-06	5.211e-07	1.042e-07	2.008e-08	3.222e-09	8.106e-10
4.6500e-05	2.1500e-05	3.814e-06	2.699e-06	1.121e-06	4.565e-07	7.438e-08	1.431e-08	2.257e-09	4.901e-10
2.1500e-05	1.0000e-05	3.715e-06	2.941e-06	1.215e-06	4.633e-07	7.819e-08	1.500e-08	2.303e-09	4.083e-10
1.0000e-05	4.6500e-06	3.438e-06	2.869e-06	1.180e-06	4.404e-07	7.491e-08	1.433e-08	2.162e-09	3.178e-10
4.6500e-06	2.1500e-06	3.075e-06	2.581e-06	1.057e-06	3.932e-07	6.467e-08	1.233e-08	1.835e-09	2.205e-10
2.1500e-06	1.0000e-06	2.688e-06	2.180e-06	8.872e-07	3.274e-07	5.060e-08	9.597e-09	1.412e-09	1.327e-10
1.0000e-06	4.6500e-07	2.277e-06	1.710e-06	6.921e-07	2.541e-07	3.548e-08	6.698e-09	9.768e-10	6.668e-11
4.6500e-07	2.1500e-07	1.002e-06	4.187e-07	1.692e-07	6.222e-08	6.892e-09	1.299e-09	1.935e-10	1.031e-11
2.1500e-07	1.0000e-09	1.994e-06	4.808e-07	1.830e-07	7.154e-08	3.951e-09	7.326e-10	1.203e-10	1.311e-12

Table 3.8 Measured and calculated integral neutron fluxes and their C/E ratios.

Energy Range	Position [mm]	Expt.	Error [8]	Calculated Reaction Rate				DOT-F-42		MCNP-J31		MCNP-J32		Calc. / Expt.	
				MCNP-J31	MCNP-J32	DOT-J-125	DOT-F-125	DOT-J-42	DOT-F-42	MCNP-J31	MCNP-J32	DOT-J-125	DOT-F-125	DOT-J-42	DOT-F-42
>10MeV	-10.0	9.350e-05	7.48	9.963e-05	9.648e-05	1.038e-04	1.039e-04	1.039e-04	1.039e-04	1.066	1.032	1.110	1.110	1.111	1.111
	127.0	1.527e-05	7.95	1.510e-05	1.502e-05	1.542e-05	1.541e-05	1.506e-05	1.506e-05	0.989	0.984	1.010	1.009	0.987	0.986
	228.6	3.316e-06	7.96	3.078e-06	3.284e-06	3.273e-06	3.270e-06	3.154e-06	3.154e-06	0.928	0.990	0.987	0.986	0.942	0.951
	330.2	7.352e-07	8.11	6.816e-07	7.089e-07	7.267e-07	7.256e-07	6.933e-07	6.920e-07	0.927	0.964	0.988	0.987	0.943	0.941
	457.2	1.104e-07	8.63	1.013e-07	1.036e-07	1.095e-07	1.095e-07	1.032e-07	1.029e-07	0.917	0.938	0.991	0.989	0.934	0.932
	609.6	1.095e-08	8.99	1.048e-08	1.042e-08	1.109e-08	1.105e-08	1.030e-08	1.026e-08	0.957	0.952	1.013	1.009	0.941	0.937
	762.0	1.114e-09	9.16	1.056e-09	1.126e-09	1.146e-09	1.141e-09	1.050e-09	1.045e-09	0.948	1.011	1.029	1.024	0.943	0.938
	914.4	9.724e-11	16.16	8.776e-11	9.659e-11	9.897e-11	9.841e-11	9.036e-11	9.979e-11	0.902	0.993	1.018	1.012	0.929	0.923
0.1-1MeV	-10.0	1.051e-04	5.00	1.010e-04	1.002e-04	1.044e-04	1.068e-04	9.036e-05	9.214e-05	0.961	0.953	0.993	1.016	0.859	0.876
	127.0	3.944e-05	5.00	4.138e-05	4.051e-05	4.172e-05	4.216e-05	3.598e-05	3.610e-05	1.049	1.027	1.058	1.069	0.912	0.915
	228.6	1.773e-05	5.00	1.509e-05	1.535e-05	1.526e-05	1.525e-05	1.309e-05	1.293e-05	0.960	0.976	0.970	0.970	0.832	0.822
	330.2	4.269e-06	5.00	4.515e-06	4.667e-06	4.623e-06	4.558e-06	3.956e-06	3.838e-06	0.967	1.000	0.990	0.976	0.847	0.822
	457.2	1.354e-06	5.00	1.326e-06	1.301e-06	1.336e-06	1.303e-06	1.126e-06	1.077e-06	0.980	0.961	0.987	0.963	0.832	0.795
	609.6	2.204e-07	5.00	2.194e-07	2.214e-07	2.207e-07	2.087e-07	1.853e-07	1.707e-07	0.996	1.005	1.002	0.947	0.841	0.775
	762.0	4.839e-08	5.00	3.762e-08	3.865e-08	3.820e-08	3.444e-08	3.144e-08	2.754e-08	0.777	0.799	0.789	0.712	0.650	0.569
	914.4	1.948e-08	5.00	1.534e-08	1.507e-08	1.535e-08	1.279e-08	1.191e-08	9.668e-09	0.788	0.774	0.788	0.657	0.612	0.496
10-100keV	-10.0	3.318e-05	5.00	3.181e-05	3.020e-05	3.507e-05	4.068e-05	4.206e-05	5.004e-05	0.959	0.910	1.057	1.226	1.268	1.508
	127.0	1.258e-05	5.00	1.122e-05	1.105e-05	1.222e-05	1.279e-05	1.321e-05	1.407e-05	0.893	0.878	0.972	1.017	1.050	1.119
	228.6	5.750e-06	5.00	4.799e-06	4.742e-06	5.176e-06	5.335e-06	5.534e-06	5.749e-06	0.835	0.825	0.900	0.928	0.962	1.000
	330.2	1.225e-06	5.00	1.630e-06	1.608e-06	1.709e-06	1.726e-06	1.807e-06	1.826e-06	0.847	0.835	0.888	0.897	0.939	0.949
	457.2	5.253e-07	5.00	4.421e-07	4.490e-07	4.856e-07	5.006e-07	5.520e-07	5.731e-07	0.842	0.855	0.925	0.953	1.051	1.091
	609.6	1.030e-07	5.00	8.361e-08	8.944e-08	9.422e-08	9.315e-08	1.045e-07	1.029e-07	0.860	0.867	0.915	0.904	1.014	0.999
	762.0	1.495e-08	5.00	2.009e-08	1.950e-08	2.085e-08	1.946e-08	2.356e-08	2.124e-08	1.344	1.344	1.395	1.302	1.576	1.421
	914.4	1.267e-08	5.00	1.120e-08	1.059e-08	1.167e-08	1.023e-08	1.388e-08	1.151e-08	0.884	0.836	0.921	0.807	1.096	0.909
10-100keV	-10.0									8.539e-06	9.366e-06	9.215e-06	9.379e-06	9.459e-06	
	127.0	7.078e-06	20.00	7.343e-06	7.678e-06	7.860e-06	7.334e-06	7.604e-06	7.006e-06	1.037	1.085	1.110	1.036	1.074	0.990
	228.6	3.453e-06	20.00	3.061e-06	3.167e-06	3.342e-06	3.074e-06	3.219e-06	3.208e-06	0.886	0.917	0.968	0.890	0.932	0.842
	330.2	1.161e-06	20.00	1.120e-06	1.147e-06	1.156e-06	1.043e-06	1.106e-06	9.721e-07	0.964	0.988	0.995	0.998	0.952	0.837
	457.2	2.651e-07	25.00	2.288e-07	2.374e-07	2.592e-07	2.170e-07	2.417e-07	1.970e-07	0.863	0.895	0.977	0.818	0.912	0.743
	609.6	5.621e-08	25.00	4.384e-08	5.032e-08	5.196e-08	4.233e-08	4.817e-08	3.790e-08	0.869	0.904	0.924	0.753	0.857	0.674
	762.0	1.111e-08	25.00	8.651e-09	9.226e-09	9.026e-09	6.881e-09	8.132e-09	5.971e-09	0.779	0.830	0.812	0.619	0.732	0.537
	914.4	2.022e-09	2.109e-09	2.181e-09	1.416e-09	2.009e-09	1.311e-09								

Table 3.8 Continued.

Energy Range	Position [mm]	Expt.	Error [8]	Calculated Reaction Rate						Calc. / Expt.							
				MCNP- J31	MCNP- J32	DOT- F-125	DOT- F-125	DOT- F-42	DOT- F-42	MCNP- J31	MCNP- J32	DCT- F-125	DCT- F-42				
1-10eV	-10.0	6.197e-06	10.00	6.396e-06	6.334e-06	7.069e-06	7.072e-06	6.959e-06	7.062e-06	1.032	1.010	1.026	0.986	0.989	0.945		
	127.0	2.878e-06	10.00	2.649e-06	2.654e-06	6.261e-06	6.156e-06	6.109e-06	6.125e-06	5.857e-06	5.857e-06	0.920	0.922	0.931	0.878	0.893	0.833
	228.6	1.018e-06	10.00	9.139e-07	9.315e-07	9.358e-07	8.658e-07	8.911e-07	8.083e-07	8.915	0.919	0.919	0.851	0.875	0.794		
	330.2	1.895e-07	12.00	1.706e-07	1.767e-07	1.849e-07	1.613e-07	1.722e-07	1.469e-07	0.900	0.912	0.976	0.851	0.909	0.770		
	457.2	6.851e-09	12.00	3.671e-08	3.521e-08	3.676e-08	3.114e-08	3.404e-08	2.782e-08	0.956	0.997	0.998	0.845	0.924	0.756		
	609.6	3.683e-08	12.00	5.438e-09	5.980e-09	6.058e-09	4.807e-09	5.422e-09	4.152e-09	0.794	0.873	0.884	0.702	0.797	0.606		
	762.0	9.144e-09	12.00	8.774e-10	9.950e-10	9.412e-10	5.716e-10	8.559e-10	5.150e-10								
<1eV	-10.0					1.338e-05	1.324e-05	1.317e-05	1.322e-05								
	127.0	4.470e-06	10.00	5.208e-06	6.115e-06	4.679e-06	4.416e-06	4.463e-06	4.214e-06	1.165	1.368	1.047	0.983	0.998	0.943		
	228.6	2.137e-06	10.00	2.446e-06	2.400e-06	1.892e-06	1.748e-06	1.790e-06	1.642e-06	1.145	1.123	0.885	0.818	0.838	0.769		
	330.2	8.367e-07	10.00	9.280e-07	8.757e-07	6.671e-07	6.040e-07	6.266e-07	5.594e-07	1.109	1.047	0.797	0.722	0.749	0.669		
	457.2	7.041e-08	10.00	7.054e-08	8.332e-08	6.846e-08	6.073e-08	6.201e-08	5.371e-08	1.002	1.183	0.972	0.863	0.881	0.763		
	609.6	1.351e-08	10.00	1.657e-08	1.572e-08	1.341e-08	1.152e-08	1.209e-08	1.007e-08	1.227	1.164	0.992	0.853	0.894	0.745		
	762.0	2.079e-09	10.00	2.386e-09	2.472e-09	2.203e-09	1.809e-09	1.962e-09	1.543e-09	1.147	1.189	1.059	0.868	0.944	0.742		
	914.4			1.011e-10	8.219e-11	1.179e-10	7.497e-11	1.066e-10	6.605e-11								

Table 3.9 Measured and calculated gamma-ray heating rates in [Gy/Source Neutron] and their C/E ratios.

Position [mm]	Expt.	Error [8]	Calculated Reaction Rate						Calculated Reaction Rate				Calculated Reaction Rate				
			MCNP- J31	Error [8]	MCNP- J32	Error [8]	DOT- F-125	DOT- F-125	DOT- F-42	DOT- F-42	MCNP- J31	Error [8]	MCNP- J32	Error [8]	DOT- F-125	DOT- F-125	
-1.0	1.123e-15	23.11	1.350e-15	4.10	1.286e-15	3.54	1.441e-15	1.460e-15	1.514e-15	1.507e-15	1.202	4.93	1.145	4.05	1.283	1.349	1.342
127.0	5.267e-16	7.88	7.540e-16	2.90	6.820e-16	2.35	7.571e-16	7.545e-16	7.961e-16	7.703e-16	1.432	4.15	1.295	3.05	1.438	1.433	1.514
228.6	1.899e-16	14.65	2.529e-16	3.00	2.222e-16	2.71	2.508e-16	2.467e-16	2.602e-16	2.473e-16	1.332	3.99	1.170	3.17	1.321	1.299	1.370
330.2	5.623e-17	11.79	7.818e-17	2.69	6.818e-17	2.64	7.939e-17	7.687e-17	8.130e-17	7.571e-17	1.390	3.74	1.213	3.21	1.412	1.367	1.446
457.2	9.263e-18	8.89	1.233e-17	3.46	1.060e-17	3.05	1.273e-17	1.225e-17	1.297e-17	1.190e-17	1.331	4.61	1.144	3.49	1.375	1.322	1.400
609.6	1.949e-18	3.58	1.705e-18	3.37	1.984e-18	1.88	1.858e-18	1.991e-18	1.770e-18	1.233	4.42	1.078	3.64	1.255	1.175	1.260	1.120
762.0	2.566e-19	10.06	2.815e-19	2.88	2.409e-19	2.55	3.053e-19	2.762e-19	3.016e-19	2.572e-19	1.097	3.16	0.939	2.39	1.190	1.076	1.175
914.4	3.018e-20	21.03	2.659e-20	4.39	2.674e-20	4.42	2.815e-20	2.658e-20	2.785e-20	2.522e-20	0.881	3.87	0.886	3.92	0.933	0.884	0.923

Table 3.10 Gamma-ray spectra at the four positions in the assembly calculated by MCNP with the FSXLIB-J3 library.

Energy [MeV] Lower	Upper	Flux / Lethargy / Source Neutron			
		457 mm	610 mm	762 mm	914 mm
1.000e-03	2.000e-03	2.907e-21	4.134e-22	4.864e-23	5.938e-24
2.000e-03	3.000e-03	7.582e-21	1.101e-21	1.233e-22	1.584e-23
3.000e-03	4.500e-02	3.808e-12	1.064e-12	3.549e-14	1.933e-14
4.500e-02	6.000e-02	1.632e-09	4.648e-10	1.607e-11	7.733e-12
6.000e-02	8.000e-02	1.825e-08	4.944e-09	2.182e-10	5.949e-11
8.000e-02	1.000e-01	1.073e-07	1.814e-08	1.411e-09	2.312e-10
1.000e-01	1.500e-01	3.482e-07	3.799e-08	5.123e-09	6.582e-10
1.500e-01	2.000e-01	4.706e-07	7.117e-08	9.449e-09	9.888e-10
2.000e-01	3.000e-01	5.587e-07	8.329e-08	1.123e-08	1.058e-09
3.000e-01	4.000e-01	5.833e-07	9.088e-08	1.092e-08	1.190e-09
4.000e-01	5.000e-01	7.035e-07	1.251e-07	1.418e-08	1.353e-09
5.000e-01	5.200e-01	8.261e-07	1.579e-07	1.705e-08	1.626e-09
5.200e-01	6.000e-01	6.351e-07	1.133e-07	1.323e-08	1.295e-09
6.000e-01	7.000e-01	4.510e-07	6.106e-08	8.484e-09	9.972e-10
7.000e-01	8.000e-01	5.100e-07	7.244e-08	9.060e-09	1.059e-09
8.000e-01	9.000e-01	4.828e-07	6.399e-08	8.064e-09	8.939e-10
9.000e-01	1.000e+00	3.664e-07	4.975e-08	6.145e-09	7.079e-10
1.000e+00	1.125e+00	2.974e-07	4.519e-08	5.153e-09	6.196e-10
1.125e+00	1.250e+00	3.086e-07	4.755e-08	5.413e-09	6.141e-10
1.250e+00	1.375e+00	3.364e-07	5.152e-08	6.335e-09	6.438e-10
1.375e+00	1.500e+00	3.473e-07	5.084e-08	7.382e-09	6.969e-10
1.500e+00	1.750e+00	3.308e-07	4.156e-08	8.044e-09	7.107e-10
1.750e+00	2.000e+00	2.911e-07	4.031e-08	7.104e-09	5.961e-10
2.000e+00	2.250e+00	2.628e-07	4.249e-08	5.902e-09	5.618e-10
2.250e+00	2.500e+00	2.501e-07	3.862e-08	5.412e-09	6.002e-10
2.500e+00	3.000e+00	2.418e-07	3.863e-08	5.540e-09	6.487e-10
3.000e+00	3.500e+00	2.518e-07	3.806e-08	5.679e-09	7.916e-10
3.500e+00	4.000e+00	2.712e-07	3.571e-08	5.570e-09	8.449e-10
4.000e+00	4.500e+00	2.641e-07	3.765e-08	5.586e-09	7.666e-10
4.500e+00	5.000e+00	2.389e-07	4.005e-08	5.693e-09	6.792e-10
5.000e+00	5.500e+00	2.399e-07	4.301e-08	6.287e-09	6.573e-10
5.500e+00	6.000e+00	2.698e-07	4.740e-08	7.214e-09	6.732e-10
6.000e+00	6.500e+00	2.980e-07	5.059e-08	7.824e-09	6.640e-10
6.500e+00	7.000e+00	3.404e-07	5.776e-08	9.021e-09	6.965e-10
7.000e+00	7.500e+00	4.822e-07	8.166e-08	1.297e-08	9.383e-10
7.500e+00	8.000e+00	6.031e-07	1.006e-07	1.597e-08	1.123e-09
8.000e+00	9.000e+00	3.622e-07	6.070e-08	9.100e-09	6.178e-10
9.000e+00	1.000e+01	8.688e-08	1.348e-08	1.881e-09	1.083e-10
1.000e+01	1.200e+01	1.186e-08	1.273e-09	2.066e-10	6.500e-12
1.200e+01	1.400e+01	1.566e-10	1.378e-10	2.602e-12	6.449e-14

Table 3.11 Gamma-ray spectra at the four positions in the assembly calculated by MCNP with the FSXLIB-J3R2 library.

Energy Lower	Energy Upper	457 mm	Flux / Lethargy / Source Neutron		
			610 mm	762 mm	914 mm
1.000e-03	2.000e-03	2.341e-21	4.168e-22	5.195e-23	1.887e-12
2.000e-03	3.000e-03	6.051e-21	1.110e-21	1.366e-22	3.135e-13
3.000e-03	4.500e-02	3.280e-12	1.161e-12	1.763e-13	5.557e-14
4.500e-02	6.000e-02	1.448e-09	4.820e-10	6.935e-11	2.088e-11
6.000e-02	8.000e-02	1.686e-08	4.369e-09	4.846e-10	1.030e-10
8.000e-02	1.000e-01	8.237e-08	1.734e-08	1.743e-09	2.132e-10
1.000e-01	1.500e-01	2.387e-07	4.369e-08	5.243e-09	6.032e-10
1.500e-01	2.000e-01	4.140e-07	6.568e-08	9.285e-09	1.004e-09
2.000e-01	3.000e-01	5.238e-07	8.082e-08	1.089e-08	1.136e-09
3.000e-01	4.000e-01	5.335e-07	8.467e-08	1.124e-08	1.164e-09
4.000e-01	5.000e-01	6.559e-07	1.064e-07	1.316e-08	1.366e-09
5.000e-01	5.200e-01	6.900e-07	1.289e-07	1.644e-08	1.742e-09
5.200e-01	6.000e-01	5.180e-07	1.010e-07	1.225e-08	1.367e-09
6.000e-01	7.000e-01	3.568e-07	6.501e-08	7.033e-09	8.517e-10
7.000e-01	8.000e-01	4.044e-07	6.762e-08	8.622e-09	1.047e-09
8.000e-01	9.000e-01	4.725e-07	6.561e-08	9.332e-09	1.209e-09
9.000e-01	1.000e+00	4.029e-07	5.122e-08	7.604e-09	1.024e-09
1.000e+00	1.125e+00	3.189e-07	4.063e-08	6.173e-09	7.489e-10
1.125e+00	1.250e+00	3.081e-07	3.940e-08	5.888e-09	6.193e-10
1.250e+00	1.375e+00	3.210e-07	4.207e-08	5.892e-09	5.964e-10
1.375e+00	1.500e+00	3.189e-07	4.349e-08	6.161e-09	5.819e-10
1.500e+00	1.750e+00	3.081e-07	4.056e-08	6.333e-09	5.551e-10
1.750e+00	2.000e+00	2.902e-07	3.897e-08	5.763e-09	5.524e-10
2.000e+00	2.250e+00	2.840e-07	4.334e-08	5.468e-09	5.915e-10
2.250e+00	2.500e+00	2.853e-07	4.266e-08	5.128e-09	6.020e-10
2.500e+00	3.000e+00	2.641e-07	3.876e-08	4.943e-09	6.149e-10
3.000e+00	3.500e+00	2.495e-07	3.809e-08	5.308e-09	6.739e-10
3.500e+00	4.000e+00	2.576e-07	3.628e-08	5.319e-09	7.145e-10
4.000e+00	4.500e+00	2.480e-07	3.697e-08	5.246e-09	7.347e-10
4.500e+00	5.000e+00	2.331e-07	4.000e-08	5.483e-09	7.146e-10
5.000e+00	5.500e+00	2.323e-07	4.154e-08	6.066e-09	6.868e-10
5.500e+00	6.000e+00	2.365e-07	3.937e-08	6.447e-09	6.483e-10
6.000e+00	6.500e+00	2.270e-07	3.557e-08	6.301e-09	5.906e-10
6.500e+00	7.000e+00	2.290e-07	3.847e-08	6.629e-09	6.171e-10
7.000e+00	7.500e+00	3.122e-07	5.647e-08	8.727e-09	8.653e-10
7.500e+00	8.000e+00	4.067e-07	7.143e-08	1.045e-08	1.081e-09
8.000e+00	9.000e+00	2.920e-07	4.617e-08	6.800e-09	6.866e-10
9.000e+00	1.000e+01	8.139e-08	1.447e-08	1.822e-09	1.787e-10
1.000e+01	1.200e+01	7.689e-09	2.653e-09	2.055e-10	2.219e-11
1.200e+01	1.400e+01	9.128e-11	3.677e-11	5.490e-12	2.861e-13

Table 3.12 Gamma-ray spectra at the four positions in the assembly calculated by DOT with the JSSTDL library of 125 neutron and 40 gamma-ray groups.

Lower	Upper	457 mm	Flux / Lethargy / Source Neutron		
			610 mm	762 mm	914 mm
1.000e-03	2.000e-03	3.605e-12	5.886e-13	1.106e-13	4.965e-14
2.000e-03	3.000e-03	4.511e-12	5.990e-13	8.550e-14	1.852e-14
3.000e-03	4.500e-02	6.070e-11	8.094e-12	1.118e-12	1.657e-13
4.500e-02	6.000e-02	2.550e-09	3.694e-10	5.342e-11	5.395e-12
6.000e-02	8.000e-02	2.275e-08	3.309e-09	4.807e-10	4.664e-11
8.000e-02	1.000e-01	1.025e-07	1.491e-08	2.171e-09	2.077e-10
1.000e-01	1.500e-01	3.015e-07	4.393e-08	6.398e-09	6.087e-10
1.500e-01	2.000e-01	5.535e-07	8.067e-08	1.176e-08	1.115e-09
2.000e-01	3.000e-01	6.602e-07	9.595e-08	1.397e-08	1.326e-09
3.000e-01	4.000e-01	6.264e-07	9.128e-08	1.332e-08	1.252e-09
4.000e-01	5.000e-01	7.721e-07	1.160e-07	1.730e-08	1.573e-09
5.000e-01	5.200e-01	9.213e-07	1.411e-07	2.162e-08	1.905e-09
5.200e-01	6.000e-01	7.173e-07	1.068e-07	1.590e-08	1.474e-09
6.000e-01	7.000e-01	4.618e-07	6.247e-08	8.580e-09	9.250e-10
7.000e-01	8.000e-01	4.934e-07	6.507e-08	8.911e-09	1.008e-09
8.000e-01	9.000e-01	4.649e-07	6.287e-08	8.624e-09	9.843e-10
9.000e-01	1.000e+00	3.658e-07	5.147e-08	7.195e-09	7.756e-10
1.000e+00	1.125e+00	3.181e-07	4.458e-08	6.327e-09	6.235e-10
1.125e+00	1.250e+00	3.472e-07	4.629e-08	6.526e-09	6.348e-10
1.250e+00	1.375e+00	3.800e-07	4.946e-08	6.920e-09	6.988e-10
1.375e+00	1.500e+00	3.785e-07	5.064e-08	7.057e-09	7.152e-10
1.500e+00	1.750e+00	3.511e-07	4.953e-08	6.975e-09	6.745e-10
1.750e+00	2.000e+00	3.104e-07	4.517e-08	6.664e-09	6.156e-10
2.000e+00	2.250e+00	2.921e-07	4.291e-08	6.413e-09	6.021e-10
2.250e+00	2.500e+00	2.799e-07	4.118e-08	6.140e-09	6.082e-10
2.500e+00	3.000e+00	2.731e-07	4.001e-08	5.971e-09	6.224e-10
3.000e+00	3.500e+00	2.786e-07	4.073e-08	6.068e-09	6.421e-10
3.500e+00	4.000e+00	2.769e-07	4.074e-08	6.096e-09	6.394e-10
4.000e+00	4.500e+00	2.740e-07	4.098e-08	6.202e-09	6.385e-10
4.500e+00	5.000e+00	2.686e-07	4.095e-08	6.283e-09	6.340e-10
5.000e+00	5.500e+00	2.724e-07	4.246e-08	6.617e-09	6.425e-10
5.500e+00	6.000e+00	2.868e-07	4.569e-08	7.219e-09	6.686e-10
6.000e+00	6.500e+00	3.009e-07	4.835e-08	7.733e-09	6.987e-10
6.500e+00	7.000e+00	3.448e-07	5.675e-08	9.213e-09	8.076e-10
7.000e+00	7.500e+00	4.525e-07	8.107e-08	1.320e-08	1.065e-09
7.500e+00	8.000e+00	5.289e-07	9.934e-08	1.614e-08	1.241e-09
8.000e+00	9.000e+00	3.627e-07	6.260e-08	1.026e-08	8.463e-10
9.000e+00	1.000e+01	9.184e-08	1.431e-08	2.366e-09	2.168e-10
1.000e+01	1.200e+01	1.034e-08	1.596e-09	2.537e-10	2.441e-11
1.200e+01	1.400e+01	9.442e-10	1.139e-10	1.415e-11	1.292e-12

Table 3.13 Gamma-ray spectra at the four positions in the assembly calculated by DOT with the FUSION-J3 library of 125 neutron and 40 gamma-ray groups.

Energy [MeV] Lower	Upper	457 mm	Flux / Lethargy / Source Neutron		
			610 mm	762 mm	914 mm
1.000e-03	2.000e-03	2.630e-12	4.302e-13	7.922e-14	3.486e-14
2.000e-03	3.000e-03	4.185e-12	5.489e-13	7.580e-14	1.549e-14
3.000e-03	4.500e-02	6.058e-11	8.032e-12	1.086e-12	1.623e-13
4.500e-02	6.000e-02	2.625e-09	3.722e-10	5.221e-11	5.554e-12
6.000e-02	8.000e-02	2.241e-08	3.187e-09	4.486e-10	4.586e-11
8.000e-02	1.000e-01	9.751e-08	1.387e-08	1.957e-09	1.971e-10
1.000e-01	1.500e-01	2.815e-07	4.008e-08	5.657e-09	5.651e-10
1.500e-01	2.000e-01	5.150e-07	7.337e-08	1.036e-08	1.025e-09
2.000e-01	3.000e-01	6.130e-07	8.710e-08	1.229e-08	1.215e-09
3.000e-01	4.000e-01	5.881e-07	8.375e-08	1.184e-08	1.159e-09
4.000e-01	5.000e-01	7.239e-07	1.061e-07	1.531e-08	1.461e-09
5.000e-01	5.200e-01	8.624e-07	1.288e-07	1.906e-08	1.771e-09
5.200e-01	6.000e-01	6.806e-07	9.889e-08	1.424e-08	1.383e-09
6.000e-01	7.000e-01	4.544e-07	6.045e-08	8.098e-09	8.883e-10
7.000e-01	8.000e-01	4.898e-07	6.370e-08	8.522e-09	9.737e-10
8.000e-01	9.000e-01	4.636e-07	6.183e-08	8.278e-09	9.556e-10
9.000e-01	1.000e+00	3.652e-07	5.060e-08	6.889e-09	7.561e-10
1.000e+00	1.125e+00	3.167e-07	4.363e-08	6.024e-09	6.082e-10
1.125e+00	1.250e+00	3.456e-07	4.528e-08	6.213e-09	6.199e-10
1.250e+00	1.375e+00	3.785e-07	4.843e-08	6.596e-09	6.830e-10
1.375e+00	1.500e+00	3.762e-07	4.945e-08	6.703e-09	6.973e-10
1.500e+00	1.750e+00	3.472e-07	4.802e-08	6.569e-09	6.545e-10
1.750e+00	2.000e+00	3.067e-07	4.365e-08	6.244e-09	5.969e-10
2.000e+00	2.250e+00	2.897e-07	4.160e-08	6.023e-09	5.868e-10
2.250e+00	2.500e+00	2.785e-07	4.010e-08	5.796e-09	5.961e-10
2.500e+00	3.000e+00	2.720e-07	3.906e-08	5.658e-09	6.127e-10
3.000e+00	3.500e+00	2.771e-07	3.971e-08	5.740e-09	6.301e-10
3.500e+00	4.000e+00	2.747e-07	3.960e-08	5.747e-09	6.256e-10
4.000e+00	4.500e+00	2.708e-07	3.963e-08	5.812e-09	6.249e-10
4.500e+00	5.000e+00	2.640e-07	3.930e-08	5.838e-09	6.186e-10
5.000e+00	5.500e+00	2.652e-07	4.028e-08	6.068e-09	6.190e-10
5.500e+00	6.000e+00	2.762e-07	4.279e-08	6.527e-09	6.339e-10
6.000e+00	6.500e+00	2.875e-07	4.488e-08	6.925e-09	6.560e-10
6.500e+00	7.000e+00	3.275e-07	5.233e-08	8.197e-09	7.565e-10
7.000e+00	7.500e+00	4.272e-07	7.425e-08	1.167e-08	9.943e-10
7.500e+00	8.000e+00	4.965e-07	9.043e-08	1.417e-08	1.145e-09
8.000e+00	9.000e+00	3.378e-07	5.647e-08	8.916e-09	7.575e-10
9.000e+00	1.000e+01	8.530e-08	1.284e-08	2.041e-09	1.882e-10
1.000e+01	1.200e+01	9.904e-09	1.488e-09	2.281e-10	2.298e-11
1.200e+01	1.400e+01	8.754e-10	1.055e-10	1.299e-11	1.227e-12

Table 3.14 Gamma-ray spectra at the four positions in the assembly calculated by DOT with the JSSTDL library of 42 neutron and 21 gamma-ray groups.

Energy [MeV] Lower	Upper	457 mm	Flux / Lethargy / Source Neutron		
			610 mm	762 mm	914 mm
1.000e-02	1.000e-01	4.597e-09	6.595e-10	9.480e-11	9.165e-12
1.000e-01	2.000e-01	3.556e-07	5.102e-08	7.326e-09	6.960e-10
2.000e-01	4.000e-01	7.018e-07	1.007e-07	1.447e-08	1.372e-09
4.000e-01	1.000e+00	7.104e-07	1.021e-07	1.472e-08	1.397e-09
1.000e+00	1.500e+00	4.006e-07	5.462e-08	7.631e-09	7.426e-10
1.500e+00	2.000e+00	3.294e-07	4.585e-08	6.511e-09	6.244e-10
2.000e+00	2.500e+00	2.892e-07	4.166e-08	6.092e-09	5.872e-10
2.500e+00	3.000e+00	2.753e-07	3.952e-08	5.783e-09	6.029e-10
3.000e+00	3.500e+00	2.748e-07	3.938e-08	5.756e-09	6.162e-10
3.500e+00	4.000e+00	2.717e-07	3.921e-08	5.780e-09	6.106e-10
4.000e+00	4.500e+00	2.681e-07	3.935e-08	5.847e-09	6.088e-10
4.500e+00	5.000e+00	2.623e-07	3.924e-08	5.915e-09	6.045e-10
5.000e+00	5.500e+00	2.650e-07	4.058e-08	6.216e-09	6.111e-10
5.500e+00	6.000e+00	2.778e-07	4.355e-08	6.769e-09	6.338e-10
6.000e+00	6.500e+00	2.905e-07	4.603e-08	7.245e-09	6.612e-10
6.500e+00	7.000e+00	3.314e-07	5.391e-08	8.617e-09	7.627e-10
7.000e+00	7.500e+00	4.277e-07	7.596e-08	1.218e-08	9.924e-10
7.500e+00	8.000e+00	4.815e-07	8.980e-08	1.438e-08	1.116e-09
8.000e+00	1.000e+01	2.219e-07	3.695e-08	5.981e-09	5.104e-10
1.000e+01	1.200e+01	2.635e-08	4.418e-09	7.096e-10	5.855e-11
1.200e+01	1.400e+01	9.968e-10	1.177e-10	1.486e-11	1.316e-12

Table 3.15 Gamma-ray spectra at the four positions in the assembly calculated by DOT with the FUSION-40 library of 42 neutron and 21 gamma-ray groups.

Energy [MeV] Lower	Upper	457 mm	Flux / Lethargy / Source Neutron		
			610 mm	762 mm	914 mm
1.000e-02	1.000e-01	3.529e-09	4.925e-10	6.802e-11	6.966e-12
1.000e-01	2.000e-01	2.935e-07	4.095e-08	5.655e-09	5.756e-10
2.000e-01	4.000e-01	5.823e-07	8.129e-08	1.124e-08	1.127e-09
4.000e-01	1.000e+00	5.942e-07	8.303e-08	1.151e-08	1.163e-09
1.000e+00	1.500e+00	3.757e-07	4.990e-08	6.719e-09	6.841e-10
1.500e+00	2.000e+00	3.206e-07	4.344e-08	5.942e-09	5.963e-10
2.000e+00	2.500e+00	2.838e-07	3.975e-08	5.591e-09	5.675e-10
2.500e+00	3.000e+00	2.722e-07	3.806e-08	5.362e-09	5.897e-10
3.000e+00	3.500e+00	2.718e-07	3.795e-08	5.342e-09	6.021e-10
3.500e+00	4.000e+00	2.682e-07	3.767e-08	5.325e-09	5.947e-10
4.000e+00	4.500e+00	2.635e-07	3.758e-08	5.369e-09	5.934e-10
4.500e+00	5.000e+00	2.560e-07	3.715e-08	5.377e-09	5.871e-10
5.000e+00	5.500e+00	2.559e-07	3.790e-08	5.565e-09	5.849e-10
5.500e+00	6.000e+00	2.650e-07	4.008e-08	5.960e-09	5.956e-10
6.000e+00	6.500e+00	2.746e-07	4.191e-08	6.307e-09	6.142e-10
6.500e+00	7.000e+00	3.111e-07	4.872e-08	7.445e-09	7.075e-10
7.000e+00	7.500e+00	3.988e-07	6.815e-08	1.045e-08	9.215e-10
7.500e+00	8.000e+00	4.467e-07	8.012e-08	1.227e-08	1.031e-09
8.000e+00	1.000e+01	2.036e-07	3.255e-08	5.029e-09	4.493e-10
1.000e+01	1.200e+01	2.398e-08	3.851e-09	5.883e-10	4.806e-11
1.200e+01	1.400e+01	9.260e-10	1.080e-10	1.331e-11	1.209e-12

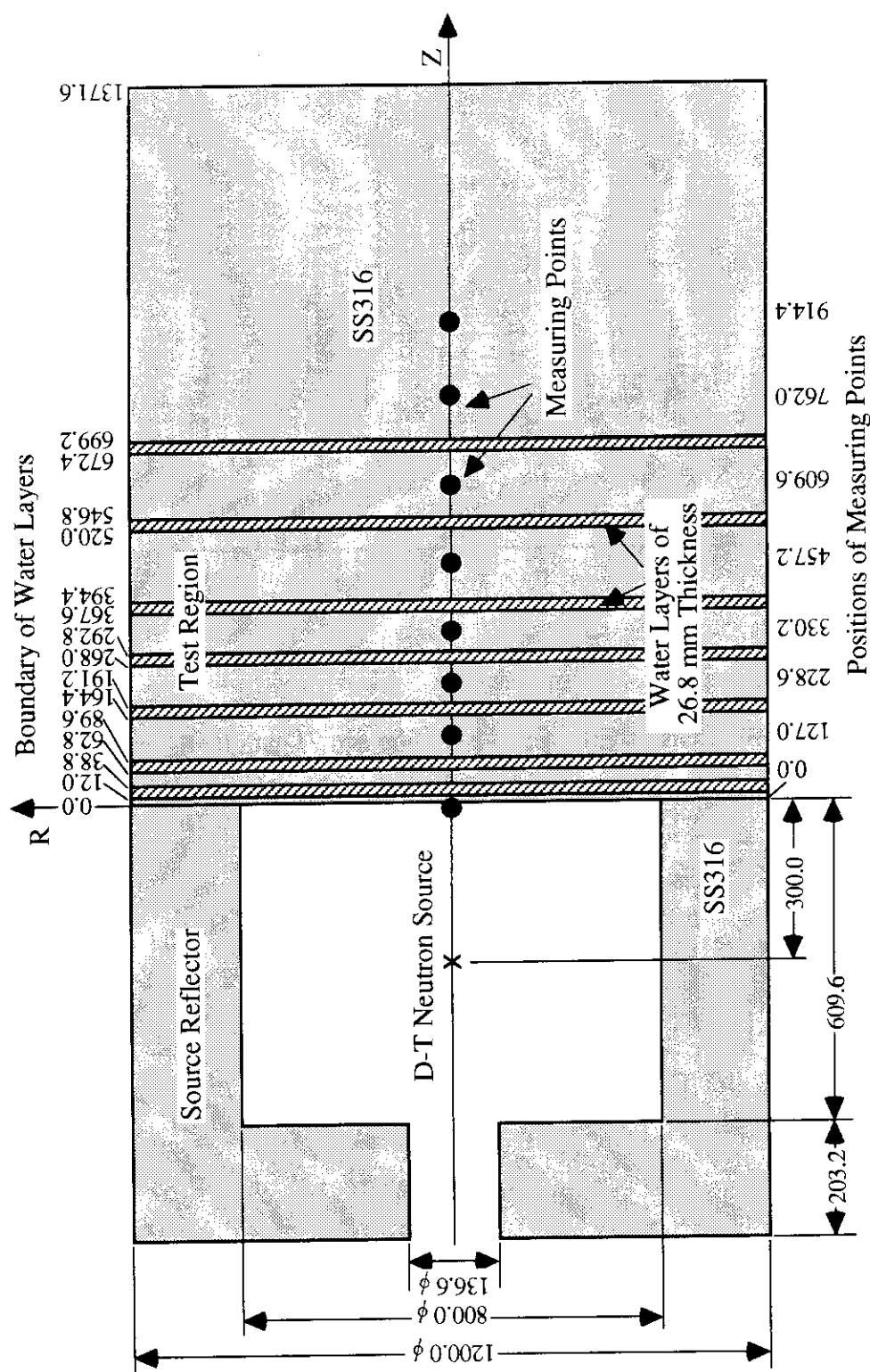


Fig. 2.1 Calculation model for the SS316/water assembly.

```

analysis of the bulk shielding experiment for SS316/H2O assembly Feb. 1993
c ****
c * cell card *
c ****
 1 4 4.9210-5 (1 -2 -30) : (2 -3 -34) #51      $ source region
51 4 4.9210-5 27 -3 -31                         $ cell for track length
 2 1 8.5855-2 3 -4 -33                           $ SS316
 3 2 9.9988-2 4 -5 -33                           $ H2O
 4 1 8.5855-2 5 -6 -33                           $ SS316
 5 2 9.9988-2 6 -7 -33                           $ H2O
 6 1 8.5855-2 7 -8 -33                           $ SS316
 7 1 8.5855-2 8 -9 -33                           $ SS316
 8 2 9.9988-2 9 -10 -33                          $ H2O
 9 1 8.5855-2 10 -11 -33                          $ SS316
10 1 8.5855-2 11 -12 -33                          $ SS316
11 2 9.9988-2 12 -13 -33                          $ H2O
12 1 8.5855-2 13 -14 -33                          $ SS316
13 1 8.5855-2 14 -15 -33                          $ SS316
14 2 9.9988-2 15 -16 -33                          $ H2O
15 1 8.5855-2 16 -17 -33                          $ SS316
16 1 8.5855-2 17 -18 -33                          $ SS316
17 2 9.9988-2 18 -19 -33                          $ H2O
18 1 8.5855-2 19 -20 -33                          $ SS316
19 1 8.5855-2 20 -21 -33                          $ SS316
20 2 9.9988-2 21 -22 -33                          $ H2O
21 1 8.5855-2 22 -23 -33                          $ SS316
22 1 8.5855-2 23 -24 -33                          $ SS316
23 1 8.5855-2 24 -25 -33                          $ SS316
24 1 8.5855-2 25 -26 -33                          $ SS316
25 1 8.5855-2 3 -4 33 -35                      $ SS316
26 2 9.9988-2 4 -5 33 -35                      $ H2O
27 1 8.5855-2 5 -6 33 -35                      $ SS316
28 2 9.9988-2 6 -7 33 -35                      $ H2O
29 1 8.5855-2 7 -8 33 -35                      $ SS316
30 1 8.5855-2 8 -9 33 -35                      $ SS316
31 2 9.9988-2 9 -10 33 -35                     $ H2O
32 1 8.5855-2 10 -11 33 -35                    $ SS316
33 1 8.5855-2 11 -12 33 -35                    $ SS316
34 2 9.9988-2 12 -13 33 -35                     $ H2O
35 1 8.5855-2 13 -14 33 -35                     $ SS316
36 1 8.5855-2 14 -15 33 -35                     $ SS316
37 2 9.9988-2 15 -16 33 -35                     $ H2O
38 1 8.5855-2 16 -17 33 -35                     $ SS316
39 1 8.5855-2 17 -18 33 -35                     $ SS316
40 2 9.9988-2 18 -19 33 -35                     $ H2O
41 1 8.5855-2 19 -20 33 -35                     $ SS316
42 1 8.5855-2 20 -21 33 -35                     $ SS316
43 2 9.9988-2 21 -22 33 -35                     $ H2O
44 1 8.5855-2 22 -23 33 -35                     $ SS316
45 1 8.5855-2 23 -24 33 -35                     $ SS316
46 1 8.5855-2 24 -25 33 -35                     $ SS316
47 1 8.5855-2 25 -26 33 -35                     $ SS316
49 3 8.5699-2 (1 -2 30 -35) : (2 -3 34 -35) $ source reflector
50 0 -1 : 26 : 35                                $ void
c ****
c * surface card *
c ****
 1   pz -51.28
 2   pz -30.96
 3   pz 30.00
 4   pz 31.20
 5   pz 33.88
 6   pz 36.28
 7   pz 38.96
 8   pz 42.70
 9   pz 46.44
10   pz 49.12
11   pz 52.86
12   pz 56.60
13   pz 59.28
14   pz 63.02
15   pz 66.76
16   pz 69.44
17   pz 75.72
18   pz 82.00
19   pz 84.68
20   pz 90.96
21   pz 97.24
22   pz 99.92
23   pz 106.20
24   pz 115.00
25   pz 121.44
26   pz 167.16
27   pz 28.00
30   cz 6.83
31   cz 4.00

```

Fig. 2.2 Input data of MCNP for the analysis of the SS316/water assembly with the FSXLIB-J3R2 library.

```

33   cz  20.00
34   cz  40.00
35   cz  60.00

c **** node card - neutron & photon ****
c **** weight window card ****
c **** materials for the assembly ****
mode n p
ext:n  0    0    0.1z  0.1z  0.1z  0.1z  0.1z  0.1z  0.1z  0.1z  0.1z
       0.1z  0.1z  0.1z  0.1z  0.1z  0.1z  0.1z  0.1z  0.1z  0.1z
       0.1z  0.1z  0.1z  0.1z  0.1z  0.1z  0.1z  0.1z  0.1z  0.1z
       0.1z  0.1z  0.1z  0.1z  0.1z  0.1z  0.1z  0.1z  0.1z  0.1z
       0.1z  0.1z  0.1z  0.1z  0.1z  0.1z  0.1z  0.1z  0.1z  0.1z
wwe:n  3.2241e-7 1.0  5.0  13.0 100.0
wwp:n  5 3 5 0 0
wwn1:n $ for thermal neutrons
        2.0      1r $ source void
        2.0      3r 0.8      1r 0.2      3r 0.06      2r
        0.02     1r 0.006     0.0015     1r 0.0004
        0.0001    1r 0.00003    1r
        2.0      3r 2.0      1r 0.8      3r 0.24      2r
        0.08     1r 0.024     0.006     1r 0.0016
        0.0004    1r 0.00012    1r
        2.0      -1 $ source reflector, external void
wwn2:n $ for eV, keV neutrons
        3.4      1r $ source void
        0.1      3r 0.05      1r 0.025     3r 0.008     2r
        0.002     1r 0.001     0.0005     1r 0.00025
        0.00012    1r 0.00003    1r
        0.4      3r 0.2      1r 0.1      3r 0.032     2r
        0.008     1r 0.004     0.002     1r 0.001
        0.00048    1r 0.00012    1r
        0.4      -1 $ source reflector, external void
wwn3:n $ for 1-5MeV neutrons
        0.4      1r $ source void
        0.1      3r 0.025     1r 0.008     3r 0.002     2r
        0.0005    1r 0.0002    0.00008    1r 0.00002
        0.000005   1r 0.0000015   1r
        0.4      3r 0.1      1r 0.032     3r 0.008     2r
        0.002     1r 0.0008    0.00032    1r 0.00008
        0.00002    1r 0.00006    1r
        0.4      -1 $ source reflector, external void
wwn4:n $ for 5-13MeV neutrons
        0.4      1r $ source void
        0.1 1r 0.025 1r 0.0064 1r 0.0016 3r 0.0004 2r
        0.0001    1r 0.00025 0.0000064 1r 0.0000016
        0.000004 1r 0.000001 1r
        0.4 1r 0.1 1r 0.0256 1r 0.0064 3r 0.0016 2r
        0.0004    1r 0.0001 0.0000256 1r 0.0000064
        0.000016 1r 0.000004 1r
        0.4      -1 $ source reflector, external void
wwn5:n $ for 14MeV neutrons
        0.4      1r $ source void
        0.1      3r 0.05      1r 0.025     3r 0.008     2r
        0.002     1r 0.0008    0.0002     1r 0.000064
        0.000016   1r 0.000004   1r
        0.4      3r 0.2      1r 0.1      3r 0.032     2r
        0.008     1r 0.0032    0.0008     1r 0.000256
        0.000064   1r 0.000016   1r
        0.4      -1 $ source reflector, external void
wwe:p  100.0
wwp:p  5 3 5 0 0
wwn1:p $ for gamma-rays
        4.0      1r $ source void
        2.0      3r 1.0      1r 0.4      3r 0.1      2r
        0.03     1r 0.01      0.005     1r 0.0016
        0.0004    1r 0.0001    1r
        4.0      3r 4.0      1r 1.6      3r 0.4      2r
        0.12     1r 0.04      0.02      1r 0.0064
        0.0016    1r 0.0004    1r
        4.0      -1 $ source reflector, external void
c **** source specification cards ****
c an user supplied source subroutine is used.
c **** material specification cards ****
m1   14000.37c 1.0341-3 24000.37c 1.5482-2   $ SS316 in test region
      25055.37c 1.0355-3 26000.37c 5.7904-2
      28000.37c 9.3405-3 42000.37c 1.0585-3
m2   1001.37c 6.6659-2 8016.37c 3.3329-2   $ H2O
      14000.37c 8.1608-4 24000.37c 1.5025-2   $ SS316 in source reflector
      25055.37c 9.13561-3 26000.37c 5.8331-2
      28000.37c 9.1456-3 42000.37c 1.0254-3

```

Fig. 2.2 Continued.

```

m4    7014.37c 3.8810-5   8016.37c 1.0400-5   $ air
c ----- materials for dosimetry reactions -----
m5    2003.37c 1.0  $ He-3 (n,p)
m6    5010.03Y 1.0  $ B-10 (n,a)  a-prod.
m7    7014.37c 1.0  $ N-14 (n,p)
m8    13027.03Y 1.0  $ Al-27(n,a)
m9    22000.03Y 1.0  $ Ti-0 (n,x)Sc-46, Sc-47, Sc-48
m10   25055.03Y 1.0  $ Mn-55(n,g)
m11   26054.03Y 1.0  $ Fe-54(n,p)
m12   26056.03Y 1.0  $ Fe-56(n,p)
m13   27059.37c 1.0  $ Co-59(n,2n), (n,g), (n,a), (n,p)
m14   28058.03Y 1.0  $ Ni-58(n,2n), (n,p)
m15   29063.03Y 1.0  $ Cu-63(n,2n), (n,g), (n,a)
m16   29065.37c 1.0  $ Cu-65(n,2n), (n,g)
m17   30064.03Y 1.0  $ Zn-64(n,p)
m18   40090.03Y 1.0  $ Zr-90(n,2n)
m19   41093.03Y 1.0  $ Nb-93(n,2n)Nb-92m
m20   49115.03Y 1.0  $ In-115(n,n')In-115m
m21   74186.03Y 1.0  $ W-186(n,g)
m22   79197.03Y 1.0  $ Au-197(n,g)
m23   92235.03Y 1.0  $ U-235(n,f)
m24   92238.03Y 1.0  $ U-238(n,f)
c ----- materials for (n,g) reactions of the assembly itself -----
m31   1001.37c 1.0  $ Hydrogen
m32   8016.37c 1.0  $ Oxygen
m33   14000.37c 1.0  $ Silicon
m34   24000.37c 1.0  $ Chromium
m38   25055.37c 1.0  $ Manganese
m35   26000.37c 1.0  $ Iron
m36   28000.37c 1.0  $ Nickel
m37   42000.37c 1.0  $ Molybdenum
c ****
c * tally specification cards *
c ****
fc12 >>> neutron reaction rate surface (r=4cm) <<<<
f12:n 3 4 5 6 7 8 9 10 11 12
      13 14 15 16 17 18 19 20 21 22
      23 24 25 26
fm12 (1) (1 1 1) (1 1 2) (1 1 102)
      (1 5 103) (1 6 107) (1 6 207) (1 7 103) (1 8 107)
      (1 9 210) (1 9 211) (1 9 212) (1 10 102) (1 11 103)
      (1 12 103) (1 13 16) (1 13 102) (1 13 103) (1 13 107)
      (1 14 16) (1 14 103) (1 15 16) (1 15 102) (1 15 107)
      (1 16 16) (1 16 102) (1 17 103) (1 18 16) (1 19 16)
      (1 20 51) (1 21 102) (1 22 102) (1 23 18) (1 24 18)
      (1 33 102) (1 34 102) (1 35 102) (1 36 102) (1 37 102)
      (1 38 102)
fs12 -31
fg12 s e f m
e12 15.488
fc22 >>> neutron energy-dependent reaction rate surface (r=4cm) <<<<
f22:n 3 4 5 6 7 8 9 10 11 12
      13 14 15 16 17 18 19 20 21 22
      23 24 25 26
fm22 (1) (1 1 1) (1 1 2) (1 1 102)
      (1 5 103) (1 6 107) (1 6 207) (1 7 103) (1 8 107)
      (1 9 210) (1 9 211) (1 9 212) (1 10 102) (1 11 103)
      (1 12 103) (1 13 16) (1 13 102) (1 13 103) (1 13 107)
      (1 14 16) (1 14 103) (1 15 16) (1 15 102) (1 15 107)
      (1 16 16) (1 16 102) (1 17 103) (1 18 16) (1 19 16)
      (1 20 51) (1 21 102) (1 22 102) (1 23 18) (1 24 18)
      (1 33 102) (1 34 102) (1 35 102) (1 36 102) (1 37 102)
      (1 38 102)
fs22 -31
fq22 s m e f
e22 1e-7 1e-6 1e-5 1e-4 1e-3 1e-2 1e-1 2e-1 5e-1 1e+0
2e+0 5e+0 1e+1 15.488
fc42 >>> neutron spectrum surface (r=4cm) <<<<
f42:n 3 8 11 14 17 20 23 25
fs42 -31
fc52 >>> neutron spectrum-decade surface (r=4cm) <<<<
f52:n 3 4 5 6 7 8 9 10 11 12
      13 14 15 16 17 18 19 20 21 22
      23 24 25 26
fs52 -31
e52 1e-7 1e-6 1e-5 1e-4 1e-3 1e-2 1e-1 1 2 10 15.488
fc64 >>> neutron spectrum cell (r=4cm) <<<<
f64:n 51
fc74 >>> neutron spectrum-decade cell (r=4cm) <<<<
f74:n 51
e74 1e-7 1e-6 1e-5 1e-4 1e-3 1e-2 1e-1 1 2 10 15.488
fc102 >>> photon spectrum surface (r=4cm) <<<<
f102:p 3 4 5 6 7 8 9 10 11 12
      13 14 15 16 17 18 19 20 21 22
      23 24 25 26
e102 1.0000-02 2.0000-02 3.0000-02 4.5000-02 6.0000-02
      8.0000-02 1.0000-01 1.5000-01 2.0000-01 3.0000-01
      4.0000-01 5.0000-01 5.2000-01 6.0000-01 7.0000-01
      8.0000-01 9.0000-01 1.0000+00 1.1300+00 1.2500+00

```

Fig. 2.2 Continued.

```

1.3800+00 1.5000+00 1.7500+00 2.0000+00 2.2500+00
2.5000+00 3.0000+00 3.5000+00 4.0000+00 4.5000+00
5.0000+00 5.5000+00 6.0000+00 6.5000+00 7.0000+00
7.5000+00 8.0000+00 9.0000+00 1.0000+01 1.2000+01
1.4000+01
fs102 -31
c -----
fg0 s m e f
e0 1.0010-11 3.2241-07
5.3156-07 8.7640-07 1.4449-06 2.3823-06 3.9278-06
6.4758-06 1.0677-05 1.7603-05 2.9023-05 4.7850-05
7.8891-05 1.3007-04 2.1445-04 3.5357-04 5.8293-04
9.6110-04 1.2341-03 1.5846-03 2.0346-03 2.6125-03
3.3546-03 4.3073-03 5.5307-03 7.1016-03 9.1186-03
1.1709-02 1.5034-02 1.9304-02 2.1874-02 2.4787-02
2.8087-02 3.1827-02 3.6065-02 4.0867-02 4.6308-02
5.2474-02 5.9461-02 6.7378-02 7.6349-02 8.6515-02
9.8035-02 1.1109-01 1.2588-01 1.4264-01 1.6163-01
1.8315-01 2.0754-01 2.3517-01 2.6649-01 3.0197-01
3.4217-01 3.8774-01 4.3936-01 4.9786-01 5.6415-01
6.3927-01 7.2438-01 8.2084-01 9.3013-01 1.0540+00
1.1943+00 1.3533+00 1.5335+00 1.7377+00 1.8498+00
1.9691+00 2.0961+00 2.2313+00 2.3752+00 2.5284+00
2.6914+00 2.8650+00 3.0498+00 3.2465+00 3.4559+00
3.6787+00 3.9160+00 4.1686+00 4.4374+00 4.7236+00
5.0282+00 5.3525+00 5.6978+00 6.0652+00 6.4564+00
6.8728+00 7.3161+00 7.7879+00 8.2902+00 8.8249+00
9.3940+00 9.9999+00 1.0157+01 1.0317+01 1.0480+01
1.0645+01 1.0812+01 1.0983+01 1.1156+01 1.1331+01
1.1510+01 1.1691+01 1.1875+01 1.2062+01 1.2252+01
1.2445+01 1.2641+01 1.2840+01 1.3042+01 1.3248+01
1.3456+01 1.3668+01 1.3883+01 1.4102+01 1.4324+01
1.4550+01 1.4779+01 1.5012+01 1.5248+01 1.5488+01
c ****
c * problem cutoff cards
c ****
phys:n 16.0 0.0
phys:p 30.0 0 0
phys:e 30.0 1 1 1 1 1 1 1
cut:n 0 0.0 -0.5 -0.25 0
cut:p 0 0.0099 -0.5 -0.25 0
nps 4000000
ctme 1000000
c ****
c * user data arrays
c ****
idum 1
rdum 0.0 0.0 0.0
c ****
c * peripheral cards
c ****
prdm 500000 500000 1 1
lost 10 10
print

```

Fig. 2.2 Continued.

PNS-GRTUNCL SS316/Water Assembly (N125+G40)

0
1\$\$
 0 5 4 38 177 165
 4 5 169 156 0 300
 300 2 1 30000 10 0
 1 0 18 0 0 37
 1 1 1 1
 2**
 1.0 51.3 0.0 0.0 0.0
 T
 1**
 F0.0
 2**
 1I0.0 1.0 2.0 6I3.3 1I17.3 1I19.3 20.3 28I21.3 79.3
 1I80.3 1I81.3 3I82.5 1I85.18 1I86.38 3I87.58 1I90.26
 7I91.46 1I96.54 3I97.74 1I100.42 7I101.62 1I106.7 3I107.9
 1I110.58 7I111.78 1I116.86 3I118.06 1I120.74 121.94
 122.62 123.62 125.02 127.02 129.02 130.42 131.42 1I132.1
 3I133.3 1I135.98 137.18 137.86 138.86 140.26 142.26
 144.26 145.66 146.66 1I147.34 3I148.54 1I151.22 152.42
 3I153.42 218.5
 3**
 F0.0
 4**
 2I0.0 6.0 6.383 6.7 7.3 14I8.0 1I38.0 1I40.0 41.0
 7I42.0 58.0 1I59.0 60.0
 6**
 1.0
 7**
 1.0
 8\$\$
 4R1 34R4 14Q38
 24R1 14R4 32Q38
 38R2 1Q38 38R3 3Q38 38R2 1Q38
 38R2 1Q38 38R3 3Q38 38R2 1Q38
 38R2 7Q38
 38R2 1Q38 38R3 3Q38 38R2 1Q38
 38R2 32Q38
 9\$\$
 -241 -247 -253 -259
 10\$\$
 ' 241 = AIR / 247 = SUS316 / 253 = H2O / 259 = SUS316
 4I241 246 2Q6
 4I247 252 9Q6
 4I253 258 2Q6
 4I259 264 9Q6
 11\$\$
 6Z 4I61 66 4I67 72
 6Z 4I163 168 4I139 144 4I187 192
 4I55 60 4I97 102 4I145 150
 4I103 108 4I109 114 4I151 156
 6Z 4I1 6 4I67 72
 6Z 4I163 168 4I139 144 4I187 192
 4I55 60 4I97 102 4I145 150
 4I103 108 4I109 114 4I151 156
 12**
 6R0.0 6R3.8810-5 6R1.0400-5
 6R0.0 6R9.3405-3 6R1.5482-2 6R1.0585-3 6R1.1931-4 6R1.0341-3
 6R1.0355-3 6R4.3954-5 6R1.9366-6 6R5.7904-2
 6R0.0 6R6.6659-2 6R3.3329-2
 6R0.0 6R9.1456-3 6R1.5025-2 6R1.0254-3 6R1.9855-4 6R8.1608-4
 6R1.3561-3 6R4.7828-5 6R4.5072-6 6R5.8331-2
 13**
 ' LONG WATER COOLED TARGET - ANGULAR COSINE DISTRIBUTION TABLE
 -1.0 -0.996195 -0.984808 -0.965926 -0.939693 -0.906308
 -0.866025 -0.819152 -0.766044 -0.707107 -0.642788 -0.573576
 -0.5 -0.422618 -0.342020 -0.258809 -0.173648 -0.087156
 0.0 0.087156 0.173648 0.258809 0.342020 0.422618
 0.5 0.573576 0.642788 0.707107 0.766044 0.819152
 0.866025 0.906308 0.939693 0.965926 0.984808 0.996195
 1.0
 14**
 ' LONG WATER COOLED TARGET - ANGULAR SOURCE INTENSITY TABLE
 1.1567 1.1785 0.97312 1.0221 0.99500 0.91711
 0.74641 0.73360 0.79463 0.88820 1.0175 1.0581
 1.0532 1.0657 1.0783 1.0797 1.0840 1.0945
 1.0902 0.82512 0.93854 1.0180 1.0603 1.0782
 1.0872 1.1009 1.1043 1.1113 1.1204 1.1200

Fig. 2.3 Input data of FNSUNCL for the DOT analysis of the SS316/water assembly with the FUSION-J3 library (125-n + 40-γ).

1.1219	1.1216	1.1314	1.1266	1.1284	1.1314
1.1312					
15**					
LONG WATER COOLED TARGET - ANGULAR SOURCE SPECTRA TABLE					
DETECTOR NO. 37 ANGLE = 180.0					
0.0	0.0	0.0	0.0	0.0	0.0
0.0	2.8133E-07	1.1132E-05	7.0699E-05	2.9725E-04	5.8035E-03
1.1174E-01	5.0083E-01	2.9325E-01	3.5948E-02	1.9167E-03	2.2345E-03
2.1223E-03	1.5259E-03	9.3736E-04	7.3617E-04	5.2773E-04	2.7017E-04
1.7821E-04	1.8328E-04	2.3002E-04	2.3362E-04	4.2295E-04	2.3769E-04
2.2497E-04	2.1734E-04	8.6941E-04	1.1876E-03	1.5784E-03	1.3262E-03
1.4116E-03	1.4346E-03	2.1877E-03	2.2324E-03	2.4385E-03	2.5503E-03
2.5201E-03	2.8223E-03	2.9695E-03	3.1546E-03	3.6912E-03	3.6241E-03
3.5154E-03	4.0251E-03	4.0676E-03	4.2225E-03	4.3285E-03	4.1782E-03
4.0598E-03	3.8551E-03	3.7352E-03	3.8356E-03	4.0109E-03	4.0103E-03
7.3721E-03	7.7382E-03	7.6206E-03	7.2109E-03	6.8743E-03	6.8912E-03
6.9001E-03	6.5590E-03	5.9411E-03	5.7141E-03	5.3731E-03	4.8503E-03
4.5656E-03	3.9063E-03	3.5676E-03	3.1742E-03	2.8645E-03	2.5666E-03
2.1491E-03	1.6690E-03	1.5357E-03	1.4715E-03	1.1850E-03	7.2317E-04
6.0680E-04	4.8332E-04	4.6588E-04	4.9846E-04	3.4555E-04	2.2581E-04
1.7049E-04	1.9573E-04	1.3086E-04	1.1007E-04	1.4885E-04	9.4420E-05
1.7731E-04	9.3409E-05	7.5281E-05	4.8565E-05	1.4022E-04	5.9894E-05
3.6855E-05	4.8798E-05	1.7405E-05	2.5103E-05	2.5085E-05	2.4342E-05
3.7830E-05	1.1205E-05	4.9533E-06	2.2206E-05	5.0575E-06	1.4315E-06
4.4221E-07	2.1665E-07	1.2984E-07	1.1197E-07	1.2533E-07	7.9222E-08
4.8207E-08	2.9786E-08	1.7825E-08	1.0563E-08	1.7191E-08	
40R0.0					
DETECTOR NO. 36 ANGLE = 175.0					
0.0	0.0	0.0	0.0	0.0	0.0
0.0	3.7835E-07	1.1441E-05	7.1589E-05	3.2069E-04	5.9072E-03
1.1362E-01	5.0424E-01	2.9650E-01	3.6687E-02	2.1034E-03	2.3824E-03
2.3643E-03	1.5373E-03	1.0950E-03	9.0216E-04	5.8232E-04	3.0937E-04
1.9418E-04	2.2513E-04	2.5174E-04	3.7938E-04	3.7668E-04	3.6816E-04
2.6841E-04	2.4088E-04	9.4038E-04	1.2670E-03	2.5181E-03	1.6416E-03
1.5187E-03	1.5842E-03	2.2275E-03	2.2738E-03	2.5485E-03	2.6521E-03
2.7587E-03	2.9765E-03	3.1518E-03	3.3321E-03	3.8155E-03	3.8634E-03
3.8329E-03	4.2131E-03	4.2484E-03	4.3953E-03	4.5454E-03	4.4384E-03
4.3055E-03	4.0501E-03	3.9252E-03	3.9979E-03	4.2933E-03	4.2104E-03
7.8070E-03	8.1364E-03	8.0442E-03	7.6252E-03	7.1929E-03	7.2062E-03
7.1945E-03	6.8679E-03	6.1286E-03	5.7872E-03	5.8984E-03	5.1340E-03
4.6260E-03	4.0971E-03	3.6996E-03	3.2870E-03	3.2319E-03	2.6774E-03
2.2376E-03	1.7009E-03	1.5526E-03	1.6186E-03	1.2897E-03	7.4667E-04
5.9701E-04	4.7018E-04	4.7219E-04	4.6062E-04	3.4094E-04	2.4816E-04
1.6731E-04	1.9320E-04	1.3040E-04	1.0584E-04	1.4500E-04	9.1075E-05
1.5279E-04	9.8490E-05	7.8313E-05	5.6966E-05	1.2022E-04	5.5179E-05
3.4974E-05	4.1840E-05	1.7134E-05	2.4323E-05	2.4930E-05	1.8584E-05
4.2462E-05	1.3667E-05	4.8839E-06	1.7358E-05	4.4998E-06	5.5091E-07
3.9295E-07	2.9448E-07	2.7264E-07	2.3974E-07	2.0566E-07	1.2782E-07
7.7551E-08	4.7355E-08	2.8479E-08	1.6972E-08	2.6943E-08	
40RC.0					
DETECTOR NO. 35 ANGLE = 170.0					
0.0	0.0	0.0	0.0	0.0	0.0
0.0	3.6185E-07	9.5040E-06	5.8872E-05	2.8999E-04	4.7439E-03
1.5019E-01	3.5413E-01	2.5513E-01	2.4816E-02	1.7208E-03	1.9255E-03
1.9925E-03	1.2381E-03	1.2442E-03	8.6672E-04	5.0687E-04	2.7164E-04
2.0134E-04	1.9040E-04	1.9574E-04	2.9987E-04	2.9225E-04	3.6524E-04
2.8297E-04	2.3123E-04	7.8890E-04	1.0449E-03	1.3277E-03	1.1490E-03
1.1557E-03	1.2977E-03	1.6929E-03	1.7493E-03	2.0090E-03	2.0004E-03
2.1562E-03	2.3733E-03	2.7334E-03	2.7047E-03	2.9446E-03	3.2352E-03
4.5391E-03	3.3228E-03	3.3184E-03	3.7626E-03	3.6943E-03	3.5435E-03
4.8576E-03	3.3648E-03	3.3153E-03	3.2196E-03	3.5733E-03	3.3254E-03
6.7419E-03	6.7177E-03	7.3722E-03	6.3825E-03	6.0115E-03	5.9379E-03
5.6789E-03	5.7026E-03	5.1413E-03	4.6794E-03	5.7318E-03	3.8717E-03
3.7424E-03	3.3807E-03	3.0274E-03	2.6121E-03	2.6251E-03	1.8869E-03
1.7138E-03	1.1776E-03	1.1197E-03	1.7472E-03	1.2439E-03	5.9356E-04
4.4854E-04	3.3661E-04	3.3863E-04	3.3456E-04	2.4365E-04	1.8998E-04
1.1907E-04	1.1157E-04	4.0102E-05	3.6947E-05	1.1068E-04	6.7082E-05
8.6911E-05	4.8253E-05	4.7431E-05	6.2276E-05	7.4372E-05	3.5246E-05
1.7196E-05	2.2051E-05	9.4176E-06	1.8920E-05	1.7962E-05	9.0355E-06
3.3089E-05	8.9171E-06	1.6759E-06	7.9120E-06	1.8300E-06	6.4386E-07
2.3745E-07	1.2144E-07	1.1283E-07	7.6016E-08	4.5987E-08	2.7550E-08
1.6531E-08	9.9574E-09	5.8651E-09	3.3952E-09	4.5389E-09	
40R0.0					
DETECTOR NO. 34 ANGLE = 165.0					
0.0	0.0	0.0	0.0	0.0	0.0
0.0	5.1082E-07	1.1670E-05	7.0606E-05	4.2223E-04	6.0348E-03
2.1281E-01	3.4467E-01	2.7046E-01	1.5885E-02	1.7828E-03	1.8549E-03
1.7356E-03	1.1338E-03	7.8382E-04	6.0876E-04	4.0911E-04	2.3795E-04
1.3771E-04	1.5310E-04	1.7963E-04	2.1663E-04	2.7483E-04	3.0444E-04
2.4874E-04	2.1519E-04	7.7115E-04	1.0766E-03	1.3225E-03	1.0973E-03
1.0457E-03	1.2748E-03	1.7166E-03	1.7760E-03	1.8308E-03	1.9160E-03
2.1251E-03	2.2543E-03	2.5858E-03	2.5611E-03	2.8428E-03	2.9902E-03
2.9110E-03	3.1924E-03	3.2355E-03	3.7441E-03	3.6503E-03	3.3356E-03
3.3900E-03	3.1860E-03	3.0971E-03	3.1019E-03	3.3434E-03	3.1527E-03
5.2305E-03	6.4802E-03	6.4301E-03	6.0320E-03	5.7398E-03	5.7555E-03
5.6117E-03	5.5303E-03	4.9000E-03	4.6177E-03	4.9295E-03	4.0625E-03
3.6606E-03	3.2393E-03	2.9173E-03	2.5212E-03	2.3047E-03	1.9101E-03
1.6915E-03	1.2459E-03	1.1716E-03	1.3675E-03	9.7259E-04	5.6789E-04
4.6392E-04	3.5134E-04	3.2277E-04	2.9870E-04	2.1404E-04	1.7976E-04

Fig. 2.3 Continued.

1.1890E-04	1.1646E-04	5.0052E-05	5.5373E-05	1.1692E-04	6.9411E-05
1.0414E-04	6.2000E-05	5.1281E-05	8.9099E-05	9.3171E-05	4.3286E-05
2.3677E-05	3.2742E-05	1.0195E-05	2.2316E-05	2.0126E-05	1.3144E-05
3.2913E-05	9.9547E-06	2.7943E-06	7.1506E-06	1.9256E-06	7.2235E-07
6.9051E-07	4.3253E-07	1.8998E-07	5.8739E-08	3.5327E-08	2.1339E-08
1.2501E-08	7.0393E-09	4.0867E-09	2.3189E-09	3.6063E-09	
40R0.0					
' DETECTOR NO. 33 ANGLE = 160.0					
0.0	0.0	0.0	0.0	0.0	0.0
0.0	6.7487E-07	1.3181E-05	8.1451E-05	5.1859E-04	9.0841E-03
2.1863E-01	3.9434E-01	2.1507E-01	4.7857E-03	1.3917E-03	1.5682E-03
1.4746E-03	9.7756E-04	7.3315E-04	5.3407E-04	3.6160E-04	1.9848E-04
1.8629E-04	1.4586E-04	1.6584E-04	2.0129E-04	2.0772E-04	2.3660E-04
1.9806E-04	1.9433E-04	6.8231E-04	1.0178E-03	1.2018E-03	9.7392E-04
9.2581E-04	1.1802E-03	1.5383E-03	1.6285E-03	1.5696E-03	1.7448E-03
1.7410E-03	2.0592E-03	2.1806E-03	2.2943E-03	2.4707E-03	2.6902E-03
2.5402E-03	2.8614E-03	2.9290E-03	3.4241E-03	3.2323E-03	2.8926E-03
2.9612E-03	2.8695E-03	2.7537E-03	2.7800E-03	2.9559E-03	2.8356E-03
5.4665E-03	5.8099E-03	5.7228E-03	5.4298E-03	5.2356E-03	5.1995E-03
5.1038E-03	4.9578E-03	4.4405E-03	4.2069E-03	3.8507E-03	3.5177E-03
3.3137E-03	2.8949E-03	2.6330E-03	2.2811E-03	2.0353E-03	1.7130E-03
1.5128E-03	1.1546E-03	1.0909E-03	1.1571E-03	8.3544E-04	5.1003E-04
4.1129E-04	3.1477E-04	2.7525E-04	2.5511E-04	1.8714E-04	1.6139E-04
1.1163E-04	1.1493E-04	4.8959E-05	5.5486E-05	1.1391E-04	6.5659E-05
1.0277E-04	6.4725E-05	5.0868E-05	7.0970E-05	8.3075E-05	4.1826E-05
2.1846E-05	2.7435E-05	8.8435E-06	2.4692E-05	1.9525E-05	1.3839E-05
2.6915E-05	1.1308E-05	3.5200E-06	6.7376E-06	2.1735E-06	3.9223E-07
2.3959E-07	1.4161E-07	7.7039E-08	7.7988E-08	5.0946E-08	3.0675E-08
1.8100E-08	1.0424E-08	6.0555E-09	3.4685E-09	5.3803E-09	
40RC.0					
' DETECTOR NO. 32 ANGLE = 155.0					
0.0	0.0	0.0	0.0	0.0	0.0
0.0	8.9791E-07	1.4586E-05	9.5698E-05	5.6608E-04	2.6967E-02
1.9132E-01	3.9240E-01	1.6671E-01	3.8048E-03	1.3617E-03	1.3263E-03
1.2102E-03	8.8958E-04	7.5102E-04	4.8041E-04	3.2739E-04	1.8630E-04
1.9849E-04	1.3412E-04	1.5276E-04	1.7149E-04	1.6488E-04	1.8827E-04
1.4737E-04	1.4125E-04	5.8666E-04	9.2285E-04	1.1113E-03	8.3773E-04
8.4104E-04	1.0331E-03	1.3060E-03	1.4303E-03	1.3361E-03	1.5202E-03
1.5421E-03	1.8882E-03	1.9012E-03	2.0756E-03	2.1427E-03	2.3393E-03
2.3223E-03	2.5239E-03	2.6141E-03	2.9561E-03	2.8357E-03	2.5353E-03
2.6349E-03	2.5420E-03	2.4548E-03	2.4387E-03	2.6031E-03	2.5276E-03
4.8102E-03	5.1441E-03	5.0666E-03	4.8717E-03	4.7288E-03	4.6509E-03
4.5458E-03	4.4021E-03	3.9861E-03	3.7728E-03	3.3999E-03	3.0991E-03
2.9660E-03	2.5794E-03	2.3559E-03	2.0473E-03	1.7990E-03	1.5004E-03
1.3428E-03	1.0309E-03	9.7457E-04	1.0035E-03	7.1358E-04	4.4090E-04
3.6019E-04	2.8148E-04	2.3747E-04	2.1923E-04	1.6562E-04	1.3953E-04
9.6636E-05	1.0480E-04	4.7050E-05	4.9619E-05	1.0190E-04	6.0504E-05
9.2283E-05	5.7845E-05	4.5599E-05	4.8541E-05	6.929CE-05	3.9698E-05
2.3074E-05	2.2337E-05	7.0312E-06	2.2823E-05	1.6930E-05	1.4584E-05
2.2601E-05	8.4404E-06	3.3708E-06	5.5248E-06	1.9803E-06	3.1467E-07
1.1544E-07	1.1136E-07	6.8319E-08	4.0515E-08	3.0920E-08	2.0354E-08
1.3326E-08	6.5807E-09	3.7466E-09	2.0959E-09	2.9469E-09	
40RC.0					
' DETECTOR NO. 31 ANGLE = 150.0					
0.0	0.0	0.0	0.0	0.0	0.0
0.0	1.1210E-06	1.5006E-05	1.0060E-04	5.2316E-04	2.2578E-02
2.2494E-01	2.7657E-01	9.8913E-02	3.5616E-03	1.3244E-03	1.1043E-03
9.6955E-04	7.9390E-04	6.9932E-04	4.4349E-04	3.4276E-04	1.8292E-04
2.4814E-04	1.3386E-04	1.4963E-04	1.8128E-04	1.3764E-04	1.6132E-04
1.2904E-04	1.1531E-04	4.8660E-04	8.5456E-04	1.0188E-03	6.9732E-04
7.4484E-04	9.3855E-04	1.1452E-03	1.2785E-03	1.1886E-03	1.3201E-03
1.3301E-03	1.6687E-03	1.6385E-03	1.8017E-03	1.8697E-03	2.0389E-03
2.0579E-03	2.2140E-03	2.3498E-03	2.6237E-03	2.4751E-03	2.2369E-03
2.3388E-03	2.2566E-03	2.1950E-03	2.1379E-03	2.2828E-03	2.2342E-03
4.2100E-03	4.5225E-03	4.4508E-03	4.3349E-03	4.2050E-03	4.1278E-03
3.9950E-03	3.8727E-03	3.5175E-03	3.3076E-03	2.9602E-03	2.6811E-03
2.6115E-03	2.2597E-03	2.0636E-03	1.8064E-03	1.5735E-03	1.2990E-03
1.1844E-03	9.0201E-04	8.5816E-04	8.6443E-04	6.0849E-04	3.8430E-04
3.1181E-04	2.4748E-04	2.0782E-04	1.8709E-04	1.5327E-04	1.2630E-04
9.5958E-05	9.1331E-05	4.4863E-05	4.5554E-05	8.6432E-05	5.3778E-05
7.8548E-05	4.9695E-05	3.7560E-05	3.3195E-05	5.9252E-05	3.5652E-05
1.7451E-05	2.0285E-05	4.7895E-06	1.8249E-05	1.5183E-05	1.4572E-05
1.9134E-05	7.6785E-06	2.8089E-06	3.6283E-06	1.4016E-06	2.6963E-07
1.1540E-07	4.7313E-08	3.6275E-08	3.7447E-08	3.0101E-08	1.6947E-08
6.5259E-09	2.4384E-09	1.3198E-09	6.9724E-10	1.0039E-09	
40R0.C					
' DETECTOR NO. 30 ANGLE = 145.0					
0.0	0.0	0.0	0.0	0.0	0.0
0.0	1.6949E-06	2.1978E-05	1.3643E-04	6.0091E-04	2.3480E-02
2.6318E-01	2.7600E-01	5.4050E-02	3.2500E-03	1.2919E-03	1.0160E-03
8.5611E-04	7.1990E-04	6.3299E-04	4.2210E-04	3.4271E-04	1.9814E-04
2.3532E-04	1.4259E-04	1.4960E-04	1.7688E-04	1.2743E-04	1.2620E-04
1.2203E-04	1.0976E-04	4.6639E-04	8.1490E-04	9.8662E-04	6.6162E-04
7.6303E-04	9.2414E-04	1.1079E-03	1.2367E-03	1.1609E-03	1.2308E-03
1.2418E-03	1.5900E-03	1.5573E-03	1.7221E-03	1.7437E-03	1.8929E-03
1.9941E-03	2.1000E-03	2.2515E-03	2.5008E-03	2.3070E-03	2.1394E-03
2.2162E-03	2.1584E-03	2.1062E-03	2.0473E-03	2.1780E-03	2.1356E-03
4.0013E-03	4.3099E-03	4.2048E-03	4.1103E-03	3.9833E-03	3.9063E-03
3.7788E-03	3.6355E-03	3.3137E-03	3.1030E-03	2.7784E-03	2.5073E-03

Fig. 2.3 Continued.

2.4569E-03	2.1258E-03	1.9309E-03	1.6933E-03	1.4796E-03	1.2275E-03
1.1158E-03	8.5627E-04	8.1476E-04	8.0224E-04	5.6604E-04	3.5453E-04
2.8569E-04	2.3434E-04	1.9996E-04	1.7156E-04	1.5059E-04	1.1994E-04
8.3085E-05	8.4877E-05	4.9478E-05	4.6774E-05	8.0741E-05	5.2202E-05
7.5314E-05	4.2304E-05	3.3567E-05	2.8351E-05	5.3527E-05	3.0993E-05
1.6388E-05	1.8109E-05	6.9991E-06	1.7221E-05	1.4210E-05	1.3371E-05
1.7076E-05	4.4784E-06	1.5095E-06	4.4346E-06	1.6978E-06	2.6603E-07
8.8200E-08	1.0072E-07	1.4891E-07	1.3208E-07	8.9108E-08	4.9790E-08
2.1794E-08	1.1539E-08	6.7703E-09	3.9349E-09	6.0322E-09	
40R0.0					
DETECTOR NO. 29 ANGLE = 140.0					
0.0	0.0	0.0	0.0	0.0	0.0
8.3758E-09	3.2259E-06	3.6848E-05	1.9696E-04	7.5786E-04	2.8071E-02
3.6635E-01	2.6706E-01	1.7009E-02	2.9138E-03	1.3014E-03	9.8912E-04
7.9827E-04	6.6673E-04	6.0671E-04	4.1567E-04	3.3070E-04	2.1432E-04
2.4904E-04	1.5170E-04	1.5436E-04	1.4332E-04	1.2830E-04	1.1970E-04
1.1459E-04	1.1102E-04	4.7404E-04	8.0617E-04	9.7136E-04	6.5863E-04
8.2244E-04	9.7565E-04	1.0950E-03	1.2550E-03	1.1613E-03	1.2151E-03
1.2302E-03	1.5517E-03	1.5489E-03	1.7214E-03	1.7282E-03	1.8651E-03
2.0120E-03	2.1197E-03	2.2769E-03	2.4929E-03	2.2883E-03	2.1430E-03
2.2366E-03	2.1648E-03	2.0825E-03	2.0127E-03	2.1776E-03	2.1173E-03
3.9451E-03	4.2898E-03	4.1755E-03	4.0607E-03	3.9507E-03	3.8711E-03
3.7580E-03	3.5891E-03	3.2842E-03	3.0715E-03	2.7721E-03	2.4871E-03
2.4433E-03	2.1114E-03	1.9100E-03	1.6739E-03	1.4647E-03	1.2191E-03
1.1111E-03	8.6411E-04	8.1556E-04	7.8804E-04	5.6044E-04	3.4677E-04
2.7549E-04	2.3238E-04	2.0242E-04	1.6774E-04	1.4996E-04	1.1996E-04
8.8578E-05	8.9432E-05	6.1748E-05	5.2939E-05	7.9992E-05	5.4394E-05
7.6257E-05	4.5755E-05	3.6237E-05	3.1611E-05	5.1836E-05	2.7927E-05
1.9274E-05	1.6869E-05	7.9097E-06	1.8214E-05	1.4095E-05	1.1872E-05
1.8913E-05	4.2903E-06	1.3943E-06	6.0019E-06	1.6842E-06	3.9013E-07
2.0573E-07	3.0670E-07	2.9182E-07	1.2486E-07	7.4879E-08	4.5499E-08
2.6566E-08	1.4635E-08	8.5884E-09	4.9522E-09	7.6450E-09	
40R0.0					
DETECTOR NO. 28 ANGLE = 135.0					
0.0	0.0	0.0	0.0	0.0	0.0
6.6301E-08	7.0022E-06	6.0610E-05	3.0120E-04	1.1054E-03	8.7910E-02
4.5054E-01	2.2314E-01	8.7039E-03	2.5413E-03	1.3146E-03	1.0274E-03
7.7033E-04	6.4257E-04	5.1682E-04	3.9690E-04	3.3611E-04	2.2998E-04
2.7166E-04	1.6956E-04	1.6884E-04	1.4875E-04	1.4039E-04	1.3160E-04
1.2650E-04	1.2339E-04	5.1868E-04	8.3099E-04	9.5169E-04	6.6309E-04
8.2152E-04	9.6828E-04	1.1113E-03	1.2520E-03	1.1899E-03	1.2335E-03
1.2741E-03	1.5875E-03	1.6245E-03	1.8029E-03	1.7928E-03	1.9302E-03
2.0497E-03	2.1811E-03	2.3036E-03	2.5041E-03	2.3271E-03	2.1892E-03
2.2790E-03	2.1897E-03	2.0963E-03	2.0463E-03	2.2020E-03	2.1441E-03
3.9834E-03	4.3372E-03	4.2133E-03	4.0817E-03	3.9724E-03	3.9057E-03
3.8220E-03	3.6130E-03	3.3144E-03	3.1137E-03	2.8229E-03	2.5167E-03
2.4615E-03	2.1303E-03	1.9255E-03	1.6999E-03	1.4891E-03	1.2549E-03
1.1354E-03	8.9488E-04	8.3718E-04	7.9595E-04	5.7350E-04	3.4863E-04
2.6964E-04	2.2675E-04	2.0970E-04	1.7849E-04	1.6461E-04	1.2741E-04
9.9796E-05	9.6615E-05	7.5223E-05	5.9055E-05	7.8031E-05	5.5161E-05
7.8496E-05	5.2523E-05	4.4599E-05	3.7881E-05	5.6352E-05	2.7468E-05
1.9952E-05	1.7650E-05	1.0450E-05	1.7764E-05	1.3308E-05	1.2003E-05
1.9138E-05	4.9426E-06	1.1253E-06	6.6121E-06	2.0351E-06	7.2957E-07
1.2222E-06	6.9884E-07	2.5650E-07	1.2777E-07	8.1596E-08	4.9696E-08
2.9194E-08	1.6330E-08	9.6405E-09	5.6648E-09	8.9422E-09	
40R0.0					
DETECTOR NO. 27 ANGLE = 130.0					
0.0	0.0	0.0	0.0	0.0	0.0
2.2355E-07	1.3946E-05	9.7231E-05	4.9304E-04	4.3809E-03	1.5888E-01
5.9957E-01	1.2934E-01	5.9629E-03	2.2007E-03	1.3389E-03	1.0226E-03
7.5445E-04	5.9669E-04	5.2290E-04	3.8106E-04	3.1829E-04	2.3544E-04
2.5732E-04	1.7797E-04	1.7706E-04	1.5935E-04	1.5720E-04	1.4166E-04
1.3660E-04	1.3429E-04	5.6647E-04	8.3879E-04	9.1136E-04	6.5701E-04
8.6825E-04	9.8927E-04	1.1826E-03	1.3017E-03	1.2510E-03	1.2741E-03
1.3552E-03	1.6826E-03	1.7276E-03	1.9284E-03	1.8946E-03	2.0313E-03
2.1083E-03	2.2246E-03	2.3216E-03	2.5221E-03	2.3616E-03	2.2390E-03
2.3086E-03	2.2094E-03	2.1091E-03	2.0756E-03	2.2469E-03	2.1756E-03
4.0428E-03	4.4142E-03	4.2691E-03	4.1176E-03	4.0365E-03	3.9712E-03
3.9220E-03	3.6633E-03	3.3799E-03	3.1996E-03	2.9137E-03	2.5972E-03
2.5078E-03	2.1761E-03	1.9691E-03	1.7425E-03	1.5346E-03	1.2927E-03
1.1557E-03	9.3503E-04	8.6952E-04	8.1876E-04	6.0651E-04	3.6738E-04
2.8595E-04	2.3679E-04	2.0954E-04	1.7714E-04	1.7153E-04	1.3969E-04
1.1067E-04	1.0034E-04	8.4935E-05	6.6903E-05	7.9046E-05	5.6364E-05
8.5317E-05	5.9717E-05	5.2391E-05	4.5358E-05	5.7759E-05	3.0117E-05
2.6913E-05	2.0625E-05	1.2195E-05	1.8492E-05	1.4476E-05	9.8925E-06
1.8589E-05	5.0499E-06	2.0118E-06	8.0632E-06	3.2367E-06	3.1658E-06
1.1346E-06	3.5995E-07	1.2803E-07	7.6927E-08	5.1571E-08	3.1477E-08
1.8233E-08	9.7204E-09	5.6876E-09	3.2586E-09	5.5706E-09	
40R0.0					
DETECTOR NO. 26 ANGLE = 125.0					
0.0	0.0	0.0	0.0	0.0	0.0
8.5582E-07	2.2739E-05	1.3161E-04	7.7918E-04	6.1183E-03	3.1671E-01
5.9319E-01	1.9254E-02	4.2549E-03	1.8912E-03	1.2685E-03	9.9572E-04
7.1559E-04	5.6036E-04	5.0357E-04	3.6113E-04	2.8606E-04	2.4805E-04
2.5531E-04	1.8159E-04	1.6519E-04	1.5199E-04	1.6071E-04	1.4352E-04
1.3665E-04	1.4310E-04	5.7015E-04	8.1935E-04	9.1369E-04	6.8028E-04
8.9815E-04	1.0154E-03	1.2839E-03	1.3774E-03	1.3314E-03	1.3337E-03
1.4193E-03	1.6868E-03	1.7090E-03	1.9331E-03	1.8861E-03	2.0201E-03
2.0664E-03	2.2012E-03	2.2858E-03	2.4728E-03	2.3247E-03	2.2206E-03

Fig. 2.3 Continued.

JAERI-Research 95-018

2.2796E-03	2.1704E-03	2.0723E-03	2.0613E-03	2.2326E-03	2.1488E-03
3.9762E-03	4.3459E-03	4.2034E-03	4.0561E-03	3.9872E-03	3.9286E-03
3.8897E-03	3.6131E-03	3.3366E-03	3.1493E-03	2.8801E-03	2.5846E-03
2.4904E-03	2.1592E-03	1.9439E-03	1.7274E-03	1.5526E-03	1.3002E-03
1.1447E-03	9.3905E-04	8.6726E-04	8.1126E-04	6.1134E-04	3.6682E-04
2.8080E-04	2.3767E-04	2.1721E-04	1.8225E-04	1.7178E-04	1.3597E-04
1.0931E-04	1.0084E-04	9.0884E-05	7.4498E-05	8.6072E-05	5.9279E-05
8.6327E-05	5.7765E-05	5.9750E-05	4.8184E-05	5.8773E-05	3.7165E-05
3.1479E-05	1.8343E-05	1.0464E-05	1.7527E-05	1.5228E-05	1.1005E-05
1.9083E-05	5.1425E-06	2.2032E-06	1.0534E-05	6.3183E-06	2.2495E-06
6.1526E-07	1.8923E-07	4.3189E-08	2.6625E-08	2.0829E-08	1.2829E-08
6.9631E-09	2.9984E-09	1.6296E-09	8.2994E-10	1.6024E-09	
40R0.0					
' DETECTOR NO. 25 ANGLE = 120.0					
0.0	0.0	0.0	0.0	0.0	0.0
2.2944E-06	3.3811E-05	2.0585E-04	1.5900E-03	7.8871E-03	5.6856E-01
3.4946E-01	7.6500E-03	3.1351E-03	1.6418E-03	1.2196E-03	9.4631E-04
6.8750E-04	5.2345E-04	4.6385E-04	3.3053E-04	2.6771E-04	2.3717E-04
2.3658E-04	1.8547E-04	1.5747E-04	1.4898E-04	1.5736E-04	1.4089E-04
1.3291E-04	1.4087E-04	5.5408E-04	8.4586E-04	9.6960E-04	7.7944E-04
9.8683E-04	0.0752E-03	1.2825E-03	1.3533E-03	1.3243E-03	1.3264E-03
1.4078E-03	1.6601E-03	1.6755E-03	1.8912E-03	1.8535E-03	1.9788E-03
1.9998E-03	2.1421E-03	2.1830E-03	2.3896E-03	2.2551E-03	2.1527E-03
2.2215E-03	2.1034E-03	2.0160E-03	2.0111E-03	2.1694E-03	2.0831E-03
3.8573E-03	4.2221E-03	4.0743E-03	3.9483E-03	3.8728E-03	3.8028E-03
3.7698E-03	3.4982E-03	3.2364E-03	3.0578E-03	2.7958E-03	2.5239E-03
2.4336E-03	2.1076E-03	1.8878E-03	1.6749E-03	1.4965E-03	1.2732E-03
1.1155E-03	9.3412E-04	8.5527E-04	7.7762E-04	5.8585E-04	3.4910E-04
2.7138E-04	2.4068E-04	2.1652E-04	1.7720E-04	1.6964E-04	1.3553E-04
1.0859E-04	1.0309E-04	8.9797E-05	7.1544E-05	8.7058E-05	6.2362E-05
8.9898E-05	6.3702E-05	5.9993E-05	4.5523E-05	5.5730E-05	3.6701E-05
2.9748E-05	1.5837E-05	1.1124E-05	2.2795E-05	1.4229E-05	8.8521E-06
1.9648E-05	5.1785E-06	5.5667E-06	7.2296E-06	6.5238E-06	2.9807E-06
5.7698E-07	1.8522E-07	7.1894E-08	4.5585E-08	3.1981E-08	1.9536E-08
1.0981E-08	5.5515E-09	3.1608E-09	1.7897E-09	2.8533E-09	
40R0.0					
' DETECTOR NO. 24 ANGLE = 115.0					
0.0	0.0	0.0	0.0	0.0	1.4415E-08
4.4834E-06	4.7137E-05	3.0702E-04	2.8316E-03	1.8619E-02	8.4279E-01
8.1891E-02	4.7301E-03	2.4430E-03	1.5379E-03	1.1489E-03	8.7505E-04
6.4023E-04	4.8227E-04	4.3108E-04	3.0496E-04	2.5063E-04	2.3437E-04
2.3187E-04	2.0034E-04	1.5201E-04	1.5186E-04	1.6844E-04	1.4502E-04
1.3759E-04	1.4760E-04	5.7055E-04	8.7709E-04	1.0182E-03	8.6560E-04
1.0445E-03	1.1305E-03	1.2765E-03	1.3224E-03	1.3054E-03	1.3152E-03
1.3994E-03	1.6094E-03	1.6300E-03	1.8327E-03	1.8031E-03	1.9288E-03
1.9485E-03	2.0799E-03	2.1175E-03	2.3097E-03	2.2058E-03	2.1046E-03
2.1662E-03	2.0429E-03	1.9604E-03	1.9571E-03	2.0955E-03	2.0126E-03
3.7415E-03	4.1118E-03	3.9645E-03	3.8493E-03	3.7739E-03	3.7071E-03
3.6781E-03	3.4034E-03	3.1671E-03	3.0000E-03	2.7342E-03	2.4611E-03
2.3599E-03	2.0534E-03	1.8559E-03	1.6405E-03	1.4539E-03	1.2337E-03
1.0920E-03	9.2547E-04	8.4566E-04	7.5657E-04	5.7723E-04	3.5307E-04
2.7371E-04	2.2411E-04	1.9684E-04	1.7383E-04	1.7130E-04	1.3713E-04
1.0535E-04	1.0217E-04	9.1919E-05	7.0141E-05	8.3613E-05	6.3252E-05
9.2454E-05	6.7626E-05	5.7599E-05	4.4719E-05	5.5483E-05	3.7441E-05
2.8970E-05	1.6255E-05	1.2075E-05	2.3158E-05	1.5932E-05	9.1442E-06
2.0923E-05	7.3523E-06	7.5554E-06	7.5417E-06	6.3468E-06	1.4703E-06
4.2676E-07	2.5603E-07	1.2244E-07	7.5931E-08	4.9930E-08	3.0287E-08
1.7540E-08	9.4677E-09	5.5093E-09	3.1850E-09	5.2187E-09	
40R0.0					
' DETECTOR NO. 23 ANGLE = 110.0					
0.0	0.0	0.0	0.0	0.0	2.8857E-08
8.4050E-06	6.7246E-05	4.9937E-04	6.4064E-03	6.9774E-02	8.8061E-01
6.3306E-03	3.1939E-03	1.9961E-03	1.4631E-03	1.1140E-03	8.1587E-04
5.9222E-04	4.5432E-04	4.0108E-04	2.8284E-04	2.3983E-04	2.5734E-04
2.4407E-04	2.2296E-04	1.8480E-04	1.7862E-04	1.9698E-04	1.7189E-04
1.6452E-04	1.7347E-04	6.6770E-04	9.1612E-04	9.8309E-04	8.9031E-04
1.0275E-03	1.1093E-03	1.2229E-03	1.2982E-03	1.2804E-03	1.2930E-03
1.3701E-03	1.5650E-03	1.6012E-03	1.7724E-03	1.7565E-03	1.8926E-03
1.9026E-03	2.0189E-03	2.0568E-03	2.2317E-03	2.1508E-03	2.0385E-03
2.1040E-03	1.9729E-03	1.9102E-03	1.9021E-03	2.0363E-03	1.9592E-03
3.6355E-03	4.0035E-03	3.8620E-03	3.7363E-03	3.6580E-03	3.5985E-03
3.5666E-03	3.2867E-03	3.0703E-03	2.9282E-03	2.6590E-03	2.3968E-03
2.3009E-03	2.0002E-03	1.7962E-03	1.5949E-03	1.4262E-03	1.2106E-03
1.0581E-03	8.9560E-04	8.0717E-04	7.3452E-04	5.5559E-04	3.4747E-04
2.7755E-04	2.2014E-04	1.9227E-04	1.7518E-04	1.6971E-04	1.3485E-04
1.0288E-04	9.6823E-05	8.8290E-05	6.5954E-05	8.0897E-05	6.1697E-05
9.1331E-05	7.1904E-05	5.6933E-05	4.5038E-05	5.0421E-05	3.4796E-05
3.6050E-05	1.9702E-05	1.4569E-05	2.2191E-05	1.3973E-05	8.5006E-06
2.0144E-05	8.7232E-06	6.8648E-06	6.3568E-06	3.9792E-06	2.5051E-06
1.0405E-06	2.5855E-07	1.0838E-07	6.6257E-08	4.3805E-08	2.6631E-08
1.5380E-08	8.2229E-09	4.7720E-09	2.7969E-09	4.7150E-09	
40R0.0					
' DETECTOR NO. 22 ANGLE = 105.0					
0.0	0.0	0.0	0.0	0.0	2.4873E-07
1.3231E-05	9.2865E-05	8.7947E-04	1.3776E-02	5.4827E-01	4.0248E-01
4.2705E-03	2.3001E-03	1.7099E-03	1.4454E-03	1.0999E-03	7.5577E-04
5.4657E-04	4.3171E-04	3.7012E-04	2.7472E-04	2.4669E-04	2.6774E-04
2.4633E-04	2.3636E-04	2.0276E-04	1.9019E-04	2.0703E-04	1.8552E-04
1.7636E-04	1.9123E-04	7.1085E-04	8.9644E-04	9.4240E-04	8.7186E-04

Fig. 2.3 Continued.

9.8223E-04	1.0780E-03	1.1703E-03	1.2653E-03	1.2398E-03	1.2590E-03
1.3328E-03	1.5009E-03	1.5371E-03	1.7079E-03	1.6953E-03	1.6319E-03
1.8430E-03	1.9497E-03	1.9829E-03	2.1372E-03	2.0793E-03	1.9679E-03
2.0431E-03	1.9088E-03	1.8442E-03	1.8315E-03	1.9621E-03	1.8867E-03
3.5061E-03	3.8795E-03	3.7337E-03	3.6138E-03	3.5382E-03	3.4833E-03
3.4601E-03	3.1937E-03	2.9823E-03	2.8333E-03	2.5601E-03	2.3144E-03
2.2220E-03	1.9272E-03	1.7283E-03	1.5299E-03	1.3665E-03	1.1669E-03
1.0239E-03	8.7194E-04	7.8028E-04	7.0345E-04	5.4430E-04	3.3167E-04
2.6637E-04	2.1845E-04	1.8906E-04	1.6148E-04	1.5728E-04	1.3204E-04
9.6734E-05	8.4057E-05	8.5157E-05	6.6669E-05	7.7763E-05	5.9391E-05
9.3587E-05	6.9867E-05	5.6189E-05	4.3179E-05	4.9298E-05	3.1133E-05
2.9982E-05	2.0273E-05	1.5702E-05	2.0473E-05	1.5198E-05	9.2796E-06
1.8551E-05	1.0498E-05	4.8483E-05	8.7398E-06	2.1959E-06	2.5108E-06
1.0289E-06	1.7426E-07	5.2550E-08	3.2498E-08	2.3054E-08	1.4153E-08
7.8995E-09	3.8570E-09	2.1661E-09	1.1424E-09	2.1773E-09	
40R0.0					
' DETECTOR NO. 21		ANGLE = 100.0			
0.0	0.0	0.0	0.0	0.0	6.7023E-07
2.9288E-05	1.7547E-04	1.8057E-03	2.0560E-02	9.4450E-01	8.1780E-03
2.9787E-03	1.8119E-03	1.5798E-03	1.4520E-03	1.1037E-03	7.3572E-04
5.3950E-04	4.3129E-04	3.7038E-04	2.9151E-04	2.7802E-04	2.6086E-04
2.4018E-04	2.2862E-04	2.0259E-04	1.8758E-04	2.0163E-04	1.3093E-04
1.7206E-04	1.8755E-04	6.9083E-04	8.4623E-04	9.0626E-04	8.6180E-04
9.5296E-04	1.0568E-03	1.1042E-03	1.1929E-03	1.1642E-03	1.2073E-03
1.2857E-03	1.4376E-03	1.5100E-03	1.6570E-03	1.6449E-03	1.7720E-03
1.7847E-03	1.8966E-03	1.9153E-03	2.0644E-03	2.0157E-03	1.9035E-03
1.9710E-03	1.8495E-03	1.7900E-03	1.7761E-03	1.8985E-03	1.8279E-03
3.3926E-03	3.7559E-03	3.6132E-03	3.4778E-03	3.4071E-03	3.3684E-03
3.3436E-03	3.0840E-03	2.8801E-03	2.7284E-03	2.4570E-03	2.2382E-03
2.1482E-03	1.8546E-03	1.6710E-03	1.4796E-03	1.3114E-03	1.1202E-03
9.7835E-04	8.3622E-04	7.5337E-04	6.7702E-04	5.2798E-04	3.1833E-04
2.4811E-04	2.0853E-04	1.8748E-04	1.5595E-04	1.4415E-04	1.2448E-04
9.1237E-05	7.7455E-05	8.2274E-05	6.6356E-05	7.3316E-05	5.3120E-05
8.4060E-05	7.3440E-05	6.0267E-05	4.3339E-05	4.4719E-05	2.7196E-05
2.7864E-05	1.8710E-05	1.5473E-05	1.9280E-05	1.4095E-05	8.9170E-06
1.7487E-05	1.0095E-05	4.8414E-06	8.2697E-06	2.2037E-06	2.5050E-06
1.0648E-06	2.2204E-07	8.2337E-08	5.0716E-08	3.3780E-08	2.0615E-08
1.1878E-08	6.3301E-09	3.6336E-09	2.0456E-09	3.5337E-09	
40R0.0					
' DETECTOR NO. 20		ANGLE = 95.0			
0.0	0.0	0.0	0.0	0.0	1.4046E-06
3.9778E-05	2.5477E-04	3.3630E-03	2.5387E-02	9.5634E-01	6.4895E-03
2.1419E-03	1.4871E-03	1.4673E-03	1.4270E-03	1.0912E-03	7.1690E-04
5.2895E-04	4.2708E-04	3.6821E-04	3.0136E-04	2.8959E-04	2.4770E-04
2.2306E-04	2.2121E-04	1.9980E-04	1.8731E-04	1.9661E-04	1.7747E-04
1.6918E-04	1.8426E-04	6.7558E-04	8.0302E-04	8.5648E-04	8.1939E-04
8.9015E-04	9.9780E-04	1.0439E-03	1.1423E-03	1.1137E-03	1.1570E-03
1.2344E-03	1.3704E-03	1.4148E-03	1.5532E-03	1.5615E-03	1.6768E-03
1.7000E-03	1.8129E-03	1.8290E-03	1.9551E-03	1.9263E-03	1.8264E-03
1.8945E-03	1.7729E-03	1.7197E-03	1.6925E-03	1.8124E-03	1.7424E-03
3.2420E-03	3.5927E-03	3.4370E-03	3.3142E-03	3.2422E-03	3.2039E-03
3.1738E-03	2.9484E-03	2.7409E-03	2.5879E-03	2.3215E-03	2.1129E-03
2.0283E-03	1.7507E-03	1.5692E-03	1.3886E-03	1.2308E-03	1.0486E-03
9.1460E-04	7.8486E-04	7.0981E-04	6.4303E-04	5.0014E-04	2.8954E-04
2.2995E-04	1.9871E-04	1.8200E-04	1.4800E-04	1.2882E-04	1.0521E-04
8.2438E-05	7.8330E-05	7.9630E-05	6.2280E-05	7.0263E-05	5.1060E-05
7.5034E-05	6.2809E-05	5.5296E-05	4.0284E-05	4.1991E-05	2.6341E-05
2.6559E-05	1.4645E-05	1.2265E-05	2.0126E-05	1.3817E-05	7.4286E-06
1.8492E-05	6.2082E-06	5.5262E-06	7.6592E-06	1.6990E-06	9.9804E-07
1.3780E-06	1.0828E-06	2.0834E-07	8.5500E-08	5.1594E-08	3.1123E-08
1.9026E-08	1.2006E-08	7.0108E-09	4.1456E-09	6.9302E-09	
40R0.0					
' DETECTOR NO. 19		ANGLE = 90.0			
0.0	0.0	0.0	0.0	0.0	2.6828E-06
4.9304E-05	4.3044E-04	4.5219E-03	3.6843E-01	6.2044E-01	4.4165E-03
1.6714E-03	1.2353E-03	1.3836E-03	1.3818E-03	1.0702E-03	7.2665E-04
5.2066E-04	4.2389E-04	3.6410E-04	3.2302E-04	3.0313E-04	2.3882E-04
2.1957E-04	2.1217E-04	1.8963E-04	1.8424E-04	1.8838E-04	1.6722E-04
1.5826E-04	1.6668E-04	6.3204E-04	7.3883E-04	8.1574E-04	8.0422E-04
8.5016E-04	9.6558E-04	9.6664E-04	1.0409E-03	1.0134E-03	1.0532E-03
1.1208E-03	1.2207E-03	1.2703E-03	1.3956E-03	1.4004E-03	1.5054E-03
1.5289E-03	1.6224E-03	1.6339E-03	1.7429E-03	1.7278E-03	1.6368E-03
1.6871E-03	1.5817E-03	1.5405E-03	1.5197E-03	1.6182E-03	1.5665E-03
2.9085E-03	3.1983E-03	3.0694E-03	2.9755E-03	2.8787E-03	2.8382E-03
2.7967E-03	2.6078E-03	2.4184E-03	2.2669E-03	2.0277E-03	1.8401E-03
1.7767E-03	1.5362E-03	1.3773E-03	1.2101E-03	1.0562E-03	8.9893E-04
8.0502E-04	6.8155E-04	6.1733E-04	5.5606E-04	4.2983E-04	2.5980E-04
2.0319E-04	1.7180E-04	1.5901E-04	1.3691E-04	1.2339E-04	9.7985E-05
7.1828E-05	6.9509E-05	6.9582E-05	5.2570E-05	6.2568E-05	4.8259E-05
6.8235E-05	5.5222E-05	4.4250E-05	3.1273E-05	3.7422E-05	2.3115E-05
2.2231E-05	1.5281E-05	1.0289E-05	1.5313E-05	1.2484E-05	9.1578E-06
1.6309E-05	6.0638E-06	4.8678E-06	6.7599E-06	1.4570E-06	9.0732E-07
1.3230E-06	1.0470E-06	1.9881E-07	8.0852E-08	4.8765E-08	2.9420E-08
1.7933E-08	1.1210E-08	6.6058E-09	3.9022E-09	6.5140E-09	
40R0.0					
' DETECTOR NO. 18		ANGLE = 85.0			
0.0	0.0	0.0	0.0	1.0166E-08	5.5161E-06
8.9111E-05	9.0599E-04	6.8726E-03	6.4956E-01	7.3033E-02	3.1950E-03
1.4338E-03	1.1701E-03	1.3489E-03	1.3599E-03	1.0767E-03	7.2963E-04

Fig. 2.3 Continued.

5.3264E-04	4.1977E-04	3.6503E-04	3.2931E-04	3.0611E-04	2.3516E-04
2.1871E-04	2.1070E-04	1.8664E-04	1.8397E-04	1.9202E-04	1.6646E-04
1.5757E-04	1.6826E-04	6.3366E-04	7.3237E-04	8.3473E-04	8.2533E-04
8.5153E-04	9.8543E-04	9.8212E-04	1.0595E-03	1.0410E-03	1.0816E-03
1.1654E-03	1.2663E-03	1.3201E-03	1.4170E-03	1.4354E-03	1.5281E-03
1.5546E-03	1.6281E-03	1.6405E-03	1.7547E-03	1.7367E-03	1.6520E-03
1.6955E-03	1.6004E-03	1.5535E-03	1.5316E-03	1.6141E-03	1.5723E-03
2.9170E-03	3.1741E-03	3.0198E-03	2.9366E-03	2.7976E-03	2.8100E-03
2.7606E-03	2.5510E-03	2.3652E-03	2.2246E-03	1.9448E-03	1.7463E-03
1.7303E-03	1.5038E-03	1.3386E-03	1.1876E-03	1.0354E-03	8.7665E-04
7.7155E-04	6.5809E-04	6.0815E-04	5.4971E-04	4.2063E-04	2.6302E-04
2.0267E-04	1.7238E-04	1.6174E-04	1.4221E-04	1.2788E-04	1.0105E-04
7.0055E-05	6.7549E-05	7.2053E-05	5.6457E-05	6.5195E-05	4.7695E-05
7.9798E-05	6.1868E-05	4.2659E-05	3.0063E-05	3.6289E-05	2.6279E-05
2.0017E-05	1.5513E-05	1.2495E-05	1.6743E-05	1.0830E-05	7.9878E-06
2.1308E-05	5.9946E-06	5.1503E-06	8.1263E-06	1.2702E-06	7.2907E-07
4.4338E-07	3.6439E-07	5.5582E-07	3.7402E-07	1.8067E-07	2.8611E-08
1.5286E-08	9.5458E-09	5.6370E-09	3.3185E-09	5.5899E-09	
40R0.0					
' DETECTOR NO. 17		ANGLE = 80.0			
0.0	0.0	0.0	0.0	2.3878E-08	1.0544E-05
1.8519E-04	1.6538E-03	1.0816E-01	7.1456E-01	1.5762E-02	2.6287E-03
1.3261E-03	1.1602E-03	1.3148E-03	1.3167E-03	1.0841E-03	7.5529E-04
5.5354E-04	4.3299E-04	3.7586E-04	3.4959E-04	3.1741E-04	2.4063E-04
2.3158E-04	2.1510E-04	1.9088E-04	1.9297E-04	1.9441E-04	1.7414E-04
1.6386E-04	1.7360E-04	6.6292E-04	7.4120E-04	8.4013E-04	8.5734E-04
8.7795E-04	1.0191E-03	1.0347E-03	1.1174E-03	1.1055E-03	1.1517E-03
1.2447E-03	1.3279E-03	1.3772E-03	1.4707E-03	1.4973E-03	1.5992E-03
1.6204E-03	1.7024E-03	1.7138E-03	1.8177E-03	1.8126E-03	1.7223E-03
1.7587E-03	1.6764E-03	1.6192E-03	1.5907E-03	1.6772E-03	1.6316E-03
3.0416E-03	3.3236E-03	3.1819E-03	3.0740E-03	2.9742E-03	2.9831E-03
2.9305E-03	2.7131E-03	2.5184E-03	2.3636E-03	2.0752E-03	1.8659E-03
1.8309E-03	1.5909E-03	1.4219E-03	1.2679E-03	1.1063E-03	9.3905E-04
8.2479E-04	7.0931E-04	6.4839E-04	5.8755E-04	4.5714E-04	2.8884E-04
2.2711E-04	1.8667E-04	1.5855E-04	1.3488E-04	1.2288E-04	1.0976E-04
8.7947E-05	8.0806E-05	7.6735E-05	6.2897E-05	7.1697E-05	5.2502E-05
8.7301E-05	6.5613E-05	5.3394E-05	3.8823E-05	3.9314E-05	2.8753E-05
2.3133E-05	1.8132E-05	1.4915E-05	1.9154E-05	1.1728E-05	7.5911E-06
2.0805E-05	9.6445E-06	5.7105E-06	8.5326E-06	1.6539E-06	9.4138E-07
5.5908E-07	2.8838E-07	4.9062E-07	3.3325E-07	1.5755E-07	1.7383E-08
8.5610E-09	5.3897E-09	3.0829E-09	1.7877E-09	3.4571E-09	
40RC.0					
' DETECTOR NO. 16		ANGLE = 75.0			
0.0	0.0	0.0	0.0	2.2318E-07	2.2255E-05
3.9825E-04	2.5265E-03	3.5056E-01	5.5144E-01	1.3327E-02	2.3236E-03
1.2385E-03	1.1170E-03	1.2420E-03	1.2400E-03	1.0749E-03	7.8256E-04
5.6608E-04	4.3968E-04	3.7872E-04	3.5368E-04	3.1739E-04	2.4216E-04
2.4465E-04	2.1454E-04	1.9569E-04	2.0039E-04	2.0182E-04	1.7927E-04
1.6839E-04	1.7872E-04	6.7726E-04	7.3764E-04	8.2728E-04	8.5409E-04
8.6874E-04	1.0237E-03	1.0587E-03	1.1269E-03	1.1190E-03	1.1638E-03
1.2530E-03	1.3543E-03	1.3971E-03	1.5003E-03	1.5241E-03	1.6261E-03
1.6411E-03	1.7332E-03	1.7295E-03	1.8282E-03	1.8336E-03	1.7555E-03
1.7895E-03	1.7023E-03	1.6464E-03	1.6209E-03	1.7131E-03	1.6620E-03
3.1089E-03	3.4109E-03	3.2748E-03	3.1455E-03	3.0663E-03	3.0608E-03
3.0054E-03	2.7878E-03	2.5995E-03	2.4593E-03	2.1692E-03	1.9486E-03
1.8820E-03	1.6456E-03	1.4709E-03	1.3131E-03	1.1472E-03	9.8646E-04
8.6628E-04	7.4817E-04	6.8025E-04	6.1160E-04	4.8038E-04	2.9675E-04
2.3276E-04	1.9360E-04	1.6598E-04	1.4068E-04	1.2654E-04	1.1221E-04
9.0381E-05	8.2116E-05	8.0541E-05	6.9845E-05	8.0983E-05	6.1836E-05
9.3860E-05	6.5677E-05	5.6538E-05	4.1692E-05	4.3132E-05	3.1265E-05
2.5027E-05	1.8536E-05	1.9040E-05	1.9259E-05	1.0511E-05	7.5556E-06
2.1955E-05	9.3876E-06	6.5787E-06	9.0364E-06	2.0560E-06	1.1151E-06
6.5154E-07	2.5708E-07	1.0707E-07	6.4376E-08	8.1014E-08	1.2122E-07
7.7811E-08	4.7237E-08	2.8465E-08	1.7090E-08	2.6844E-08	
40R0.0					
' DETECTOR NO. 15		ANGLE = 70.0			
0.0	0.0	0.0	0.0	7.7782E-07	5.2595E-05
7.5123E-04	4.7888E-02	5.7281E-01	3.3010E-01	8.9590E-03	2.0751E-03
1.1994E-03	1.0713E-03	1.1364E-03	1.1560E-03	1.0542E-03	7.9346E-04
5.4692E-04	4.3020E-04	3.7762E-04	3.5515E-04	3.0422E-04	2.3629E-04
2.3976E-04	1.9564E-04	1.9345E-04	2.0040E-04	1.9935E-04	1.8046E-04
1.6845E-04	1.7878E-04	6.7576E-04	7.5044E-04	8.4707E-04	8.6777E-04
9.9037E-04	1.0131E-03	1.0346E-03	1.1089E-03	1.1141E-03	1.1598E-03
1.2446E-03	1.3627E-03	1.4025E-03	1.5033E-03	1.5299E-03	1.6211E-03
1.6494E-03	1.7320E-03	1.7293E-03	1.8182E-03	1.8307E-03	1.7591E-03
1.7849E-03	1.7078E-03	1.6439E-03	1.6295E-03	1.7217E-03	1.6746E-03
3.1275E-03	3.4198E-03	3.2991E-03	3.1711E-03	3.1125E-03	3.0912E-03
3.0324E-03	2.8076E-03	2.6166E-03	2.4834E-03	2.2050E-03	1.9859E-03
1.8982E-03	1.6671E-03	1.4915E-03	1.3296E-03	1.1674E-03	1.0062E-03
8.8371E-04	7.6388E-04	6.8899E-04	6.1848E-04	4.9084E-04	2.9260E-04
2.3361E-04	2.0547E-04	1.7937E-04	1.4753E-04	1.2821E-04	1.1149E-04
9.1668E-05	8.1336E-05	7.8904E-05	7.1644E-05	6.0441E-05	6.0722E-05
9.3289E-05	6.9941E-05	6.5292E-05	4.6833E-05	4.3983E-05	3.1640E-05
2.0825E-05	1.8432E-05	1.9671E-05	2.3562E-05	1.2986E-05	9.0666E-06
2.3132E-05	7.9316E-06	6.9761E-06	9.6681E-06	2.0929E-06	1.1084E-06
5.9873E-07	2.9066E-07	1.3132E-07	7.9156E-08	8.8177E-08	1.2256E-07
7.8423E-08	4.7559E-08	2.8614E-08	1.7126E-08	2.6742E-08	
40R0.0					
' DETECTOR NO. 14		ANGLE = 65.0			

Fig. 2.3 Continued.

0.0	0.0	0.0	0.0	1.9562E-06	1.2755E-04
1.2063E-03	1.9135E-01	6.1978E-01	1.6045E-01	6.3671E-03	1.8480E-03
1.1307E-03	1.0451E-03	1.0358E-03	1.0666E-03	1.0362E-03	8.0016E-04
5.3339E-04	4.1712E-04	3.6654E-04	3.4455E-04	2.8471E-04	2.3380E-04
2.3689E-04	1.9314E-04	1.9577E-04	2.0532E-04	2.0731E-04	1.9019E-04
1.7325E-04	1.8417E-04	6.9621E-04	7.4204E-04	8.3368E-04	8.5276E-04
8.7532E-04	1.0034E-03	1.0412E-03	1.1091E-03	1.1107E-03	1.1556E-03
1.2319E-03	1.3513E-03	1.3846E-03	1.4856E-03	1.5137E-03	1.6017E-03
1.6308E-03	1.7277E-03	1.7248E-03	1.8110E-03	1.8121E-03	1.7514E-03
1.7725E-03	1.7052E-03	1.6309E-03	1.6149E-03	1.7132E-03	1.6658E-03
3.1046E-03	3.4110E-03	3.2979E-03	3.1550E-03	3.1200E-03	3.0953E-03
3.0338E-03	2.8070E-03	2.6136E-03	2.4853E-03	2.2143E-03	1.9892E-03
1.8933E-03	1.6677E-03	1.5037E-03	1.3422E-03	1.1744E-03	1.0117E-03
8.8660E-04	7.7632E-04	7.0195E-04	6.1751E-04	4.8891E-04	2.8975E-04
2.3363E-04	2.1094E-04	1.8258E-04	1.5218E-04	1.2861E-04	1.0813E-04
9.7056E-05	8.6960E-05	8.0155E-05	7.1826E-05	7.8111E-05	6.1098E-05
9.2801E-05	7.0573E-05	6.4900E-05	4.7292E-05	4.2566E-05	3.2921E-05
2.4179E-05	1.9804E-05	1.9515E-05	2.3860E-05	1.4156E-05	1.0367E-05
2.0492E-05	1.0410E-05	7.4388E-06	8.5969E-06	1.5732E-06	8.5457E-07
5.1938E-07	2.4669E-07	1.0740E-07	6.4748E-08	3.9023E-08	2.3383E-08
1.4071E-08	8.5408E-09	4.9476E-09	2.7333E-09	4.7424E-09	
40R0.0					
' DETECTOR NO. 13		ANGLE = 60.0			
0.0	0.0	0.0	0.0	5.9532E-06	2.6198E-04
1.4414E-02	3.3191E-01	5.5806E-01	7.9752E-02	4.7307E-03	1.6740E-03
1.0805E-03	1.0206E-03	9.3813E-04	9.9104E-04	1.0087E-03	7.8931E-04
5.1065E-04	3.8443E-04	3.4150E-04	3.2008E-04	2.6003E-04	2.4655E-04
2.4155E-04	2.0105E-04	1.9932E-04	2.1921E-04	2.2135E-04	2.0344E-04
1.8524E-04	1.9041E-04	7.4509E-04	7.5728E-04	8.3953E-04	8.5940E-04
8.8859E-04	9.9778E-04	1.0280E-03	1.0903E-03	1.1018E-03	1.1433E-03
1.2263E-03	1.3371E-03	1.3818E-03	1.4658E-03	1.5080E-03	1.5765E-03
1.6227E-03	1.7199E-03	1.7083E-03	1.7803E-03	1.7907E-03	1.7470E-03
1.7588E-03	1.6962E-03	1.6207E-03	1.6113E-03	1.7090E-03	1.6555E-03
3.0851E-03	3.4021E-03	3.2957E-03	3.1183E-03	3.0875E-03	3.0743E-03
3.0192E-03	2.7912E-03	2.5943E-03	2.4662E-03	2.2127E-03	1.9926E-03
1.8760E-03	1.6447E-03	1.4916E-03	1.3451E-03	1.1843E-03	1.0199E-03
8.8048E-04	7.5858E-04	6.9201E-04	6.2460E-04	4.9639E-04	2.9693E-04
2.4041E-04	2.0869E-04	1.8176E-04	1.6059E-04	1.3826E-04	1.1435E-04
1.0208E-04	9.0115E-05	8.1079E-05	7.6198E-05	7.9405E-05	5.6080E-05
8.5967E-05	6.5998E-05	6.5094E-05	4.6335E-05	4.5554E-05	2.9622E-05
2.1753E-05	1.8346E-05	2.1639E-05	2.5875E-05	1.9039E-05	1.1490E-05
2.0781E-05	1.1063E-05	4.9804E-06	9.3706E-06	1.3486E-06	7.0381E-07
4.2008E-07	2.0875E-07	8.7309E-08	5.2502E-08	3.1486E-08	1.8896E-08
1.1396E-08	6.9027E-09	3.8807E-09	2.1421E-09	3.8837E-09	
40R0.0					
' DETECTOR NO. 12		ANGLE = 55.0			
0.0	0.0	0.0	0.0	1.0534E-05	4.4914E-04
1.0360E-01	3.9431E-01	4.5995E-01	4.1881E-02	3.7296E-03	1.5312E-03
1.0673E-03	9.6853E-04	8.6461E-04	9.1042E-04	9.7229E-04	7.8333E-04
4.9395E-04	3.5350E-04	3.1187E-04	2.9130E-04	2.3041E-04	2.4749E-04
2.3849E-04	2.0849E-04	2.0425E-04	2.2271E-04	2.3291E-04	2.1382E-04
1.9354E-04	1.9858E-04	7.6865E-04	7.7927E-04	8.7092E-04	8.8183E-04
9.2347E-04	1.0026E-03	1.0176E-03	1.0749E-03	1.0825E-03	1.1210E-03
1.1982E-03	1.3280E-03	1.3668E-03	1.4442E-03	1.4927E-03	1.5537E-03
1.6002E-03	1.7090E-03	1.6875E-03	1.7623E-03	1.7645E-03	1.7236E-03
1.7336E-03	1.6827E-03	1.6075E-03	1.6019E-03	1.6981E-03	1.6504E-03
3.0738E-03	3.3814E-03	3.2615E-03	3.0775E-03	3.0590E-03	3.0505E-03
3.0073E-03	2.7769E-03	2.5694E-03	2.4419E-03	2.1989E-03	1.9854E-03
1.8687E-03	1.6393E-03	1.4838E-03	1.3380E-03	1.1798E-03	1.0063E-03
8.6956E-04	7.5608E-04	6.9336E-04	6.3247E-04	5.0724E-04	2.9806E-04
2.3863E-04	2.0210E-04	1.7402E-04	1.5606E-04	1.3090E-04	1.1074E-04
9.9812E-05	8.8783E-05	8.6213E-05	8.1647E-05	7.6750E-05	5.2700E-05
8.1286E-05	6.8496E-05	7.2987E-05	4.9490E-05	4.5489E-05	2.9095E-05
2.3067E-05	1.9540E-05	2.0037E-05	2.3146E-05	1.7797E-05	1.3401E-05
2.2731E-05	9.6903E-06	6.8688E-06	8.7348E-06	1.2134E-06	3.5725E-07
2.4049E-07	2.1997E-07	1.6912E-07	1.0378E-07	6.2541E-08	3.7647E-08
2.2737E-08	1.3700E-08	7.9958E-09	4.6399E-09	7.7541E-09	
40R0.0					
' DETECTOR NO. 11		ANGLE = 50.0			
0.0	0.0	0.0	0.0	2.9960E-05	1.0799E-03
2.0287E-01	4.2829E-01	3.4188E-01	3.1311E-02	2.8746E-03	1.4187E-03
1.0827E-03	9.3500E-04	8.0656E-04	8.5483E-04	9.4226E-04	7.7785E-04
4.7988E-04	3.3737E-04	2.8232E-04	2.6826E-04	2.2865E-04	2.3055E-04
2.2224E-04	1.9600E-04	1.8977E-04	2.0760E-04	2.2084E-04	2.0433E-04
1.8394E-04	1.9514E-04	7.3193E-04	7.6984E-04	9.0637E-04	9.0276E-04
9.5760E-04	1.0159E-03	1.0244E-03	1.0765E-03	1.0786E-03	1.1123E-03
1.1828E-03	1.3297E-03	1.3569E-03	1.4346E-03	1.4856E-03	1.5516E-03
1.5901E-03	1.6960E-03	1.6715E-03	1.7349E-03	1.7403E-03	1.7009E-03
1.7139E-03	1.6615E-03	1.5935E-03	1.5962E-03	1.6924E-03	1.6419E-03
3.0607E-03	3.3648E-03	3.2370E-03	3.0458E-03	3.0329E-03	3.0235E-03
2.9858E-03	2.7584E-03	2.5523E-03	2.4249E-03	2.1785E-03	1.9525E-03
1.8354E-03	1.6336E-03	1.4832E-03	1.3306E-03	1.1709E-03	1.0042E-03
8.7870E-04	7.5714E-04	6.8492E-04	6.2603E-04	5.1249E-04	2.9945E-04
2.2841E-04	1.9410E-04	1.7445E-04	1.5113E-04	1.2869E-04	1.1623E-04
1.0409E-04	9.4238E-05	8.6824E-05	7.7165E-05	7.4482E-05	5.7007E-05
9.1044E-05	7.2310E-05	6.3841E-05	4.5727E-05	4.5969E-05	3.2256E-05
2.3603E-05	1.7262E-05	2.1740E-05	2.3276E-05	1.5754E-05	1.6049E-05
2.4448E-05	8.9675E-06	6.5154E-06	8.4586E-06	1.3307E-06	4.0630E-07
2.6942E-07	2.3497E-07	1.7611E-07	1.0784E-07	6.5000E-08	3.9156E-08

Fig. 2.3 Continued.

2.3556E-08	1.4243E-08	8.3154E-09	4.8047E-09	8.0264E-09	
40R0.0					
' DETECTOR NO. 10	ANGLE = 45.0				
0.0	0.0	0.0	0.0	5.9829E-05	3.1221E-02
2.6880E-01	4.4411E-01	2.6127E-01	8.6141E-03	2.3038E-03	1.3610E-03
1.1030E-03	8.9468E-04	7.4529E-04	8.1224E-04	9.1756E-04	7.7524E-04
4.7823E-04	3.0710E-04	2.6233E-04	2.4956E-04	2.2194E-04	2.0771E-04
2.0422E-04	1.7785E-04	1.7364E-04	1.9002E-04	2.0733E-04	1.8931E-04
1.7044E-04	1.7926E-04	6.8096E-04	7.4221E-04	9.0116E-04	8.9378E-04
9.5723E-04	1.0062E-03	1.0498E-03	1.0997E-03	1.0933E-03	1.1347E-03
1.1933E-03	1.3269E-03	1.3579E-03	1.4277E-03	1.4941E-03	1.5452E-03
1.5858E-03	1.6852E-03	1.6446E-03	1.7124E-03	1.7103E-03	1.6780E-03
1.6951E-03	1.6444E-03	1.5752E-03	1.5845E-03	1.6794E-03	1.6312E-03
3.0316E-03	3.3351E-03	3.2137E-03	3.0248E-03	3.0167E-03	2.9925E-03
2.9527E-03	2.7297E-03	2.5412E-03	2.4071E-03	2.1436E-03	1.9214E-03
1.8109E-03	1.6221E-03	1.4795E-03	1.3335E-03	1.1622E-03	9.9937E-04
8.7974E-04	7.6241E-04	6.9005E-04	6.1246E-04	4.9454E-04	2.9491E-04
2.3394E-04	1.9833E-04	1.7511E-04	1.4793E-04	1.2522E-04	1.1638E-04
1.0237E-04	9.5500E-05	8.6911E-05	8.0443E-05	7.8750E-05	5.7068E-05
8.3543E-05	7.4430E-05	6.7446E-05	5.1181E-05	4.6957E-05	3.1365E-05
2.3033E-05	1.6642E-05	2.0401E-05	2.0789E-05	1.5248E-05	1.2511E-05
2.5409E-05	9.0416E-06	6.0714E-06	9.0294E-06	2.6953E-06	9.3249E-07
2.5819E-07	1.7280E-07	1.3520E-07	8.3016E-08	5.0045E-08	3.0050E-08
1.8023E-08	1.0855E-08	6.3268E-09	3.6719E-09	6.0908E-09	
40R0.0					
' DETECTOR NO. 9	ANGLE = 40.0				
0.0	0.0	0.0	0.0	1.3996E-04	1.0331E-01
2.8163E-01	4.6378E-01	1.6850E-01	7.1715E-03	1.9089E-03	1.3190E-03
1.1338E-03	8.5898E-04	6.9993E-04	7.8126E-04	8.9814E-04	7.6692E-04
4.7796E-04	2.9565E-04	2.5043E-04	2.4040E-04	2.1936E-04	1.9152E-04
1.9310E-04	1.6345E-04	1.6161E-04	1.7706E-04	1.9853E-04	1.7757E-04
1.5871E-04	1.7462E-04	6.4380E-04	7.1504E-04	8.6012E-04	8.5586E-04
9.2161E-04	9.7908E-04	1.0783E-03	1.1219E-03	1.1054E-03	1.1444E-03
1.1942E-03	1.3285E-03	1.3615E-03	1.4330E-03	1.4852E-03	1.5481E-03
1.5741E-03	1.6717E-03	1.6370E-03	1.5978E-03	1.6889E-03	1.6592E-03
1.6804E-03	1.6353E-03	1.5566E-03	1.5768E-03	1.6708E-03	1.6243E-03
3.0117E-03	3.3042E-03	3.1761E-03	2.9987E-03	2.9907E-03	2.9598E-03
2.9280E-03	2.7098E-03	2.5171E-03	2.3856E-03	2.1321E-03	1.9087E-03
1.8036E-03	1.6182E-03	1.4688E-03	1.3150E-03	1.1414E-03	9.7603E-04
8.6670E-04	7.7426E-04	6.9665E-04	6.0340E-04	4.8056E-04	2.8773E-04
2.3921E-04	2.0155E-04	1.7450E-04	1.5123E-04	1.2805E-04	1.1154E-04
9.3509E-05	8.7624E-05	8.4361E-05	8.2482E-05	8.0636E-05	5.8733E-05
9.2101E-05	7.4686E-05	6.7448E-05	4.8317E-05	4.7162E-05	3.4191E-05
2.3325E-05	1.7143E-05	2.0718E-05	2.1674E-05	1.3023E-05	1.2117E-05
2.4798E-05	1.3958E-05	6.1917E-06	8.2243E-06	2.4272E-06	8.3598E-07
2.0562E-07	2.0224E-07	1.5484E-07	9.4669E-08	5.7097E-08	3.4255E-08
2.0626E-08	1.2315E-08	7.1074E-09	4.0827E-09	6.8717E-09	
40R0.0					
DETector NO. 8	ANGLE = 35.0				
0.0	0.0	0.0	0.0	4.1913E-04	1.5996E-01
3.0105E-01	4.3809E-01	1.1940E-01	6.4152E-03	1.6222E-03	1.3283E-03
1.1491E-03	8.1603E-04	6.8095E-04	7.4528E-04	8.9898E-04	7.6990E-04
4.7809E-04	2.9282E-04	2.4285E-04	2.3599E-04	2.0814E-04	1.7588E-04
1.7058E-04	1.5014E-04	1.4986E-04	1.6306E-04	1.8668E-04	1.6549E-04
1.4603E-04	1.6300E-04	5.9247E-04	6.9080E-04	8.1929E-04	8.1899E-04
8.9359E-04	9.4978E-04	1.0647E-03	1.0973E-03	1.0853E-03	1.1233E-03
1.1846E-03	1.3391E-03	1.3924E-03	1.4501E-03	1.5003E-03	1.5621E-03
1.5794E-03	1.6683E-03	1.6326E-03	1.6905E-03	1.6764E-03	1.6491E-03
1.6659E-03	1.6197E-03	1.5347E-03	1.5594E-03	1.6564E-03	1.6091E-03
2.9835E-03	3.2754E-03	3.1564E-03	2.9920E-03	2.9681E-03	2.9339E-03
2.9043E-03	2.6837E-03	2.4896E-03	2.3512E-03	2.1032E-03	1.8944E-03
1.7980E-03	1.6152E-03	1.4551E-03	1.2959E-03	1.1272E-03	9.6810E-04
8.5145E-04	7.4843E-04	6.8634E-04	6.0530E-04	4.8117E-04	2.8667E-04
2.3559E-04	2.0274E-04	1.7747E-04	1.5195E-04	1.2465E-04	1.0979E-04
9.5892E-05	8.3639E-05	7.6711E-05	7.8702E-05	8.0279E-05	6.3120E-05
1.0108E-04	7.9701E-05	6.9887E-05	4.6751E-05	3.9903E-05	3.0345E-05
2.4885E-05	2.1616E-05	2.0341E-05	2.4461E-05	1.3215E-05	8.7597E-06
2.2180E-05	9.7950E-06	7.7113E-06	8.9265E-06	3.5902E-06	1.1282E-06
3.5944E-07	1.5413E-07	1.1587E-07	7.1016E-08	4.2723E-08	2.5589E-08
1.5301E-08	8.8523E-09	5.1182E-09	2.8637E-09	4.8088E-09	
40R0.0					
' DETECTOR NO. 7	ANGLE = 30.0				
0.0	0.0	0.0	0.0	5.7086E-03	2.0313E-01
3.4256E-01	3.5342E-01	1.1747E-01	6.0931E-03	1.4287E-03	1.4204E-03
1.1384E-03	7.7202E-04	6.7450E-04	7.2070E-04	8.9082E-04	7.7423E-04
4.7798E-04	2.8679E-04	2.3616E-04	2.3275E-04	2.0146E-04	1.6525E-04
1.6174E-04	1.4281E-04	1.4237E-04	1.5778E-04	1.7932E-04	1.5983E-04
1.3940E-04	1.5677E-04	5.6929E-04	6.6617E-04	7.8352E-04	7.8659E-04
8.5941E-04	9.2590E-04	1.0342E-03	1.0732E-03	1.0652E-03	1.0973E-03
1.1479E-03	1.3096E-03	1.3893E-03	1.4300E-03	1.4801E-03	1.5339E-03
1.5829E-03	1.6731E-03	1.6451E-03	1.7007E-03	1.6850E-03	1.6530E-03
1.6677E-03	1.6241E-03	1.5243E-03	1.5507E-03	1.6476E-03	1.5910E-03
2.9444E-03	3.2511E-03	3.1372E-03	2.9650E-03	2.9302E-03	2.8942E-03
2.8695E-03	2.6609E-03	2.4700E-03	2.3426E-03	2.1016E-03	1.8753E-03
1.7698E-03	1.5920E-03	1.4435E-03	1.2843E-03	1.1163E-03	9.5419E-04
8.3201E-04	7.2743E-04	6.7339E-04	5.9617E-04	4.7903E-04	2.8857E-04
2.3697E-04	2.0056E-04	1.7503E-04	1.5399E-04	1.2891E-04	1.1010E-04
9.7865E-05	8.9814E-05	8.0720E-05	7.8833E-05	7.6789E-05	5.9752E-05
8.7582E-05	7.5921E-05	7.3410E-05	4.8773E-05	4.0289E-05	3.0871E-05

Fig. 2.3 Continued.

2.7906E-05	2.9608E-05	2.0893E-05	1.9881E-05	1.0227E-05	6.9839E-06
2.1185E-05	9.5356E-06	4.9158E-05	8.7443E-06	4.6806E-06	1.2961E-06
8.3175E-07	3.8999E-07	1.7327E-07	6.5953E-08	3.9684E-08	2.3774E-08
1.4209E-08	8.1587E-09	4.7467E-09	2.6400E-09	4.5597E-09	
40R0.0					
' DETECTOR NO.	6	ANGLE = 25.0			
0.0	0.0	0.0	0.0	3.8666E-02	2.2939E-01
3.3095E-01	3.3021E-01	9.3995E-02	5.7748E-03	1.3284E-03	1.5651E-03
1.1285E-03	7.3454E-04	6.8679E-04	7.1726E-04	8.8338E-04	7.8329E-04
4.9505E-04	2.8393E-04	2.3034E-04	2.1753E-04	1.9359E-04	1.5405E-04
1.4901E-04	1.3575E-04	1.3328E-04	1.4897E-04	1.6912E-04	1.5314E-04
1.3019E-04	1.5184E-04	5.4781E-04	6.4799E-04	7.5490E-04	7.5899E-04
8.3096E-04	9.1007E-04	1.0036E-03	1.0466E-03	1.0406E-03	1.0637E-03
1.1182E-03	1.2864E-03	1.3749E-03	1.4145E-03	1.4632E-03	1.5146E-03
1.5819E-03	1.6683E-03	1.6411E-03	1.6883E-03	1.6725E-03	1.6440E-03
1.6606E-03	1.6229E-03	1.5220E-03	1.5454E-03	1.6419E-03	1.5849E-03
2.9275E-03	3.2433E-03	3.1182E-03	2.9351E-03	2.9160E-03	2.8715E-03
2.8305E-03	2.6224E-03	2.4450E-03	2.3252E-03	2.0954E-03	1.8628E-03
1.7558E-03	1.5741E-03	1.4265E-03	1.2648E-03	1.1047E-03	9.5547E-04
8.3558E-04	7.2603E-04	6.5534E-04	5.7904E-04	4.7082E-04	2.7839E-04
2.2549E-04	1.9047E-04	1.7006E-04	1.5598E-04	1.3475E-04	1.1748E-04
1.0489E-04	9.0442E-05	8.1647E-05	7.7729E-05	7.5620E-05	5.6844E-05
8.9702E-05	8.0144E-05	6.8059E-05	4.5187E-05	4.1228E-05	3.0566E-05
2.3431E-05	2.2742E-05	2.1660E-05	2.0622E-05	1.1209E-05	8.4085E-06
1.7808E-05	1.0298E-05	5.2494E-06	8.2153E-06	3.5754E-06	1.5450E-06
8.7961E-07	4.7170E-07	2.252CE-07	9.7260E-08	5.8581E-08	3.5205E-08
2.1067E-08	1.2426E-08	7.2480E-09	4.1349E-09	7.0998E-09	
40R0.0					
' DETECTOR NO.	5	ANGLE = 20.0			
0.0	0.0	0.0	0.0	7.6544E-02	2.2132E-01
3.1814E-01	3.8291E-01	3.4905E-02	5.8395E-03	1.2750E-03	1.7827E-03
1.1025E-03	6.8570E-04	6.8120E-04	7.3260E-04	8.7682E-04	7.9218E-04
5.0512E-04	2.8311E-04	2.1602E-04	2.2385E-04	1.9659E-04	1.5251E-04
1.4793E-04	1.3661E-04	1.3285E-04	1.5120E-04	1.7352E-04	1.5529E-04
1.3504E-04	1.5183E-04	4.5416E-04	6.1833E-04	7.1022E-04	7.2093E-04
7.9444E-04	8.9578E-04	9.8190E-04	1.0184E-03	1.0287E-03	1.0290E-03
1.0924E-03	1.2622E-03	1.3534E-03	1.3981E-03	1.4492E-03	1.4955E-03
1.5684E-03	1.6488E-03	1.6149E-03	1.6691E-03	1.6561E-03	1.6225E-03
1.6345E-03	1.6064E-03	1.5180E-03	1.5344E-03	1.6301E-03	1.5749E-03
2.9180E-03	3.2297E-03	3.0938E-03	2.9176E-03	2.9116E-03	2.8641E-03
2.8057E-03	2.6012E-03	2.4296E-03	2.3015E-03	2.0661E-03	1.8444E-03
1.7446E-03	1.5571E-03	1.4156E-03	1.2644E-03	1.1025E-03	9.3544E-04
8.1769E-04	7.1642E-04	6.4228E-04	5.6621E-04	4.5696E-04	2.7154E-04
2.3180E-04	1.9441E-04	1.7134E-04	1.5510E-04	1.3729E-04	1.2175E-04
1.0496E-04	8.5439E-05	7.7958E-05	7.7721E-05	7.3330E-05	5.3915E-05
9.6865E-05	7.0045E-05	6.6897E-05	4.5110E-05	4.3305E-05	3.3620E-05
2.5810E-05	1.9527E-05	1.8963E-05	1.9758E-05	1.2475E-05	9.2707E-06
1.8139E-05	1.1218E-05	5.3872E-06	6.1711E-06	2.0929E-06	1.4805E-06
1.1278E-06	6.5364E-07	3.3031E-07	1.5163E-07	9.0138E-08	5.4359E-08
3.2685E-08	1.9477E-08	1.1495E-08	6.7662E-09	1.1124E-08	
40R0.0					
' DETECTOR NO.	4	ANGLE = 15.0			
0.0	0.0	0.0	0.0	9.1941E-02	2.6806E-01
3.5410E-01	2.8455E-01	3.2023E-02	4.8461E-03	1.2358E-03	2.0603E-03
1.0759E-03	6.7031E-04	6.6643E-04	7.3884E-04	8.9195E-04	7.9234E-04
5.2071E-04	2.8768E-04	2.0132E-04	2.2158E-04	1.9788E-04	1.4742E-04
1.4473E-04	1.3321E-04	1.2870E-04	1.5005E-04	1.7026E-04	1.5342E-04
1.3192E-04	1.4871E-04	5.3126E-04	6.0732E-04	6.9376E-04	7.0117E-04
7.7627E-04	8.9175E-04	6.6989E-04	9.9074E-04	1.0226E-03	1.0021E-03
1.0707E-03	1.2298E-03	1.3213E-03	1.3779E-03	1.4275E-03	1.4615E-03
1.5526E-03	1.6304E-03	1.5927E-03	1.6467E-03	1.6342E-03	1.5957E-03
1.6134E-03	1.5853E-03	1.5077E-03	1.5229E-03	1.6144E-03	1.5653E-03
2.9025E-03	3.2096E-03	3.0809E-03	2.9141E-03	2.8996E-03	2.8396E-03
2.7857E-03	2.5861E-03	2.4237E-03	2.2855E-03	2.0432E-03	1.8232E-03
1.7259E-03	1.5415E-03	1.4042E-03	1.2599E-03	1.0975E-03	9.2556E-04
8.0366E-04	7.0323E-04	6.2444E-04	5.6185E-04	4.5837E-04	2.6533E-04
2.2894E-04	1.9414E-04	1.7044E-04	1.5106E-04	1.3568E-04	1.2392E-04
1.0823E-04	8.4122E-05	7.4565E-05	7.3861E-05	7.2207E-05	5.2297E-05
9.5607E-05	6.7757E-05	6.2308E-05	4.4581E-05	4.7764E-05	3.4515E-05
2.5261E-05	1.7102E-05	1.5733E-05	1.8448E-05	1.2361E-05	1.0694E-05
1.9815E-05	1.1722E-05	7.1133E-06	6.4887E-06	1.8255E-06	1.0600E-06
9.2490E-07	6.6269E-07	4.1861E-07	2.0459E-07	1.2210E-07	7.3560E-08
4.4279E-08	2.6361E-08	1.5602E-08	9.1799E-09	1.5191E-08	
40R0.0					
' DETECTOR NO.	3	ANGLE = 10.0			
0.0	0.0	0.0	0.0	1.1642E-01	2.4857E-01
3.7951E-01	2.5645E-01	3.1773E-02	5.0555E-03	1.1759E-03	2.3546E-03
1.0686E-03	6.6974E-04	6.5115E-04	7.2396E-04	9.2523E-04	8.2654E-04
5.2118E-04	2.7361E-04	2.0154E-04	2.2045E-04	1.9245E-04	1.4187E-04
1.3708E-04	1.2634E-04	1.2305E-04	1.4648E-04	1.6297E-04	1.4879E-04
1.2701E-04	1.4336E-04	5.1024E-04	5.9242E-04	6.7615E-04	6.8078E-04
7.5623E-04	8.8024E-04	9.5945E-04	9.7981E-04	1.0240E-03	9.9095E-04
1.0535E-03	1.2090E-03	1.2945E-03	1.3748E-03	1.4029E-03	1.4366E-03
1.5434E-03	1.6300E-03	1.5819E-03	1.6339E-03	1.6272E-03	1.5797E-03
1.6010E-03	1.5715E-03	1.5045E-03	1.5171E-03	1.6040E-03	1.5597E-03
2.8824E-03	3.1881E-03	3.0645E-03	2.9009E-03	2.8743E-03	2.8130E-03
2.7809E-03	2.5844E-03	2.4068E-03	2.2711E-03	2.0330E-03	1.8064E-03
1.7137E-03	1.5327E-03	1.3928E-03	1.2488E-03	1.0872E-03	9.1786E-04
8.0149E-04	7.0332E-04	6.3267E-04	5.7016E-04	4.5988E-04	2.5871E-04

Fig. 2.3 Continued.

2.2756E-04 1.9569E-04 1.6185E-04 1.4402E-04 1.3226E-04 1.2078E-04
 1.0637E-04 8.5644E-05 7.3601E-05 7.2192E-05 7.0134E-05 5.1037E-05
 8.9122E-05 6.9435E-05 6.3116E-05 4.7055E-05 4.7573E-05 3.1909E-05
 2.5920E-05 1.8250E-05 1.6779E-05 1.7771E-05 9.5596E-06 8.6683E-06
 2.3414E-05 1.2816E-05 7.3184E-06 7.6131E-06 1.4451E-06 7.4222E-07
 3.5597E-07 1.8033E-07 1.8698E-07 2.3515E-07 2.0601E-07 1.2793E-07
 7.7136E-08 4.6172E-08 2.7579E-08 1.6328E-08 2.6362E-08

40R0.0

' DETECTOR NO. 2 ANGLE = 5.0

0.0 0.0 0.0 1.4266E-01 2.2369E-01
 4.0507E-01 2.3227E-01 3.1489E-02 5.3793E-03 1.1292E-03 2.5848E-03
 1.0645E-03 6.4579E-04 6.5864E-04 7.1080E-04 9.4891E-04 8.6205E-04
 5.2667E-04 2.5473E-04 2.0836E-04 2.1582E-04 1.8610E-04 1.3986E-04
 1.3221E-04 1.2093E-04 1.2374E-04 1.4268E-04 1.5861E-04 1.4520E-04
 1.2411E-04 1.3578E-04 4.9796E-04 6.0630E-04 6.8574E-04 6.8783E-04
 7.5621E-04 8.7105E-04 9.4153E-04 9.6907E-04 1.0076E-03 9.8066E-04
 1.0426E-03 1.2051E-03 1.2847E-03 1.3882E-03 1.3985E-03 1.4358E-03
 1.5402E-03 1.6277E-03 1.5742E-03 1.6337E-03 1.6307E-03 1.5723E-03
 1.5991E-03 1.5654E-03 1.5048E-03 1.5144E-03 1.5942E-03 1.5624E-03
 2.8944E-03 3.2043E-03 3.0698E-03 2.8950E-03 2.8734E-03 2.8135E-03
 2.7915E-03 2.5905E-03 2.4036E-03 2.2680E-03 2.0441E-03 1.8205E-03
 1.7223E-03 1.5388E-03 1.3907E-03 1.2428E-03 1.0760E-03 9.2398E-04
 8.1254E-04 7.1105E-04 6.4349E-04 5.7403E-04 4.5807E-04 2.5445E-04
 2.2634E-04 2.0022E-04 1.6712E-04 1.4737E-04 1.3227E-04 1.1642E-04
 9.7519E-05 8.0751E-05 7.2335E-05 7.2465E-05 7.1767E-05 5.1826E-05
 9.0182E-05 7.0994E-05 6.2513E-05 4.8815E-05 4.4413E-05 3.0197E-05
 2.8196E-05 1.9477E-05 1.7146E-05 1.7372E-05 9.2661E-06 8.5143E-06
 2.2875E-05 1.2712E-05 6.8685E-06 7.6081E-06 2.3506E-06 7.9421E-07
 7.6540E-07 6.7491E-07 3.9386E-07 2.0421E-07 6.3820E-08 3.6800E-08
 2.1770E-08 1.2588E-08 7.1652E-09 3.9247E-09 6.9538E-09

40R0.0

' DETECTOR NO. 1 ANGLE = 0.0

0.0 0.0 0.0 1.4276E-01 2.2369E-01
 4.0519E-01 2.3206E-01 3.1364E-02 5.3721E-03 1.1067E-03 2.6708E-03
 1.0556E-03 6.4016E-04 6.5564E-04 7.0786E-04 9.5418E-04 8.7356E-04
 5.2460E-04 2.4759E-04 2.0933E-04 2.1838E-04 1.8675E-04 1.4421E-04
 1.3431E-04 1.2190E-04 1.2642E-04 1.4100E-04 1.5964E-04 1.4779E-04
 1.2673E-04 1.3230E-04 4.9914E-04 5.9420E-04 6.7795E-04 6.8043E-04
 7.4273E-04 8.5947E-04 9.3079E-04 9.6374E-04 1.0082E-03 9.7555E-04
 1.0459E-03 1.2120E-03 1.2893E-03 1.3998E-03 1.3949E-03 1.4353E-03
 1.5248E-03 1.6310E-03 1.5700E-03 1.6284E-03 1.6304E-03 1.5676E-03
 1.5963E-03 1.5660E-03 1.5070E-03 1.5116E-03 1.5890E-03 1.5658E-03
 2.8900E-03 3.1949E-03 3.0651E-03 2.9025E-03 2.8823E-03 2.8147E-03
 2.7917E-03 2.5861E-03 2.4082E-03 2.2762E-03 2.0587E-03 1.8216E-03
 1.7222E-03 1.5293E-03 1.3852E-03 1.2447E-03 1.0821E-03 9.4058E-04
 8.2187E-04 7.0538E-04 6.3363E-04 5.7113E-04 4.6877E-04 2.6606E-04
 2.2815E-04 1.9156E-04 1.6297E-04 1.4476E-04 1.2221E-04 1.0639E-04
 9.7926E-05 8.0374E-05 6.9982E-05 6.6729E-05 6.6152E-05 5.3031E-05
 1.0042E-04 7.6437E-05 7.0560E-05 4.7636E-05 3.9790E-05 2.7772E-05
 2.6856E-05 1.9386E-05 1.8523E-05 1.9948E-05 1.1482E-05 9.8805E-06
 1.9937E-05 1.0053E-05 6.7864E-06 6.9047E-06 2.0054E-06 1.3301E-06
 1.1166E-06 8.5386E-07 4.0943E-07 2.1118E-07 6.9261E-08 3.9982E-08
 2.3521E-08 1.3766E-08 7.9062E-09 4.4338E-09 7.5075E-09

40R0.0

T T

Fig. 2.3 Continued.

FNS-DOT3.5 SS316/Water Assembly (N125+G40)

61\$
 0 5 4 38 177 165
 4 5 169 156 0 0
 300 1 160 1 1 0
 0 0 1 15 15 3
 6 2 0 0 0 0
 0 0 0 0 0 0
 0 0 0 0 0 0
 0 0 2 1 1 0
 0 0 0 0 0 8

62\$
 0 0 0 0 0 0
 0 0 0 0 8 0
 0 0 0 0 0 0

63**
 0.0 1.000E-02 0.0 0.0 0.0 0.0
 0.0 0.0 0.0 0.0 0.0 0.0
 0.0 0.0 0.0 0.0 0.0 0.0

7**
 -0.21082 -0.14907 1M1

Fig. 2.4 Input data of the DOT analysis for the SS316/water assembly with the FUSION-J3 library (125-n + 40- γ).

JAERI-Research 95-018

```

-0.42164 -0.39441 -0.14907 1M2
-0.55777 -0.53748 -0.39441 -0.14907 1M3
-0.66667 -0.64979 -0.53748 -0.39441 -0.14907 1M4
-0.76012 -0.74536 -0.64979 -0.53748 -0.39441 -0.14907
1M5
-0.84327 -0.82999 -0.74536 -0.64979 -0.53748 -0.39441
-0.14907 1M6
-0.91894 -0.90676 -0.82999 -0.74536 -0.64979 -0.53748
-0.39441 -0.14907 1M7
-0.98883 -0.97753 -0.90676 -0.82999 -0.74536 -0.64979
-0.53748 -0.39441 -0.14907 1M8
1Q80
3R-0.97753 5R-0.90676 7R-0.82999 9R-0.74536 11R-0.64979 13R-0.53748
15R-0.39441 17R-0.14907 3R0.97753 5R0.90676 7R0.82999 9R0.74536
11R0.64979 13R0.53748 15R0.39441 17R0.14907
T
6**
0.0 2R0.13586-1 0.0 4R0.97681-2
0.0 0.64738-2 0.50390-2 0.64738-2 1N3
0.0 0.64634-2 2R0.71124-2 0.64634-2 1N4
0.0 0.64634-2 0.14381-2 0.36342-2 0.14381-2 0.64634-2
1N5
0.0 0.64738-2 0.71124-2 0.36342-2 1N3 1Q6
0.0 0.97681-2 0.50390-2 0.71124-2 0.14381-2 0.71124-2
0.0 0.50390-2 0.97681-2 1N7
0.0 0.13586-1 0.97681-2 2R0.64738-2 1N4 1Q8
1Q80
T
3**
F0.0
T
1**
F0.0
2**
1I0.0 1.0 2.0 6I3.3 1I17.3 1I19.3 20.3 28I21.3 79.3
1I80.3
1I81.3 3I82.5 1I85.18 1I86.38 3I87.58 1I90.26
7I91.46 1I96.54 3I97.74 1I100.42 7I101.62 1I106.7 3I107.9
1I110.58 7I111.78 1I116.86 3I118.06 1I120.74 121.94
122.62 123.62 125.02 127.02 129.02 130.42 131.42 1I132.1
3I133.3 1I135.98 137.18 137.86 138.86 140.26 142.26
144.26 145.66 146.66 1I147.34 3I148.54 1I151.22 152.42
3I153.42 218.5
4**
2I0.0 6.0 6.383 6.7 7.3 14I8.0 1I38.0 1I40.0 41.0
7I42.0 58.0 1I59.0 60.0
5**
F1.0
8$$
4R1 34R4 14Q38
24R1 14R4 32Q38
38R2 1Q38 38R3 3Q38 38R2 1Q38
38R2 1Q38 38R3 3Q38 38R2 1Q38
38R2 7Q38
38R2 1Q38 38R3 3Q38 38R2 1Q38
38R2 1Q38 38R3 3Q38 38R2 1Q38
38R2 32Q38
9$$
-241 -247 -253 -259
10$$
1241 = AIR / 247 = SUS316 / 253 = H2O
4I241 246 2Q6
4I247 252 9Q6
4I253 258 2Q6
4I259 264 9Q6
11$$
6Z 4I61 66 4I67 72
6Z 4I163 168 4I139 144 4I187 192
4I55 60 4I97 102 4I145 150
4I103 108 4I109 114 4I151 156
6Z 4I11 6 4I67 72
6Z 4I163 168 4I139 144 4I187 192
4I55 60 4I97 102 4I145 150
4I103 108 4I109 114 4I151 156
12**
6R0.0 6R3.8810-5 6R1.0400-5
6R0.0 6R9.3405-3 6R1.5482-2 6R1.0585-3 6R1.1931-4 6R1.0341-3
6R1.0355-3 6R4.3954-5 6R1.9366-6 6R5.7904-2
6R0.0 6R6.6659-2 6R3.3329-2
6R0.0 6R9.1456-3 6R1.5025-2 6R1.0254-3 6R1.9855-4 6R8.1608-4
6R1.3561-3 6R4.7828-5 6R4.5072-6 6R5.8331-2
T T

```

Fig. 2.4 Continued.

JAERI-Research 95-018

```

FNS-GRTUNCL      SS316/Water Assembly (N42+G21)
O
1$$
      0      5      4      38      177      63
      4      5      67      156      0      300
    300      2      1      30000      10      0
      1      0      18      0      0      37
      1      1      1
2**
  1.0      51.3      0.0      0.0      0.0
T
1**
  F0.0
2**
  1I0.0  1.0  2.0  6I3.3  1I17.3  1I19.3  20.3  28I21.3  79.3
  1I80.3  1I81.3  3I82.5  1I85.18  1I86.38  3I87.58  1I90.26
  7I91.46  1I96.54  3I97.74  1I100.42  7I101.62  1I106.7  3I107.9
  1I110.58  7I111.78  1I116.86  3I118.06  1I120.74  121.94
  122.62  123.62  125.02  127.02  129.02  130.42  131.42  1I132.1
  3I133.3  1I135.98  137.18  137.86  138.86  140.26  142.26
  144.26  145.66  146.66  1I147.34  3I148.54  1I151.22  152.42
  3I153.42  218.5
3**
  F0.0
4**
  2I0.0  6.0  6.383  6.7  7.3  14I8.0  1I38.0  1I40.0  41.0
  7I42.0  58.0  1I59.0  60.0
6**
  1.0
7**
  1.0
8$$
  4R1   34R4   14Q38
  24R1  14R4   32Q38
  38R2   1Q38   38R3   3Q38   38R2   1Q38
  38R2   1Q38   38R3   3Q38   38R2   1Q38
  38R2   7Q38
  38R2   1Q38   38R3   3Q38   38R2   1Q38
  38R2   32Q38
9$$
  -241  -247  -253  -259
10$$
  241 = AIR / 247 = SUS316 / 253 = H2O / 259 = SUS316
        4I241   246   2Q6
        4I247   252   9Q6
        4I253   258   2Q6
        4I259   264   9Q6
11$$
  6Z     4I61     66     4I67     72
  6Z     4I163    168     4I139    144     4I187    192
  4I55     60     4I97     102     4I145    150
  4I103    108     4I109    114     4I151    156
  6Z     4I1     6     4I67     72
  6Z     4I163    168     4I139    144     4I187    192
  4I55     60     4I97     102     4I145    150
  4I103    108     4I109    114     4I151    156
12**
  6R0.0   6R3.8810-5  6R1.0400-5
  6R0.0   6R9.3405-3  6R1.5482-2  6R1.0585-3  6R1.1931-4  6R1.0341-3
  6R1.0355-3  6R4.3954-5  6R1.9366-6  6R5.7904-2
  6R0.0   6R6.6659-2  6R3.3329-2
  6R0.0   6R9.1456-3  6R1.5025-2  6R1.0254-3  6R1.9855-4  6R8.1608-4
  6R1.3561-3  6R4.7828-5  6R4.5072-6  6R5.8331-2
13**
  LONG WATER COOLED TARGET - ANGULAR COSINE DISTRIBUTION TABLE
  -1.0    -0.996195   -0.984808   -0.965926   -0.939693   -0.906308
  -0.866025   -0.819152   -0.766044   -0.707107   -0.642788   -0.573576
  -0.5    -0.422618   -0.342020   -0.258809   -0.173648   -0.087156
  0.0     0.087156   0.173648   0.258809   0.342020   0.422618
  0.5     0.573576   0.642788   0.707107   0.766044   0.819152
  0.866025   0.906308   0.939693   0.965926   0.984808   0.996195
  1.0
14**
  LONG WATER COOLED TARGET - ANGULAR SOURCE INTENSITY TABLE
  1.1567   1.1785   0.97312   1.0221   0.99500   0.91711
  0.74641   0.73360   0.79463   0.88820   1.0175   1.0581
  1.0532   1.0657   1.0783   1.0797   1.0840   1.0945
  1.0902   0.82512   0.93854   1.0180   1.0603   1.0782
  1.0872   1.1009   1.1043   1.1113   1.1204   1.1200

```

Fig. 2.5 Input data of FNSUNCL for the DOT analysis of the SS316/water assembly with the FUSION-40 library (42-n + 21- γ).

1.1219 1.1216 1.1314 1.1266 1.1284 1.1314
 1.1312
 15**
 ' LONG WATER COOLED TARGET - ANGULAR SOURCE SPECTRA TABLE
 ' DETECTOR NO. 37 ANGLE = 180.0
 0.4793E-02 0.9460E+00 0.7066E-02 0.1480E-02 0.1812E-02 0.2678E-02
 0.2526E-02 0.3422E-02 0.4506E-02 0.4909E-02 0.5521E-02 0.6431E-02
 0.1414E-01 0.1580E-01 0.1805E-01 0.1774E-01 0.1672E-01 0.1540E-01
 0.1738E-01 0.1488E-01 0.1154E-01 0.8511E-02 0.5765E-02 0.3866E-02
 0.3299E-02 0.1005E-02 0.3998E-03 0.2581E-03 0.1176E-03 0.7449E-04
 0.4676E-04 0.1107E-04 0.2489E-04 0.3854E-05 0.5468E-06 0.2313E-06
 0.1803E-06 0.1314E-06 0.6025E-07 0.2851E-07 0.8407E-08 0.1652E-07
 21R0.0
 ' DETECTOR NO. 36 ANGLE = 175.0
 0.4897E-02 0.9557E+00 0.7782E-02 0.1637E-02 0.2036E-02 0.3704E-02
 0.3028E-02 0.3610E-02 0.4643E-02 0.5214E-02 0.5858E-02 0.6742E-02
 0.1500E-01 0.1660E-01 0.1903E-01 0.1872E-01 0.1765E-01 0.1611E-01
 0.1856E-01 0.1573E-01 0.1194E-01 0.9087E-02 0.5965E-02 0.4116E-02
 0.3281E-02 0.1014E-02 0.3794E-03 0.2443E-03 0.1071E-03 0.6865E-04
 0.5159E-04 0.1235E-04 0.1975E-04 0.2706E-05 0.5471E-06 0.4220E-06
 0.3445E-06 0.2131E-06 0.9651E-07 0.4552E-07 0.1348E-07 0.2589E-07
 21R0.0
 ' DETECTOR NO. 35 ANGLE = 170.0
 0.3967E-02 0.7880E+00 0.6903E-02 0.1369E-02 0.1846E-02 0.2294E-02
 0.2210E-02 0.2837E-02 0.3610E-02 0.4005E-02 0.4820E-02 0.5421E-02
 0.1350E-01 0.1378E-01 0.1682E-01 0.1560E-01 0.1539E-01 0.1331E-01
 0.1523E-01 0.1345E-01 0.9662E-02 0.7250E-02 0.4322E-02 0.3812E-02
 0.2484E-02 0.6255E-03 0.2230E-03 0.1786E-03 0.5739E-04 0.4655E-04
 0.3855E-04 0.6554E-05 0.8832E-05 0.1525E-05 0.2967E-06 0.1714E-06
 0.9649E-07 0.4646E-07 0.2047E-07 0.9401E-08 0.2664E-08 0.4362E-08
 21R0.0
 ' DETECTOR NO. 34 ANGLE = 165.0
 0.5095E-02 0.8479E+00 0.5683E-02 0.1185E-02 0.1719E-02 0.2313E-02
 0.2054E-02 0.2833E-02 0.3491E-02 0.3857E-02 0.4588E-02 0.5168E-02
 0.1143E-01 0.1320E-01 0.1491E-01 0.1471E-01 0.1404E-01 0.1283E-01
 0.1476E-01 0.1272E-01 0.9429E-02 0.6792E-02 0.4389E-02 0.3252E-02
 0.2336E-02 0.6540E-03 0.2584E-03 0.2312E-03 0.7763E-04 0.5574E-04
 0.3950E-04 0.8236E-05 0.8176E-05 0.1675E-05 0.9104E-06 0.3708E-06
 0.7442E-07 0.3582E-07 0.1512E-07 0.6565E-08 0.1839E-08 0.3466E-08
 21R0.0
 ' DETECTOR NO. 33 ANGLE = 160.0
 0.7523E-02 0.8371E+00 0.4936E-02 0.1046E-02 0.1465E-02 0.2135E-02
 0.1821E-02 0.2576E-02 0.3106E-02 0.3355E-02 0.4016E-02 0.4541E-02
 0.1017E-01 0.1176E-01 0.1326E-01 0.1307E-01 0.1257E-01 0.1165E-01
 0.1334E-01 0.1081E-01 0.8454E-02 0.6088E-02 0.3973E-02 0.2852E-02
 0.2081E-02 0.6214E-03 0.2563E-03 0.2018E-03 0.6899E-04 0.5780E-04
 0.3422E-04 0.9699E-05 0.7897E-05 0.1436E-05 0.3108E-06 0.1440E-06
 0.1015E-06 0.5158E-07 0.2206E-07 0.9734E-08 0.2750E-08 0.5170E-08
 21R0.0
 ' DETECTOR NO. 32 ANGLE = 155.0
 0.2119E-01 0.7627E+00 0.4385E-02 0.9556E-03 0.1209E-02 0.1955E-02
 0.1610E-02 0.2219E-02 0.2688E-02 0.2938E-02 0.3599E-02 0.4027E-02
 0.9020E-02 0.1030E-01 0.1173E-01 0.1155E-01 0.1119E-01 0.1046E-01
 0.1190E-01 0.9600E-02 0.7543E-02 0.5422E-02 0.3519E-02 0.2490E-02
 0.1812E-02 0.5532E-03 0.2312E-03 0.1622E-03 0.6006E-04 0.5357E-04
 0.2873E-04 0.7980E-05 0.6582E-05 0.1260E-05 0.1756E-06 0.1182E-06
 0.5567E-07 0.3352E-07 0.1544E-07 0.6044E-08 0.1650E-08 0.2832E-08
 21R0.0
 ' DETECTOR NO. 31 ANGLE = 150.0
 0.1781E-01 0.6112E+00 0.3859E-02 0.9849E-03 0.1026E-02 0.1796E-02
 0.1384E-02 0.1979E-02 0.2395E-02 0.2549E-02 0.3144E-02 0.3499E-02
 0.7941E-02 0.9107E-02 0.1038E-01 0.1015E-01 0.9884E-02 0.9285E-02
 0.1047E-01 0.8370E-02 0.6612E-02 0.4755E-02 0.3079E-02 0.2157E-02
 0.1583E-02 0.4928E-03 0.1984E-03 0.1310E-03 0.5239E-04 0.4674E-04
 0.2492E-04 0.7003E-05 0.4379E-05 0.9406E-06 0.1372E-06 0.6014E-07
 0.5246E-07 0.2844E-07 0.6983E-08 0.2150E-08 0.5498E-09 0.9646E-09
 21R0.0
 ' DETECTOR NO. 30 ANGLE = 145.0
 0.1862E-01 0.6039E+00 0.3540E-02 0.9799E-03 0.9510E-03 0.1727E-02
 0.1368E-02 0.1932E-02 0.2236E-02 0.2386E-02 0.2972E-02 0.3309E-02
 0.7532E-02 0.8640E-02 0.9916E-02 0.9669E-02 0.9362E-02 0.8791E-02
 0.9867E-02 0.7848E-02 0.6212E-02 0.4463E-02 0.2911E-02 0.2020E-02
 0.1481E-02 0.4770E-03 0.1839E-03 0.1158E-03 0.4944E-04 0.4422E-04
 0.2122E-04 0.3956E-05 0.5335E-05 0.1076E-05 0.1436E-06 0.2066E-06
 0.1737E-06 0.8433E-07 0.2582E-07 0.1087E-07 0.3117E-08 0.5797E-08
 21R0.0
 ' DETECTOR NO. 28 ANGLE = 135.0
 0.6833E-01 0.7078E+00 0.3241E-02 0.1072E-02 0.1031E-02 0.1706E-02
 0.1426E-02 0.1981E-02 0.2366E-02 0.2419E-02 0.3040E-02 0.3445E-02
 0.7745E-02 0.8754E-02 0.1001E-01 0.9684E-02 0.3351E-02 0.8787E-02

Fig. 2.5 Continued.

0.9880E-02	0.7910E-02	0.6220E-02	0.4485E-02	0.2990E-02	0.2040E-02
0.1483E-02	0.5491E-03	0.2068E-03	0.1297E-03	0.5417E-04	0.4347E-04
0.2328E-04	0.3828E-05	0.7688E-05	0.1764E-05	0.1571E-05	0.5530E-06
0.1850E-06	0.8322E-07	0.3523E-07	0.1547E-07	0.4498E-08	0.8593E-08
21RC.0	DETECTOR NO. 27	ANGLE = 130.0			
0.1258E+00	0.7769E+00	0.3150E-02	0.1104E-02	0.1112E-02	0.1672E-02
0.1466E-02	0.2066E-02	0.2475E-02	0.2532E-02	0.3227E-02	0.3667E-02
0.7990E-02	0.8872E-02	0.1013E-01	0.9839E-02	0.9462E-02	0.8939E-02
0.1007E-01	0.8149E-02	0.6355E-02	0.4605E-02	0.3080E-02	0.2120E-02
0.1539E-02	0.5949E-03	0.2268E-03	0.1433E-03	0.6267E-04	0.4397E-04
0.2244E-04	0.4769E-05	0.9775E-05	0.4765E-05	0.1286E-05	0.2822E-06
0.1010E-06	0.5262E-07	0.2165E-07	0.9124E-08	0.2604E-08	0.5353E-08
21R0.0	DETECTOR NO. 26	ANGLE = 125.0			
0.2479E+00	0.6962E+00	0.2991E-02	0.1100E-02	0.1125E-02	0.1659E-02
0.1517E-02	0.2184E-02	0.2628E-02	0.2655E-02	0.3232E-02	0.3661E-02
0.7896E-02	0.8742E-02	0.1001E-01	0.9693E-02	0.9328E-02	0.8838E-02
0.9955E-02	0.8054E-02	0.6305E-02	0.4579E-02	0.3078E-02	0.2115E-02
0.1548E-02	0.6113E-03	0.2330E-03	0.1548E-03	0.6937E-04	0.4431E-04
0.2315E-04	0.5011E-05	0.1387E-04	0.5280E-05	0.6935E-06	0.1224E-06
0.3692E-07	0.2129E-07	0.7743E-08	0.2643E-08	0.6703E-09	0.1540E-08
21R0.0	DETECTOR NO. 25	ANGLE = 120.0			
0.4421E+00	0.4997E+00	0.2810E-02	0.1062E-02	0.1103E-02	0.1743E-02
0.1697E-02	0.2244E-02	0.2598E-02	0.2638E-02	0.3179E-02	0.3588E-02
0.7674E-02	0.8452E-02	0.9732E-02	0.9407E-02	0.9051E-02	0.8570E-02
0.9647E-02	0.7830E-02	0.6152E-02	0.4455E-02	0.3024E-02	0.2049E-02
0.1512E-02	0.6097E-03	0.2453E-03	0.1488E-03	0.6551E-04	0.4692E-04
0.2339E-04	0.8378E-05	0.1069E-04	0.6106E-05	0.6550E-06	0.1520E-06
0.6078E-07	0.3258E-07	0.1282E-07	0.5105E-08	0.1422E-08	0.2742E-08
21R0.0	DETECTOR NO. 24	ANGLE = 115.0			
0.6628E+00	0.2940E+00	0.2608E-02	0.1078E-02	0.1141E-02	0.1824E-02
0.1834E-02	0.2296E-02	0.2551E-02	0.2617E-02	0.3094E-02	0.3484E-02
0.7456E-02	0.8227E-02	0.9456E-02	0.9127E-02	0.8815E-02	0.8354E-02
0.9412E-02	0.7662E-02	0.5992E-02	0.4351E-02	0.2963E-02	0.2011E-02
0.1479E-02	0.6046E-03	0.2511E-03	0.1474E-03	0.6611E-04	0.4944E-04
0.2570E-04	0.1155E-04	0.1092E-04	0.4503E-05	0.5559E-06	0.2349E-06
0.9902E-07	0.5073E-07	0.2031E-07	0.8860E-08	0.2536E-08	0.5015E-08
21R0.0	DETECTOR NO. 23	ANGLE = 110.0			
0.7465E+00	0.2254E+00	0.2442E-02	0.1216E-02	0.1326E-02	0.1824E-02
0.1841E-02	0.2226E-02	0.2500E-02	0.2569E-02	0.3022E-02	0.3384E-02
0.7281E-02	0.7981E-02	0.9181E-02	0.8878E-02	0.8574E-02	0.8103E-02
0.9113E-02	0.7464E-02	0.5832E-02	0.4242E-02	0.2880E-02	0.1936E-02
0.1465E-02	0.5837E-03	0.2524E-03	0.1406E-03	0.7773E-04	0.4652E-04
0.2544E-04	0.1161E-04	0.8481E-05	0.4450E-05	0.1136E-05	0.2206E-06
0.8657E-07	0.4457E-07	0.1829E-07	0.7692E-08	0.2232E-08	0.4531E-08
21RC.0	DETECTOR NO. 22	ANGLE = 105.0			
0.8691E+00	0.1076E+00	0.2312E-02	0.1279E-02	0.1411E-02	0.1765E-02
0.1779E-02	0.2147E-02	0.2427E-02	0.2498E-02	0.2903E-02	0.3261E-02
0.7040E-02	0.7691E-02	0.8870E-02	0.8572E-02	0.8293E-02	0.7842E-02
0.8849E-02	0.7206E-02	0.5625E-02	0.4072E-02	0.2789E-02	0.1871E-02
0.1405E-02	0.5557E-03	0.2502E-03	0.1349E-03	0.7204E-04	0.4693E-04
0.2477E-04	0.1059E-04	0.9917E-05	0.3611E-05	0.1075E-05	0.1266E-06
0.4350E-07	0.2355E-07	0.9119E-08	0.3490E-08	0.9216E-09	0.2092E-08
21R0.0	DETECTOR NO. 21	ANGLE = 100.0			
0.9733E+00	0.1124E+00	0.2342E-02	0.1251E-02	0.1371E-02	0.1685E-02
0.1739E-02	0.2086E-02	0.2285E-02	0.2397E-02	0.2810E-02	0.3169E-02
0.6823E-02	0.7439E-02	0.8590E-02	0.8299E-02	0.8008E-02	0.7568E-02
0.8547E-02	0.6939E-02	0.5430E-02	0.3925E-02	0.2672E-02	0.1807E-02
0.1341E-02	0.5271E-03	0.2414E-03	0.1291E-03	0.6698E-04	0.4428E-04
0.2347E-04	0.1033E-04	0.9451E-05	0.3610E-05	0.1137E-05	0.1784E-06
0.6643E-07	0.3445E-07	0.1410E-07	0.5851E-08	0.1636E-08	0.3396E-08
21R0.0	DETECTOR NO. 20	ANGLE = 95.0			
0.9903E+00	0.9511E+00	0.2334E-02	0.1209E-02	0.1340E-02	0.1596E-02
0.1640E-02	0.1952E-02	0.2185E-02	0.2299E-02	0.2663E-02	0.2984E-02
0.6494E-02	0.7109E-02	0.8226E-02	0.7923E-02	0.7628E-02	0.7199E-02
0.8141E-02	0.6556E-02	0.5119E-02	0.3683E-02	0.2502E-02	0.1710E-02
0.1252E-02	0.4893E-03	0.2168E-03	0.1209E-03	0.5879E-04	0.4289E-04
0.2248E-04	0.8902E-05	0.8579E-05	0.1882E-05	0.1949E-05	0.6530E-06
0.1084E-06	0.5244E-07	0.2396E-07	0.1129E-07	0.3307E-08	0.6660E-08
21R0.0	DETECTOR NO. 19	ANGLE = 90.0			
0.9972E+00	0.8147E+00	0.2357E-02	0.1166E-02	0.1248E-02	0.1499E-02
0.1587E-02	0.1850E-02	0.1992E-02	0.2090E-02	0.2384E-02	0.2680E-02
0.5824E-02	0.6350E-02	0.7353E-02	0.7096E-02	0.6824E-02	0.6382E-02
0.7187E-02	0.5737E-02	0.4488E-02	0.3194E-02	0.2171E-02	0.1479E-02
0.1118E-02	0.4347E-03	0.1920E-03	0.1004E-03	0.5267E-04	0.3776E-04
0.2050E-04	0.8168E-05	0.7549E-05	0.1674E-05	0.1875E-05	0.6285E-06
0.1025E-06	0.4955E-07	0.2251E-07	0.1061E-07	0.3112E-08	0.6260E-08
21R0.0	DETECTOR NO. 18	ANGLE = 85.0			
0.7330E+00	0.7503E+00	0.2376E-02	0.1163E-02	0.1249E-02	0.1513E-02
0.1608E-02	0.1883E-02	0.2035E-02	0.2158E-02	0.2476E-02	0.2737E-02

Fig. 2.5 Continued.

0.5893E-02 0.6391E-02 0.7400E-02 0.7092E-02 0.6730E-02 0.6264E-02
 0.7049E-02 0.5540E-02 0.4365E-02 0.3125E-02 0.2102E-02 0.1457E-02
 0.1132E-02 0.4430E-03 0.2098E-03 0.1003E-03 0.5333E-04 0.3704E-04
 0.2529E-04 0.8411E-05 0.8818E-05 0.1357E-05 0.6366E-06 0.7508E-06
 0.4445E-06 0.9272E-07 0.1918E-07 0.9044E-08 0.2648E-08 0.5372E-08

21R0.0
 ' DETECTOR NO. 17 ANGLE = 80.0
 0.8423E+00 0.7192E-02 0.2467E-02 0.1200E-02 0.1299E-02 0.1528E-02
 0.1664E-02 0.1965E-02 0.2153E-02 0.2300E-02 0.2596E-02 0.2848E-02
 0.6156E-02 0.6654E-02 0.7705E-02 0.7397E-02 0.7066E-02 0.6653E-02
 0.7496E-02 0.5903E-02 0.4626E-02 0.3335E-02 0.2254E-02 0.1562E-02
 0.1187E-02 0.5010E-03 0.2320E-03 0.1178E-03 0.6171E-04 0.4055E-04
 0.2637E-04 0.1097E-04 0.9429E-05 0.1757E-05 0.7000E-06 0.6499E-06
 0.3938E-06 0.7231E-07 0.1077E-07 0.4983E-08 0.1444E-08 0.3322E-08

21R0.0
 ' DETECTOR NO. 16 ANGLE = 75.0
 0.9200E+00 0.6842E-02 0.2508E-02 0.1233E-02 0.1328E-02 0.1512E-02
 0.1652E-02 0.1990E-02 0.2176E-02 0.2321E-02 0.2639E-02 0.2901E-02
 0.6250E-02 0.6733E-02 0.7843E-02 0.7564E-02 0.7252E-02 0.6840E-02
 0.7709E-02 0.6156E-02 0.4778E-02 0.3458E-02 0.2371E-02 0.1635E-02
 0.1228E-02 0.5287E-03 0.2486E-03 0.1274E-03 0.6799E-04 0.4031E-04
 0.2740E-04 0.1169E-04 0.1015E-04 0.2127E-05 0.7684E-06 0.2184E-06
 0.1096E-06 0.1645E-06 0.9663E-07 0.4550E-07 0.1356E-07 0.2580E-07

21R0.0
 ' DETECTOR NO. 15 ANGLE = 70.0
 0.9621E+00 0.6493E-02 0.2471E-02 0.1200E-02 0.1330E-02 0.1543E-02
 0.1686E-02 0.1959E-02 0.2151E-02 0.2310E-02 0.2649E-02 0.2909E-02
 0.6254E-02 0.6723E-02 0.7865E-02 0.7604E-02 0.7304E-02 0.6923E-02
 0.7767E-02 0.6246E-02 0.4836E-02 0.3511E-02 0.2419E-02 0.1658E-02
 0.1261E-02 0.5280E-03 0.2569E-03 0.1368E-03 0.6430E-04 0.4850E-04
 0.2824E-04 0.1132E-04 0.1080E-04 0.2135E-05 0.7384E-06 0.2578E-06
 0.1272E-06 0.1684E-06 0.9736E-07 0.4575E-07 0.1359E-07 0.2570E-07

21R0.0
 ' DETECTOR NO. 14 ANGLE = 65.0
 0.9907E+00 0.6139E-02 0.2406E-02 0.1206E-02 0.1370E-02 0.1522E-02
 0.1657E-02 0.1955E-02 0.2149E-02 0.2295E-02 0.2622E-02 0.2876E-02
 0.6204E-02 0.6685E-02 0.7810E-02 0.7564E-02 0.7285E-02 0.6934E-02
 0.7764E-02 0.6259E-02 0.4839E-02 0.3538E-02 0.2439E-02 0.1667E-02
 0.1271E-02 0.5348E-03 0.2571E-03 0.1366E-03 0.6929E-04 0.5103E-04
 0.2684E-04 0.1311E-04 0.9459E-05 0.1630E-05 0.6376E-06 0.2146E-06
 0.8209E-07 0.3944E-07 0.1747E-07 0.7933E-08 0.2187E-08 0.4557E-08

21R0.0
 ' DETECTOR NO. 13 ANGLE = 60.0
 0.9904E+00 0.5816E-02 0.2273E-02 0.1259E-02 0.1454E-02 0.1541E-02
 0.1676E-02 0.1938E-02 0.2122E-02 0.2277E-02 0.2604E-02 0.2852E-02
 0.6154E-02 0.6616E-02 0.7773E-02 0.7527E-02 0.7245E-02 0.6877E-02
 0.7718E-02 0.6240E-02 0.4793E-02 0.3547E-02 0.2420E-02 0.1672E-02
 0.1301E-02 0.5554E-03 0.2395E-03 0.1364E-03 0.6605E-04 0.5934E-04
 0.2761E-04 0.1102E-04 0.1010E-04 0.1367E-05 0.5212E-06 0.1778E-06
 0.6646E-07 0.3186E-07 0.1414E-07 0.6275E-08 0.1720E-08 0.3732E-08

21R0.0
 ' DETECTOR NO. 12 ANGLE = 55.0
 0.1005E+01 0.5524E-02 0.2134E-02 0.1283E-02 0.1509E-02 0.1593E-02
 0.1732E-02 0.1934E-02 0.2089E-02 0.2230E-02 0.2578E-02 0.2816E-02
 0.6084E-02 0.6532E-02 0.7707E-02 0.7493E-02 0.7165E-02 0.6821E-02
 0.7670E-02 0.6196E-02 0.4774E-02 0.3528E-02 0.2397E-02 0.1690E-02
 0.1276E-02 0.5554E-03 0.2414E-03 0.1421E-03 0.6715E-04 0.5662E-04
 0.2924E-04 0.1215E-04 0.9405E-05 0.9462E-06 0.3587E-06 0.2708E-06
 0.1316E-06 0.6342E-07 0.2816E-07 0.1285E-07 0.3701E-08 0.7451E-08

21R0.0
 ' DETECTOR NO. 11 ANGLE = 50.0
 0.1009E+01 0.5332E-02 0.2044E-02 0.1200E-02 0.1447E-02 0.1621E-02
 0.1785E-02 0.1954E-02 0.2098E-02 0.2203E-02 0.2569E-02 0.2799E-02
 0.6050E-02 0.6445E-02 0.7645E-02 0.7459E-02 0.7105E-02 0.6762E-02
 0.7618E-02 0.6134E-02 0.4727E-02 0.3511E-02 0.2405E-02 0.1680E-02
 0.1253E-02 0.5650E-03 0.2529E-03 0.1376E-03 0.6771E-04 0.5731E-04
 0.3105E-04 0.1140E-04 0.9189E-05 0.1052E-05 0.3949E-06 0.2843E-06
 0.1367E-06 0.6592E-07 0.2921E-07 0.1336E-07 0.3832E-08 0.7713E-08

21R0.0
 ' DETECTOR NO. 10 ANGLE = 45.0
 0.1017E+01 0.5169E-02 0.1961E-02 0.1100E-02 0.1346E-02 0.1592E-02
 0.1776E-02 0.1967E-02 0.2126E-02 0.2241E-02 0.2570E-02 0.2791E-02
 0.6016E-02 0.6351E-02 0.7572E-02 0.7395E-02 0.7054E-02 0.6708E-02
 0.7552E-02 0.6057E-02 0.4681E-02 0.3502E-02 0.2409E-02 0.1656E-02
 0.1250E-02 0.5722E-03 0.2498E-03 0.1448E-03 0.6520E-04 0.5105E-04
 0.3148E-04 0.1100E-04 0.1048E-04 0.2225E-05 0.3471E-06 0.2153E-06
 0.1053E-06 0.5063E-07 0.2232E-07 0.1017E-07 0.2927E-08 0.5853E-08

21R0.0
 ' DETECTOR NO. 9 ANGLE = 40.0
 0.1027E+01 0.5054E-02 0.1919E-02 0.1028E-02 0.1276E-02 0.1525E-02
 0.1705E-02 0.1965E-02 0.2162E-02 0.2254E-02 0.2574E-02 0.2798E-02
 0.5991E-02 0.6289E-02 0.7518E-02 0.7344E-02 0.6982E-02 0.6643E-02
 0.7489E-02 0.6014E-02 0.4661E-02 0.3450E-02 0.2392E-02 0.1641E-02
 0.1254E-02 0.5524E-03 0.2601E-03 0.1441E-03 0.6710E-04 0.4945E-04
 0.3303E-04 0.1381E-04 0.9530E-05 0.1998E-05 0.3151E-06 0.2482E-06
 0.1200E-06 0.5775E-07 0.2546E-07 0.1145E-07 0.3258E-08 0.6603E-08

21R0.0
 ' DETECTOR NO. 8 ANGLE = 35.0
 0.1028E+01 0.4976E-02 0.1892E-02 0.9430E-03 0.1184E-02 0.1461E-02

Fig. 2.5 Continued.

0.1643E-02	0.1922E-02	0.2119E-02	0.2222E-02	0.2605E-02	0.2834E-02
0.6010E-02	0.6254E-02	0.7439E-02	0.7277E-02	0.6948E-02	0.6590E-02
0.7417E-02	0.5940E-02	0.4642E-02	0.3408E-02	0.2344E-02	0.1634E-02
0.1251E-02	0.5377E-03	0.2794E-03	0.1335E-03	0.7167E-04	0.4952E-04
0.2800E-04	0.1304E-04	0.1085E-04	0.2851E-05	0.4313E-06	0.1869E-06
0.8998E-07	0.4314E-07	0.1868E-07	0.8220E-08	0.2285E-08	0.4621E-08
21R0.0					
' DETECTOR NO. 7 ANGLE = 30.0					
0.1031E+01	0.4906E-02	0.1869E-02	0.8988E-03	0.1138E-02	0.1403E-02
0.1579E-02	0.1870E-02	0.2075E-02	0.2164E-02	0.2565E-02	0.2800E-02
0.5989E-02	0.6284E-02	0.7419E-02	0.7201E-02	0.6896E-02	0.6504E-02
0.7348E-02	0.5915E-02	0.4580E-02	0.3376E-02	0.2293E-02	0.1612E-02
0.1256E-02	0.5465E-03	0.2614E-03	0.1375E-03	0.8326E-04	0.4058E-04
0.2660E-04	0.1012E-04	0.1123E-04	0.3562E-05	0.1018E-05	0.3380E-06
0.8357E-07	0.4008E-07	0.1730E-07	0.7606E-08	0.2111E-08	0.4382E-08
21R0.0					
' DETECTOR NO. 6 ANGLE = 25.0					
0.1032E+01	0.4899E-02	0.1857E-02	0.8429E-03	0.1092E-02	0.1357E-02
0.1526E-02	0.1827E-02	0.2024E-02	0.2103E-02	0.2525E-02	0.2769E-02
0.5956E-02	0.6247E-02	0.7398E-02	0.7171E-02	0.6846E-02	0.6458E-02
0.7254E-02	0.5881E-02	0.4536E-02	0.3337E-02	0.2294E-02	0.1571E-02
0.1225E-02	0.5600E-03	0.2619E-03	0.1327E-03	0.7243E-04	0.4367E-04
0.2380E-04	0.1087E-04	0.1012E-04	0.3290E-05	0.1112E-05	0.4268E-06
0.1233E-06	0.5929E-07	0.2590E-07	0.1163E-07	0.3305E-08	0.6823E-08
21R0.0					
' DETECTOR NO. 5 ANGLE = 20.0					
0.1042E+01	0.4884E-02	0.1866E-02	0.8471E-03	0.1093E-02	0.1284E-02
0.1454E-02	0.1792E-02	0.1984E-02	0.2047E-02	0.2479E-02	0.2737E-02
0.5888E-02	0.6170E-02	0.7337E-02	0.7139E-02	0.6801E-02	0.6441E-02
0.7198E-02	0.5814E-02	0.4498E-02	0.3323E-02	0.2251E-02	0.1535E-02
0.1229E-02	0.5530E-03	0.2577E-03	0.1364E-03	0.7043E-04	0.4420E-04
0.2468E-04	0.1151E-04	0.7297E-05	0.2537E-05	0.1455E-05	0.6119E-06
0.1914E-06	0.9148E-07	0.4032E-07	0.1844E-07	0.5389E-08	0.1069E-07
21R0.0					
' DETECTOR NO. 4 ANGLE = 15.0					
0.1038E+01	0.4915E-02	0.1870E-02	0.8282E-03	0.1069E-02	0.1257E-02
0.1418E-02	0.1777E-02	0.1950E-02	0.2002E-02	0.2419E-02	0.2694E-02
0.5803E-02	0.6082E-02	0.7263E-02	0.7097E-02	0.6779E-02	0.6400E-02
0.7161E-02	0.5759E-02	0.4452E-02	0.3305E-02	0.2218E-02	0.1516E-02
0.1214E-02	0.5485E-03	0.2479E-03	0.1393E-03	0.6521E-04	0.4327E-04
0.2681E-04	0.1350E-04	0.7482E-05	0.1978E-05	0.1269E-05	0.7107E-06
0.2586E-06	0.1238E-06	0.5461E-07	0.2501E-07	0.7316E-08	0.1460E-07
21R0.0					
' DETECTOR NO. 3 ANGLE = 10.0					
0.1041E+01	0.4997E-02	0.1867E-02	0.7934E-03	0.1030E-02	0.1226E-02
0.1379E-02	0.1755E-02	0.1939E-02	0.1978E-02	0.2375E-02	0.2667E-02
0.5756E-02	0.6038E-02	0.7222E-02	0.7054E-02	0.6744E-02	0.6347E-02
0.7139E-02	0.5721E-02	0.4421E-02	0.3276E-02	0.2209E-02	0.1533E-02
0.1189E-02	0.5400E-03	0.2425E-03	0.1400E-03	0.6703E-04	0.3831E-04
0.3058E-04	0.1431E-04	0.8407E-05	0.1448E-05	0.4438E-06	0.2901E-06
0.3407E-06	0.2133E-06	0.9531E-07	0.4413E-07	0.1299E-07	0.2533E-07
21R0.0					
' DETECTOR NO. 2 ANGLE = 5.0					
0.1044E+01	0.5059E-02	0.1867E-02	0.7745E-03	0.1005E-02	0.1248E-02
0.1386E-02	0.1730E-02	0.1913E-02	0.1956E-02	0.2361E-02	0.2674E-02
0.5745E-02	0.6029E-02	0.7204E-02	0.7078E-02	0.6748E-02	0.6348E-02
0.7151E-02	0.5740E-02	0.4438E-02	0.3260E-02	0.2233E-02	0.1545E-02
0.1196E-02	0.5227E-03	0.2454E-03	0.1372E-03	0.7030E-04	0.3757E-04
0.2997E-04	0.1380E-04	0.8877E-05	0.1952E-05	0.1126E-05	0.6908E-06
0.2196E-06	0.6280E-07	0.2657E-07	0.1154E-07	0.3146E-08	0.6682E-08
21R0.0					
' DETECTOR NO. 1 ANGLE = 0.0					
0.1044E+01	0.5070E-02	0.1869E-02	0.7831E-03	0.1006E-02	0.1229E-02
0.1366E-02	0.1709E-02	0.1907E-02	0.1954E-02	0.2372E-02	0.2684E-02
0.5729E-02	0.6016E-02	0.7197E-02	0.7069E-02	0.6748E-02	0.6359E-02
0.7151E-02	0.5763E-02	0.4426E-02	0.3270E-02	0.2247E-02	0.1542E-02
0.1186E-02	0.4938E-03	0.2672E-03	0.1327E-03	0.6920E-04	0.4381E-04
0.2605E-04	0.1226E-04	0.7991E-05	0.2345E-05	0.1565E-05	0.7789E-06
0.2293E-06	0.6818E-07	0.2883E-07	0.1272E-07	0.3540E-08	0.7214E-08
21R0.0					
T	T				

Fig. 2.5 Continued.

Fig. 2.6 Input data of the DOT analysis for the SS316/water assembly with the FUSION-40 library (42-n + 21-y).

38R2 32Q38
 9\$\$ -241 -247 -253 -259
 10\$\$
 ' 241 = AIR / 247 = SUS316 / 253 = H2O
 4I241 246 296
 4I247 252 996
 4I253 258 296
 4I259 264 996
 11\$\$
 6Z 4I161 66 4I167 72
 6Z 4I163 168 4I139 144 4I187 192
 4I55 60 4I197 102 4I145 150
 4I103 108 4I109 114 4I151 156
 6Z 4I1 6 4I167 72
 6Z 4I163 168 4I139 144 4I187 192
 4I55 60 4I197 102 4I145 150
 4I103 108 4I109 114 4I151 156
 12**
 6R0.0 6R3.8810-5 6R1.0400-5
 6R0.0 6R9.3405-3 6R1.5482-2 6R1.0585-3 6R1.1931-4 6R1.0341-3
 6R1.0355-3 6R4.3954-5 6R1.9366-6 6R5.7904-2
 6R0.0 6R6.6559-2 6R3.3329-2
 6R0.0 6R9.1456-3 6R1.5025-2 6R1.0254-3 6R1.9855-4 6R8.1608-4
 6R1.3561-3 6R4.7828-5 6R4.5072-6 6R5.8331-2

Fig. 2.6 Continued.

Fig. 2.7 : Input data of FNSUNCL for the DOT analysis of the SS316/water assembly with the JSSTDLib library (125-n + 40- γ).

```

38R2      32Q38
9$$
   -1    -7    -13   -19
13**
' LONG WATER COOLED TARGET - ANGULAR COSINE DISTRIBUTION TABLE
-1.0      -0.996195   -0.984808   -0.965926   -0.939693   -0.906308
-0.866025  -0.819152   -0.766044   -0.707107   -0.642788   -0.573576
-0.5      -0.422618   -0.342020   -0.258809   -0.173648   -0.087156
  0.0      0.087156   0.173648   0.258809   0.342020   0.422618
  0.5      0.573576   0.642788   0.707107   0.766044   0.819152
  0.866025  0.906308   0.939693   0.965926   0.984808   0.996195
  1.0
14**
' LONG WATER COOLED TARGET - ANGULAR SOURCE INTENSITY TABLE
  1.1567    1.1785    0.97312    1.0221    0.99500    0.91711
  0.74641   0.73360   0.79463   0.88820   1.0175    1.0581
  1.0532    1.0657    1.0783    1.0797    1.0840    1.0945
  1.0902    0.82512   0.93854   1.0180    1.0603    1.0782
  1.0872    1.1009    1.1043    1.1113    1.1204    1.1200
  1.1219    1.1216    1.1314    1.1266    1.1284    1.1314
  1.1312
15**
' LONG WATER COOLED TARGET - ANGULAR SOURCE SPECTRA TABLE
' DETECTOR NO. 37   ANGLE = 180.0
  0.0      0.0      0.0      0.0      0.0      0.0
  0.0      2.8133E-07  1.1132E-05  7.0699E-05  2.9725E-04  5.8035E-03
  1.1174E-01 5.0093E-01  2.9325E-01  3.5848E-02  1.9167E-03  2.2345E-03
  4.6392E-04 3.5134E-04  3.2277E-04  2.9870E-04  2.1404E-04  1.7976E-04

```

The rest of the data are just the same as those in Fig. 2.3.

Fig. 2.7 Continued.

```

PNS-DOT3.5  SS316/Water Assembly  SELF SHIELD (N125+G40)
O
61$$
  0      5      4      38      177     165
  3      4      168     0       0       24
  24     0      160     1       1       0
  0      0      1       15      15      3
  6      2      0       0       0       0
  0      0      0       0       0       0
  0      0      0       0       3       0
  0      0      0       0       0       0
  0      0      2       1       1       0
  0      0      0       0       0       0
  0
62$$
  0      0      0       0       0       0
  0      0      0       0       8       0
  0
63**
  0.0    1.000E-02  0.0      0.0      0.0      0.0
  0.0    0.0      0.0      0.0      0.0      0.0
  0.0    0.0      0.0      0.0      0.0      0.0
T
7**
  -0.21082  -0.14907  1M1
  -0.42164  -0.39441  -0.14907  1M2
  -0.55777  -0.53748  -0.39441  -0.14907  1M3
  -0.66667  -0.64979  -0.53748  -0.39441  -0.14907  1M4
  -0.76012  -0.74536  -0.64979  -0.53748  -0.39441  -0.14907
1M5
  -0.84327  -0.82999  -0.74536  -0.64979  -0.53748  -0.3944
  -0.14907  1M6
  -0.91894  -0.90676  -0.82999  -0.74536  -0.64979  -0.53748
  -0.39441  -0.14907  1M7
  -0.98883  -0.97753  -0.90676  -0.82999  -0.74536  -0.64979
  -0.53748  -0.39441  -0.14907  1M8
1Q80
  3R-0.97753  5R-0.90676  7R-0.82999  9R-0.74536  11R-0.64979  13R-0.53748
  15R-0.39441 17R-0.14907  3R0.97753  5R0.90676  7R0.82999  9R0.74536
  11R0.64979  13R0.53748  15R0.39441  17R0.14907
T
6**
  0.0    2R0.13586-1      0.0      4R0.97681-2
  0.0    0.64738-2  0.50390-2  0.64738-2  1N3
  0.0    0.64634-2  2R0.71124-2  0.64634-2  1N4
  0.0    0.64634-2  0.14381-2  0.36342-2  0.14381-2  0.64634-2
  1N5

```

Fig. 2.8 Input data of the DOT analysis for the SS316/water assembly with the JSSTD library (125-n + 40- γ).

JAERI-Research 95-018

```

0.0      0.64738-2   0.71124-2   0.36342-2 1N3      1Q6
0.0      0.97681-2   0.50390-2   0.71124-2   0.14381-2   0.71124-2
0.0      0.50390-2   0.97681-2 1N7
0.0      0.13586-1   0.97681-2 2R0.64738-2 1N4      1Q8
1Q80
T
13$$
        4I3081 3086
        4I3261 3266
        4I3011 3016
        4I3267 3272
T
3**
F0.0
T
1**
F0.0
2**
  1I0.0  1.0   2.0   6I3.3   1I17.3   1I19.3   20.3   28I21.3   79.3
  1I80.3
    1I81.3   3I82.5   1I85.18   1I86.38   3I87.58   1I90.26
  7I91.46   1I96.54   3I97.74   1I100.42   7I101.62   1I106.7   3I107.9
  1I110.58   7I111.78   1I116.86   3I118.06   1I120.74   121.94
  122.62   123.62   125.02   127.02   129.02   130.42   131.42   1I132.1
  3I133.3   1I135.98   137.18   137.86   138.86   140.26   142.26
  144.26   145.66   146.66   1I147.34   3I148.54   1I151.22   152.42
  3I1153.42   218.5
4**
  2I0.0   6.0   6.383   6.7   7.3   14I8.0   1I38.0   1I40.0   41.0
  7I42.0   58.0   1I59.0   60.0
5**
F1.0
8$$
        4R1    34R4   14Q38
        24R1   14R4   32Q38
        38R2   1Q38   38R3   3Q38   38R2   1Q38
        38R2   1Q38   38R3   3Q38   38R2   1Q38
        38R2   7Q38
        38R2   1Q38   38R3   3Q38   38R2   1Q38
        38R2   32Q38
9$$
  1 = AIR /  7 = SUS316 /  13 = H2O /  19 = SUS316
  -1   -7   -13   -19
T
T

```

Fig. 2.8 Continued.

```

FNS-GRTUNCL      SS316/Water Assembly SELF SHIELD (N42+G21)
O
1$$
        0       5       4       38      177      63
        3       4       66      0       0       24
        24      1       1       30000     10       0
        1       0       18      0       0       37
        1       1       1       1
2**
  1.0      51.3      0.0      0.0      0.0
T
13$$
        4I3081 3086
        4I3261 3266
        4I3011 3016
        4I3267 3272
T
1**
F0.0
2**
  1I0.0  1.0   2.0   6I3.3   1I17.3   1I19.3   20.3   28I21.3   79.3
  1I80.3
    1I81.3   3I82.5   1I85.18   1I86.38   3I87.58   1I90.26
  7I91.46   1I96.54   3I97.74   1I100.42   7I101.62   1I106.7   3I107.9
  1I110.58   7I111.78   1I116.86   3I118.06   1I120.74   121.94
  122.62   123.62   125.02   127.02   129.02   130.42   131.42   1I132.1

```

Fig. 2.9 Input data of FNSUNCL for the DOT analysis of the SS316/water assembly with the JSSTDL library (42-n + 21- γ).

```

3I133.3   1I135.98   137.18   137.86   138.86   140.26   142.26
144.26   145.66   146.66   1I147.34   3I148.54   1I151.22   152.42
      3I1I53.42   218.5

3**
   F.O.0
4**
   2I0.0    6.0    6.383   6.7    7.3    14I8.0    1I38.0    1I40.0    41.0
   7I42.0   58.0   1I59.0   60.0

6**
   1.0
7**
   1.0
8$$
   4R1    34R4    14Q38
   24R1   14R4    32Q38
   38R2   1Q38    38R3    3Q38    38R2    1Q38
   38R2   1Q38    38R3    3Q38    38R2    1Q38
   38R2   7Q38
   38R2   1Q38    38R3    3Q38    38R2    1Q38
   38R2   32Q38
9$$
   -1     -7     -13    -19

13**
   LONG WATER COOLED TARGET - ANGULAR COSINE DISTRIBUTION TABLE
   -1.0    -0.996195   -0.984808   -0.965926   -0.939693   -0.906308
   -0.866025   -0.819152   -0.766044   -0.707107   -0.642788   -0.573576
   -0.5    -0.422618   -0.342020   -0.258809   -0.173648   -0.087156
   0.0     0.087156    0.173648   -0.258809   0.342020   0.422618
   0.5     0.573576    0.642788   0.707107   0.766044   0.819152
   0.866025   0.906308   0.939693   0.965926   0.984808   0.996195
   1.0

14**
   LONG WATER COOLED TARGET - ANGULAR SOURCE INTENSITY TABLE
   1.1567    1.1785    0.97312   1.0221    0.99500   0.91711
   0.74641   0.73360   0.79463   0.88820   1.0175    1.0581
   1.0532    1.0657    1.0783    1.0797    1.0840    1.0945
   1.0902    0.82512   0.93854   1.0180    1.0603    1.0782
   1.0872    1.1009    1.1043    1.1113    1.1204    1.1200
   1.1219    1.1216    1.1314    1.1266    1.1284    1.1314
   1.1312

15**
   LONG WATER COOLED TARGET - ANGULAR SOURCE SPECTRA TABLE
   DETECTOR NO. 37      ANGLE = 180.0
   0.4793E-02  0.9460E+00  0.7066E-02  0.1480E-02  0.1812E-02  0.2678E-02
   0.2626E-02  0.3422E-02  0.4506E-02  0.4909E-02  0.5521E-02  0.6431E-02
   0.1414E-01  0.1580E-01  0.1805E-01  0.1774E-01  0.1672E-01  0.1540E-01

```

The rest of the data are just the same as those in Fig. 2.5.

Fig. 2.9 Continued.

FNS-DOT3.5		SS316/Water Assembly		(N42+G21)			
61\$\$		0	5	4	38	177	63
		3	4	66	0	0	24
		24	0	160	1	1	0
		0	0	1	15	15	3
		6	2	0	0	0	0
		0	0	0	0	0	0
		0	0	0	0	3	0
		0	0	0	0	0	0
		0	0	2	1	1	0
		0	0	0	0	0	0
62\$\$		0	0	0	0	0	0
		0	0	0	0	8	0
63**		0.0	1.000E-02	0.0	0.0	0.0	0.0
		0.0	0.0	0.0	0.0	0.0	0.0

Fig. 2.10 Input data of the DOT analysis for the SS316/water assembly with the JSSTDLL library (42-n + 21- γ).

0.0 0.0 0.0 0.0 0.0 0.0
^T
 7** -0.21082 -0.14907 1M1
 -0.42164 -0.39441 -0.14907 1M2
 -0.55777 -0.53748 -0.39441 -0.14907 1M3
 -0.66667 -0.64979 -0.53748 -0.39441 -0.14907 1M4
 -0.76012 -0.74536 -0.64979 -0.53748 -0.39441 -0.14907
 1M5 -0.84327 -0.82999 -0.74536 -0.64979 -0.53748 -0.39441
 -0.14907 1M6 -0.91894 -0.90676 -0.82999 -0.74536 -0.64979 -0.53748
 -0.39441 -0.14907 1M7 -0.98883 -0.97753 -0.90676 -0.82999 -0.74536 -0.64979
 -0.53748 -0.39441 -0.14907 1M8
 1Q8C 3R-0.97753 5R-0.90676 7R-0.82999 9R-0.74536 11R-0.64979 13R-0.53748
 15R-0.39441 17R-0.14907 3R0.97753 5R0.90676 7R0.82999 9R0.74536
 11R0.64979 13R0.53748 15R0.39441 17R0.14907
^T
 6** 2R0.13586-1 0.0 4R0.97681-2
 0.0 0.64738-2 0.50390-2 0.64738-2 1N3
 0.0 0.64634-2 2R0.71124-2 0.64634-2 1N4
 0.0 0.64634-2 0.14381-2 0.36342-2 0.14381-2 0.64634-2
 1N5 0.64738-2 0.71124-2 0.36342-2 1N3 1Q6
 0.0 0.97681-2 0.50390-2 0.71124-2 0.14381-2 0.71124-2
 0.50390-2 0.97681-2 1N7
 0.0 0.13586-1 0.97681-2 2R0.64738-2 1N4 1Q8
 1Q80
^T
 13\$\$ 4I3081 3086
 4I3261 3266
 4I3011 3016
 4I3267 3272
^T
 3** FC.0
^T
 1** F0.0
 2** 1I0.0 1.0 2.0 6I3.3 1I17.3 1I19.3 20.3 28I21.3 79.3
 1I80.3 1I81.3 3I82.5 1I85.18 1I86.38 3I87.58 1I90.26
 7I91.46 1I96.54 3I97.74 1I100.42 7I101.62 1I106.7 3I107.9
 1I110.58 7I111.78 1I116.86 3I118.06 1I120.74 121.94
 122.62 123.62 125.02 127.02 129.02 130.42 131.42 1I132.1
 3I133.3 1I135.98 137.18 137.86 138.86 140.26 142.26
 144.26 145.66 146.66 1I147.34 3I148.54 1I151.22 152.42
 3I153.42 218.5
 4** 2I0.0 6.0 6.383 6.7 7.3 14I8.0 1I38.0 1I40.0 41.0
 7I42.0 58.0 1I59.0 60.0
 5** F1.0
 8\$\$ 4R1 34R4 14Q38
 24R1 14R4 32Q38
 38R2 1Q38 38R3 3Q38 38R2 1Q38
 38R2 1Q38 38R3 3Q38 38R2 1Q38
 38R2 7Q38
 38R2 1Q38 38R3 3Q38 38R2 1Q38
 38R2 32Q38
 9\$\$ 1 = AIR / 7 = SUS316 / 13 = H2O / 19 = SUS316
 -1 -7 -13 -19
^T ^T

Fig. 2.10 Continued.

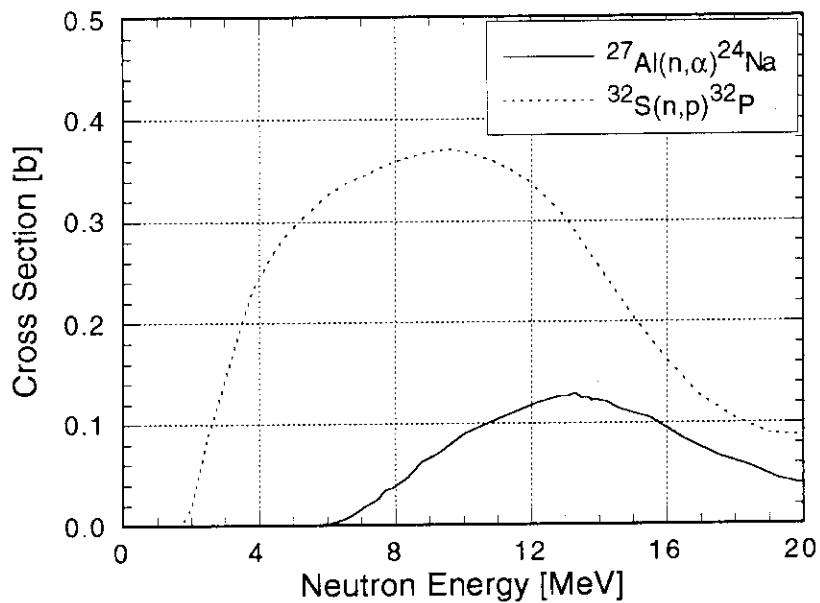


Fig. 3.1 Dosimetry reaction cross sections of the $^{27}\text{Al}(n,\alpha)^{24}\text{Na}$ and $^{32}\text{S}(n,p)^{32}\text{P}$ reactions taken from JENDL Dosimetry File.

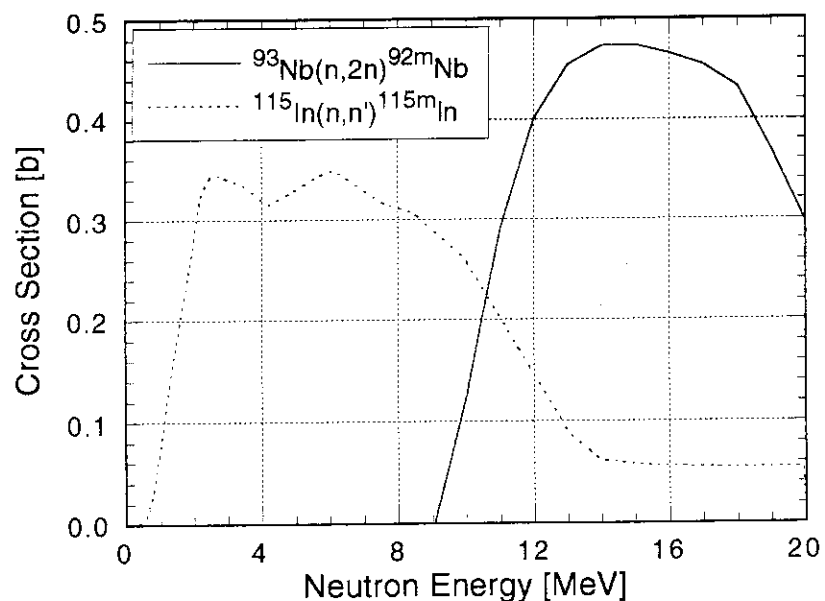


Fig. 3.2 Dosimetry reaction cross sections of the $^{93}\text{Nb}(n,2n)^{92m}\text{Nb}$ and $^{115}\text{In}(n,n')^{115m}\text{In}$ reactions taken from JENDL Dosimetry File.

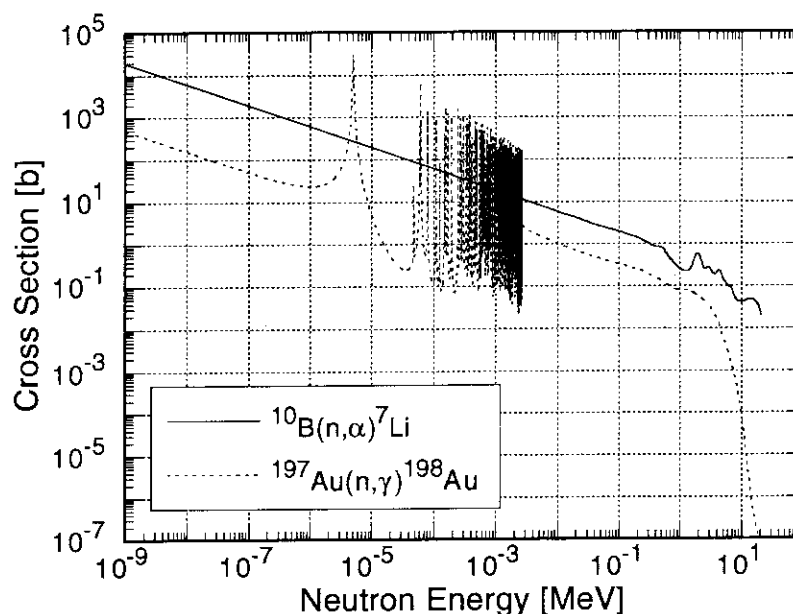


Fig. 3.3 Dosimetry reaction cross sections of the $^{10}\text{B}(\text{n},\alpha)^7\text{Li}$ and $^{197}\text{Au}(\text{n},\gamma)^{198}\text{Au}$ reactions taken from JENDL Dosimetry File.

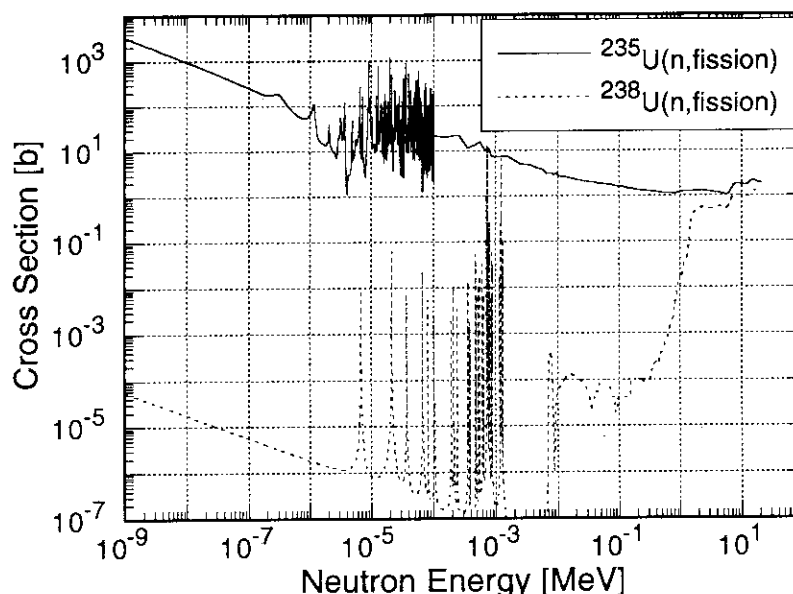


Fig. 3.4 Dosimetry reaction cross sections of the $^{235}\text{U}(\text{n,fission})$ and $^{238}\text{U}(\text{n,fission})$ reactions taken from JENDL Dosimetry File.

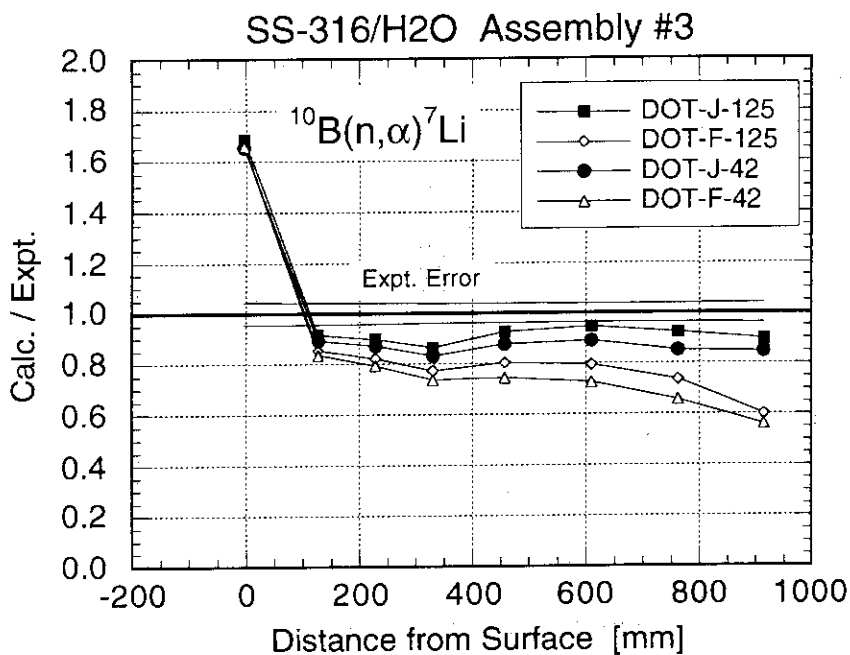


Fig. 3.5 The C/E ratios of the $^{10}\text{B}(\text{n},\alpha)^7\text{Li}$ reaction rate for four different DOT calculations.

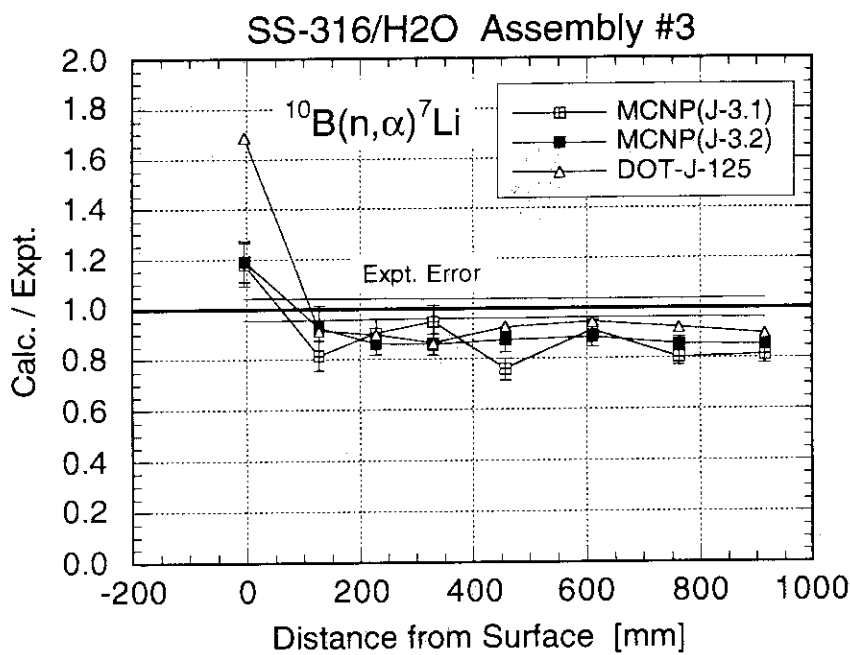


Fig. 3.6 The C/E ratios of the $^{10}\text{B}(\text{n},\alpha)^7\text{Li}$ reaction rate for MCNP and DOT calculations.

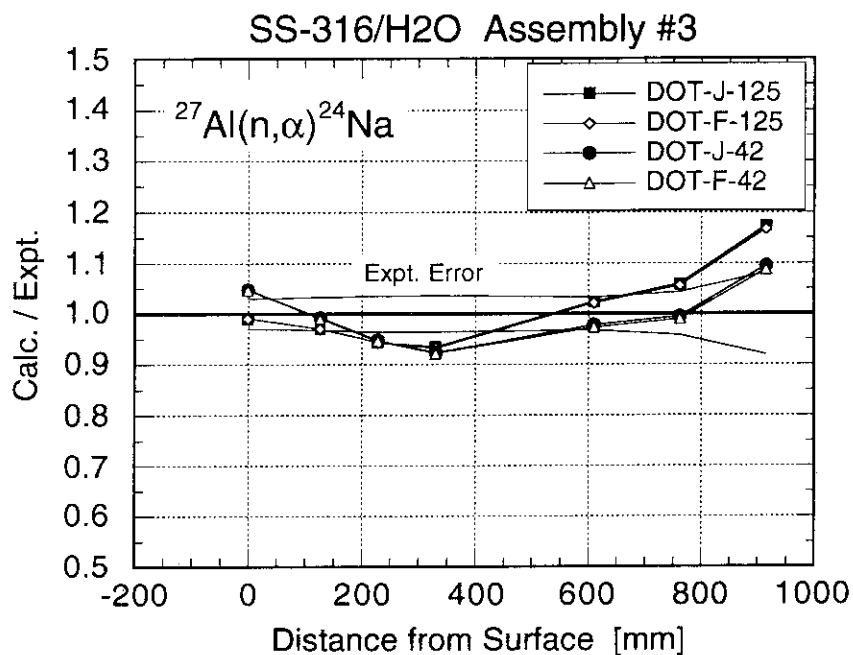


Fig. 3.7 The C/E ratios of the $^{27}\text{Al}(\text{n},\alpha)^{24}\text{Na}$ reaction rate for four different DOT calculations.

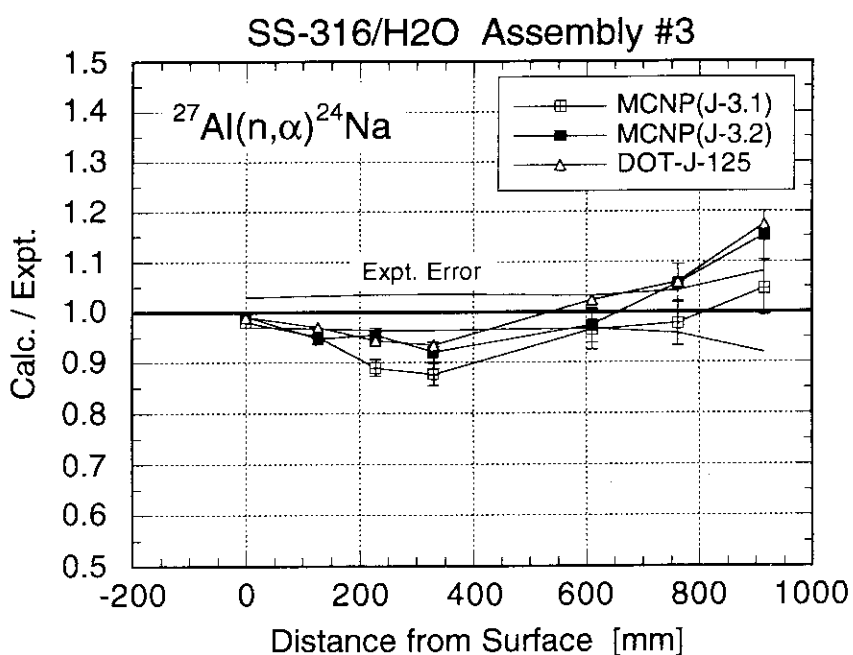


Fig. 3.8 The C/E ratios of the $^{27}\text{Al}(\text{n},\alpha)^{24}\text{Na}$ reaction rate for MCNP and DOT calculations.

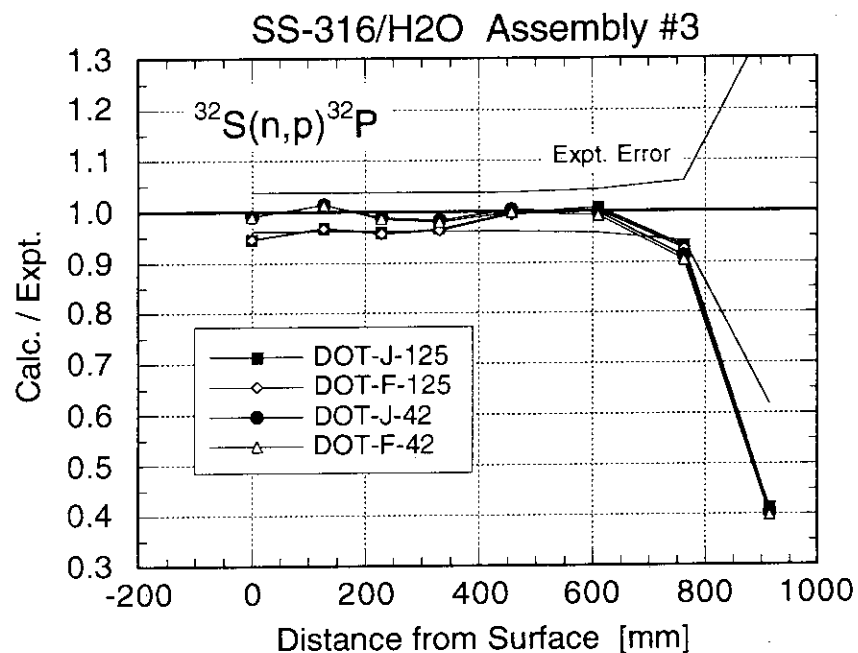


Fig. 3.9 The C/E ratios of the $^{32}\text{S}(\text{n},\text{p})^{32}\text{P}$ reaction rate for four different DOT calculations.

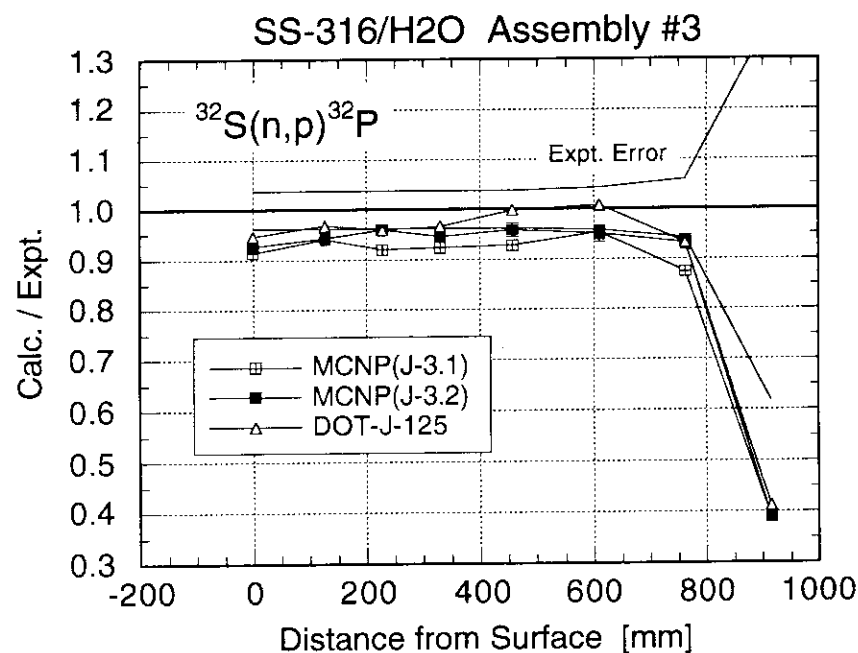


Fig. 3.10 The C/E ratios of the $^{32}\text{S}(\text{n},\text{p})^{32}\text{P}$ reaction rate for MCNP and DOT calculations.

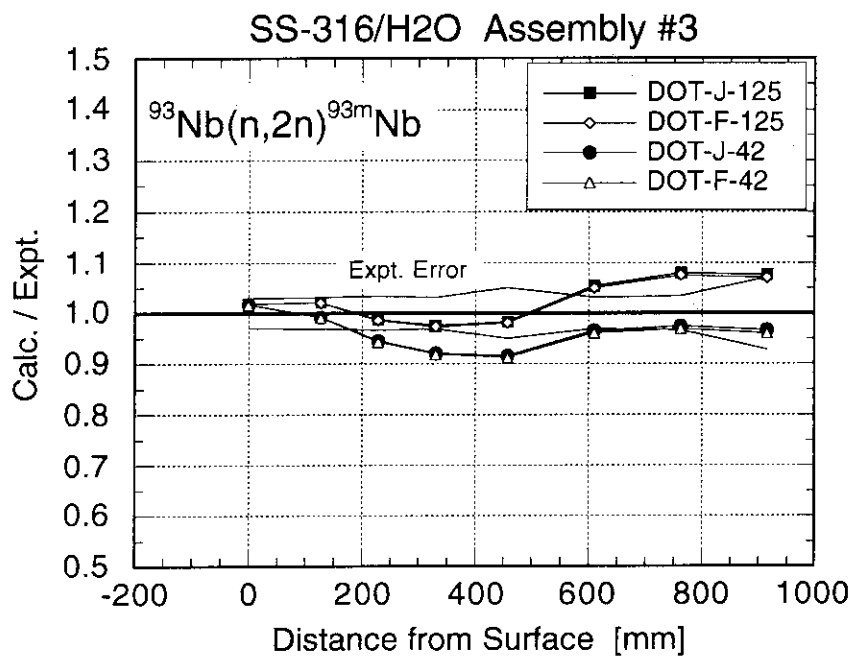


Fig. 3.11 The C/E ratios of the $^{93}\text{Nb}(n,2n)^{93\text{m}}\text{Nb}$ reaction rate for four different DOT calculations.

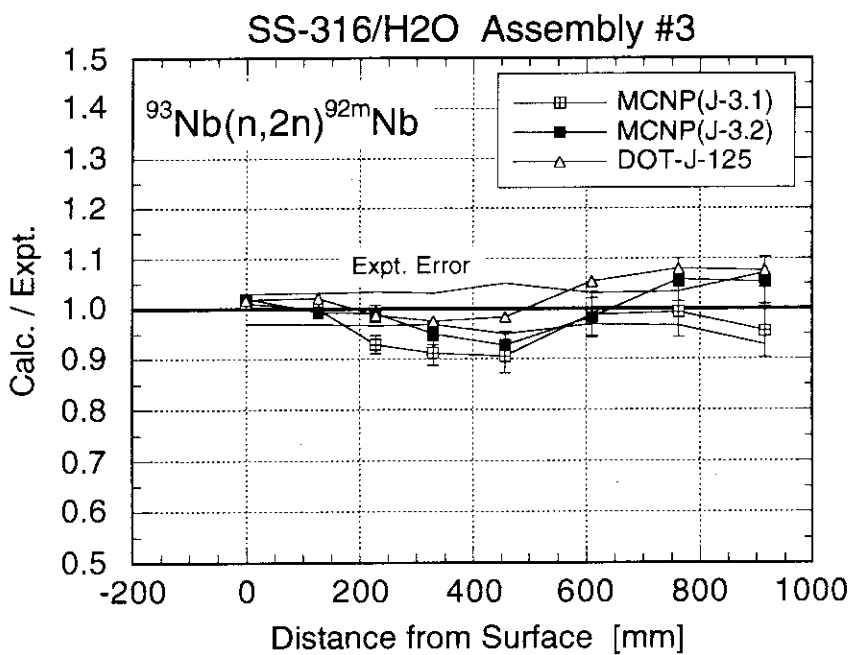


Fig. 3.12 The C/E ratios of the $^{93}\text{Nb}(n,2n)^{92\text{m}}\text{Nb}$ reaction rate for MCNP and DOT calculations.

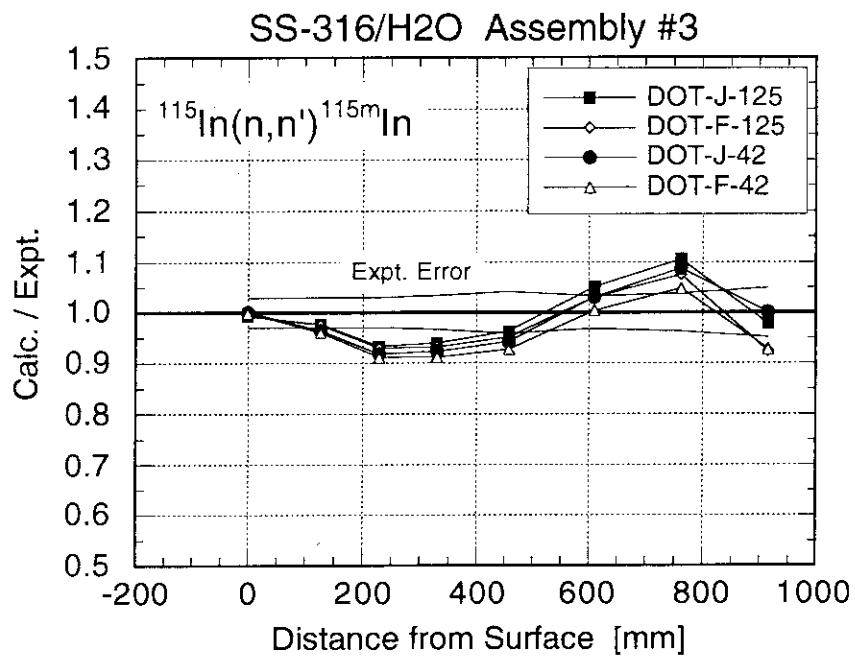


Fig. 3.13 The C/E ratios of the $^{115}\text{In}(n,n')$ $^{115\text{m}}\text{In}$ reaction rate for four different DOT calculations.

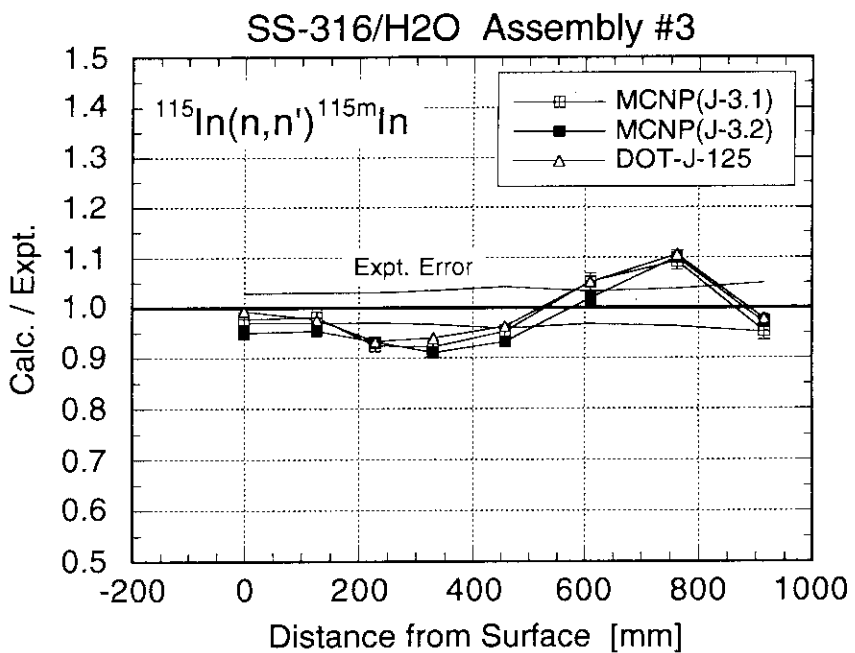


Fig. 3.14 The C/E ratios of the $^{115}\text{In}(n,n')$ $^{115\text{m}}\text{In}$ reaction rate for MCNP and DOT calculations.

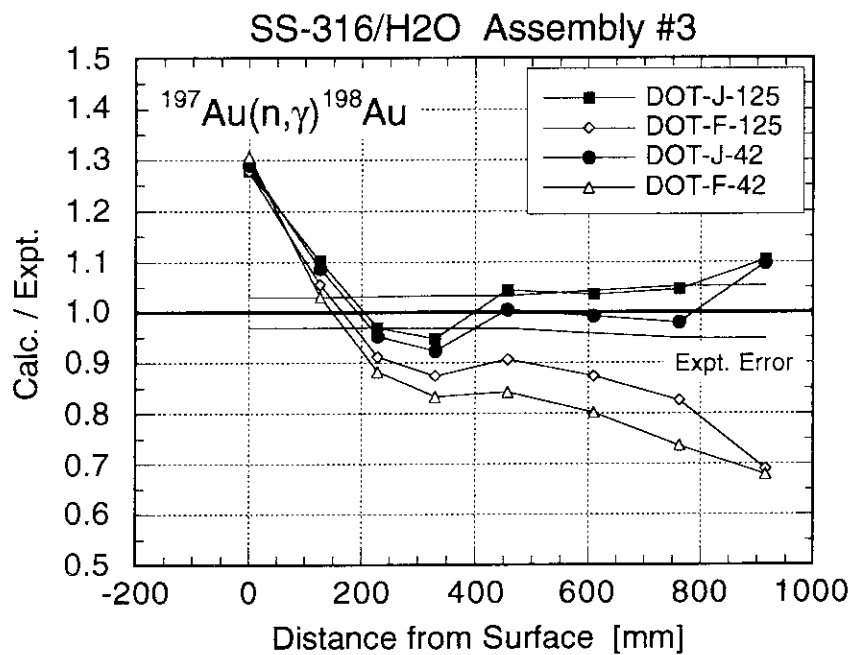


Fig. 3.15 The C/E ratios of the $^{197}\text{Au}(n,\gamma)^{198}\text{Au}$ reaction rate for four different DOT calculations.

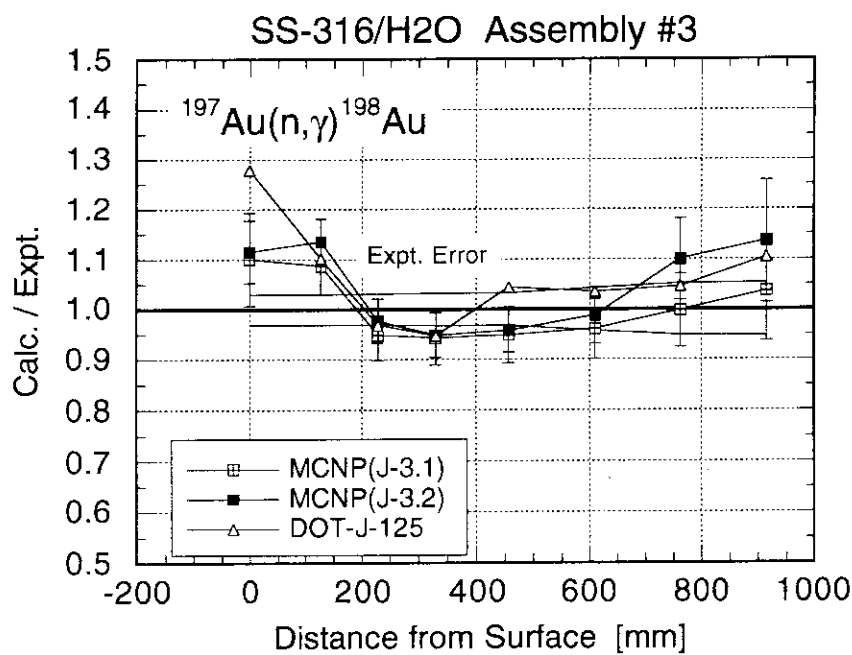


Fig. 3.16 The C/E ratios of the $^{197}\text{Au}(n,\gamma)^{198}\text{Au}$ reaction rate for MCNP and DOT calculations.

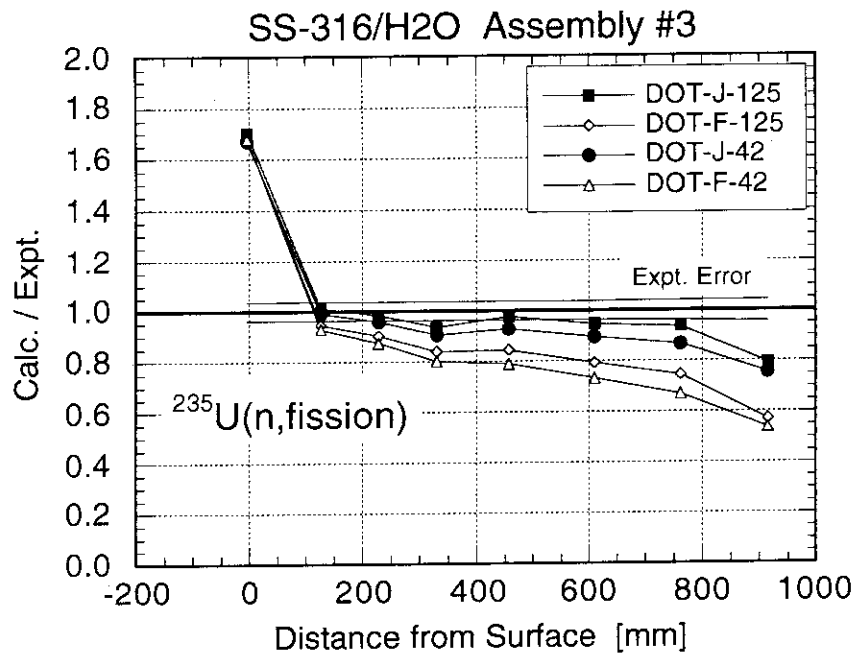


Fig. 3.17 The C/E ratios of the $^{235}\text{U}(\text{n},\text{fission})$ reaction rate for four different DOT calculations.

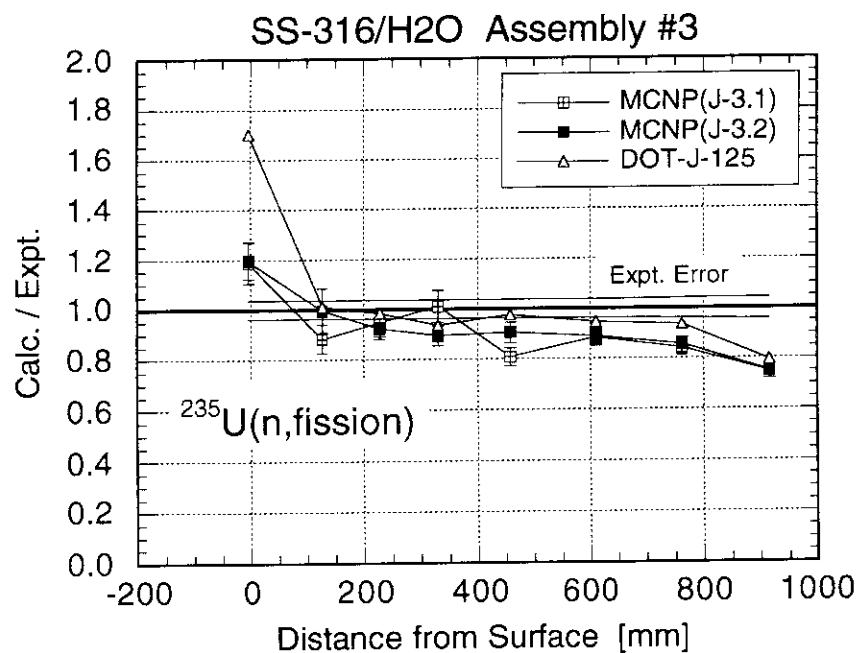


Fig. 3.18 The C/E ratios of the $^{235}\text{U}(\text{n},\text{fission})$ reaction rate for MCNP and DOT calculations.

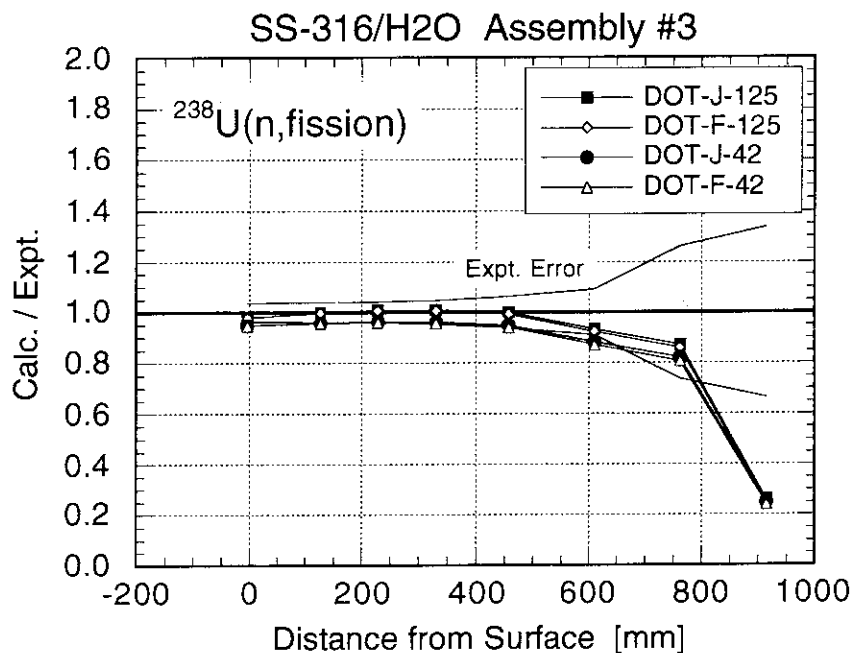


Fig. 3.19 The C/E ratios of the $^{238}\text{U}(\text{n,fission})$ reaction rate for four different DOT calculations.

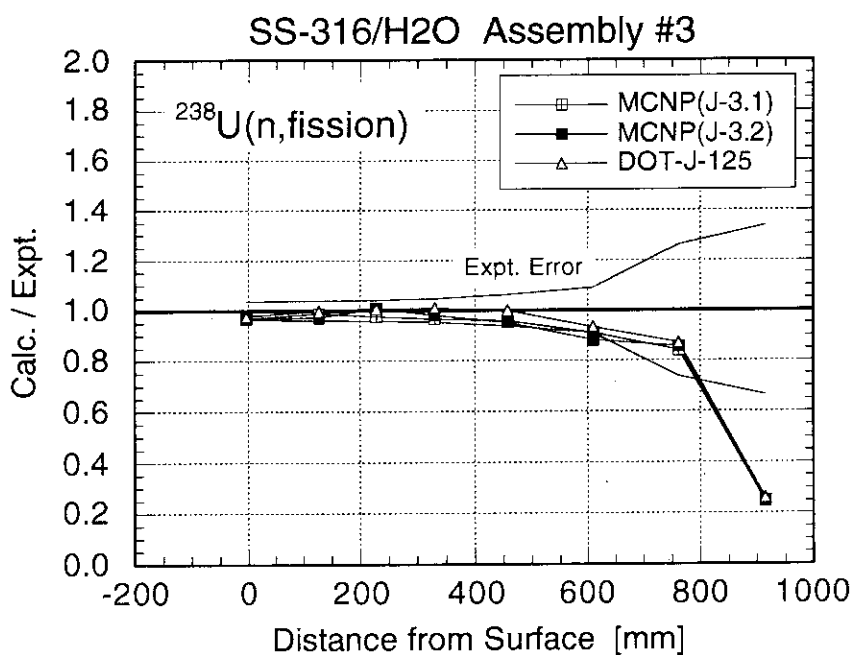


Fig. 3.20 The C/E ratios of the $^{238}\text{U}(\text{n,fission})$ reaction rate for MCNP and DOT calculations.

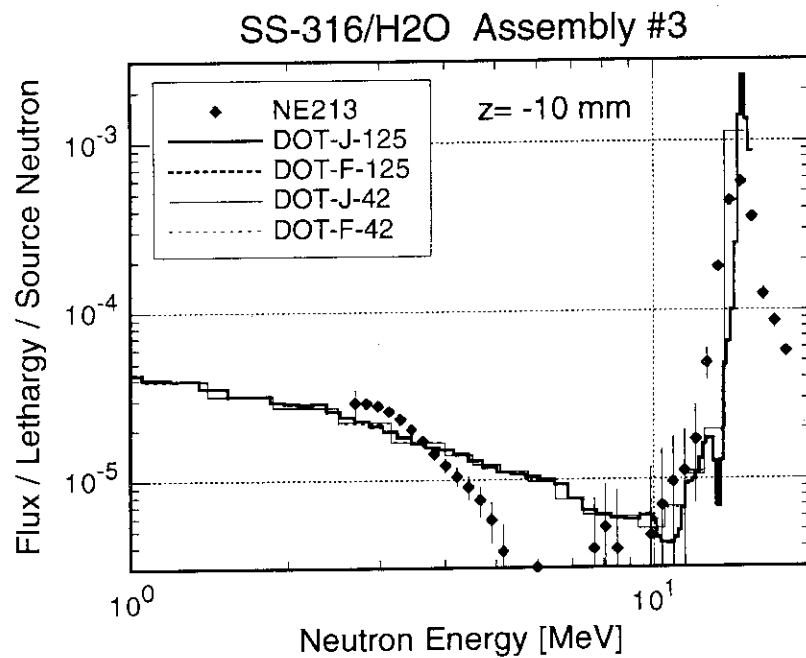


Fig. 3.21 The measured neutron spectra in MeV energy region at the front surface of the assembly in comparisons with four different DOT calculations.

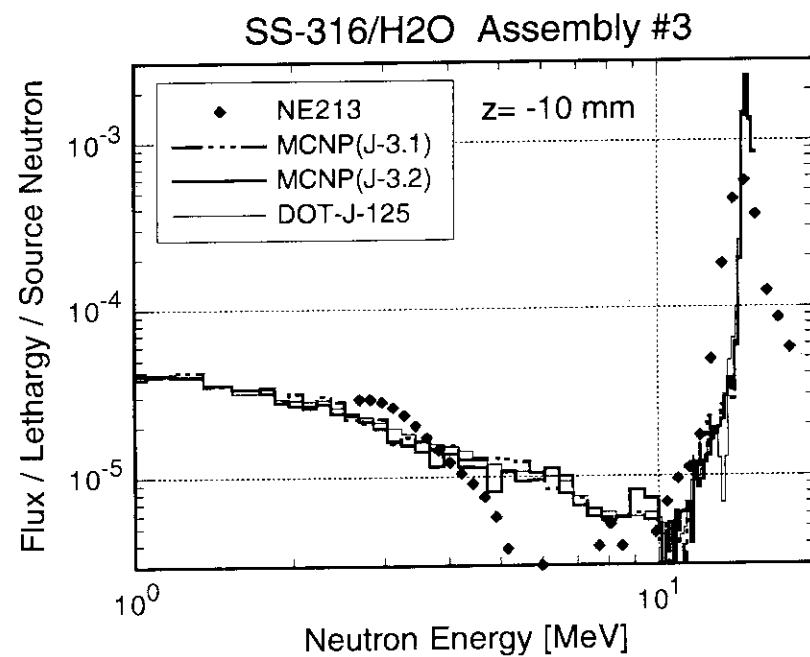


Fig. 3.22 The measured neutron spectra in MeV energy region at the front surface of the assembly in comparisons with MCNP and DOT calculations.

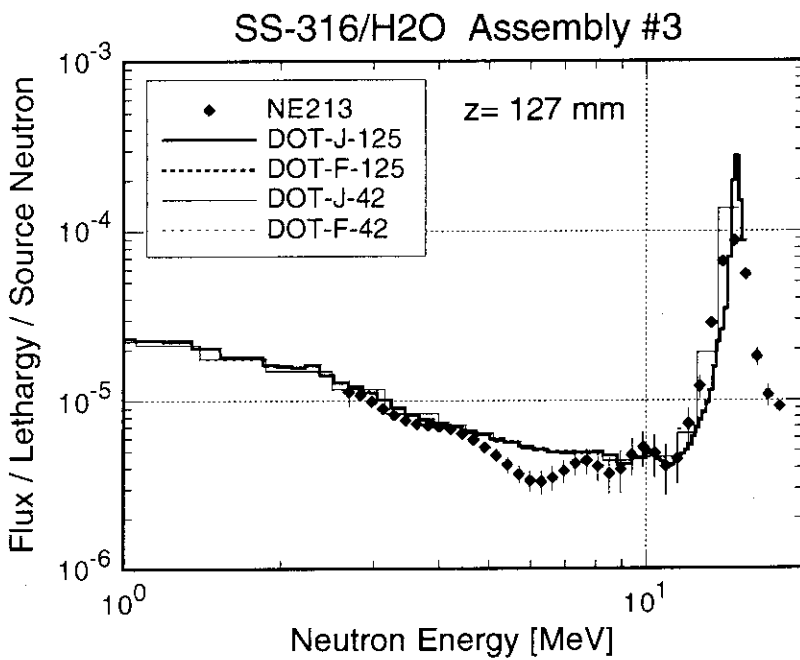


Fig. 3.23 The measured neutron spectra in MeV energy region at 127 mm depth in comparisons with four different DOT calculations.

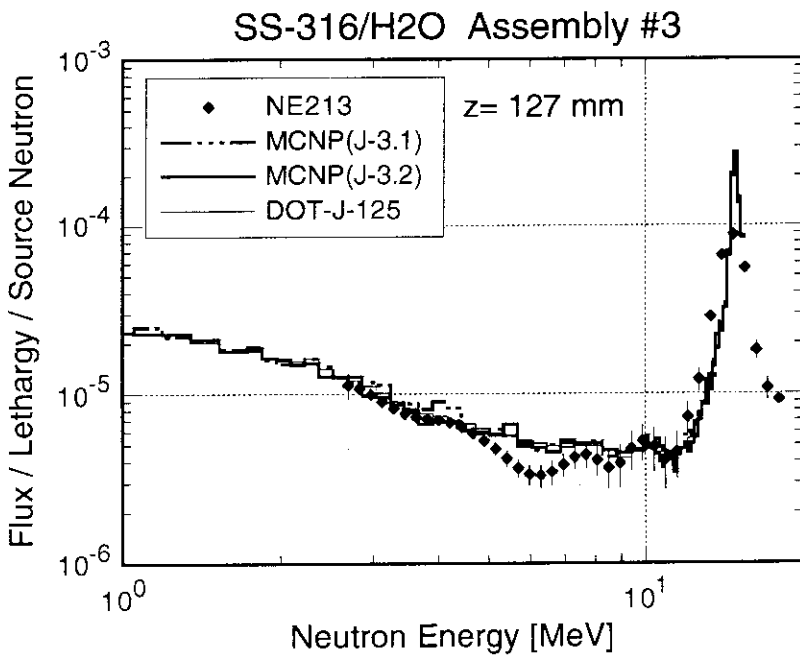


Fig. 3.24 The measured neutron spectra in MeV energy region at 127 mm depth in comparisons with MCNP and DOT calculations.

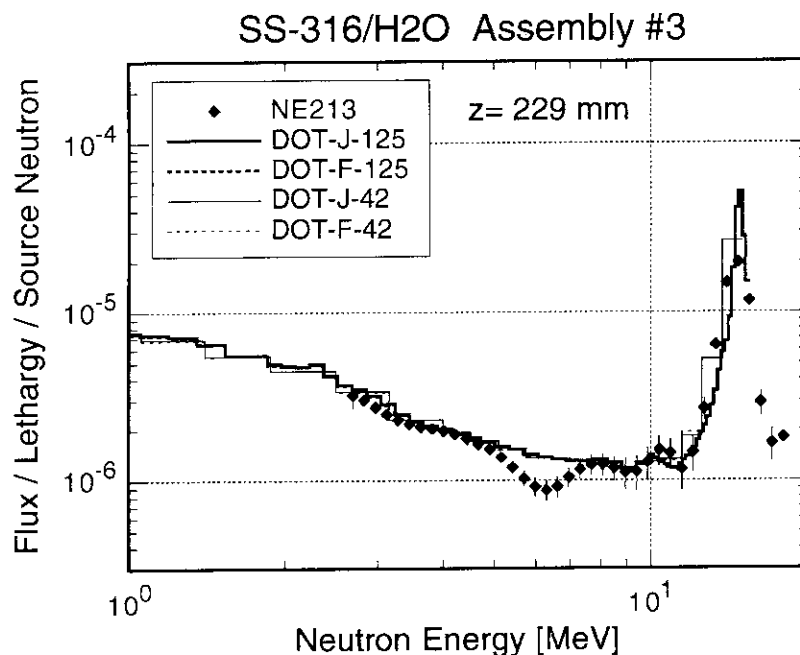


Fig. 3.25 The measured neutron spectra in MeV energy region at 229 mm depth in comparisons with four different DOT calculations.

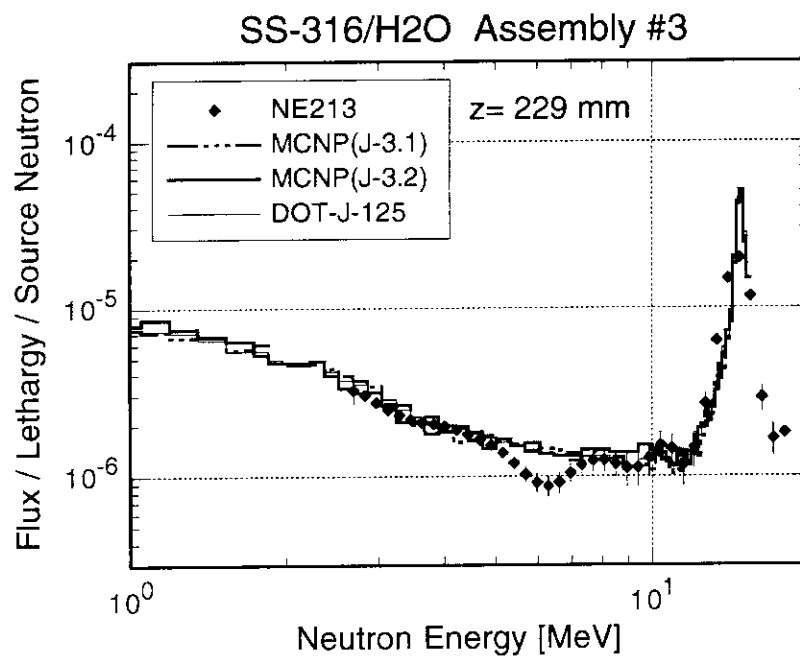


Fig. 3.26 The measured neutron spectra in MeV energy region at 229 mm depth in comparisons with MCNP and DOT calculations.

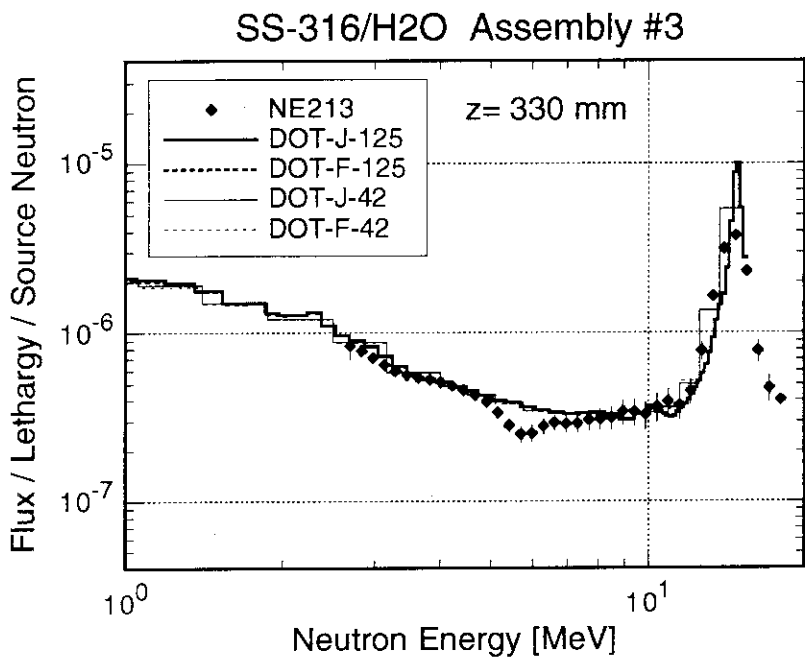


Fig. 3.27 The measured neutron spectra in MeV energy region at 330 mm depth in comparisons with four different DOT calculations.

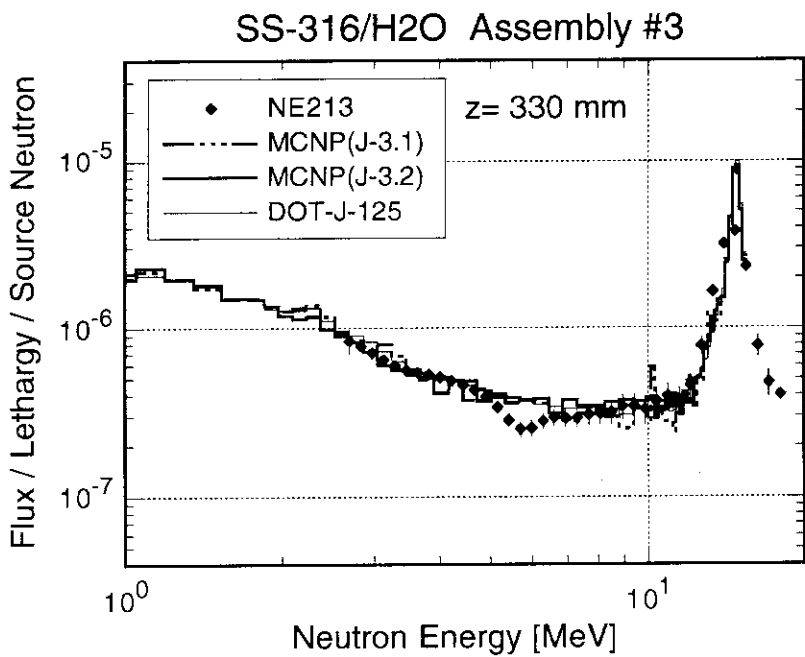


Fig. 3.28 The measured neutron spectra in MeV energy region at 330 mm depth in comparisons with MCNP and DOT calculations.

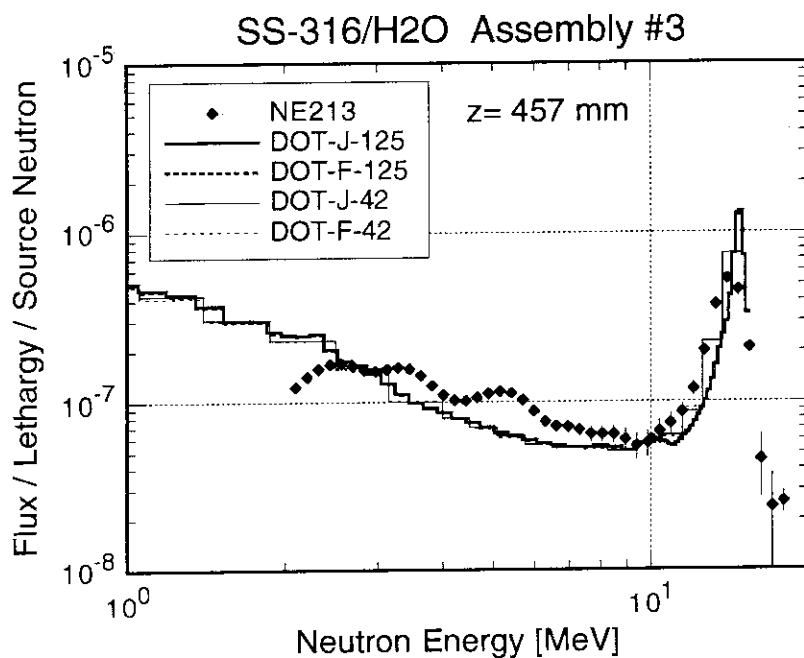


Fig. 3.29 The measured neutron spectra in MeV energy region at 457 mm depth in comparisons with four different DOT calculations.

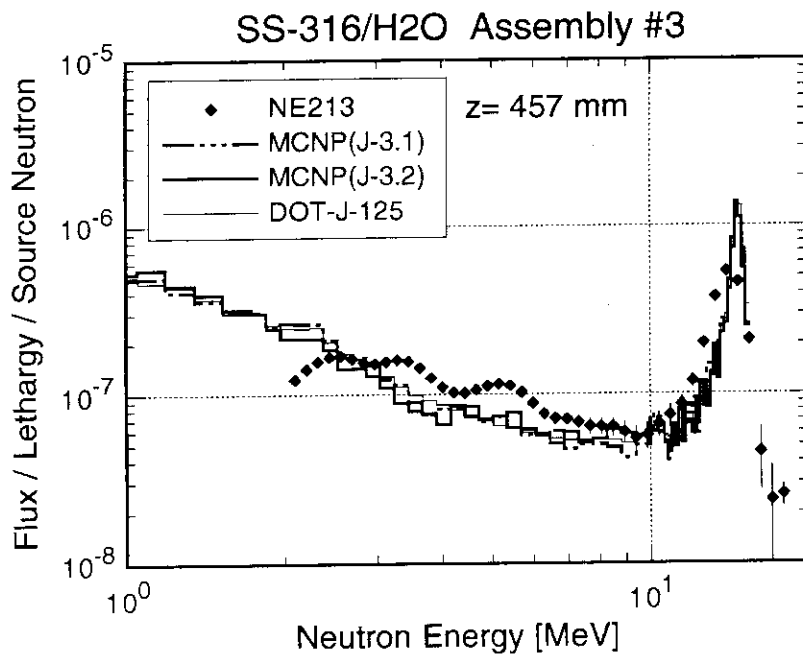


Fig. 3.30 The measured neutron spectra in MeV energy region at 457 mm depth in comparisons with MCNP and DOT calculations.

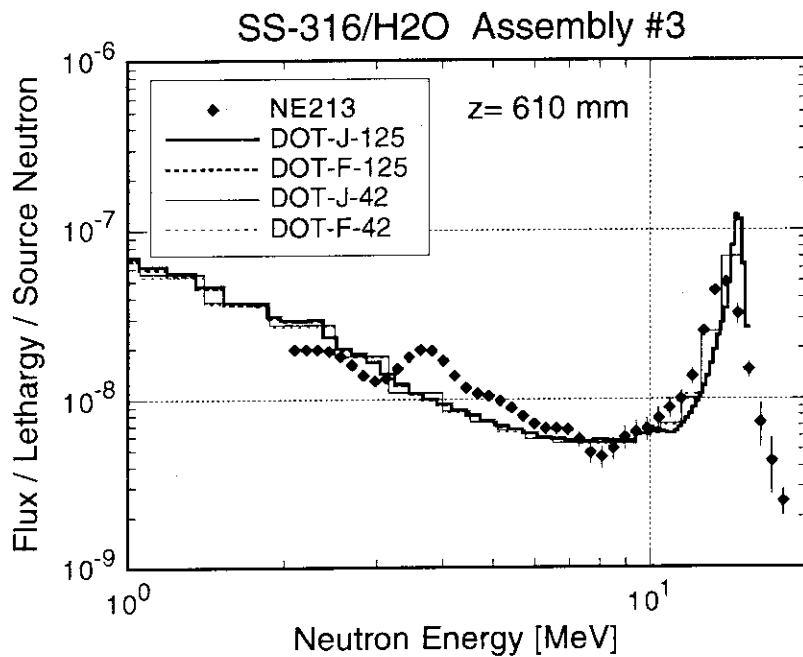


Fig. 3.31 The measured neutron spectra in MeV energy region at 610 mm depth in comparisons with four different DOT calculations.

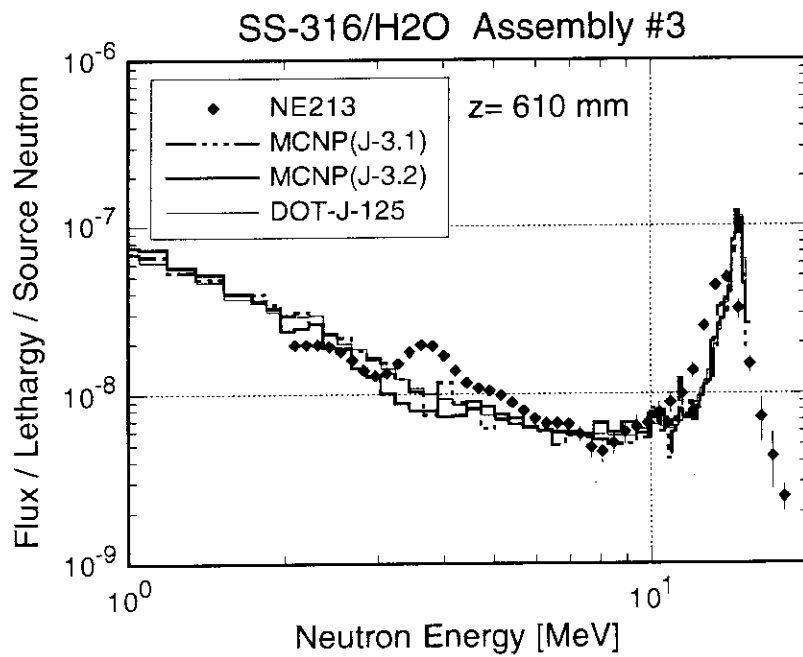


Fig. 3.32 The measured neutron spectra in MeV energy region at 610 mm depth in comparisons with MCNP and DOT calculations.

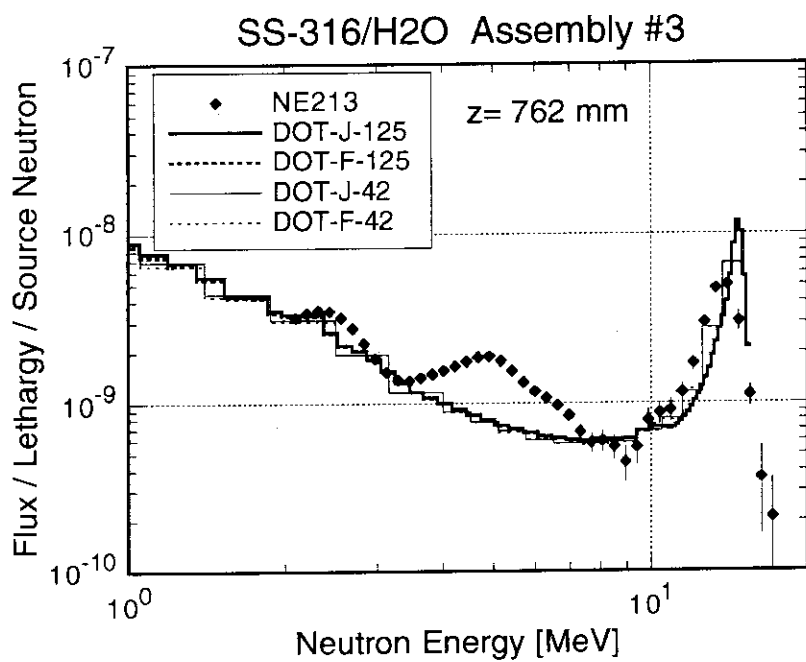


Fig. 3.33 The measured neutron spectra in MeV energy region at 762 mm depth in comparisons with four different DOT calculations.

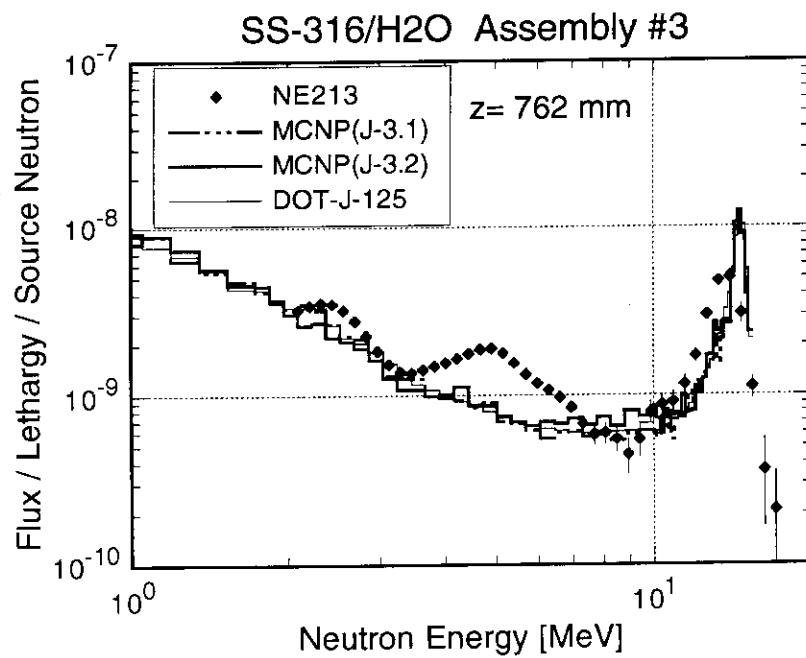


Fig. 3.34 The measured neutron spectra in MeV energy region at 762 mm depth in comparisons with MCNP and DOT calculations.

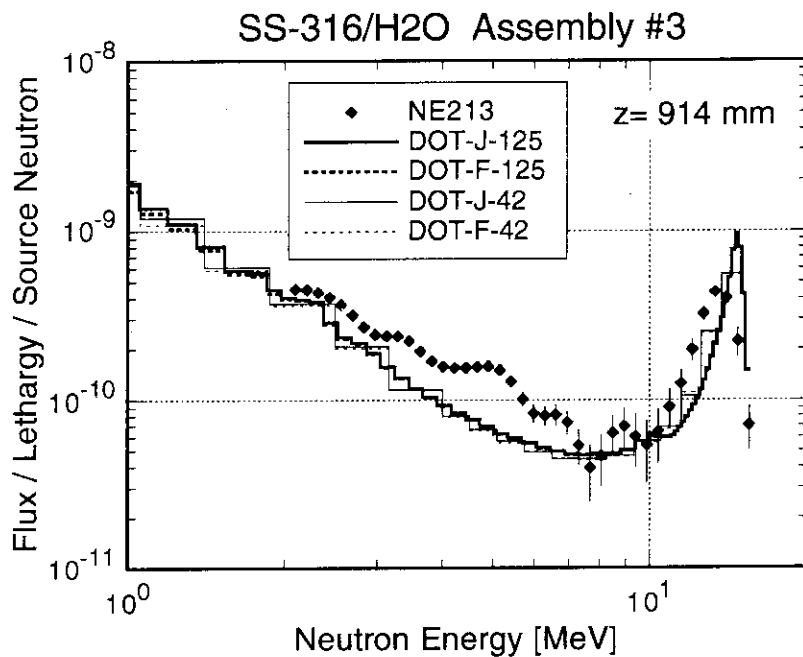


Fig. 3.35 The measured neutron spectra in MeV energy region at 914 mm depth in comparisons with four different DOT calculations.

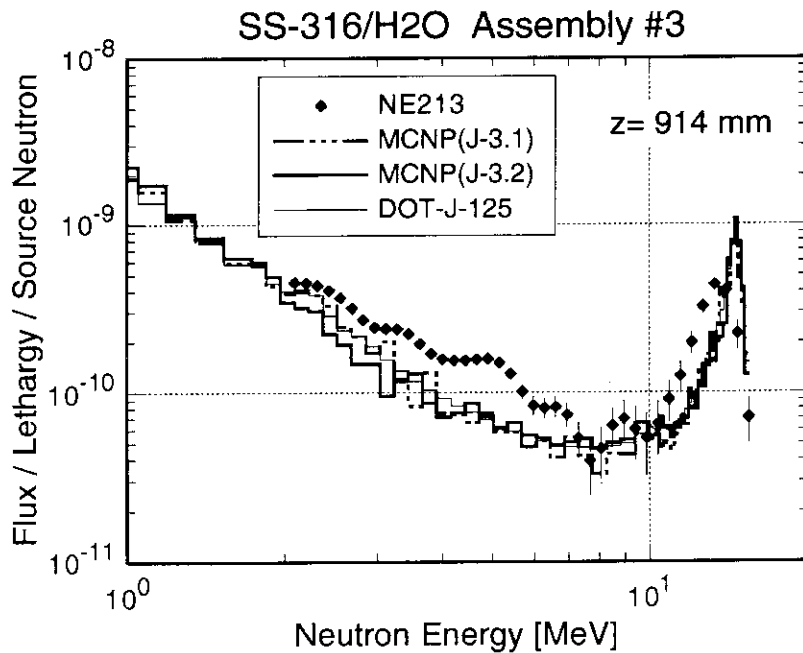


Fig. 3.36 The measured neutron spectra in MeV energy region at 914 mm depth in comparisons with MCNP and DOT calculations.

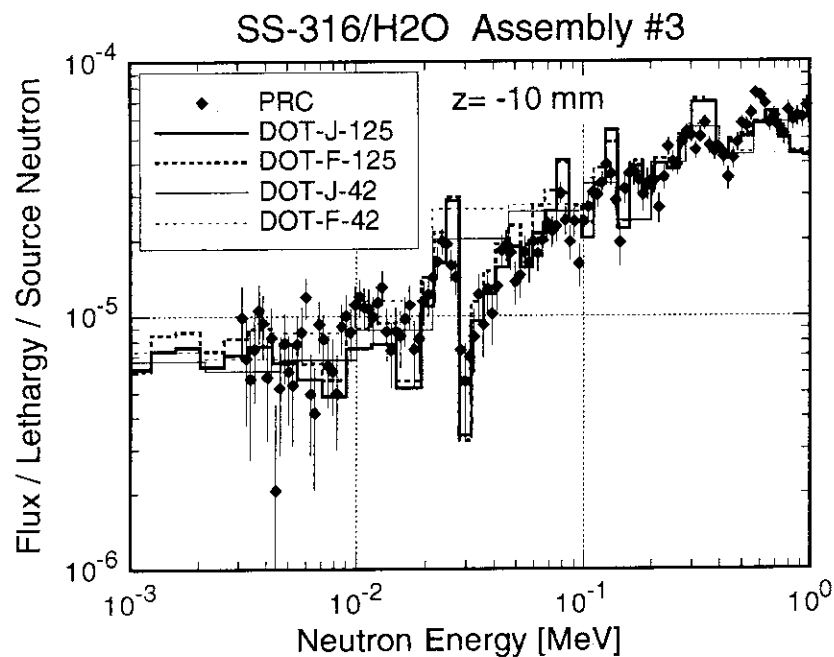


Fig. 3.37 The measured neutron spectra in keV energy region at the front surface of the assembly in comparisons with four different DOT calculations.

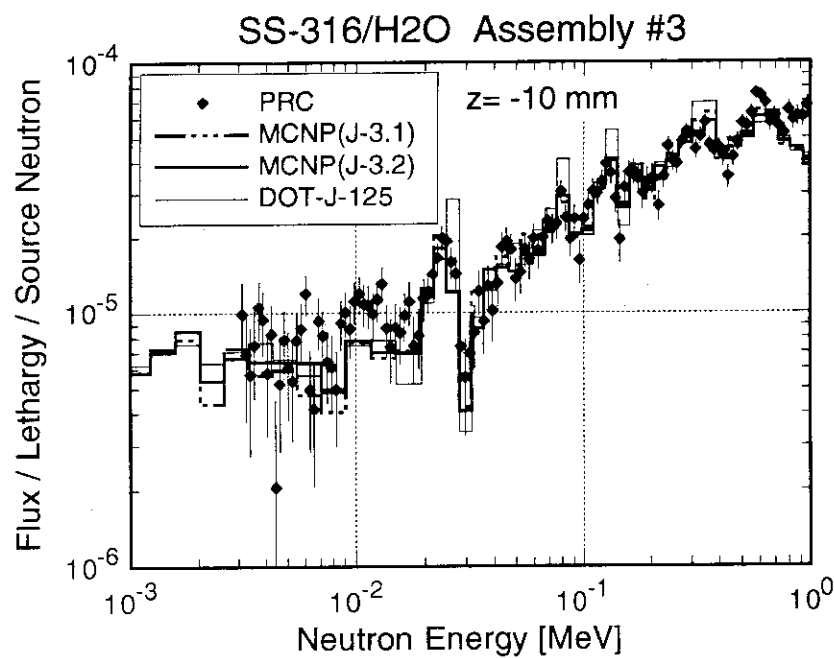


Fig. 3.38 The measured neutron spectra in keV energy region at the front surface of the assembly in comparisons with MCNP and DOT calculations.

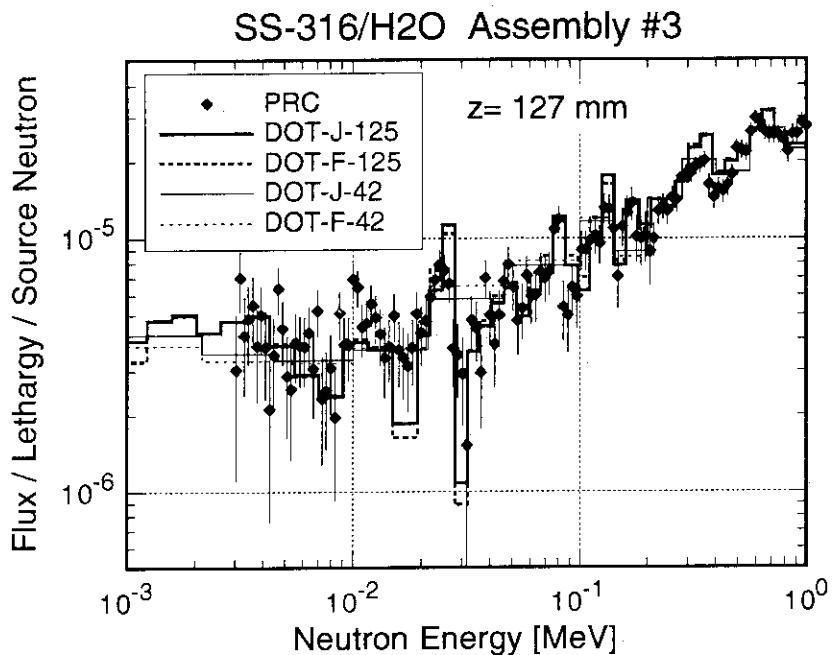


Fig. 3.39 The measured neutron spectra in keV energy region at 127 mm depth in comparisons with four different DOT calculations.

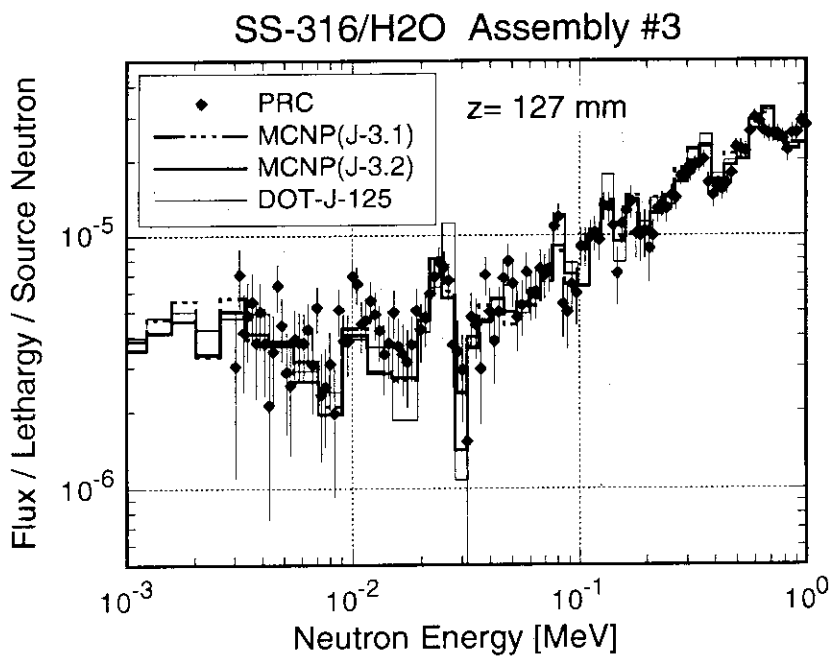


Fig. 3.40 The measured neutron spectra in keV energy region at 127 mm depth in comparisons with MCNP and DOT calculations.

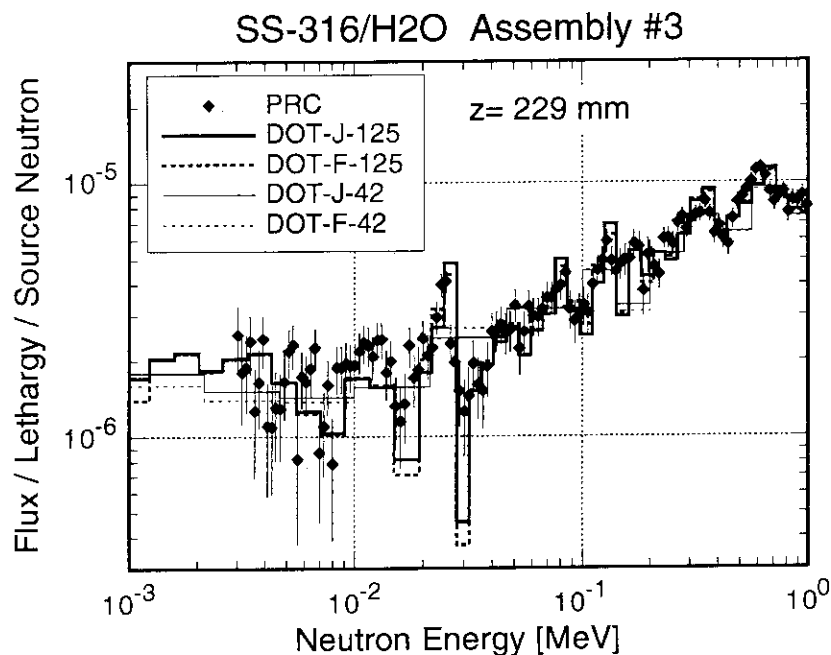


Fig. 3.41 The measured neutron spectra in keV energy region at 229 mm depth in comparisons with four different DOT calculations.

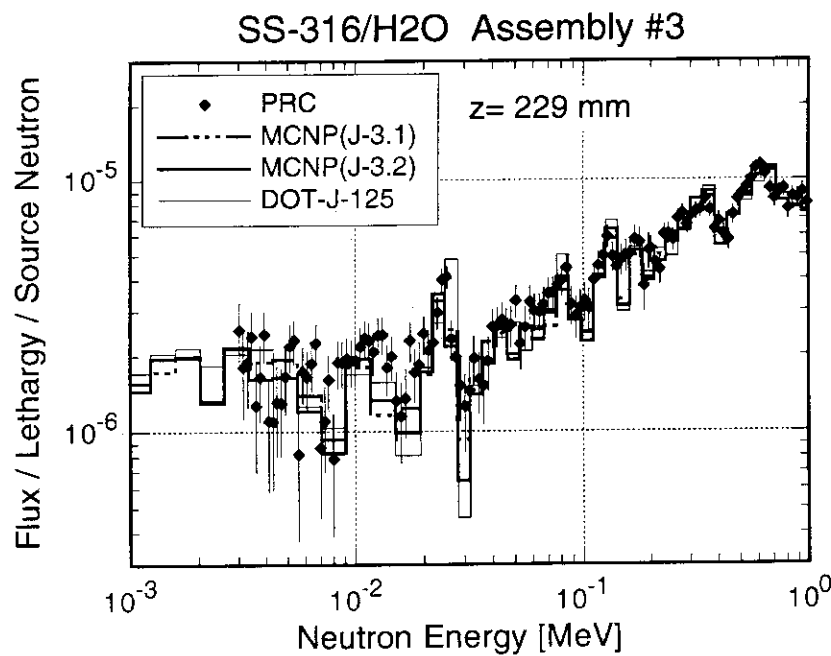


Fig. 3.42 The measured neutron spectra in keV energy region at 229 mm depth in comparisons with MCNP and DOT calculations.

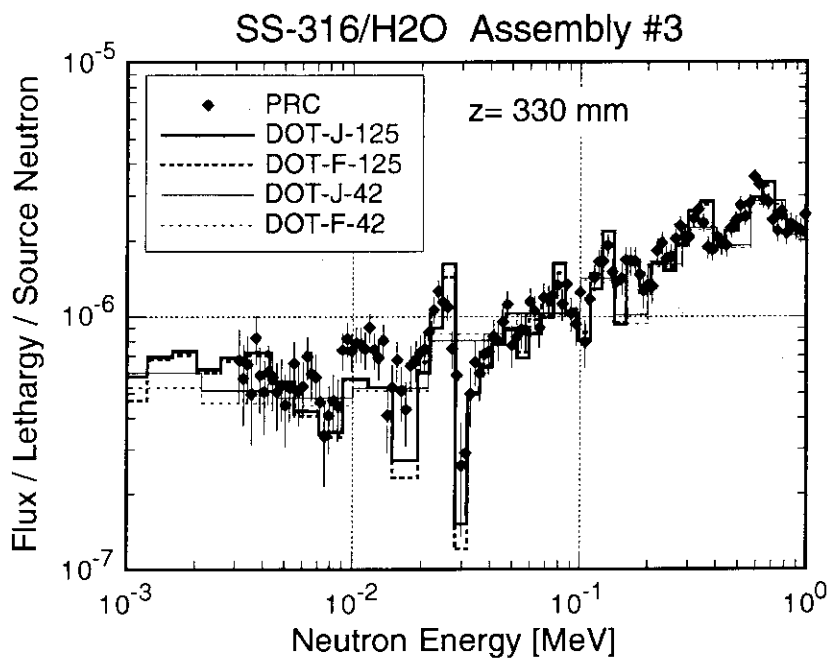


Fig. 3.43 The measured neutron spectra in keV energy region at 330 mm depth in comparisons with four different DOT calculations.

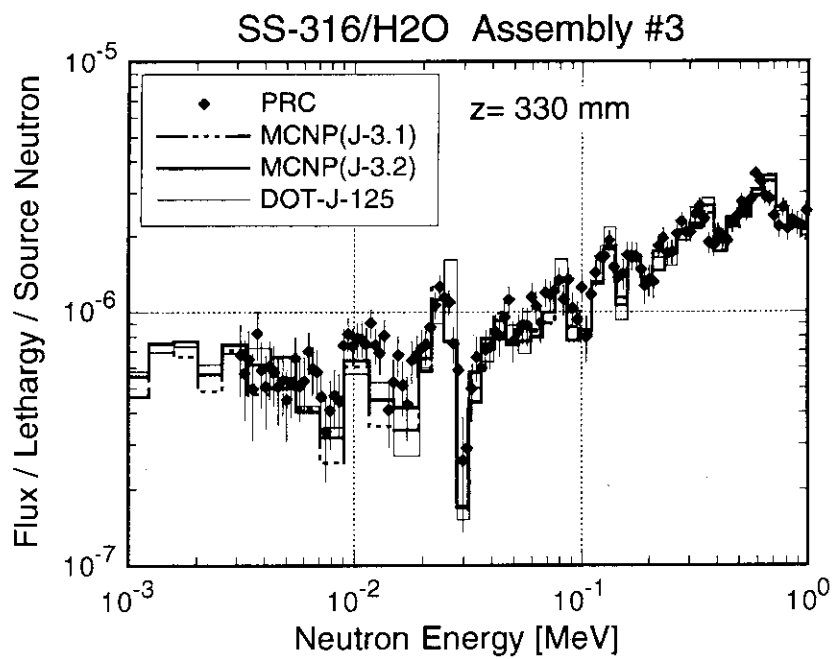


Fig. 3.44 The measured neutron spectra in keV energy region at 330 mm depth in comparisons with MCNP and DOT calculations.

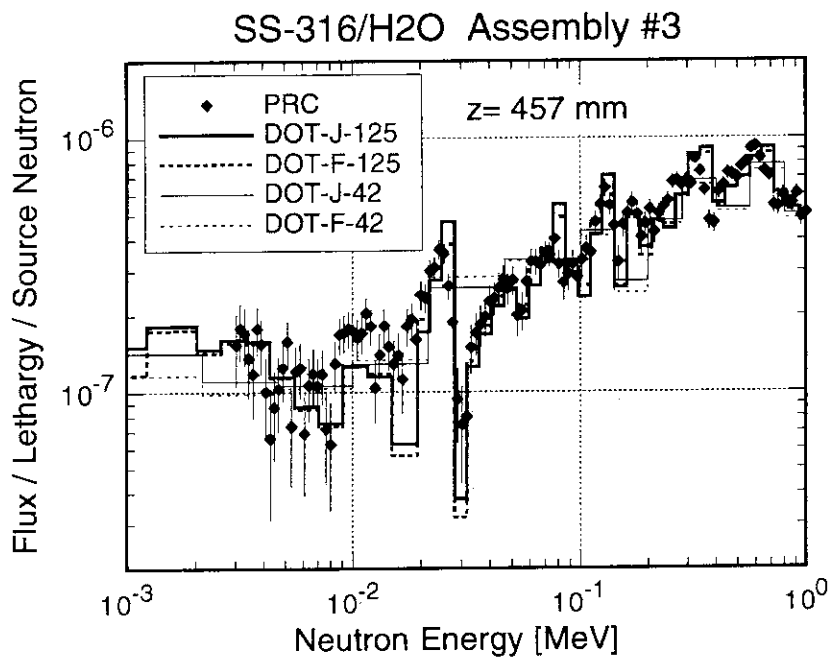


Fig. 3.45 The measured neutron spectra in keV energy region at 457 mm depth in comparisons with four different DOT calculations.

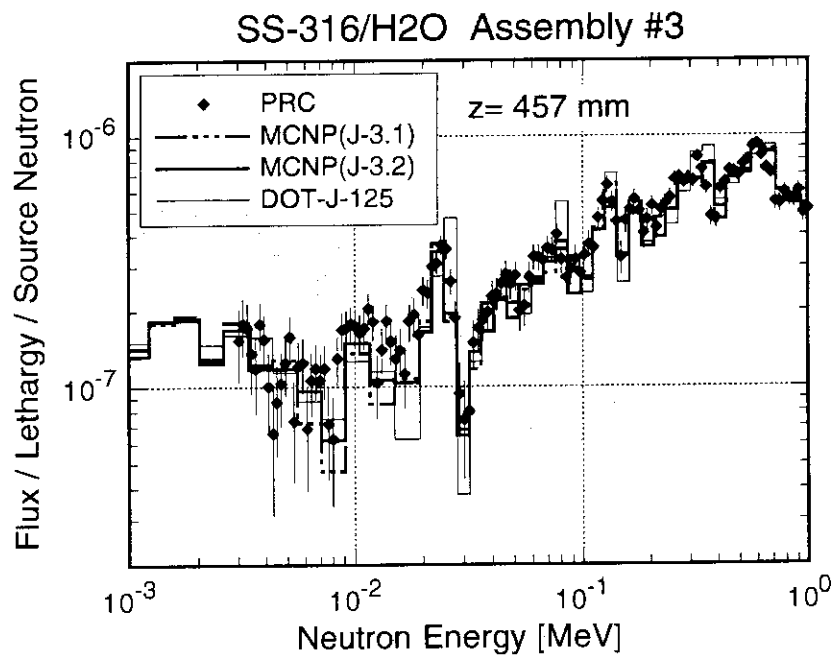


Fig. 3.46 The measured neutron spectra in keV energy region at 457 mm depth in comparisons with MCNP and DOT calculations.

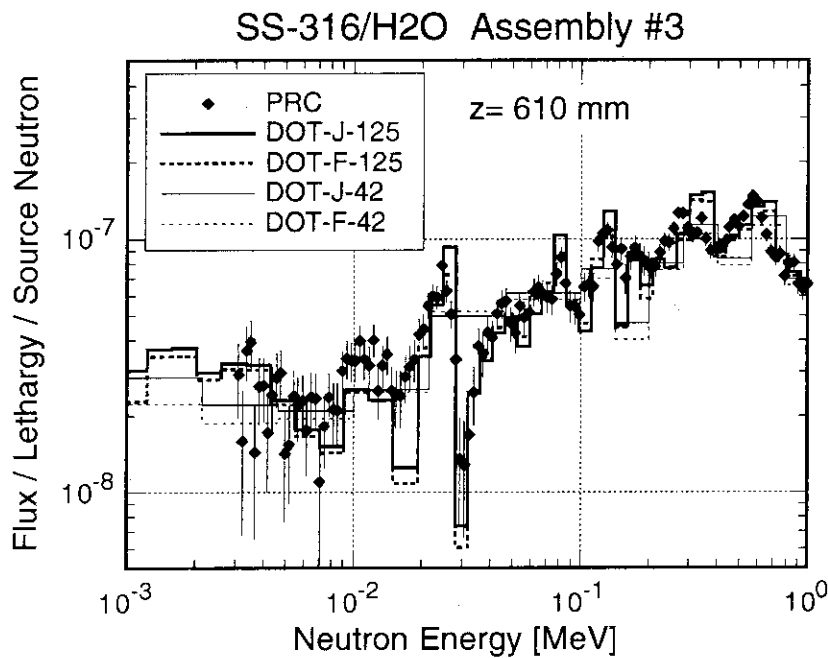


Fig. 3.47 The measured neutron spectra in keV energy region at 610 mm depth in comparisons with four different DOT calculations.

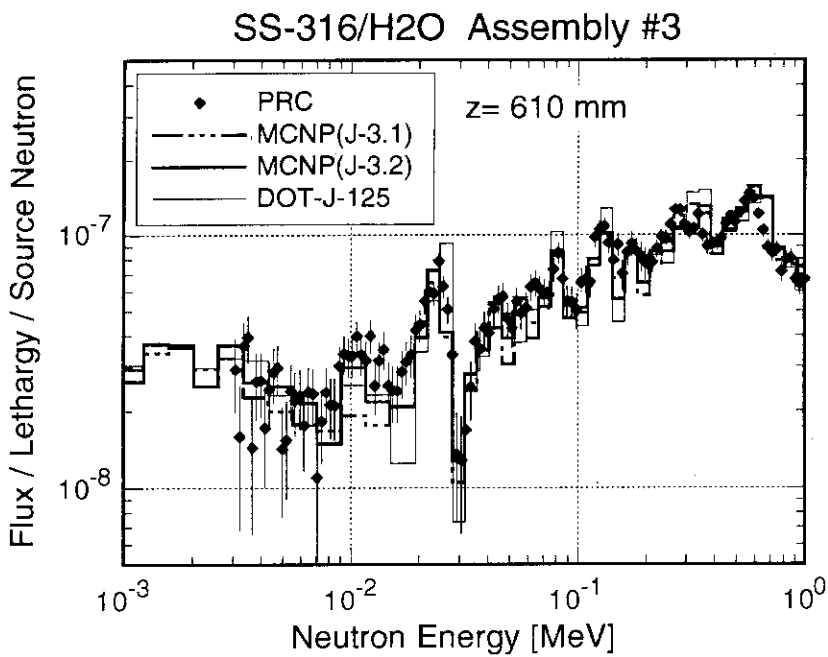


Fig. 3.48 The measured neutron spectra in keV energy region at 610 mm depth in comparisons with MCNP and DOT calculations.

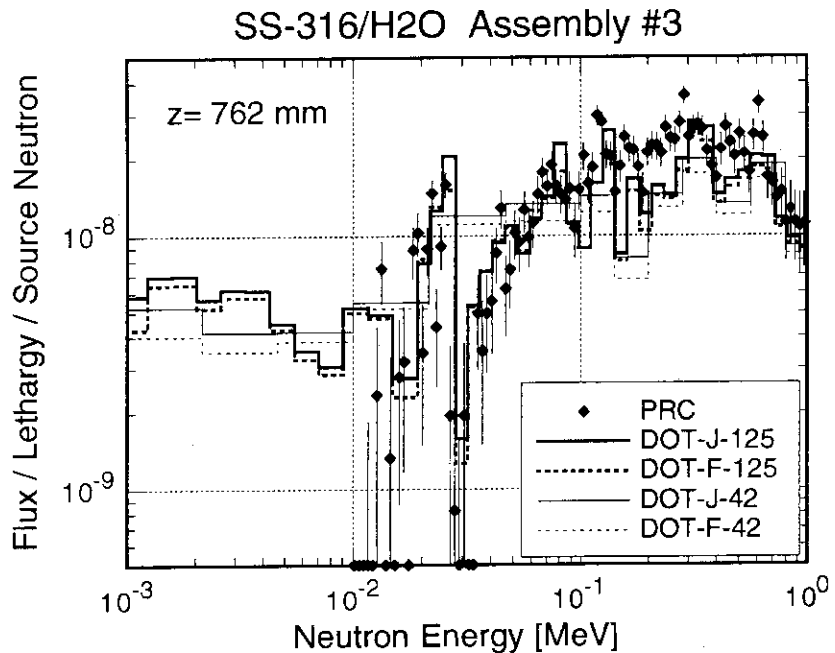


Fig. 3.49 The measured neutron spectra in keV energy region at 762 mm depth in comparisons with four different DOT calculations.

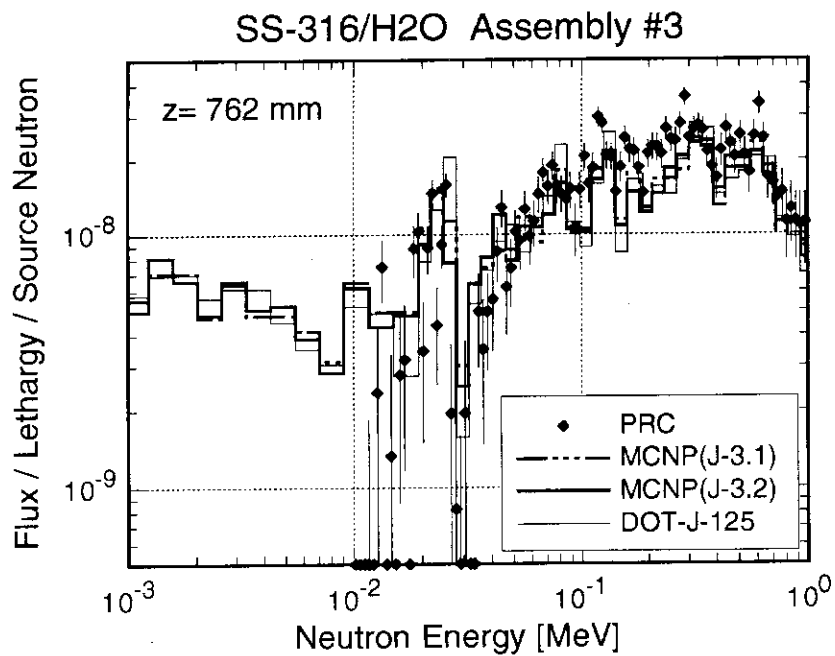


Fig. 3.50 The measured neutron spectra in keV energy region at 762 mm depth in comparisons with MCNP and DOT calculations.

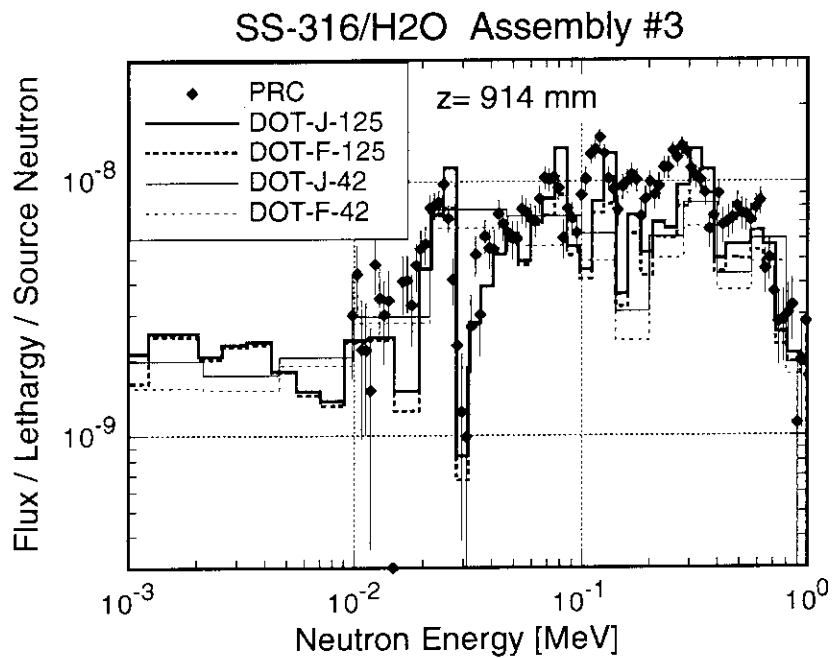


Fig. 3.51 The measured neutron spectra in keV energy region at 914 mm depth in comparisons with four different DOT calculations.

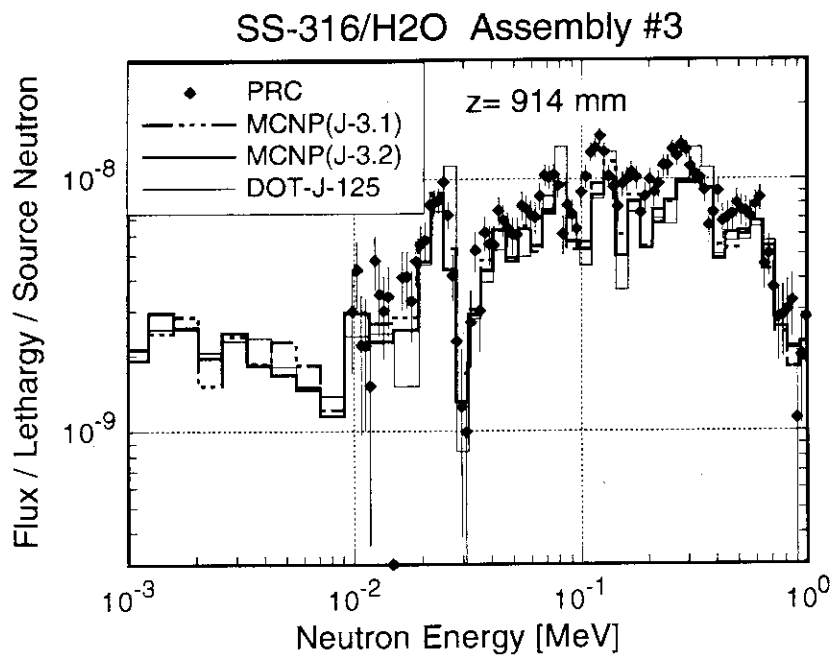


Fig. 3.52 The measured neutron spectra in keV energy region at 914 mm depth in comparisons with MCNP and DOT calculations.

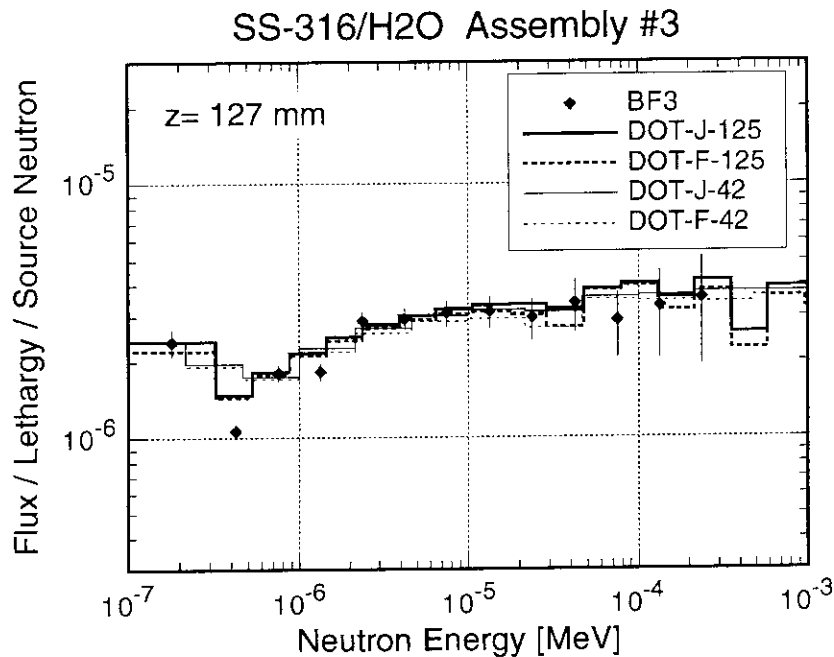


Fig. 3.53 The measured neutron spectra in eV energy region at 127 mm depth in comparisons with four different DOT calculations.

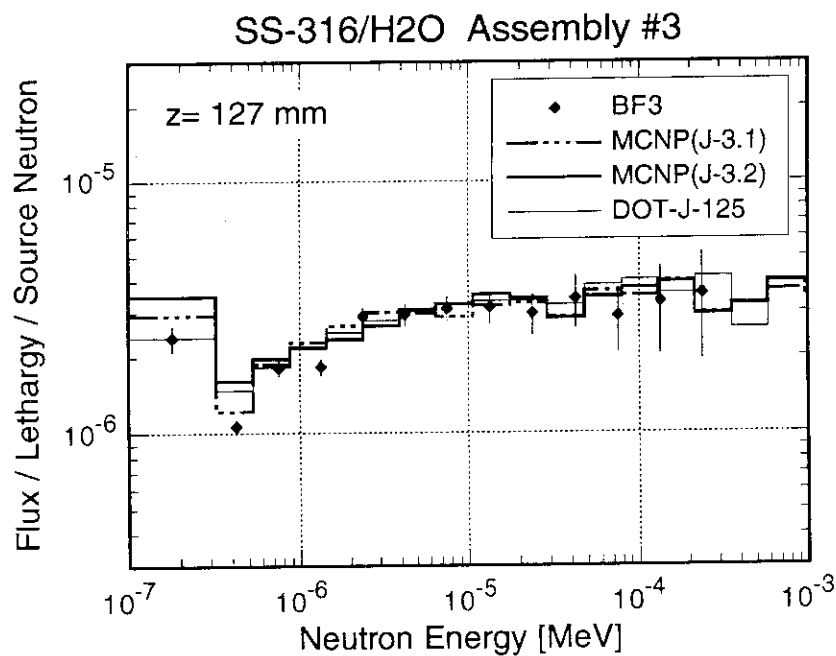


Fig. 3.54 The measured neutron spectra in eV energy region at 127 mm depth in comparisons with MCNP and DOT calculations.

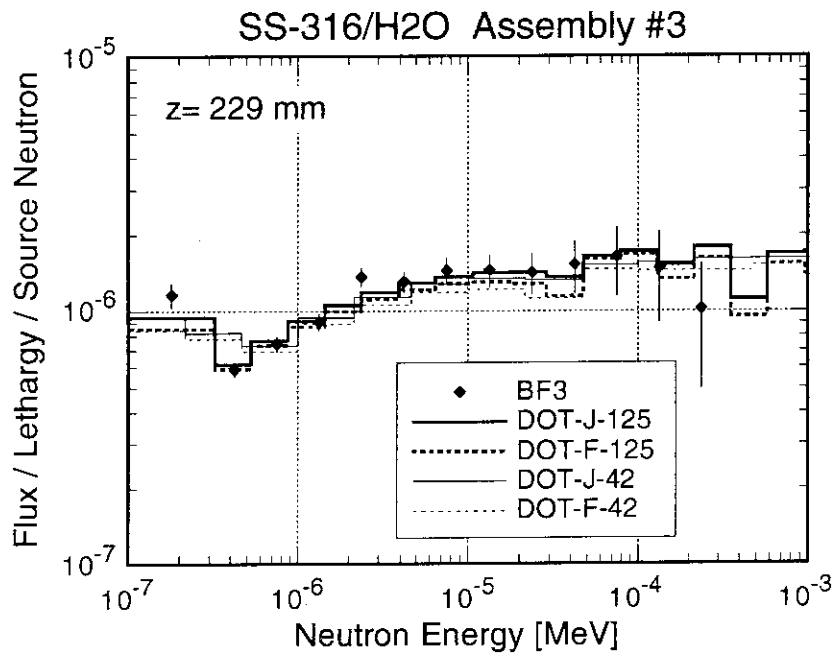


Fig. 3.55 The measured neutron spectra in eV energy region at 229 mm depth in comparisons with four different DOT calculations.

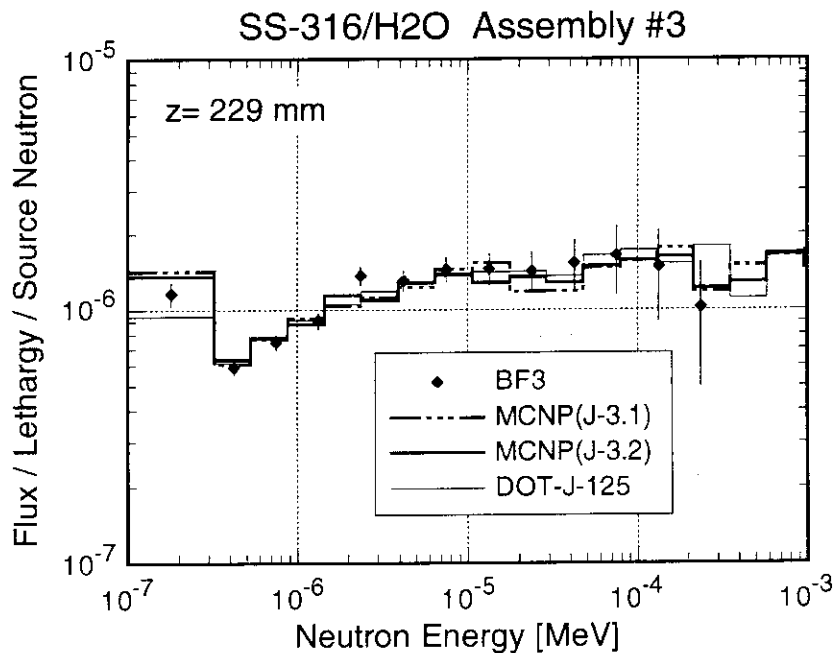


Fig. 3.56 The measured neutron spectra in eV energy region at 229 mm depth in comparisons with MCNP and DOT calculations.

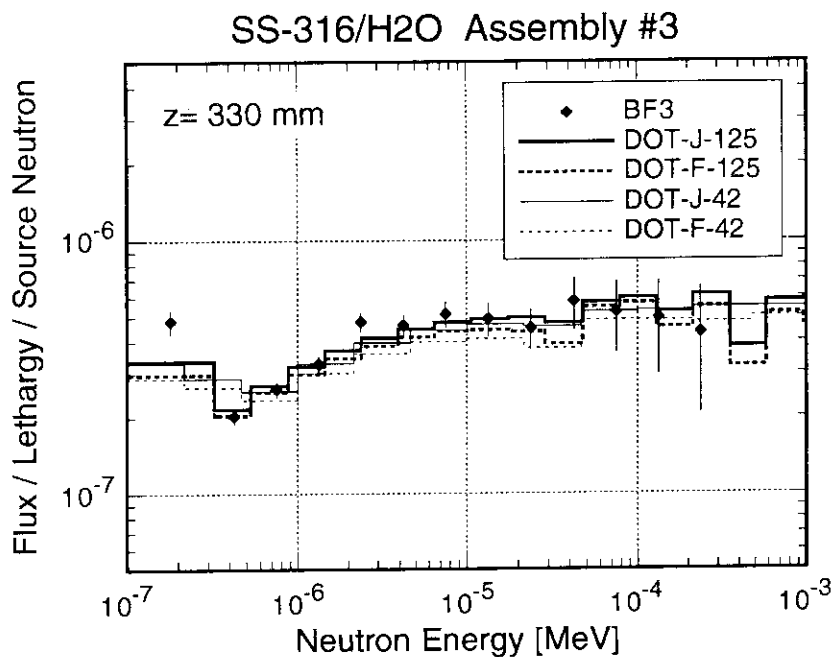


Fig. 3.57 The measured neutron spectra in eV energy region at 330 mm depth in comparisons with four different DOT calculations.

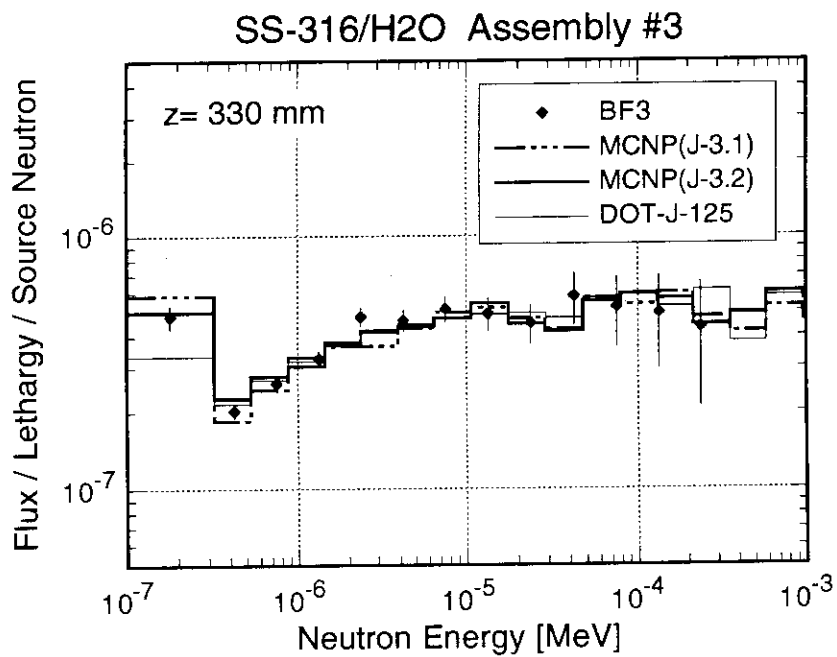


Fig. 3.58 The measured neutron spectra in eV energy region at 330 mm depth in comparisons with MCNP and DOT calculations.

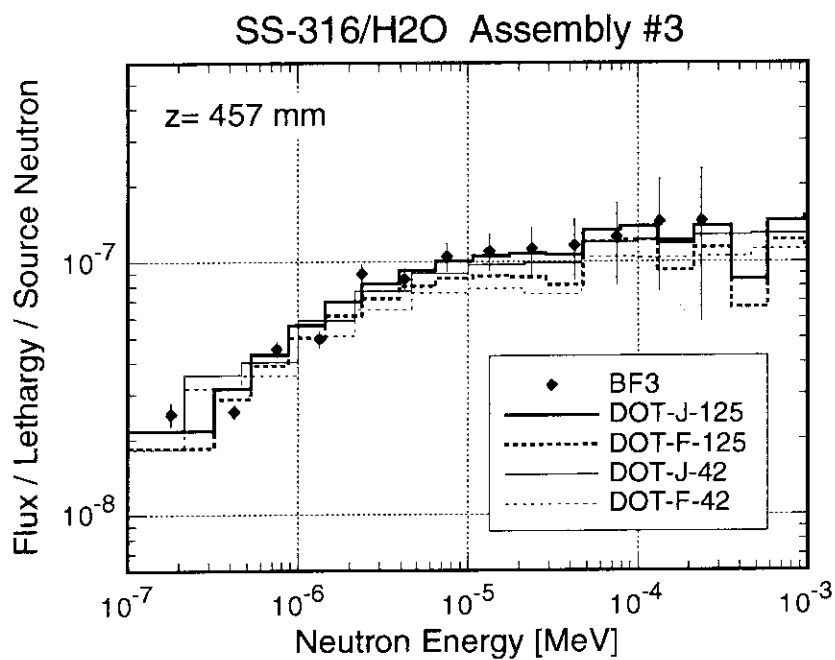


Fig. 3.59 The measured neutron spectra in eV energy region at 457 mm depth in comparisons with four different DOT calculations.

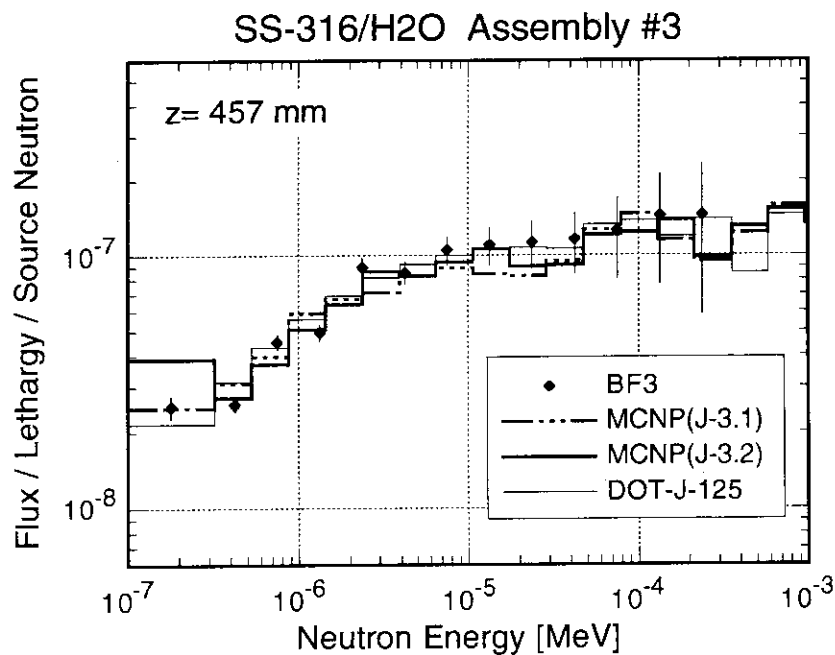


Fig. 3.60 The measured neutron spectra in eV energy region at 457 mm depth in comparisons with MCNP and DOT calculations.

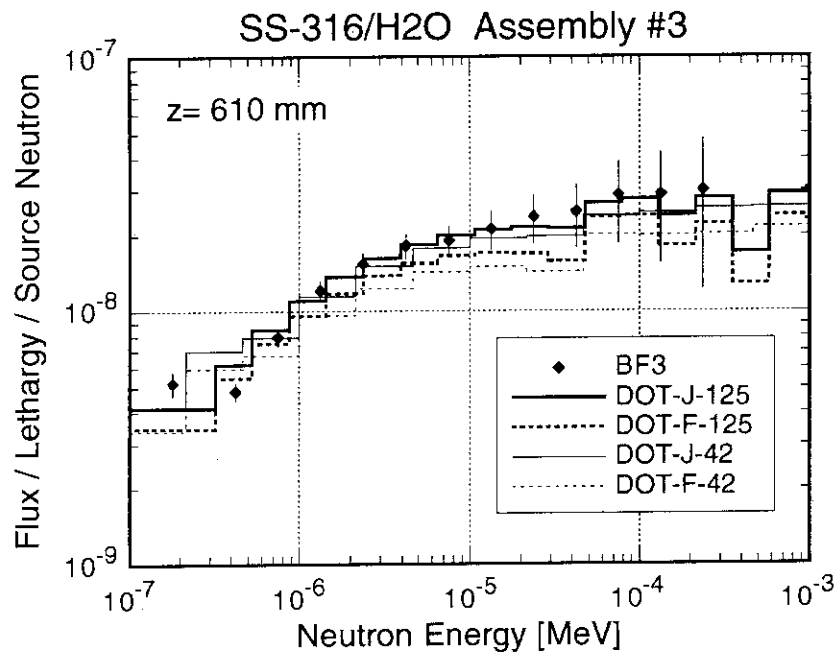


Fig. 3.61 The measured neutron spectra in eV energy region at 610 mm depth in comparisons with four different DOT calculations.

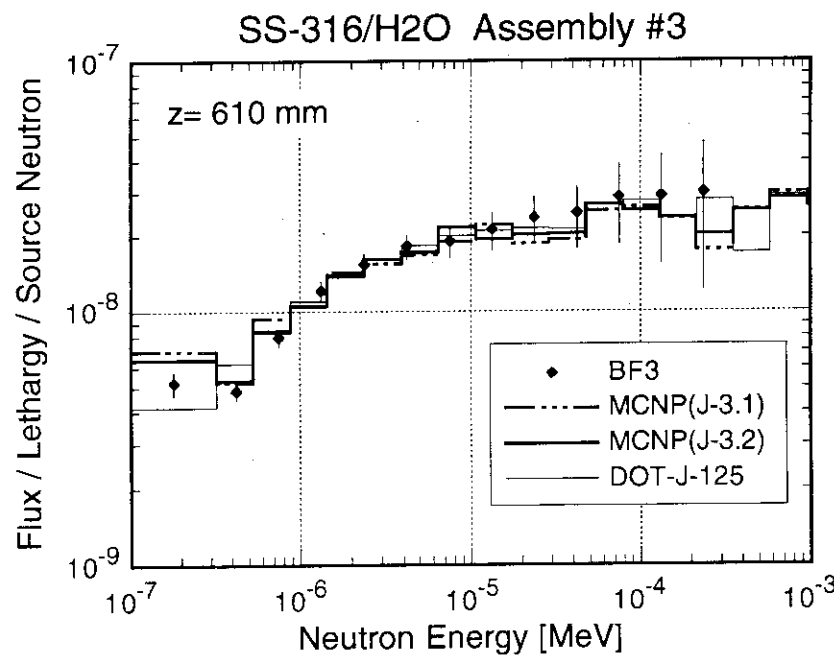


Fig. 3.62 The measured neutron spectra in eV energy region at 610 mm depth in comparisons with MCNP and DOT calculations.

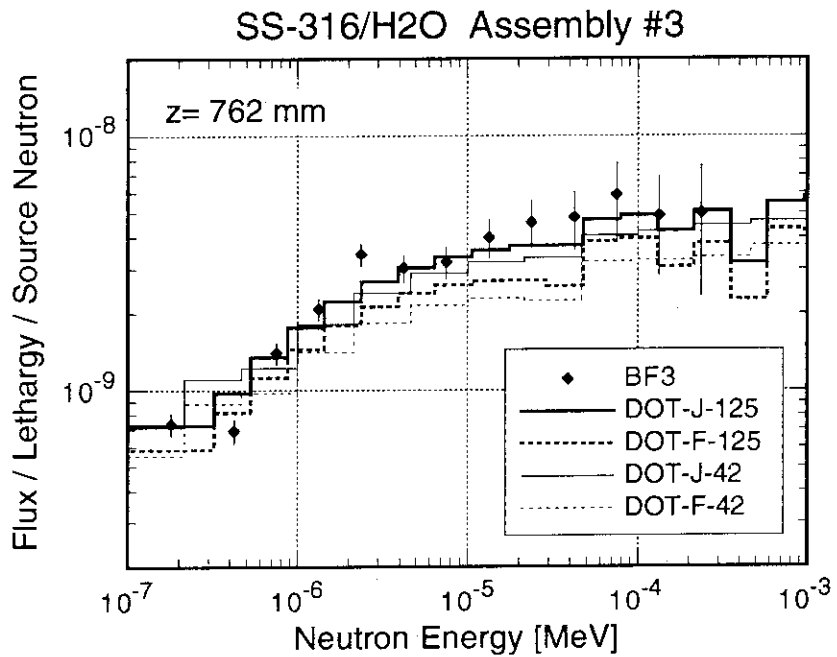


Fig. 3.63 The measured neutron spectra in eV energy region at 762 mm depth in comparisons with four different DOT calculations.

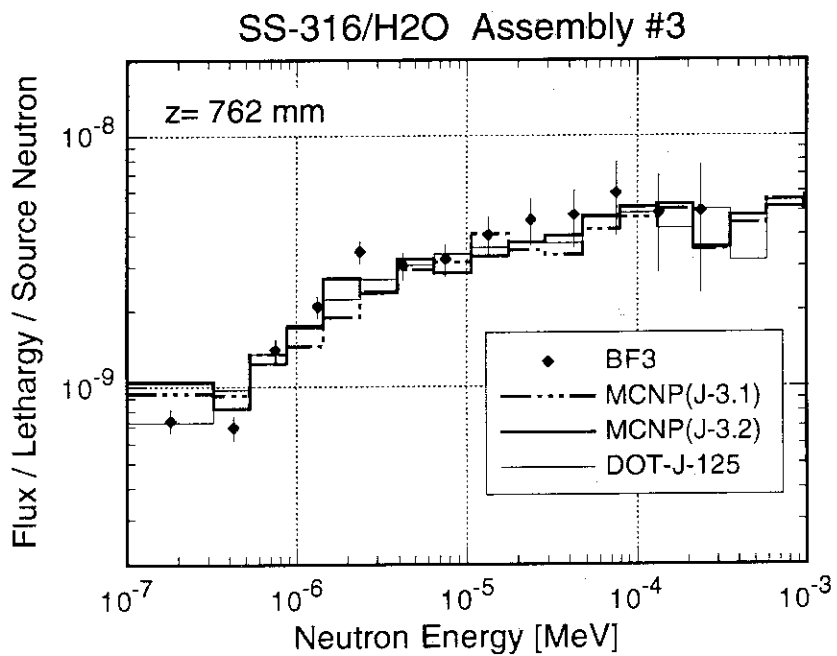


Fig. 3.64 The measured neutron spectra in eV energy region at 762 mm depth in comparisons with MCNP and DOT calculations.

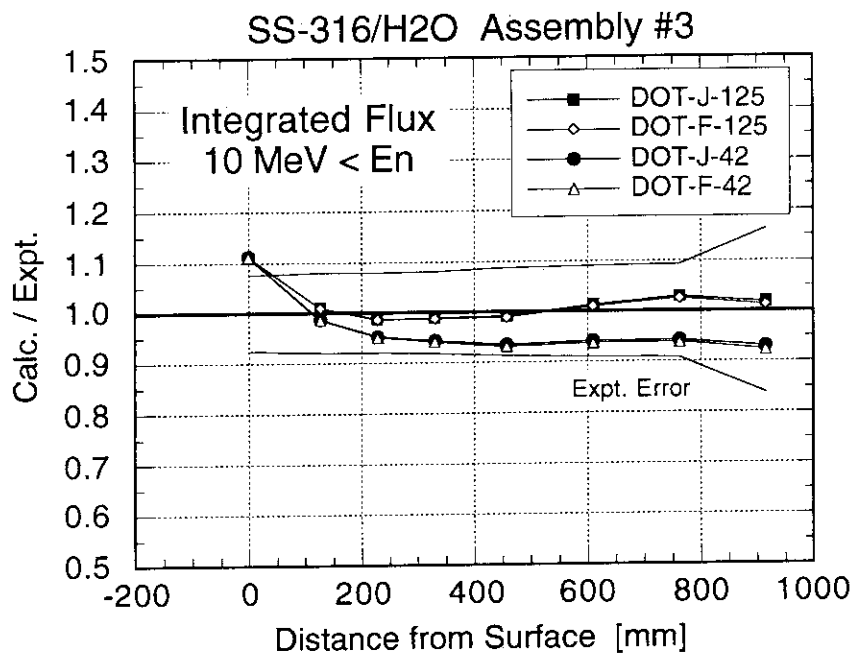


Fig. 3.65 The C/E ratios of the integrated neutron flux above 10 MeV for four different DOT calculations.

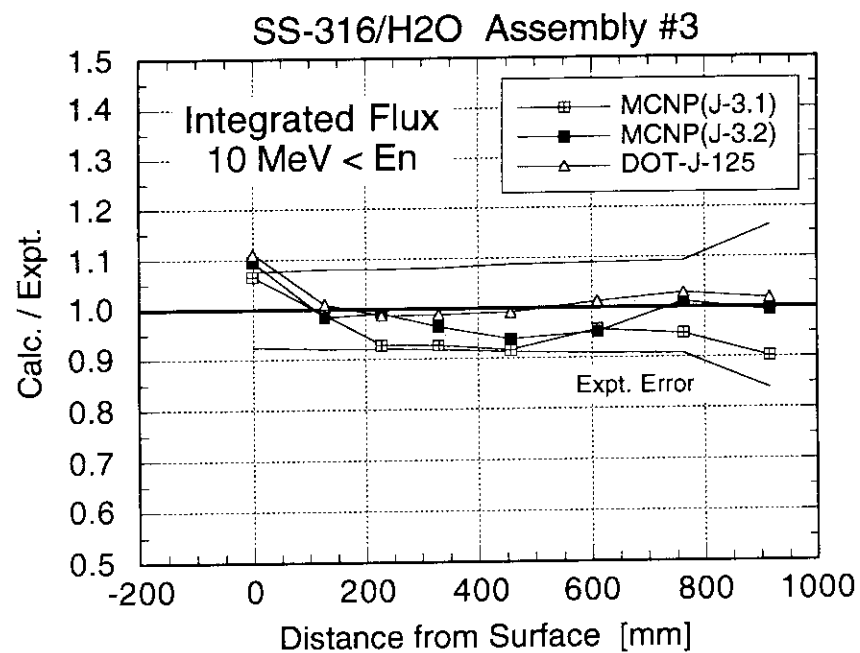


Fig. 3.66 The C/E ratios of the integrated neutron flux above 10 MeV for MCNP and DOT calculations.

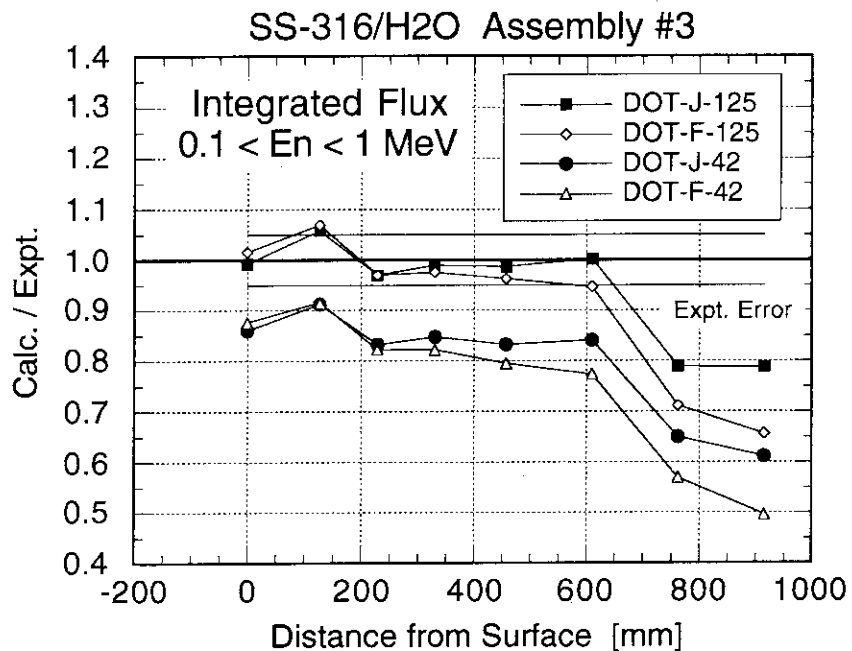


Fig. 3.67 The C/E ratios of the integrated neutron flux between 0.1 and 1 MeV for four different DOT calculations.

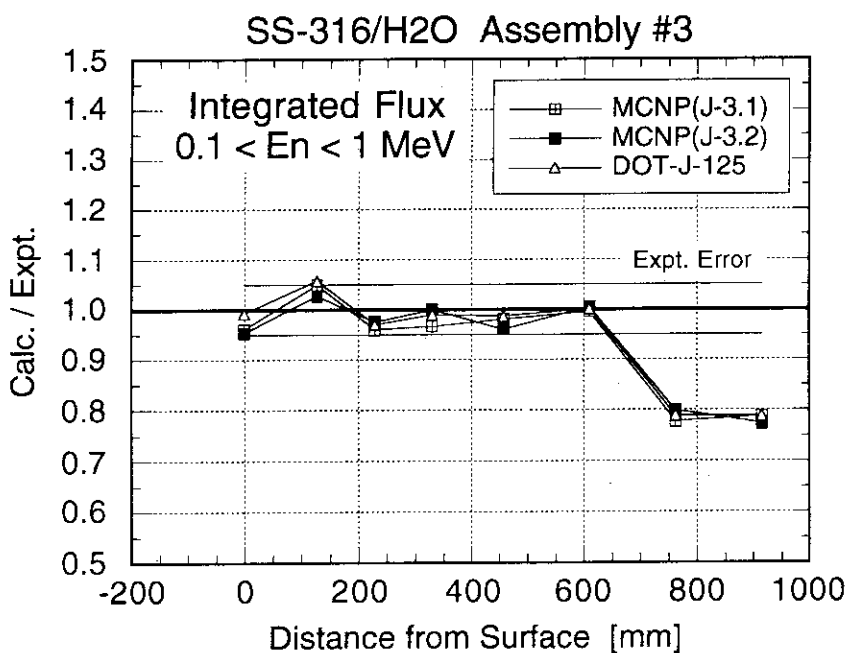


Fig. 3.68 The C/E ratios of the integrated neutron flux between 0.1 and 1 MeV for MCNP and DOT calculations.

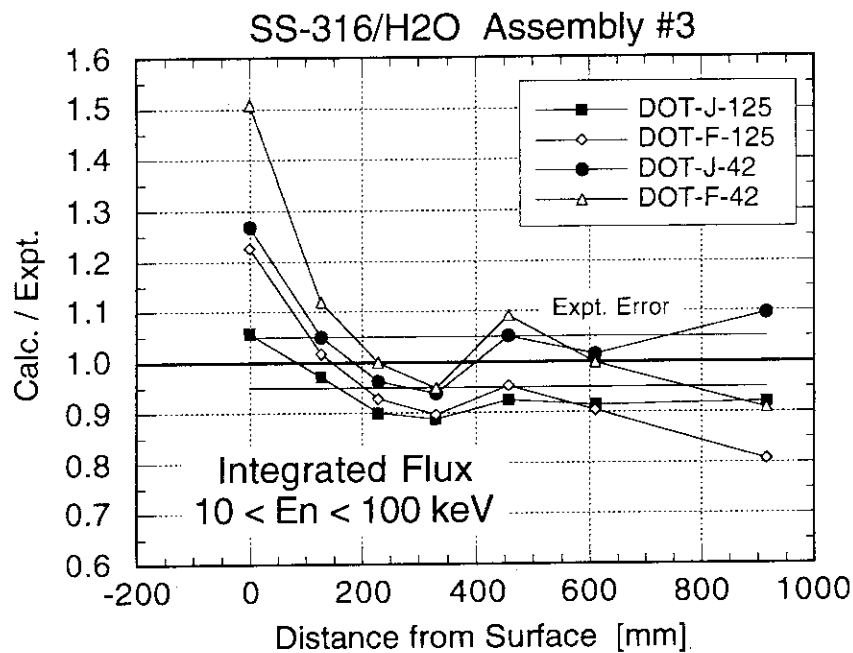


Fig. 3.69 The C/E ratios of the integrated neutron flux between 10 and 100 keV for four different DOT calculations.

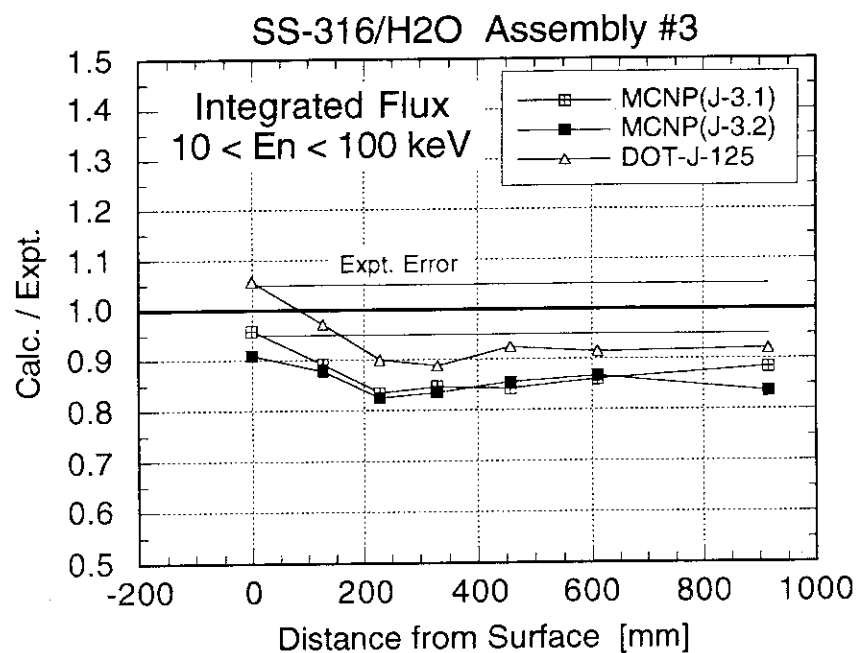


Fig. 3.70 The C/E ratios of the integrated neutron flux between 10 and 100 keV for MCNP and DOT calculations.

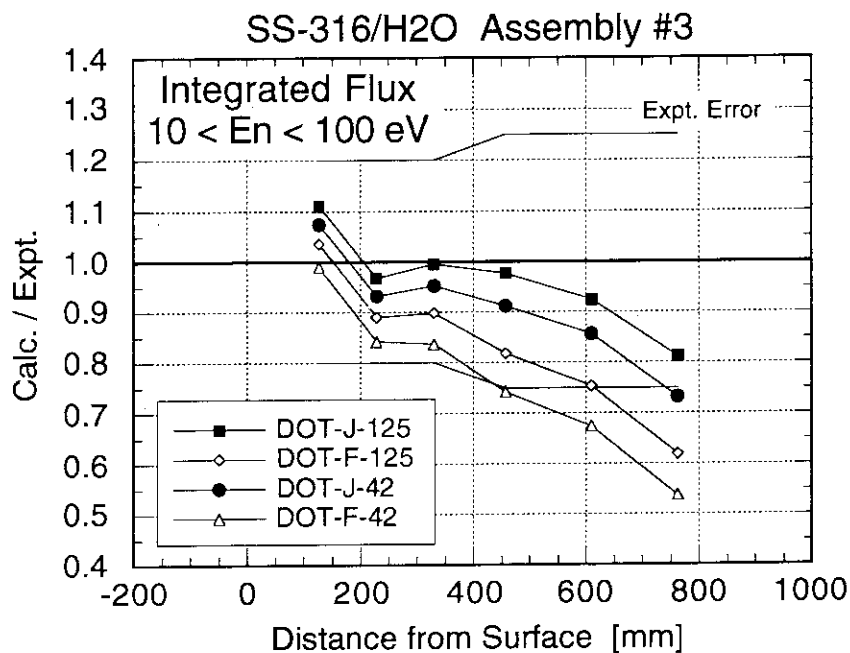


Fig. 3.71 The C/E ratios of the integrated neutron flux between 10 and 100 eV for four different DOT calculations.

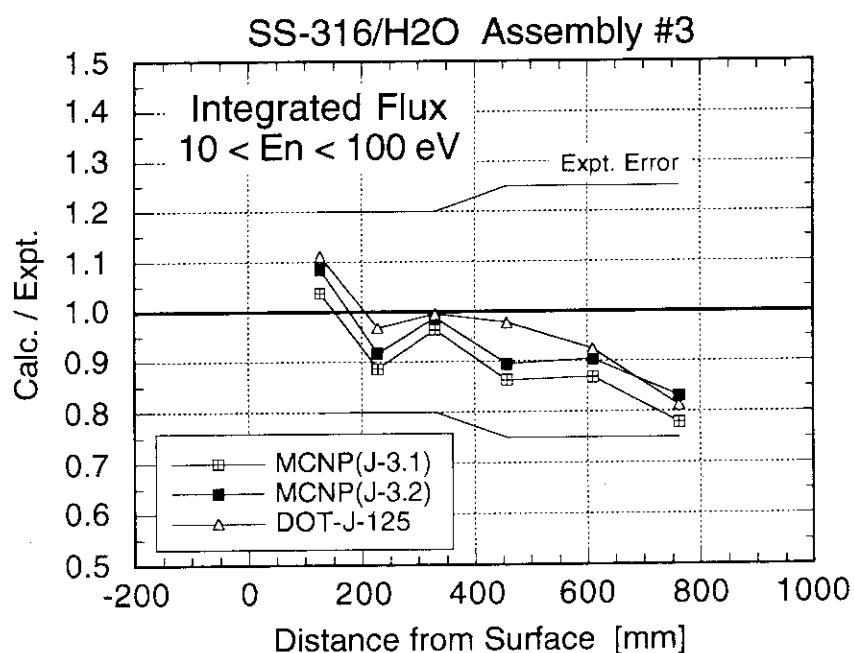


Fig. 3.72 The C/E ratios of the integrated neutron flux between 10 and 100 eV for MCNP and DOT calculations.

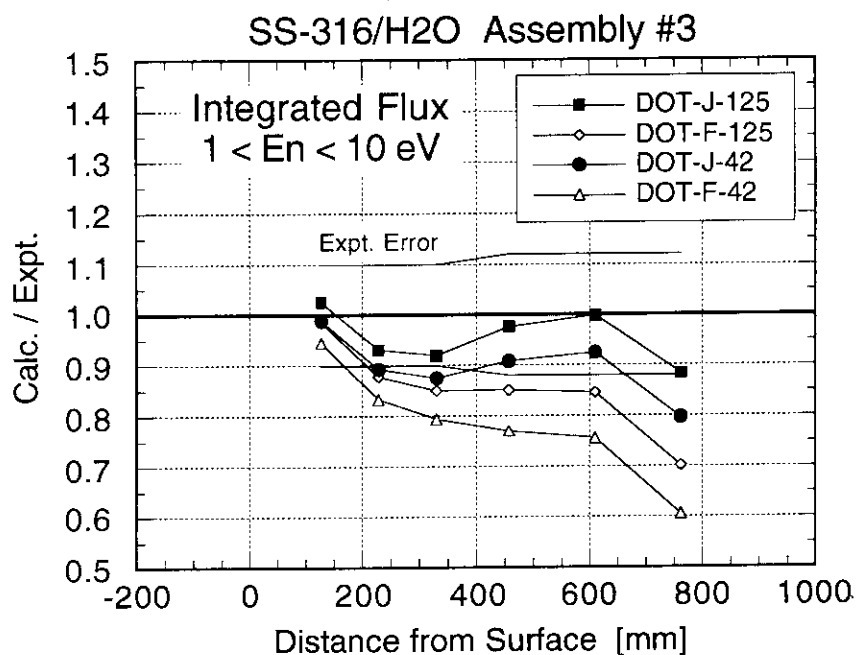


Fig. 3.73 The C/E ratios of the integrated neutron flux between 1 and 10 eV for four different DOT calculations.

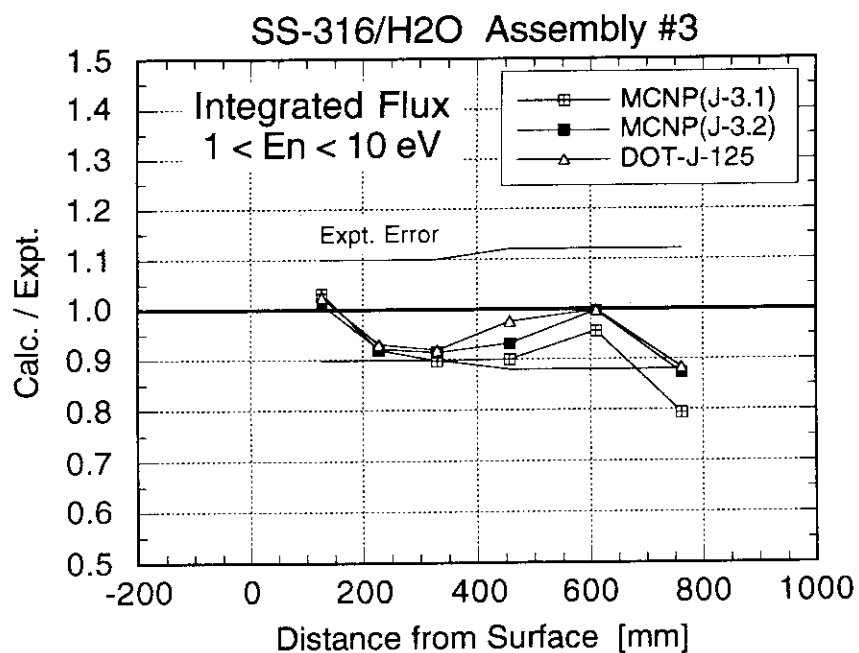


Fig. 3.74 The C/E ratios of the integrated neutron flux between 1 and 10 eV for MCNP and DOT calculations.

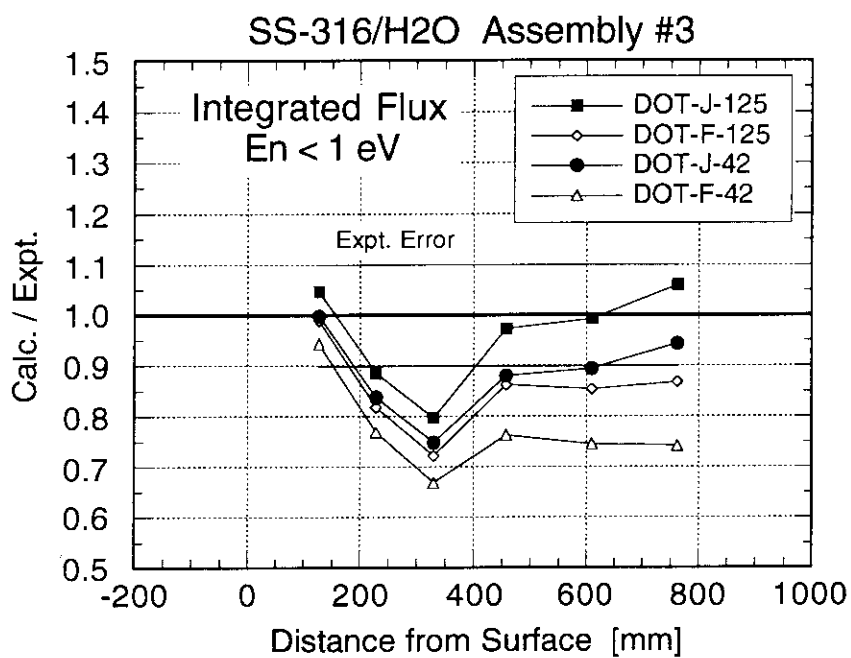


Fig. 3.75 The C/E ratios of the integrated neutron flux below 1 eV for four different DOT calculations.

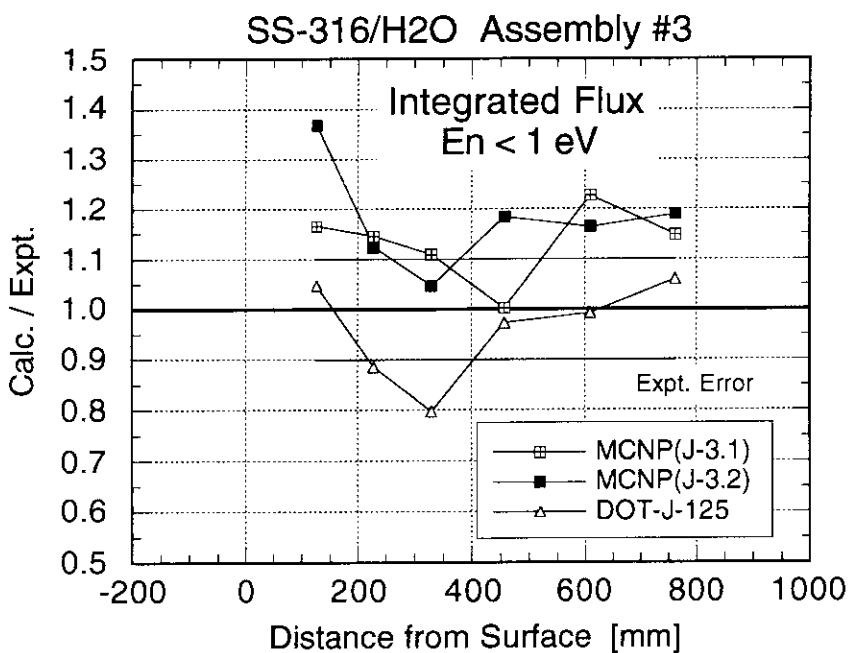


Fig. 3.76 The C/E ratios of the integrated neutron flux below 1 eV for MCNP and DOT calculations.

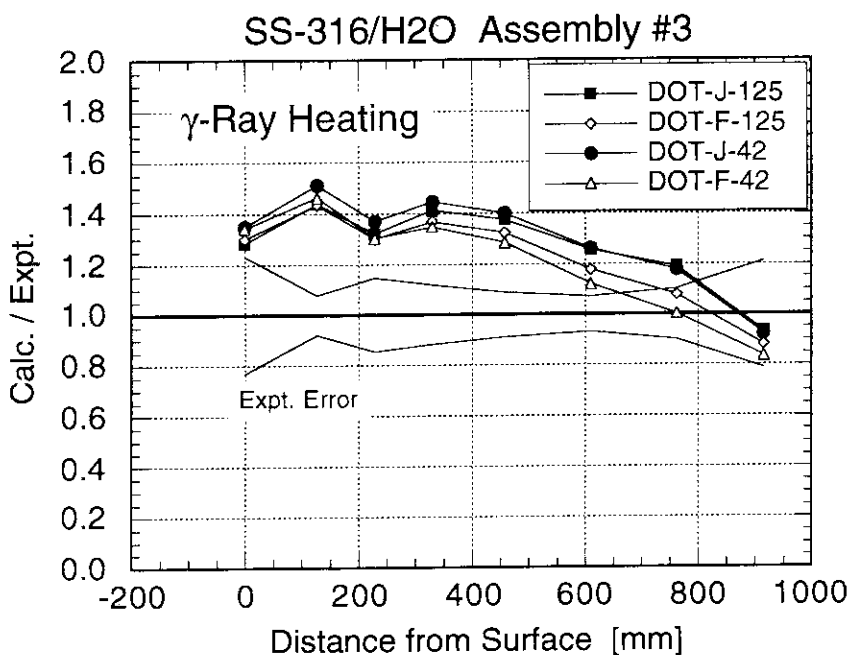


Fig. 3.77 The C/E ratios of the gamma-ray heating rate of SS316 for four different DOT calculations.

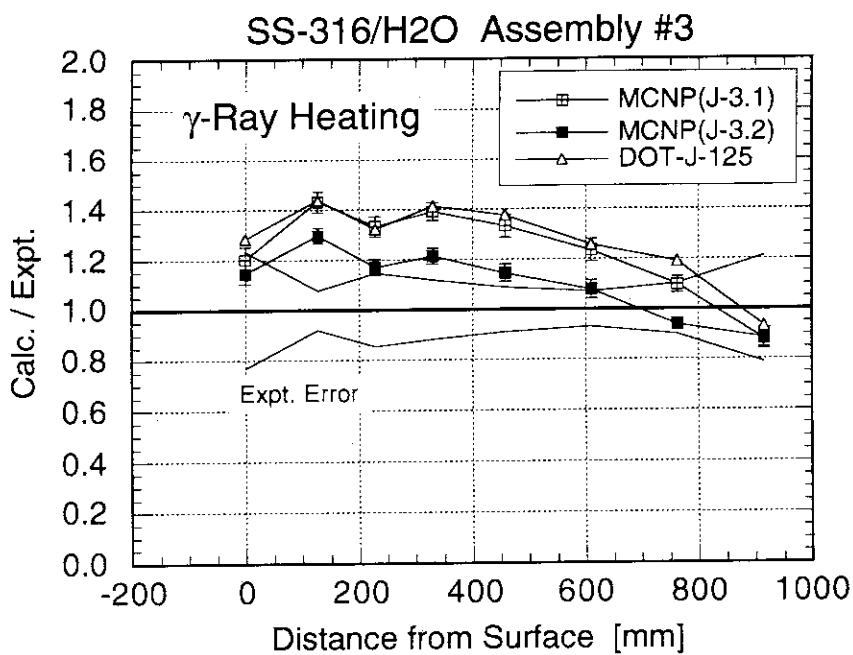


Fig. 3.78 The C/E ratios of the gamma-ray heating rate of SS316 for MCNP and DOT calculations.

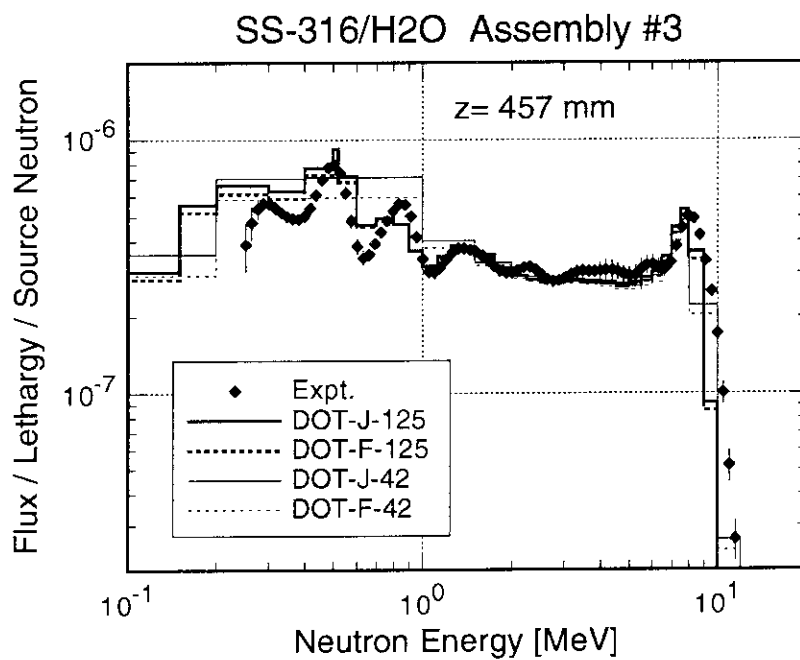


Fig. 3.79 The measured gamma-ray spectra at 457 mm depth in comparisons with four different DOT calculations.

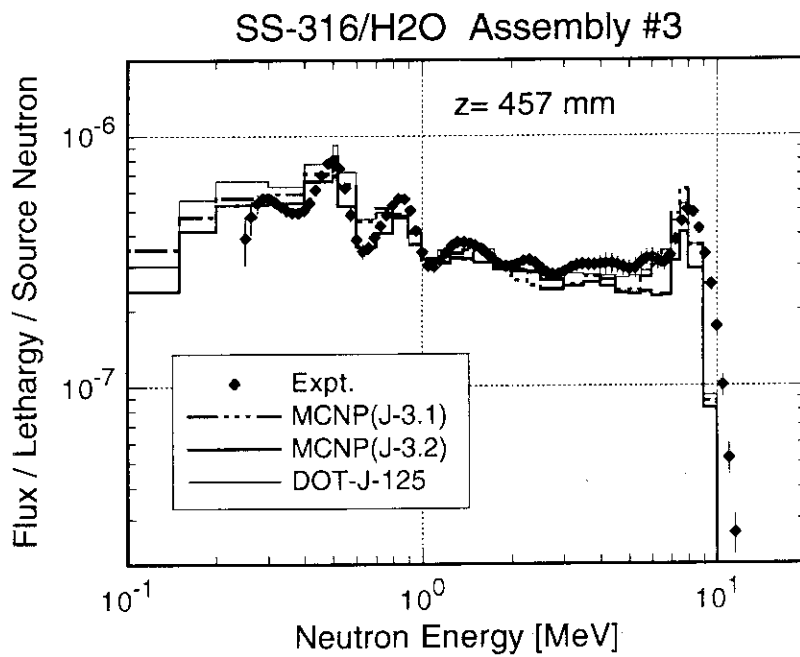


Fig. 3.80 The measured gamma-ray spectra at 457 mm depth in comparisons with MCNP and DOT calculations.

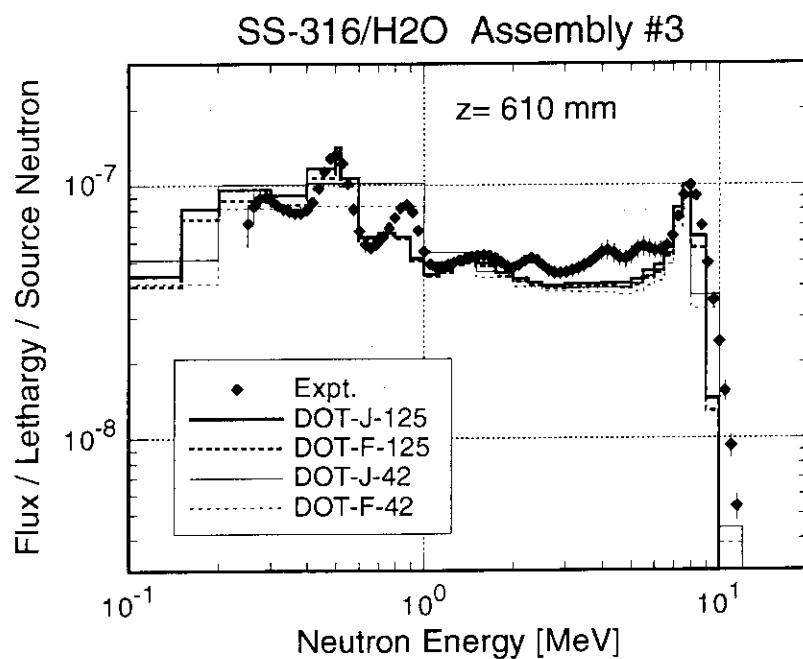


Fig. 3.81 The measured gamma-ray spectra at 610 mm depth in comparisons with four different DOT calculations.

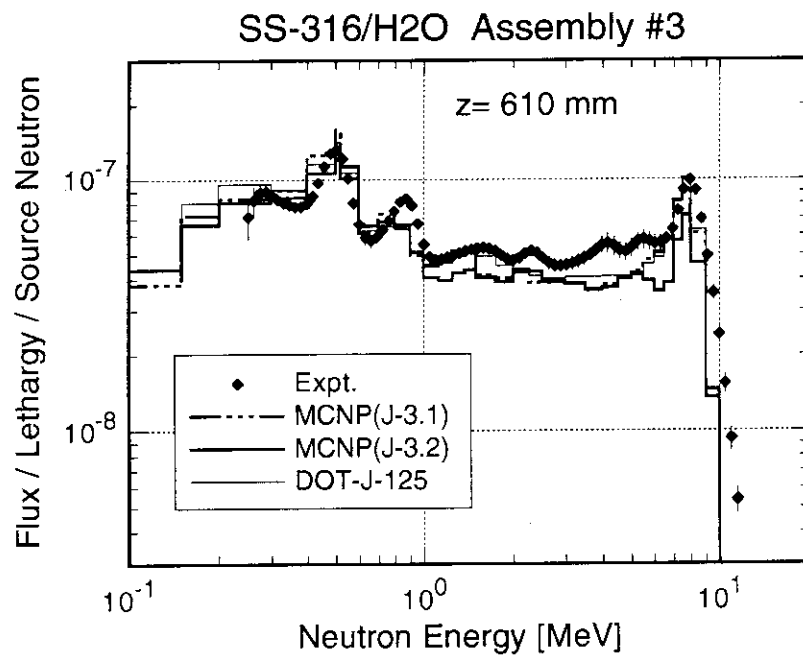


Fig. 3.82 The measured gamma-ray spectra at 610 mm depth in comparisons with MCNP and DOT calculations.

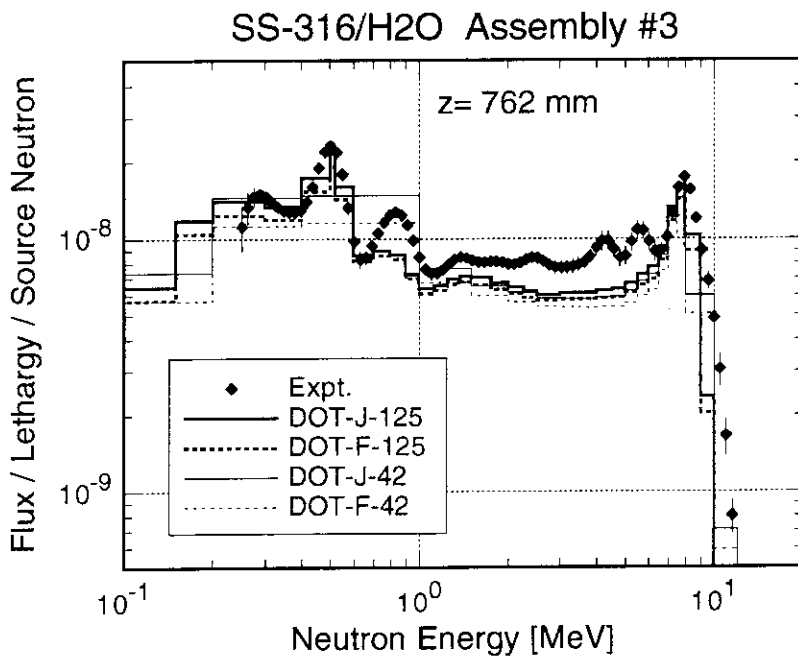


Fig. 3.83 The measured gamma-ray spectra at 762 mm depth in comparisons with four different DOT calculations.

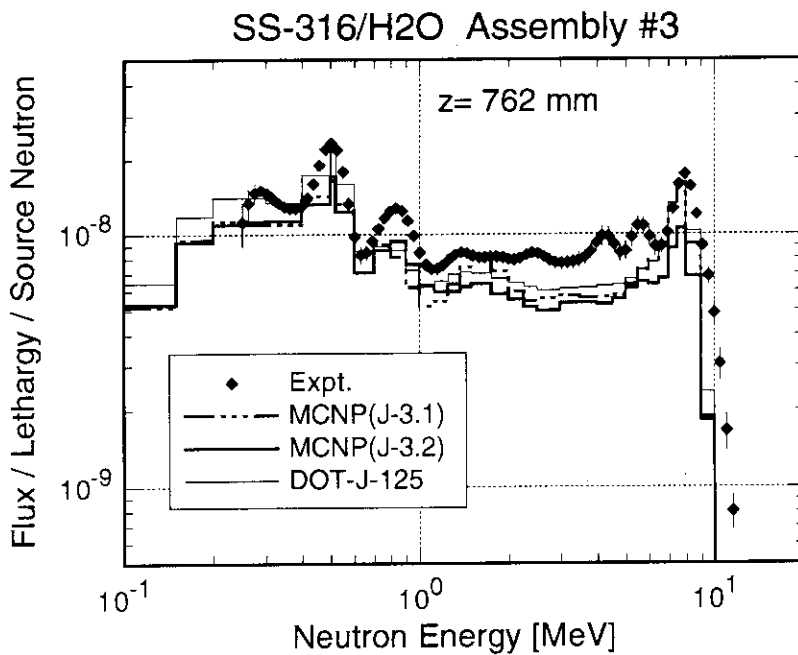


Fig. 3.84 The measured gamma-ray spectra at 762 mm depth in comparisons with MCNP and DOT calculations.

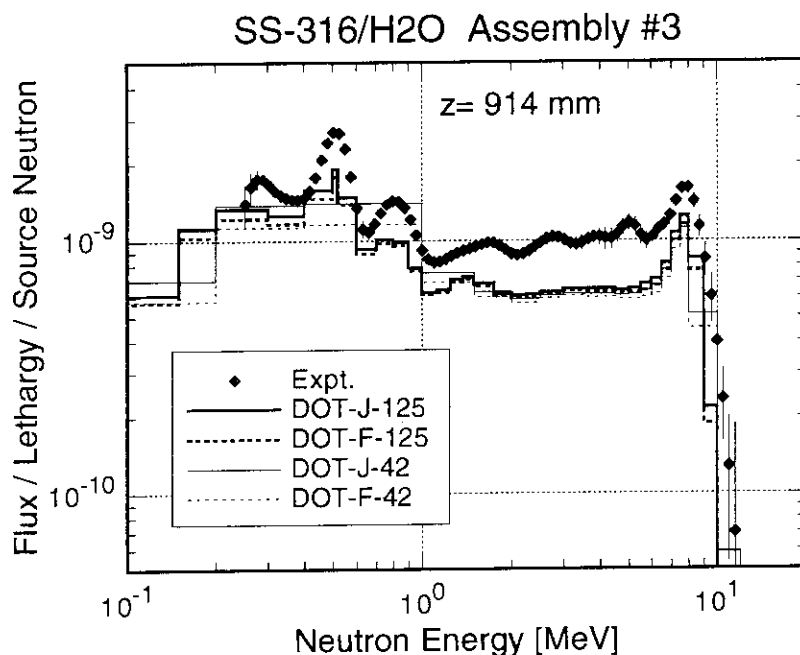


Fig. 3.85 The measured gamma-ray spectra at 914 mm depth in comparisons with four different DOT calculations.

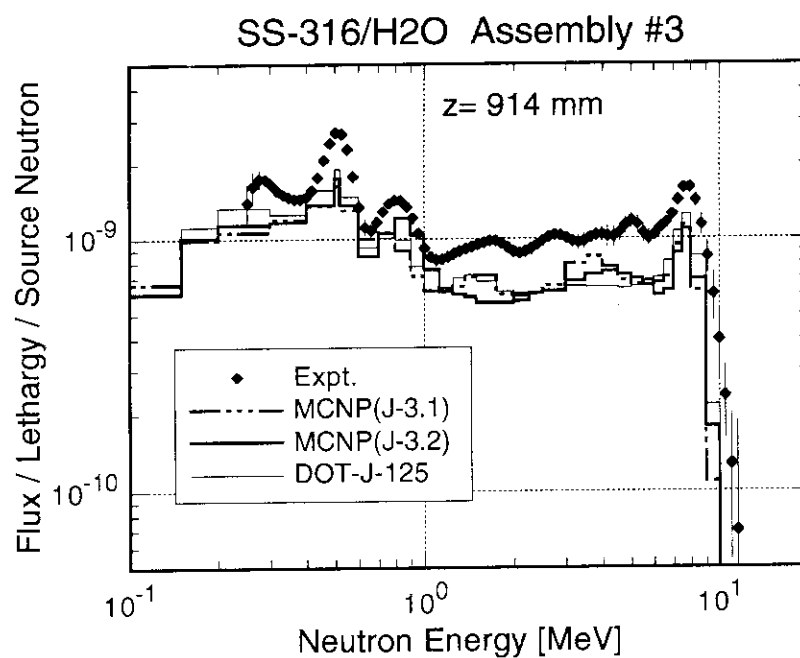
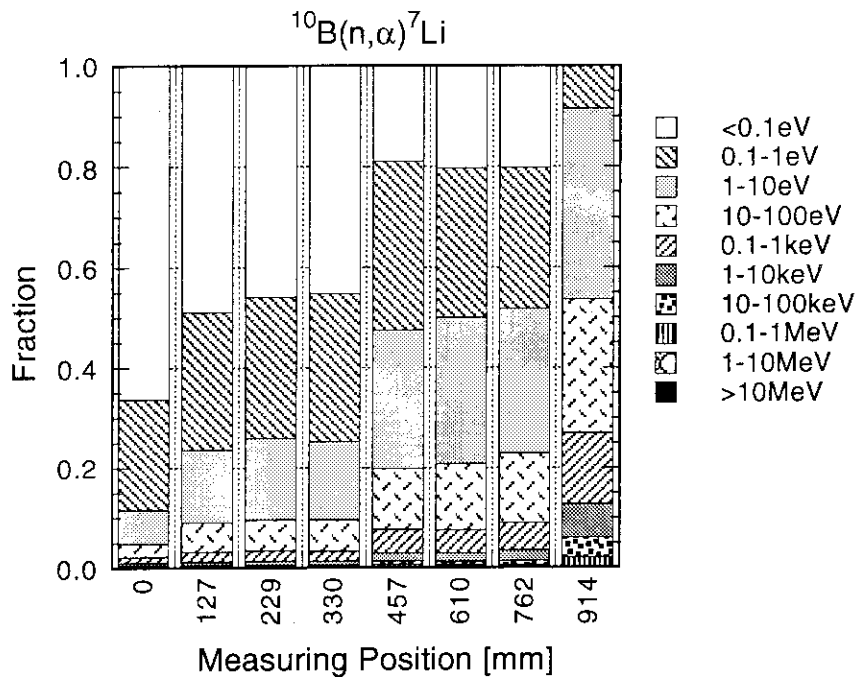
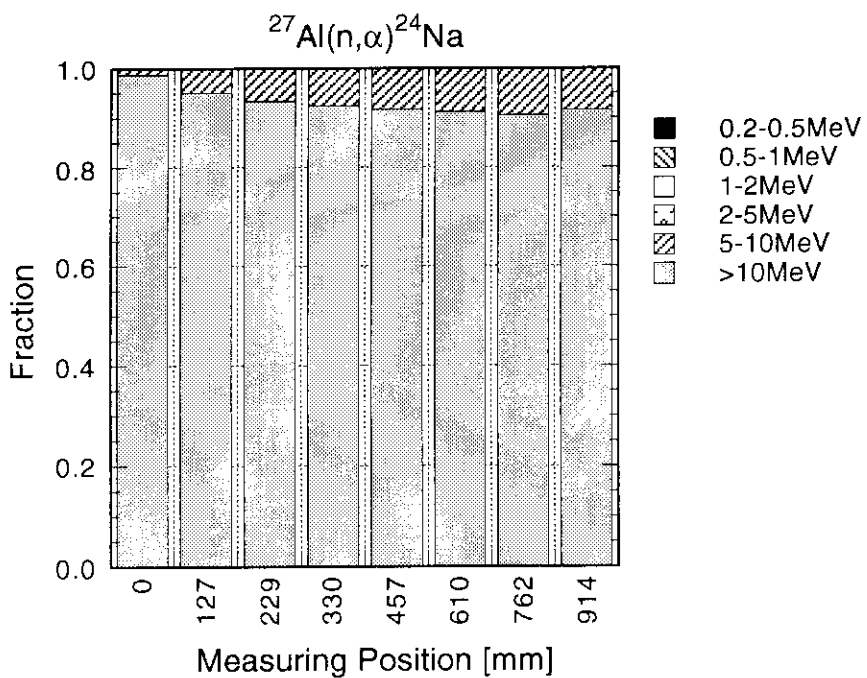
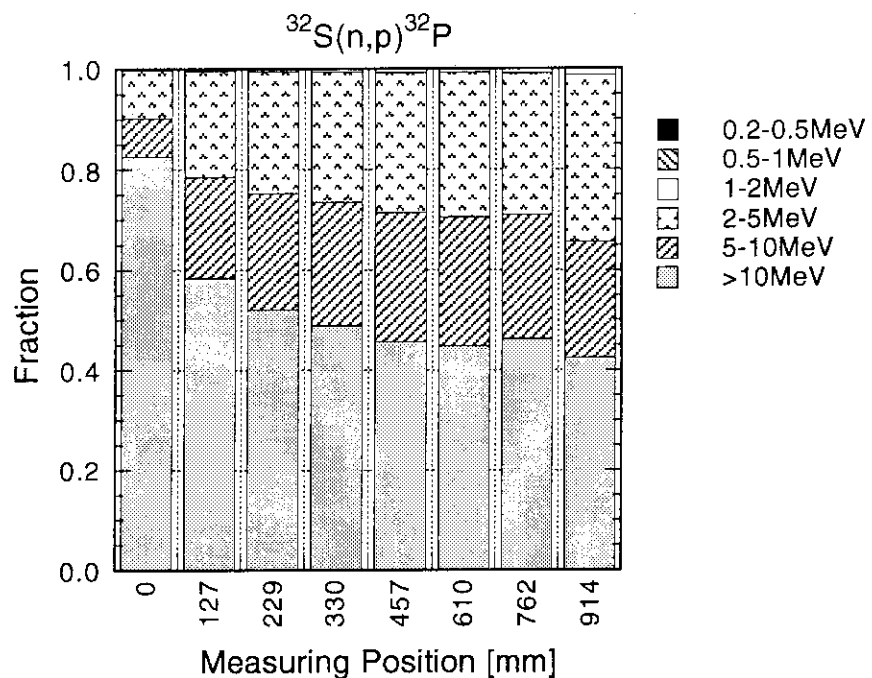
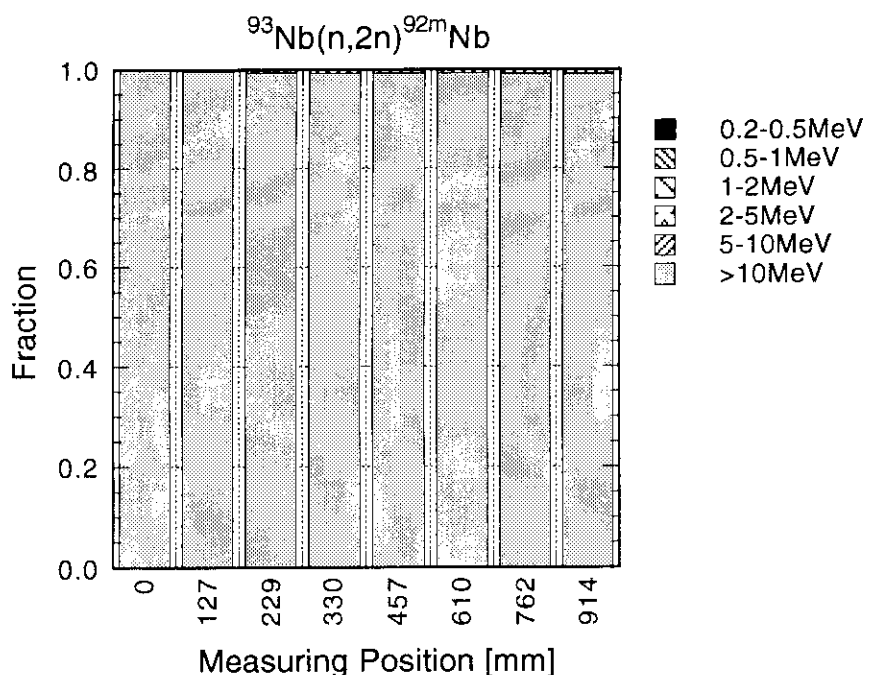
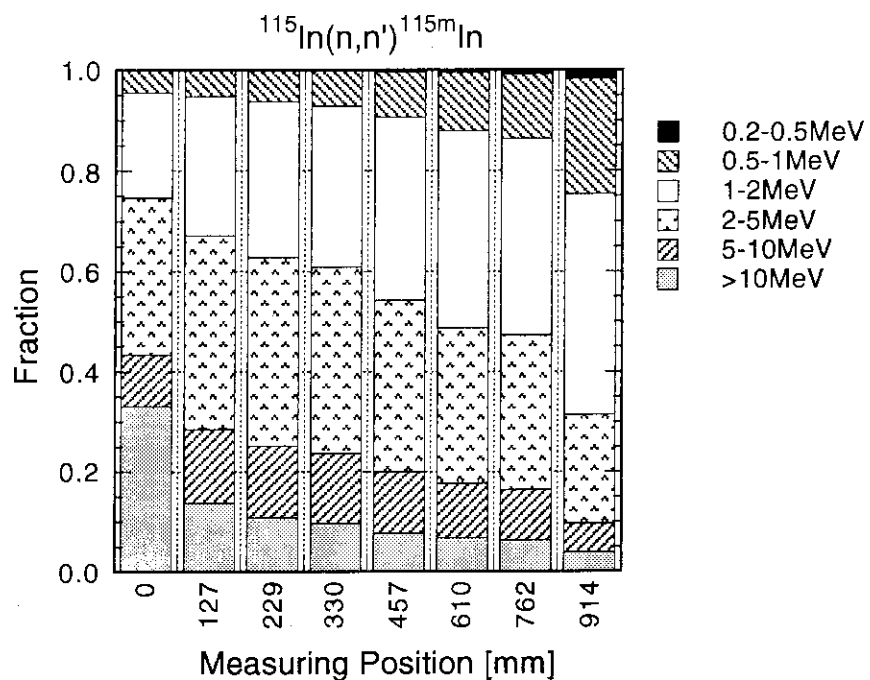
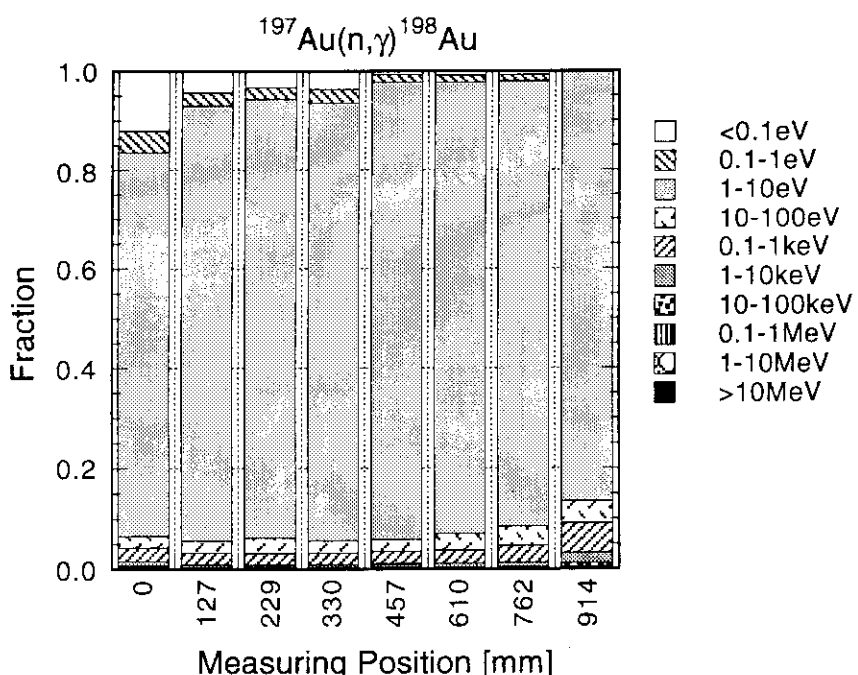


Fig. 3.86 The measured gamma-ray spectra at 914 mm depth in comparisons with MCNP and DOT calculations.

Fig. 4.1 Energy profile of $^{10}\text{B}(\text{n},\alpha)^7\text{Li}$ reaction at each measuring positions.Fig. 4.2 Energy profile of $^{27}\text{Al}(\text{n},\alpha)^{24}\text{Na}$ reaction at each measuring positions.

Fig. 4.3 Energy profile of $^{32}\text{S}(\text{n},\text{p})^{32}\text{P}$ reaction at each measuring positions.Fig. 4.4 Energy profile of $^{93}\text{Nb}(\text{n},2\text{n})^{92\text{m}}\text{Nb}$ reaction at each measuring positions.

Fig. 4.5 Energy profile of $^{115}\text{In}(n,n')^{115m}\text{In}$ reaction at each measuring positions.Fig. 4.6 Energy profile of $^{197}\text{Au}(n,\gamma)^{198}\text{Au}$ reaction at each measuring positions.

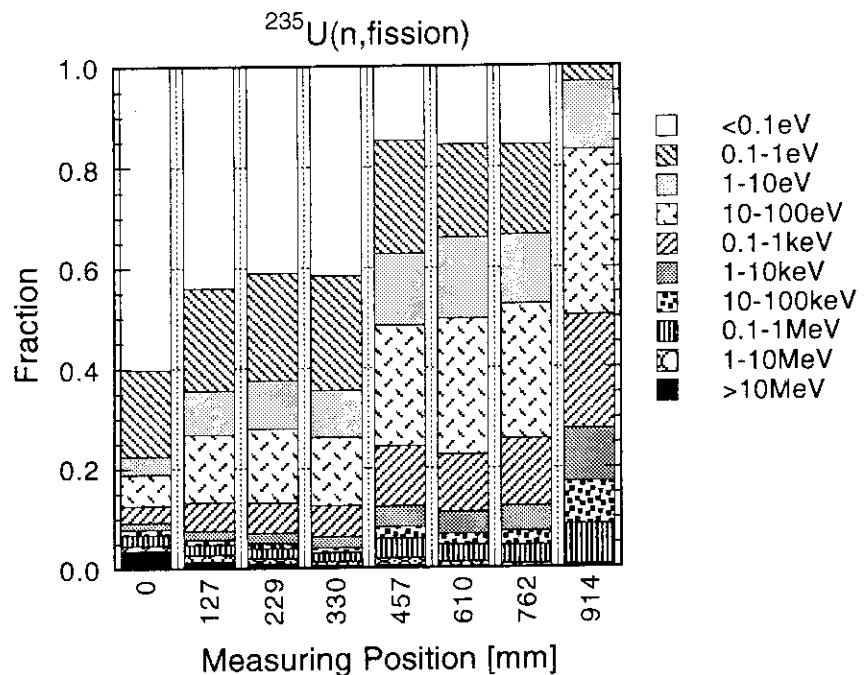


Fig. 4.7 Energy profile of $^{235}\text{U}(\text{n,fission})$ reaction at each measuring positions.

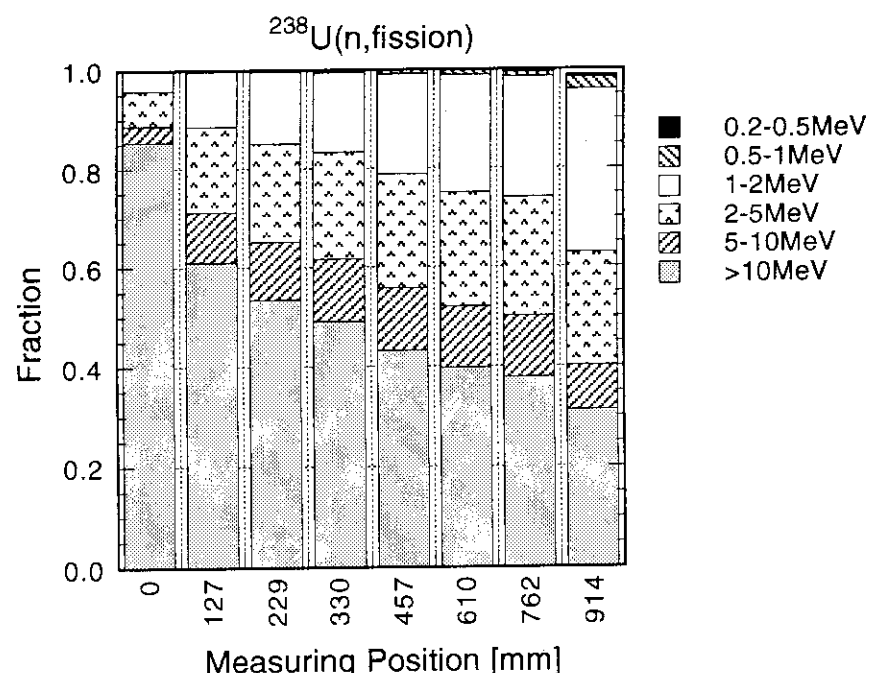


Fig. 4.8 Energy profile of $^{238}\text{U}(\text{n,fission})$ reaction at each measuring positions.